

The Role of Protein:Protein Interactions in Regulating Flagellar Assembly

Kritchai Poonchareon

Thesis submitted in partial fulfilment of the requirements of the
regulations for the degree of Doctor of Philosophy

Faculty of Medical Sciences
Institute for Cellular and Molecular Biosciences
Centre for Bacterial Cell Biology
Newcastle University
Newcastle upon Tyne

July 2013

Acknowledgements

The first person I would like to acknowledge is Dr Phillip Aldridge for his hard work to guide me through my PhD course. With his advice, determination and enthusiasm, this project has been published and contributes to the scientific society. I would like to give my great thanks to Dr Timothy Cheek for giving me a brilliant chance to be in Dr Phillip Aldridge's supervision and also for caring me every step of my life in UK. I would like to thank Professor Jeff Errington FRS to give me a good opportunity to enjoy doing research in Center for Bacterial Cell Biology. My thanks also go to Professor Colin Harwood, Professor Mike Kehoe and Dr Mark Banfield who gave me a good advice for being a good scientist. I would like to thank our lab members past and present; Christine Aldridge, Dr Jonathon Brown and Dr Christopher Birchall, for me, they have been like my family who share a good time, nice cuisine and especially great scientific ideas. All of the AUC results were intriguing and performed by Dr Alexandra Soloyva whom I would like to thank. Dr Joe Gray for his good advice and valuable "Muldi-Top" data. I would like to thank Dr Tohru Minamino and Dr Katsumi Imada for their close collaboration which was invaluable for the success of the project. Also everyone at the Center for Bacterial Cell Biology and Newcastle University who are unique and talented scientific community. I would to thank Professor Dr Prapon Wilairat for showing me the love of science. Many thank is giving to Kemmawadee Preedalikit for giving me strange and inspiration. I would like to thank Dr Sangchan Senapin for her help when I was in Thailand. For the success of this PhD, all belongs to my mother and father, Suda and Mitri Poonchareon because I used their genes for this study.

Abstract

The number of flagella in *Salmonella enterica* serovar Typhimurium cells is closely related with the activity of FlhD₄C₂, a transcriptional regulator that controls the synthesis of a flagellum. In multiflagelated cells of *S. enterica*, FlhD₄C₂ activity is negatively controlled by the Type 3 Secretion chaperone, FliT. FliT interacts with the flagellar filament cap protein FliD. FliD is thus indicated as an anti-regulator in the same aspect describing FlgM inhibition of σ^{28} activity. Protein interactions between FliT, FliD and FlhD₄C₂ were explored in detail. Two independent studies, Native gel electrophoresis and gel filtration, revealed the stoichiometry of FliT:FliD interaction to be 1 to 1. In addition, Bacterial Two Hybrid (B2H) analysis showed FliT interacting with FliD *In vivo*. FliT was also shown to interact with FlhD₄C₂ by destroying the FlhD₄C₂ complex. FlhD₄C₂ activity reduced in the presence of FliT but not all FlhD₄C₂ activity was inhibited. Biochemical analysis of the interaction between FlhD₄C₂ and DNA showed that FlhD₄C₂ bound to DNA was insensitive to FliT regulation. Using a FliT variant, FliT94, that had the last α -helix deleted, helped show that the binding site of FliT to both FliD and FlhD₄C₂ possibly overlap. The negative regulation of FliT is proposed to be a flagellar specific regulatory mechanism that effectively decreases FlhD₄C₂ activity to a minimum level rather than inhibiting all flagellar production. FliD counteracts FliT activity to increase FlhD₄C₂ activity by forming the FliT:FliD complex. Importantly, FlhD₄C₂ bound to DNA is insensitive to FliT regulation and permits a low number of cells in a population to build a low number of flagella, even during the action of FliT. This study highlighted the importance of including the regulatory protein:DNA interaction in the working model of the regulatory circuit. This model unveils a mechanism to allow bacterial cells to remain prepared to respond quickly and efficiently to the decision to control the activity of flagellation to multiple signals generated by the external environment, internal cues and flagellar specific feedback mechanisms.

Abbreviations

α -helix – alpha helix
 ATP – Adenosine triphosphate
 A – adenosine
 Amp – Ampicillin
 β -sheet – beta sheet
 BSA – Bovine serum albumin
 C-ring – cytoplamic ring
 C-terminus – Carboxy terminus
 cAMP – cyclic adenosine monophosphate
 cAMP-CRP – (cAMP) cAMP response protein
 CBD – chaperone binding domain
 CaCl_2 – Calcium chloride
 DNA – deoxyribose nucleic acid
 DMSO – Dimethyl sulphoxide
 dNTP – Deoxyribonucleotide triphosphate
 DNase – deoxyribonuclease
 EDTA –Ethylenediaminetetraacetic acid
 EM – Electron microscopy
 g – gravity
 HBB – Hook basal body
 HAPs – Hook associated proteins
 H_2O – Water
 HCl - Hydrochloric acid
 His-tag – histidine tag
 IM – Inner membrane
 IPTG - Isopropyl β -D-1-thiogalactopyranoside
 Kan – Kanamycin
 KCl – Potassium chloride
 L-ring – Lipopolysacchride ring
 L-handed – Left handed
 LB – Luria Bertani
 MgCl_2 – Magnesium chloride

mins – minutes

MALDI-TOF - Matrix-assisted laser desorption/ionization time of flight

N-terminus – Amino terminus

NaCl – Sodium chloride

OM – Outer membrane

OMP – Outer membrane protein

OD – optical density

P-ring - Peptidoglycan ring

PCR – polymerase chain reaction

PBS – phosphate buffered saline

PMT – PBS, Milk, Tween

R-handed – Right handed

RNA – ribonucleic acid

RNAP - ribonucleic acid polymerase

rpm – revolutions per minute

SPI1 – *Salmonella* pathogenicity island 1

SPI2 – *Salmonella* pathogenicity island 2

SDS – sodium dodecyl sulphate

SDS-PAGE – sodium dodecyl sulphate polyacrylamide gel electrophoresis

T3S – Type 3 secretion

T3SS - Type 3 secretion system

TLR – Toll like receptors

T5SS – Type 5 secretion system

T2SS – Type 2 secretion system

T1SS – Type 1 secretion system

T4SS – Type 4 secretion system

T3SC – Type 3 secretion chaperone

TAE – Tris-acetate EDTA

v – Volts

V1/V2 – Volume 1 / Volume 2

X-gal - 5-bromo-4-chloro-3-indolyl-b-D-galactopyranoside

5' – 5 prime

3' – 3 prime

λ – Wavelength

Table of contents

Acknowledgements.....	i
Abstract.....	ii
Abbreviations.....	iii
Table of contents.....	v
Table of figures.....	xii
Table of tables.....	xvi
1. Introduction.....	1
1.1 Bacteria in general.....	2
1.2 Salmonella Typhimurium.....	2
1.2.1 Salmonella as pathogen.....	3
1.2.2 Salmonella infection.....	4
1.3 Motility.....	6
1.3.1 The rotational motion of the flagellum.....	7
1.3.2 Filament configurations and their impact on motility	9
1.4 Chemotaxis.....	10
1.4.1 Chemotactic response control bacterial movement.....	10
1.4.2 Chemotactic sensing.....	14
1.4.3 Signal transduction: two-component system (TCS).....	14
1.5 Flagella structure.....	18
1.5.1 Flagella architecture - general principles	18
1.5.1.1 The hook basal body (HBB) or “engine”.....	18
1.5.1.2 Hook, Caps & junctions.....	19
1.5.1.3 The flagellar propeller.....	22

1.6 Type 3 secretion.....	23
1.6.1 <i>General principles.....</i>	23
1.6.2 <i>The flagellar T3S apparatus.....</i>	23
1.6.2.1 <i>T3S energy provision</i>	26
1.6.2.2 <i>The T3S substrate-specificity switch</i>	26
1.6.2.3 <i>Flagellar T3S Chaperones</i>	27
1.7 The general principles of transcriptional regulation	28
1.7.1 <i>Transcriptional regulation by Sigma Factors (σ).....</i>	28
1.7.2 <i>Other regulatory proteins</i>	31
1.7.3 <i>Post-transcriptional regulation</i>	32
1.8 Flagellar regulon.....	32
1.8.1 <i>The regulon's architecture (fla regulons).....</i>	32
1.8.2 <i>Activation of the transcriptional hierarchy.....</i>	33
1.8.3 <i>The FlhD₄C₂ component in the circuit.....</i>	34
1.8.4 <i>The HBB assembly Checkpoint and flagellar gene</i>	
<i>expression.....</i>	40
1.8.4.1 σ^{28}	40
1.8.4.2 FlgM.....	41
1.8.4.3 The σ^{28} : FlgM switch.....	42
1.9 FliT.....	44
1.10 FliD.....	46
 2. AIMS.....	 53
 3. Materials.....	 56
3.1 Bacterial strains and Plasmids.....	57
3.2 Media, agar plates and antibiotics.....	59
3.3 Primers for PCR reaction.....	60
3.4 DNA Preparation and cloning.....	61
3.5 Protein Preparation.....	61
3.6 DNA and protein analysis.....	62

3.7 Analytical instrumentation.....	62
3.8 Others.....	63
4 Methods.....	64
4.1 Bacterial growth.....	65
4.2 DNA manipulation procedure	65
4.2.1 <i>Sigma Bacterial Genomic DNA KIT.....</i>	65
4.2.2 <i>Isolation of plasmid DNA.....</i>	65
4.2.2.1 <i>Crude plasmid DNA extraction.....</i>	65
4.2.2.2 <i>Sigma PLASMID MINI-PREP KIT</i>	66
4.2.3 <i>Restriction endonuclease digestion of DNA.....</i>	66
4.2.3.1 <i>Simple Test Digests.....</i>	66
4.2.3.2 <i>Cloning Experiments.....</i>	67
4.2.4 <i>Ligation of DNA fragments.....</i>	67
4.2.5 <i>Heat shock transformation of E. coli cells.....</i>	67
4.2.5.1 <i>Preparation and storage of competent cell.....</i>	67
4.2.5.2 <i>Heat shock transformation.....</i>	68
4.2.6 <i>Oligonucleotides as primers.....</i>	68
4.2.7 <i>Polymerase Chain Reaction (PCR).....</i>	68
4.2.8 <i>Purification of a PCR fragment (DNA Precipitation).....</i>	69
4.2.8.1 <i>Ethanol precipitation.....</i>	69
4.2.8.2 <i>Sigma PCR Clean-Up Kit.....</i>	69
4.2.8.3 <i>Sigma Gel Extraction Kit.....</i>	69
4.2.9 <i>Quantitation of DNA.....</i>	69
4.2.10 <i>Agarose gel electrophoresis.....</i>	70
4.3 DNA mutagenesis (QuickChange Site-Directed Mutagenesis kit).....	70
4.4 Bacterial two hybrid system (B2H).....	72
4.4.1 <i>B-galactosidase activity assay.....</i>	72
4.5 DNA sequencing.....	73
4.6 Protein purification procedure	73
4.6.1 <i>Cell Culture and Preparation.....</i>	73
4.6.2 <i>Cell Disruption.....</i>	74

4.6.3 Purification of bacterial proteins.....	74
4.6.3.1 His tag isolation of FliT and FliD.....	74
4.6.3.2 Heparin isolation of FlhD ₄ C ₂	74
4.6.3.3 GST-protein isolation.....	75
4.6.3.4 Gel filtration of FlhD ₄ C ₂ , FliT and FliD.....	75
4.6.4 The measurement of protein concentration.....	76
4.6.5 Thrombin digestion.....	76
4.6.6 Cell lysate preparation for western blot.....	77
4.6.7 Protein gel electrophoresis (PAGE)	77
4.6.7.1 Native gel electrophoresis.....	77
4.6.7.2 SDS Protein gel electrophoresis.....	78
4.6.8 Western blot analysis	78
4.7 Protein analysis procedure.....	79
4.7.1 Analytical Ultracentrifugation (AUC).....	79
4.7.2 Isothermal calorimeter (ITC).....	79
4.7.3 Surface Plasma Resonance (SPR).....	80
4.7.4 Protein Crystallography.....	83
4.7.4.1 The Optimisation of crystallisation conditions.....	83
4.7.5 Matrix-assisted Laser Desorption/Ionization-time of flight Mass Spectroscopy (MALDI-TOF).....	83
5 Investigation of FliT / FliD interaction.....	84
5.1 Purification of FliT and FliD.....	86
5.2 Analysis of FliT:FliD interaction by native gel electrophoresis.....	90
5.3 Analysis of FliT: FliD interaction by gel purification.....	92
5.4 Analytical ultracentrifugation (AUC) of FliT: FliD complex.....	94
5.5 Isolation of FliT: FliD crystals.....	98
5.6 Discussion.....	100

6 Investigation of <i>FliT</i> and <i>FlhD₄C₂</i> interaction.....	101
6.1 Purification of <i>FlhD₄C₂</i> for further analysis.....	104
6.2 Analysis of <i>FliT</i> : <i>FlhD₄C₂</i> interaction by native gel electrophoresis.....	105
6.3 Analysis of <i>FliT</i> : <i>FlhD₄C₂</i> interaction by gel purification.....	109
6.4 MALDI-TOF MS Analysis of <i>FliT</i> incorporated in the products of the <i>FliT</i> : <i>FlhD₄C₂</i> interaction.....	115
6.5 Analysis of the <i>FliT</i> : <i>FlhD₄C₂</i> interaction by Analytical Ultra Centrifugation (AUC).....	120
6.6 Discussion.....	122
7 SPR analysis of <i>FliT</i>: <i>FlhD₄C₂</i>: DNA interaction.....	125
7.1 <i>FliT</i> regulation towards <i>FlhD₄C₂</i> :DNA interaction monitored by SPR analysis.....	127
7.2 Motility assay of overexpressed <i>FliT</i>	131
7.3 An SPR analysis shows resistance of <i>FlhD₄C₂</i> :DNA complex to <i>FliT</i>	136
7.4 <i>FliD</i> as an anti-anti- <i>FlhD₄C₂</i> factor.....	141
7.5 Discussion.....	143
8 The analysis of <i>FliT</i>: <i>FliD</i>: <i>FlhD₄C₂</i> interaction by B2H	145
8.1 <i>FliD</i> : <i>FliT</i> interaction by B2H.....	151
8.2 Expanded combination assay of all proteins in the circuit.....	154
8.3 Analysis of <i>FliT</i> point mutations (B2H).....	155
8.4 SPR analysis of <i>FliT</i> 94 mutants.....	159

9 The quantification of the concentration of FliT, FliD, and FlhD₄C₂ by western blot analysis	164
9.1 The quantification of FliT, FliD and FlhD ₄ C ₂ in natural form in a natural form in a bacterial population.....	165
9.2 FliT and FliD are more abundant than FlhD ₄ C ₂	166
9.3 Discussion.....	167
10 Discussion, conclusion and future research.....	172
10.1 Discussion.....	173
10.2 Conclusion.....	179
10.3 Future research.....	180
11 Reference.....	181
Appendix A: Growth media and solutions.....	200
Appendix B: Protein preparation for analysis.....	205
1 FliT purification.....	205
2 FliD purification.....	206
3 FlhD ₄ C ₂ purification.....	207
Appendix C: The prediction of protein concentration	208
Appendix D: Bacterial Two Hybrid system (B2H).....	209
1 Methods Illustrated for protein interaction analysis (FliT and FliD).....	209
2 The actual result on big square agar plate representing B2H experiments from different protein interaction with either C or N terminal free of all 56 combinations.....	210
3 Test digestion showing gene insert of all 16 clones.....	211
Appendix E: Thrombin digestion of proteins.....	212
Methods Illustrated for preparing digested proteins (FliT and FliD)	212

Appendix F: GST proteins purification.....	213
1 GST proteins purified by GST- affinity beads for GST-FliT mutants.....	213
2 Expression profiles of GST FliT mutants and immune blot (FliT).....	214
Appendix G: Prepare bacterial cells' sample.....	215
Appendix H: PCR information for amplifying <i>fliT</i>, <i>fliD</i> and <i>flhDC</i> gene.....	216

Tables of figures

Figure 1	<i>Infection caused by S. Typhimurium requiring the Salmonella pathogenecity islands 1 and 2 (SPI1 and SPI2).....</i>	5
Figure 2	<i>Photomicrographs of Salmonella enteridis show the peritricious arrangement of flagella.....</i>	8
Figure 3	<i>Two types of the configuration of flagella (L- and R-type straight filaments of flagella)</i>	11
Figure 4	<i>Schematic diagrams show drawing of the possible flagellar waveforms for bacterial movement.....</i>	12
Figure 5	<i>A schematic diagram showing how E.coli can utilise changes in waveform during tumbling motion to alter flagellar rotation, and ultimately swimming direction.....</i>	13
Figure 6	<i>The morphological structure of chemoreceptor arrays.....</i>	15
Figure 7	<i>Illustration of the E.coli chemotaxis system modifying flagellar activity.....</i>	17
Figure 8	<i>Flagellar components of Salmonella enteric serovar Typhimurium.....</i>	21
Figure 9	<i>Illustration of the flagellar T3S apparatus.....</i>	25
Figure 10	<i>Flagellar genes are expressed in an organized order corresponding to the sequence of flagellar assembly.....</i>	36
Figure 11	<i>Regulation of flagellar master regulator FlhD₄C₂.....</i>	38
Figure 12	<i>Structure of the FlhD₄C₂ complex</i>	39
Figure 13	<i>Structure of the A.aeolicus σ^{28} / FlgM Complex.....</i>	43
Figure 14	<i>The proposed circuit of FliT negative regulation upon the gene expression of the flagellar Class 2 operon.....</i>	48
Figure 15	<i>Molecular structure of FliT.....</i>	49
Figure 16	<i>The configuration of FliD decamer in solution.....</i>	50
Figure 17	<i>Three – dimentional density map of the cap-filament complex.....</i>	51
Figure 18	<i>Processes of the QuikChange® site-directed mutagenesis method.....</i>	71

Figure 19	<i>A sensorgram of one cyclic experiment with molecular interaction detail on the chip.....</i>	81
Figure 20	<i>Purification of FliT.....</i>	88
Figure 21	<i>Purification of FliD.....</i>	89
Figure 22	<i>Native gel- electrophoresis of FliT:FliD complex.....</i>	91
Figure 23	<i>Gel filtration profile of the FliT:FliD complex</i>	93
Figure 24	<i>AUC analysis of FliT, FliD and the FliT:FliD complex.....</i>	96
Figure 25	<i>Composite AUC profiles of FliT, FliD, and the FliT:FliD complex</i>	97
Figure 26	<i>Crystals of FliT:FliD.....</i>	99
Figure 27	<i>FliT and FlhD expressed with His Tags (except FlhC).....</i>	103
Figure 28	<i>Purification of FlhD₄C₂.....</i>	106
Figure 29	<i>Native gel analysis of FliT: FlhD₄C₂ interaction with the corresponding SDS-PAGE.....</i>	107
Figure 30	<i>Native gel analysis showing the effect of increased FlhD₄C₂ concentrations.....</i>	108
Figure 31	<i>Gel filtration analysis revealed no new peak of the FliT: FlhD₄C₂ complex but the original FlhD₄C₂ peak shifted to the right side</i>	111
Figure 32	<i>FliT interacts with FlhD₄C₂ in generating a FliT/FlhD₄C₂ complex the size of FlhD₄C₂.....</i>	113
Figure 33	<i>SDS-PAGE of gel filtration all indicates the main peak at FlhD₄C₂ region while 1:1 FliT:FlhD₄C₂ ratio, smaller complex (FliT/FlhD) and excess FliT ,larger complex (FliT:FlhD₄C₂).....</i>	114
Figure 34	<i>MALDI TOF illustrated cartoon.....</i>	117
Figure 35	<i>FlhC (A) and FlhD (B) peptide mass fingerprint obtained from MALDI-TOF experiments of FlhD₄C₂ control collected at FlhD₄C₂ peak (fraction 40).....</i>	118
Figure 36	<i>FlhC (A) and FlhD/FliT (B) peptide mass fingerprint obtained from MALDI-TOF experiments of a FliT: FlhD₄C₂ mix collected at the same region (FlhD₄C₂ peak, Fraction 39)</i>	119
Figure 37	<i>Analytical ultracentrifugation analysis of the interaction of FliT with FlhD₄C₂.....</i>	121
Figure 38	<i>The Sensogram diagram generated by SPR experiment.....</i>	128
Figure 39	<i>SPR analysis of FlhD₄C₂ and FlhD₄C₂/FliT interaction to P_{flgB} (DNA)..</i>	132

Figure 40	SPR analysis of <i>FliT</i> regulation towards <i>FlhD₄C₂</i> :DNA interaction	133
Figure 41	The motility test and swimming pattern of the wild type and the overexpressed <i>FliT</i> strain.....	135
Figure 42	SPR Profile showing the double injection of <i>FlhD₄C₂</i> and <i>P_{flgB}</i> , respectively.....	138
Figure 43	<i>FlhD₄C₂</i> departure from various <i>FlhD₄C₂</i> :DNA complex by <i>flgB</i> challenge.....	139
Figure 44	Resistance of <i>FlhD₄C₂</i> :DNA complex to <i>FliT</i>	140
Figure 45	<i>FliD</i> , an anti-anti- <i>FlhD₄C₂</i> factor.....	142
Figure 46	The principle of B2H assay showing <i>FliT</i> and <i>FliD</i> interaction.....	148
Figure 47	Different gene organisation in B2H plasmids results in free C or N terminal regions for analysis.....	149
Figure 48	The coding sequence of <i>FliT</i> showing four α regions (red underlined) and predicted <i>FliT</i> tertiary structure containing flexible region ($\alpha 4$) at C-terminus, where its deletion creates <i>FliT94</i>	150
Figure 49	The construction of recombinant plasmids or pUT18 carrying <i>fliD</i> gene (pKP11) for B2H analysis requires 2 steps.....	152
Figure 50	The B2H assay of <i>FliT</i> and <i>FliD</i> interaction	153
Figure 51	The actual result on big square agar plate representing B2H experiments from different protein interaction with either C or N terminal free	157
Figure 52	Cartoon presentation showing interaction of <i>FliT</i> / <i>FliD</i> / <i>FlhD</i> and <i>FlhC</i> specifying C and N terminal and their corresponding B2H results.....	158
Figure 53	The protein interaction test (B2H) of mutant producing different specified single amino acid substitutions of <i>FliT</i> protein at different location against wild type producing <i>FliD</i> , <i>FlhC</i> , and <i>FlhD₄C₂</i>	161
Figure 54	Mutation of <i>FliT</i> (E75A) shows both decreasing <i>FliT</i> inhibition from motility assay and weak interaction to <i>FlhD₄C₂</i>	162
Figure 55	SPR data showed <i>FliT94</i> mutation renders various inhibitory effect of several mutated <i>FliT</i> to <i>FlhD₄C₂</i>	163
Figure 56	Thrombin digestion of <i>FliT</i> and <i>FliD</i>	168
Figure 57	<i>FliT</i> quantification.....	169

Figure 58	<i>FliD</i> quantification.....	170
Figure 59	<i>FlhD₄C₂</i> quantification.....	171
Figure 60	A general mechanism applied to the regulatory circuit used for flagellar gene expression.....	174
Figure 61	The mechanism of action from each counterpart in the circuit.....	176

Tables of tables

Table 1	<i>Eσ^{70} regulate many enzymes responsible for important cell activities.....</i>	30
Table 2	<i>Several factors affect FlhD₄C₂ activity.....</i>	37
Table 3	<i>Bacterial strain table.....</i>	57
Table 4	<i>Plasmid table.....</i>	57
Table 5	<i>Antibiotic and supplement stock including working concentrations.....</i>	59
Table 6	<i>Primers used in B2H and Quick change.....</i>	60
Table 7	<i>DNA sequences used for SPR analysis.....</i>	82
Table 8	<i>Biochemical Parameters generated by SPR experiment.....</i>	134
Table 9	<i>The SPR data of FlhD₄C₂ signal from various concentrations of FliT interaction.....</i>	134
Table 10	<i>Detail of plasmids and their pairings used in the B2H experiment ...</i>	156

Chapter 1

Introduction

1 Introduction

1.1 Bacteria in general

Bacteria have a distinctive form of life and are able to survive in both favourable and unfavourable conditions. Bacteria are microscopic organisms that are found almost everywhere in the environment and associated with other organisms as either individuals or aggregations. Most bacteria consist of a single, circular DNA chromosome in the cytoplasm, due to the fact that they do not have a nucleus. The outer surfaces of bacteria are regarded as the most complex region of the cell. The cell envelope is a useful structure for protecting bacteria from the environment, but at the same time it is a target of many antibiotic drugs. As well as providing a bacterial cell with its integrity and protection, the cell envelope is utilised by bacteria to assemble a number of important bacterial appendages or structures. For example, many bacterial species may secrete a polysaccharide capsule onto their outer surface producing an extra layer of protection. Some species even generate a protein coat in the form of S-layers. The cell envelope is also the site used by bacteria to assemble the bacterial flagellum, fimbriae or pili, and virulence associated protein secretion machines. All of these appendages or structures are important for adhering to surfaces within their chosen habitat and interacting with other bacterial cells, species or the cells of higher organisms such as us. The utilisation of the cell envelope in this manner also comes at a cost as the presence of appendages such as the flagellum are monitored by hosts as a means to detect bacteria that are colonising sites that the host wishes to maintain sterile.

1.2 The *Salmonella* species

Salmonella enterica is a motile gram-negative facultative aerobe. The genus *Salmonella* contains only 2 bacterial species, i.e., *Salmonella enterica* and *Salmonella bongori*. These 2 species are identical between 95% and 99% at the DNA level. *S. enterica* can be classified into seven phylogenic subspecies, i.e., 1, 2, 3a, 3b, 4, 5, 6, and 7 (Lahiri *et al.*, 2010). *S. enterica* subspecies 1 contains more than 2,000 serological varieties (serovars), which include the pathogenic variants of *Salmonella*. All serovars resulting from serogrouping of *Salmonella* species that have

been assigned show different patterns of pathogenesis. They usually have the ability to infect multiple hosts except the serovar Typhi, which possesses a narrow host range strictly limited to humans.

The best-described pathogenic serovars are *Salmonella enterica* serovar Typhimurium and Typhi. *S. enterica* serovar Typhi is the most virulent strain that can cause death. Infections of *S. Typhi* regularly become systemic, allowing *S. Typhi* to infect the major organs of the host resulting in organ failure and often death if untreated. *S. Typhimurium* is one of the most prevalent serovars that causes foodborne gastroenteritis in humans. An infection of *S. Typhimurium* is self-limited to the gastrointestinal tract and results in diarrhoea, abdominal cramps, vomiting and nausea, which generally lasts up to 7 days. *S. Typhimurium* can also colonize important livestock including cattle, pigs and chicken. In many cases such colonization is asymptomatic meaning that livestock must be monitored on a regular basis for Salmonellosis to prevent unwanted contamination of meat products or eggs that will enter our food chain. The loss of commercial animals due to Salmonellosis is a major concern despite effective vaccination schemes.

1.2.1 *Salmonella* as pathogen

Salmonellae are frequently found in raw foods or contaminated food products. This is a result of the broad host range the majority of *S. enterica* serovars exhibit. *S. enterica* has been described to colonise many mammals including poultry, cattle, birds as well as reptiles, fish, amphibians and insects. Lettuce, a common commercial plant, is known to be susceptible to contamination with *S. Typhimurium* (Islam *et al.*, 2004). As a result, the growing importance of contaminated lettuce is becoming a global concern.

Infected people can also transfer *S. enterica* by handling foods with unwashed hands and through uncontrolled personal hygiene. Heat can kill *S. enterica* effectively and is a common way of reducing infection, one reason why the increase in Lettuce contamination is becoming a major issue due to it being a raw salad product. When infecting / colonising Animal hosts the intestinal tract is the preferred living site of *S. enterica*. However, *S. enterica* serovars can disseminate from the intestine to cause

systemic disease. One example is *S. Typhimurium* itself as in humans and cattle the infection is self-limited to the intestine while in mice the infection becomes systemic (hence its name Typhi – murium (mouse)). In certain sub groups of the human population *S. Typhimurium* can also escape the intestine and become systemic. This is often seen in the elderly or immunocompromised. Shedding of *S. enterica* via the faecal route into the environment is also known to lead to infection in others. A common household problem is infection through low hygiene standards.

1.2.2 *Salmonella* infection

Salmonellae are the common cause of enteric (typhoid) fever and gastroenteritis. In general, All *S. enterica* infections begin through entry in to the human body through oral ingestion and then achieve systemic infections by passing through intestinal epithelial cells. *S. enterica* will travel through the lymphatic system and enter the bloodstream, where the systemic infection of the liver, spleen and bone marrow occur. It is the colonisation of these major organs and the movement of *S. Typhi* through the bloodstream that leads to enteric (typhoid) fever. In the case of the localized infection, *S. enterica* colonize the intestines and invade the intestinal mucosa. This is an important aspect of all *S. enterica* infections. Unlike pathogenic *Escherichia coli* that will prevent host cell invasion or uptake, *S. enterica* exploits the hosts own mechanisms of phagocytosis to colonise. However, *S. enterica* also posses the ability to invade epithelial cells directly. The major cells types that do become infected are Enterocytes and M cells. The result being in the extrusion of infected epithelial cells into the intestinal lumen (**Figure 1**). Consequently, villi blunting and loss of absorptive surface arises. This in turn induces a pro-inflammatory response and the influx of polymorphonuclear leukocytes (PMN) into the infected mucosa. The resultant diarrhoea and associated symptoms is not a direct consequence of *S. enterica* releasing a toxin but the hosts own reaction to the PMN influx.

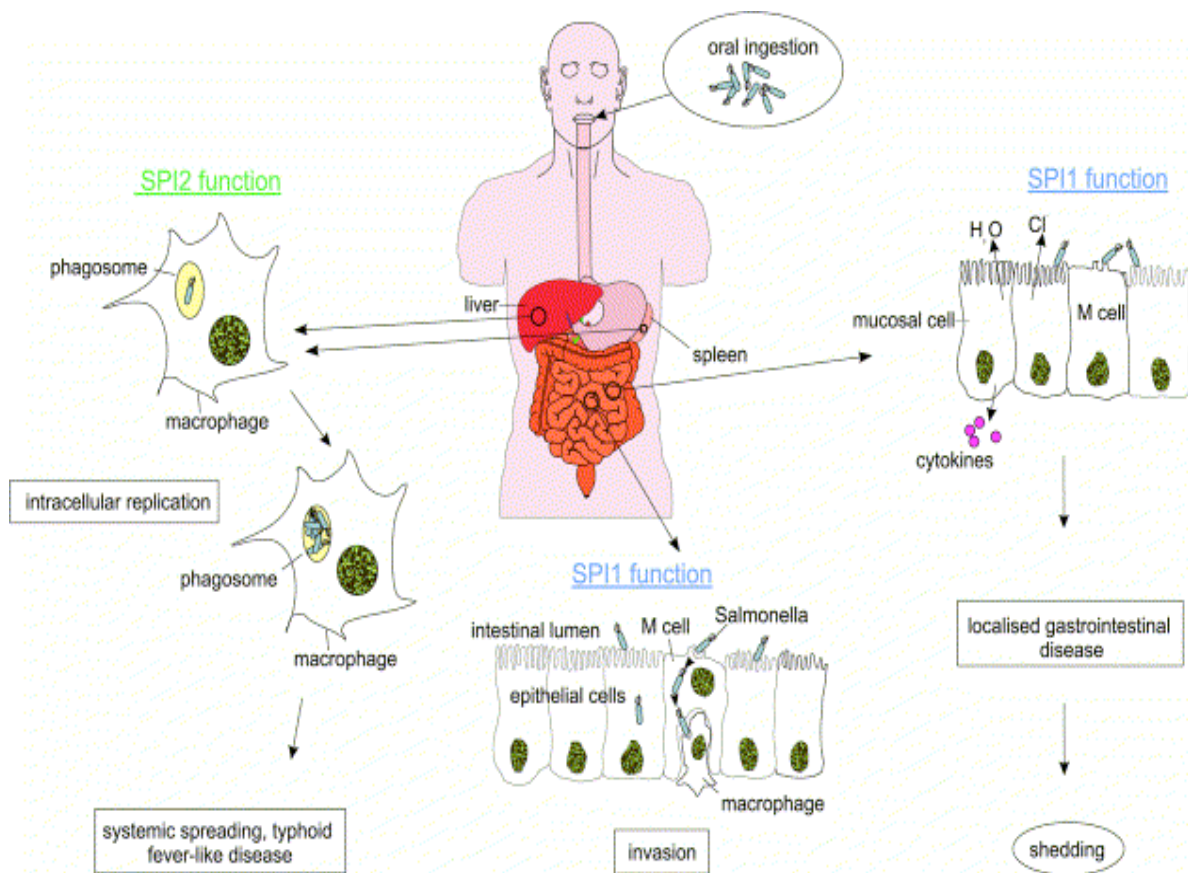


Figure 1: Infections caused by *S. Typhimurium* requiring the *Salmonella* pathogenicity islands 1 and 2 (SPI1 and SPI2)

SPI1 assists the first stage of *S. enterica* infections or salmonellosis including its penetration to the gastrointestinal epithelium, which results in the diarrhoeal symptoms due to localized gastrointestinal infections. SPI2 function is needed for further infection especially the systemic spread and the colonization of host organs. SPI2 provides the pathogen the chance of its survival and also replication in host phagocytes (**Taken from Hansen-Wester & Hensel et al., 2001**).

1.3 Motility

The bacterial flagellum is a self-assembled nanomachine. Its general structure contains three subsections; a cell envelope embedded basal body, a flexible hook and a long whip like filament. The filament can be up to 5 times the length of a bacterial cell and is comprised of the structural subunit flagellin. The ability of flagella to contribute to the invasiveness of *Salmonella* is not as clear as the role of SPI1 and SPI2. Flagellin monomers have been reported to significantly induce innate immunity, and are able to induce inflammation in the intestinal epithelium while inhibiting apoptosis. Evidence has been presented to suggest the ability to express one of two flagellins can influence systemic infections of *S. Typhimurium* in a mouse model. Other evidence suggests that flagellar gene expression is down regulated inside the host, although it has been suggested that they may be induced inside macrophages and used for escaping this cell type. Flagella are therefore not considered to be a strict pathogenicity factor of *S. enterica*. However their role in recognition by both arms of the immune system does mean their assembly and function during pathogenicity cannot be overlooked. However, the ability of the bacterial cell to coordinate flagellar assembly and flagellar gene regulation provides a superb model for the study of the regulation of gene expression.

In general, flagellar-mediated motility is considered to be an advantageous weapon of many bacteria allowing them to survive under a wide variety of environmental conditions. The main role of motility is to allow bacterial cells or populations to move towards favourable conditions or to avoid harmful environments. This movement relies on the driving force of a powerful motor attached to the flagellar filament. Flagellar-mediated motility can drive movement through liquids and over surfaces. The movement over surfaces that utilises the flagellar is known as swarming. It is a form of multicellular migration, where bacterial cells become elongated and hyper flagellated, these cells can then form multicellular rafts alike to a cooperative structure in search of nutrients as a population. An alternative mode of motility includes “gliding” motility, which is usually observed as bacteria travel in low water content environments and is flagellar independent. An important difference between flagellar-mediated swarming and gliding motility is the speed of travel. Flagellar-mediated swarming is approximately ten times faster than gliding motility.

Flagellated bacterial “swimming” has been described as the translation through a homogeneous liquid environment without the requirement of exerting thrust against another object. Speeds of swimming bacteria range from 20 to 60 $\mu\text{m}\cdot\text{s}^{-1}$. This is a fascinating phenomenon as these observed speeds are up to 30 body lengths per second (Macnab, 1984). It has been shown that flagella placement can dictate the efficacy of motility, especially in viscous conditions (Atsumi, 1996). Laterally placed flagella form a bundle that generates the necessary thrust while a single polar flagellum can also suffice. The number of flagella, their placement and the torque generated all contribute to bacterial motility. Flagella can be arranged on the cell body in different ways. The simplest arrangement is a single flagellum at one pole of the cell, while multiple flagella may be arranged tightly at the polar region in a cluster (lopotrichious) or they may be distributed randomly around the cell surface (peritrichious). Peritrichious flagella are characteristics of several commonly studied species including *E. coli*, *Bacillus subtilis*, and *S. enterica* (**Figure 2**).

1.3.1. The rotational motion of the flagellum

The force that drives bacterial swimming is the rotational movement of the flagellum. Rotation generates the movement forward through thrust, which in turn is dependent on the torque generated through the helical geometry of the flagellar filament. Rotation of the bacterial flagellum in the majority of bacterial species is via the proton motive force via the action of motor force generators associated with the base of the flagellum. The motor force generators are a complex of two proteins MotA and MotB. Rotation is proposed to occur via electrostatic forces that are maintained through energy obtained from the movement protons across the inner membrane through the MotAB complexes.

The manner of the rotation of flagella can dictate whether a cell runs (straight directional movement) or tumbles (chaotic directional movement). Tumbles are defined by a short time enabling cells to alter direction (Berg & Brown, 1972). These two types of movements can be altered in a matter of milliseconds. *E. coli* and *S. enterica* utilise the chemotaxis pathway to dictate a change in the direction of rotation of flagella from counter-clockwise (CCW), which creates running pattern, to clockwise (CW) that creates tumbling pattern that ending with changing back to CCW (Turner *et al.*, 2000, Macnab, 1977, Larsen *et al.*, 1974). In contrast, *B. subtilis* switches from CW to CCW in response to chemotactic signals (Rao *et al.*, 2004)

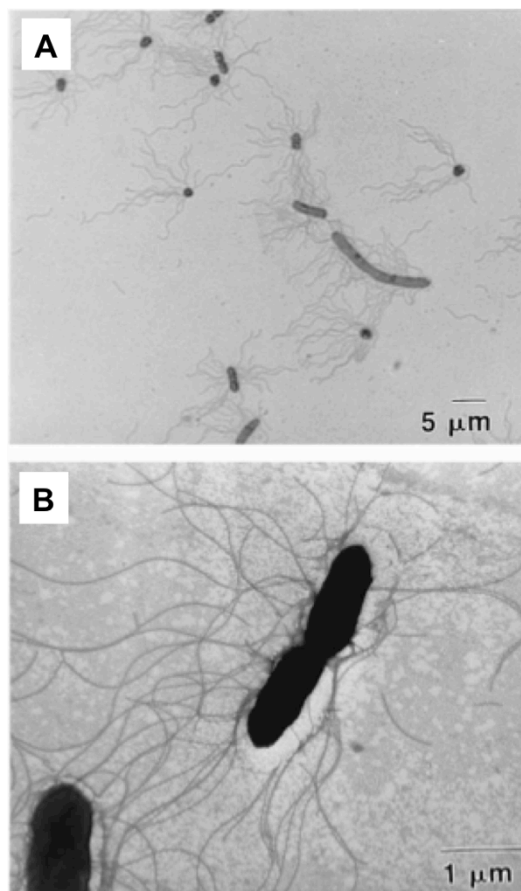


Figure 2: Photomicrographs of *Salmonella enteridis* show the peritrichous arrangement of flagella.

Light (with oil immersion) **(A)** and electron **(B)** micrographs showing the apparent random arrangement of flagella throughout the cell body of *Salmonella enteridis* after 6hrs growth. **(Taken from Holt & Chaubal *et al.*, 1997).**

1.3.2. Filament configurations and their impact on motility

The thrust generated by a flagellum depends entirely on the inter-conversion of geometrical symmetry within the filament. A typical filament of *S. enterica* consists of approximately 20,000 molecules of a single protein species, flagellin (FliC). New monomers of flagellin are passed through a thin channel and are incorporated in the growing flagellar filament at the distal end. The packing of flagellins into the filament generates 11 proto-filaments that can exist in two types: L (left)-type and R (right)-type (**Figure 3**) (Kamiya *et al.*, 1979). L or R-type describes the different handedness of the filament. R or L -type proto-filaments can exist together in a filament and dictate the degree of helical pitch within the filament. A straight filament, for example, contains only L- or R-type protofilaments. Structurally, R-type filaments are 1.7% shorter than the L-type (Yamashita *et al.*, 1998). Different combinations of both types create four distinct waveforms of flagellar filaments (**Figure 4**). The normal configuration of the filament of flagella is left-handed while the semi-coiled and curly filaments are right-handed configuration. The conversion among these forms is driven by environmental changes such as pH or mechanical twist through changes in rotation dictated by the chemotactic response.

The change from running to tumbling movement underlined by the flagellation pattern is capable of creating the random exploration of three-dimensional space around the bacterial cell. Turner and colleagues revealed that one flagellum was sufficient to drive directional change or to alter its properties to achieve tumbles (**Figure 5**) (Turner *et al.*, 2000). During an *E. coli* or *S. enterica* “run” all filaments rotate in a CCW direction allowing them to form a tight bundle. A change in the rotational direction of even just one flagellum to CW in the bundle leads to a sequence of changes in the “handedness” and pitch of that filament. The result of such a change is that the filament in question will be released from the bundle and is sufficient to generate the associated tumbling event. The important feature of these directional changes is the modulation by sensory information from the environment coordinated by the chemotaxis system.

1.4 Chemotaxis

Bacteria exhibit a phenomenon called chemotaxis in which bacteria can detect and respond to various chemicals by changing their motility pattern toward attractants or away from repellents. They are equipped with sensory devices, chemoreceptors, which are able to sense environmental benefits or hostility. Sensory cues are chemicals, which are often nutrients or related compounds, and other factors such as pH, temperature, viscosity, osmolarity, oxygen availability and light.

1.4.1 Chemotactic response control bacterial movement

The motility directed by chemotaxis is a means by which many commensal or pathogenic species colonize and invade a specific target site within a host. Bacteria tend to organize themselves in some situations into complex polysaccharide containing biofilms to protect themselves from antimicrobial agents as seen in fouling teeth and medical implants. Intercommunication between bacteria-host and predator also exists with specific chemicals triggering a chemotaxis response, for example the aggregation of rhizobia to legume root hairs (Wadhams & Armitage, 2004).

An increase in the attractant concentration, e.g., nutrients or decrease in the repellent concentration, e.g., fatty acids, can be detected and assimilated into a bacterial response by decreasing or increasing tumbling frequencies to allow directional swimming for longer periods of time (Segall *et al.*, 1986). The striking feature of the bacterial chemotactic response is the high sensitivity of bacterial sensing apparatus. The very sensitive response is regarded as only a few molecules binding to a receptor on the cell surface. This can significantly change the working pattern of the flagellar motors. It is interesting to note that bacteria have a capability to learn and to memorize a given stimulus based on the record of that particular cell, and thus, individual cells respond differently to the same stimuli according to their different experiences.

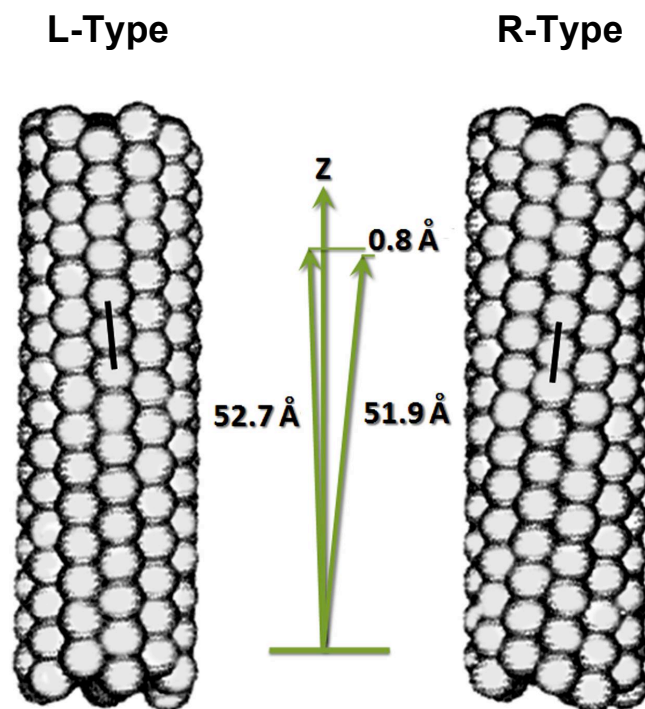


Figure 3: Two types of the configuration of flagella (L- and R-type straight filaments of flagella)

Flagellin subunits form a proto-filament with the variation of direction creating different handedness of the filament twist. This manifests itself in two configurations of filament, the R-type configuration (bending to the right), and the L-type (bending to the left). (Modified from Berg, Howard C. 2003, *E. coli in motion* p. 42, Springer-Verlag, New York,).

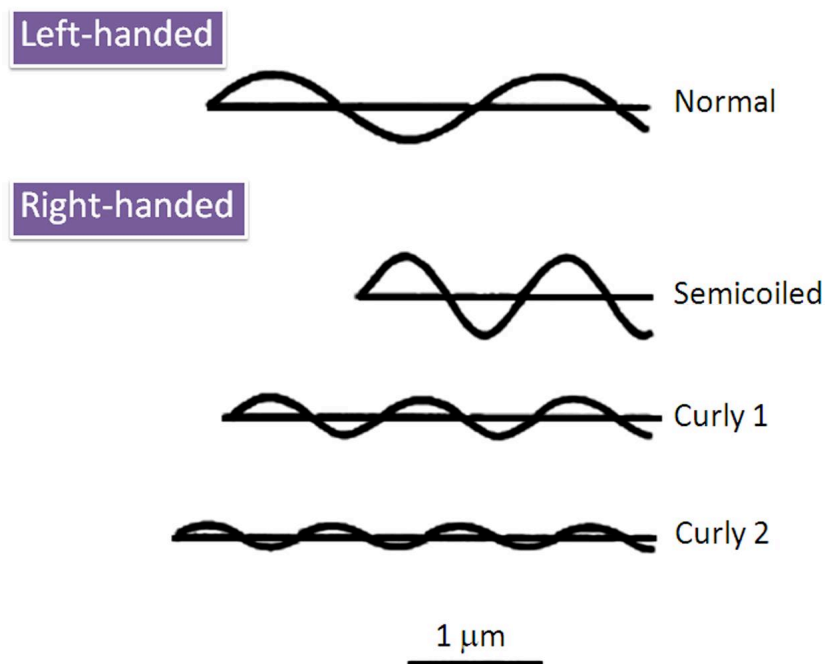


Figure 4: Schematic diagrams show drawing of the possible flagellar waveforms for bacterial movement.

The normal configuration of filament during bacterial movement is left-handed while others, needed to change movement pattern, appear to be dominated by the right-handed configuration. In spite of the equal contour length of all filaments, each configuration possesses different lengths while continuing its waveforms. It is noted that each filament possesses different combinations of L and R-type of proto-filaments, giving different configurations of flagellar filament. **(Modified from Berg, Howard C. 2003, *E. coli* in motion p. 41, Springer-Verlag, New York,).**

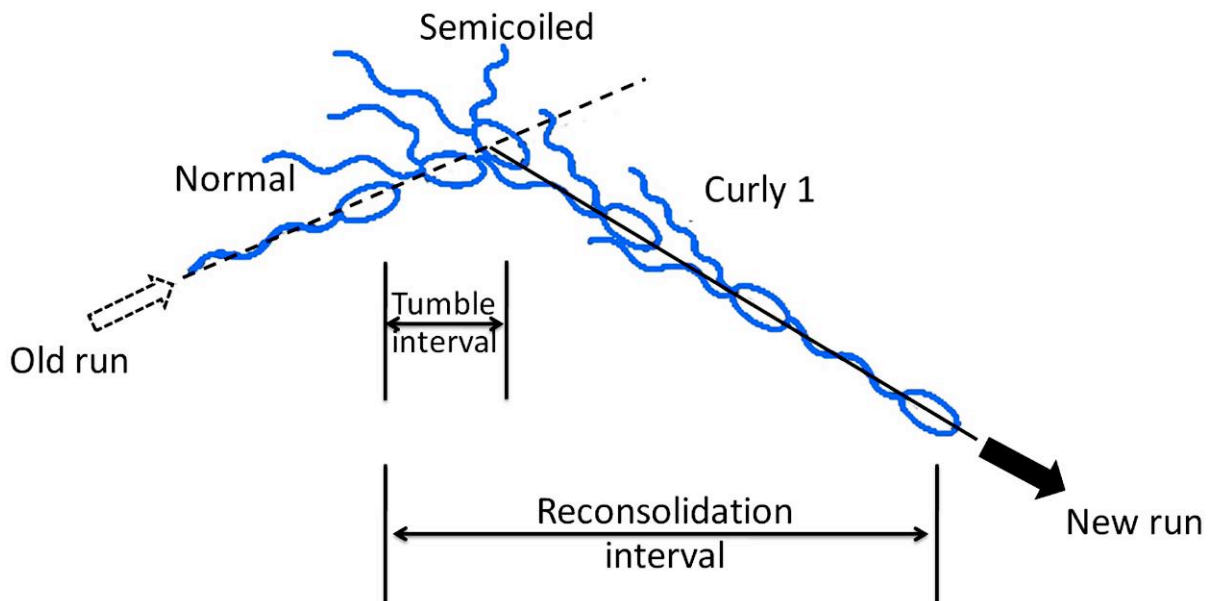


Figure 5: A schematic diagram showing how *E.coli* can utilise changes in waveform during tumbling motion to alter flagellar rotation, and ultimately swimming direction.

A cell with a bundle of two flagellar filaments is swimming and about to change its direction to the right. One filament undergoes a normal to semicoiled transformation due to a motor modification, changing its rotational direction. This change is defined as a tumble interval. As the cell starts its movement along a new track, the filament undergoes a semicoiled to a curly 1 configuration, and finally back to a normal configuration enabling a new run. The two flagellar filaments rejoin the bundle and the cell resumes at its initial speed. (Modified from Berg, Howard C. 2003, *E. coli* in motion p. 45, Springer-Verlag, New York,).

1.4.2 Chemotactic sensing

The components of the intracellular signal transduction machinery that dictate flagellar rotation were defined through the isolation of different *che* (chemotaxis) mutants. The level of genetic and biochemical data available on the chemotaxis pathway has allowed for the reconstitution of the *E. coli che* system *in silico*.

Chemoreceptors recognize or sense the chemicals via direct contact. The chemoreceptors contain domains that recognize the chemicals referred as the recognition domain. These chemoreceptors are often membrane bound proteins with the recognition domain exposed to the periplasm in Gram-negative bacteria such as *S. enterica*. *E. coli* chemoreceptors and Che proteins tend to be placed together in tight clusters at one or both poles of the cell. Thousands of receptors cluster at these polar assemblies (Maddock & Shapiro, 1993). It was shown in recent cryo-electron tomography research that the organization of *E. coli* chemoreceptor arrays needed the interaction of CheA and CheW, chemotaxis components, to form functional chemoreceptor arrays (Zhang *et al.*, 2007). **(Figure 6)**

1.4.3 Signal transduction: two-component system (TCS)

Two-component systems (TCS) are a key method by which bacteria sense the chemical world. TCS are composed of a sensor kinase and response regulator. The sensor kinase detects environmental signals and the response regulator, in most cases, regulates gene expression in response to the signals. A process of phosphoryl group transfer to a protein receiver domain controlled by the histidine protein kinase (HPK) directs the response or message to the response regulator. The wide range of response regulator access specific sites on DNA to regulate transcription and affects many processes including the modulation of the flagellar motor activity (Stock *et al.*, 2002).

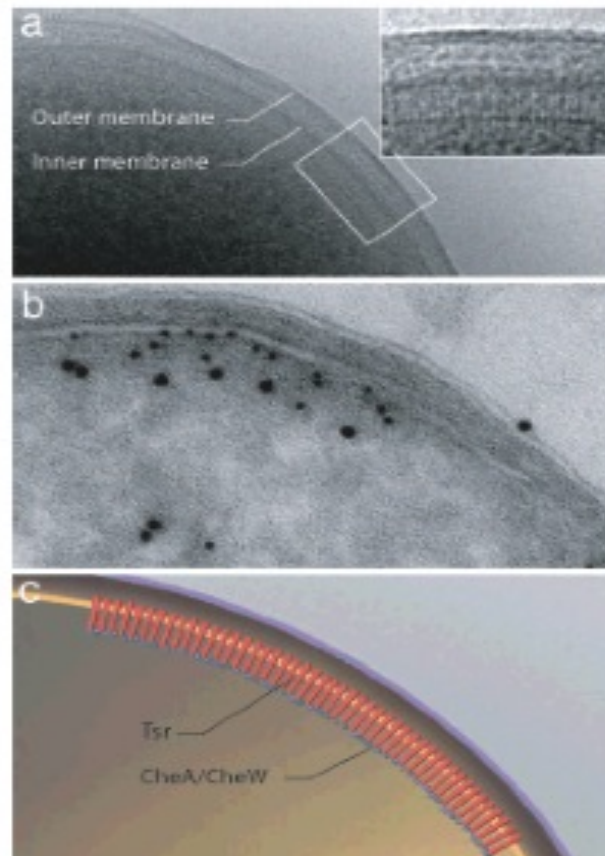


Figure 6: The morphological structure of chemoreceptor arrays

(A) A perspective cryo-projection image of the chemoreceptor array arranged in the polar region in a wild-type *E. coli* cell, shown in more detail in (B) and (C). (B) an immunolabelled image of a section from the same culture showing the membrane labelled with anti-Tsr (small black dot) and anti-CheA (large black dot) antisera. (C) an illustrated picture showing the assembly and orientation of the chemotaxis array in the polar region of wild-type *E. coli* cells, reconstructed from (A) and (B). (Taken from Zhang *et al.*, 2007)

Motile bacteria employ a two-component signal transduction system to drive chemotaxis (Stock *et al.*, 2002). Receptor-signalling complexes, containing the chemoreceptors, promote CheA autophosphorylation after being stimulated. The phosphorylation of CheA then leads to the phosphorylation of the chemotaxis response regulator, CheY generating CheY-phosphate (CheY-P). CheY-P rapidly diffuses to flagellar motors and interacts with a complex of 3 flagellar proteins associated with the base of each flagellum known collectively as the C-ring (**Figure 7**) (Sourjik & Berg, 2002, Elowitz *et al.*, 1999, Sanna *et al.*, 1995). CheY-P behaves as an allosteric regulator to promote motor switching from CCW to CW rotation and to increase tumbling movement (Alon *et al.*, 1999). The CheY-P concentration present in the swimming bacterial cells is the primary output of the chemotaxis system. The presence of the CheY-P is modulated in response to the gradient of attractant or repellent chemicals. Attractant stimuli suppress tumbles after interacting with chemoreceptors by inhibiting CheA kinase activity followed by decreasing in CheY-P concentration (Blair, 1995).

Three soluble chemotaxis components, i.e., CheZ, CheR, and CheB, also regulate CheY-P concentration. CheZ is a protein phosphatase associating with the receptor-signalling complex and enhancing the rate of CheY-P dephosphorylation (Stock *et al.*, 1987, Wang & Matsumura, 1996). The activities of CheR and CheB are to control the receptor-signalling complex via chemoreceptor methylation (CheB) and amidation (CheR) levels that are important for response adaptation (Levit *et al.*, 2002, Sourjik & Berg, 2002). The CheR and CheB modifications allow bacteria to memorize their behavioural responses. As a result, two cells never possess exactly the same complement of receptor sensitivities in a given population.

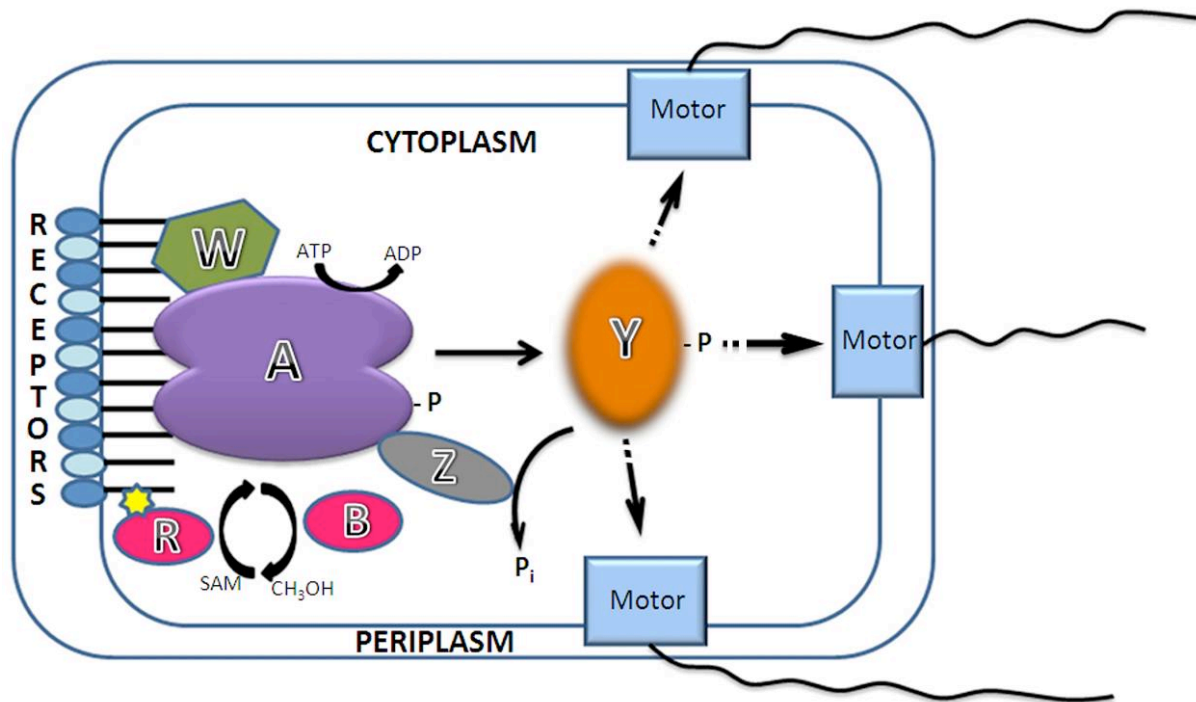


Figure 7: Illustration of the *E. coli* chemotaxis system modifying flagellar activity.

Environmental cues are received by a group of well-organized chemoreceptors at the cell pole. Receptor-signalling complexes, a group of chemoreceptors, CheW and CheA, control the transfer of phosphoryl groups from ATP to CheY by the autophosphorylation of CheA. Phosphorylated CheY is capable of interacting with flagellar motors to modify their activity in response to the environmental signal. The functional phosphorylated CheY is deactivated by the dephosphorylation from CheZ. Abbreviation: W, CheW; A, CheA; P, phosphoryl group; Z, CheZ; P_i, inorganic phosphate; R, CheR; B, CheB; SAM, S-adenosylmethionine; CH₃OH, Methanol. **(Modified from Baker *et al.*, 2005)**

1.5 Flagella structure

1.5.1. Flagella architecture - general principles

The flagellum structure extends from the cytoplasm to the outside of the bacterial cell with the majority of its structure exposed to the external environment (**Figure 8**). Its structure can be divided into three main parts: a basal body, a universal joint known as the hook, and a long whip-like propeller called the flagellar filament. Each part is composed of a well-organized group of proteins (**Figure 8**). The flagellum can be defined as a self-assembling nanomachine. Once its foundation has been laid in the inner membrane, all other components assemble with the guidance of several regulators of assembly. These regulators are involved in the efficiency of assembly rather than assembly itself.

1.5.1.1 The Hook Basal Body (HBB) or “engine”

Embedded in the inner membrane, the basal body has an integral membrane ring called the MS ring (Blair, 2006). The MS-ring acts as a foundation for flagellar assembly and the mounting plate for the rotor/switch C-ring complex. A type 3 secretion apparatus assembles at the centre of the MS-ring to direct secretion through a central channel. Approximately 26 copies of the protein FliF form the MS ring, producing a channel opening of 10 nm in diameter (Katayama *et al.*, 1996).

A rod acting as the drive shaft of the HBB is assembled onto the MS-ring in the periplasm of Gram-negative bacteria. Its structure is classified by proximal and distal subunits with respect to the MS ring. The distal rod, near the outer membrane, is composed of FlgG, the proximal rod, near the cytoplasmic membrane, contains FlgB, FlgC and FlgF (Homma *et al.*, 1990). Another rod-associated protein, FliE, is necessary for efficient subunit secretion (Lee & Hughes, 2006). FliL might also serve to stabilize the connection between proximal and distal rod as flagella lacking of FliL increasingly break at the proximal-distal rod junction on swarm agar (Attmannspacher *et al.*, 2008).

A rod cap protein, FlgJ, which has muramidase activity, controls rod assembly. This enables the growing structure to penetrate the peptidoglycan layer (Nambu *et al.*, 1999). The periplasmic P-ring FlgI and the outer membrane L-ring lipoprotein, FlgH, are perceived as bushing that holds the rod in place (Homma, 1986, Jones & Macnab, 1990). FlgI and FlgH are the only structural components, which are not secreted by the flagellar specific T3S system. Instead, their secretion is sec-dependent. At least FlgI exists as a monomer at risk of proteolysis until assembled when in the periplasm. However it can be protected by the periplasmic chaperone, FlgA (Nambu, 2000).

The C-ring is composed of FliG, FliM and FliN proteins attached to the cytoplasmic face of the MS ring. They serve as the rotor responsible for torque generation together with the Mot proteins that drive flagellar rotation. FliG, FliM, and FliN also play a key role in flagellar protein secretion (Kihara *et al.*, 2000, Kubori *et al.*, 1997). FliN is known to interact with the secretion substrate ATPase-complex protein FliH (Paul *et al.*, 2006). FliG, FliM and FliN form morphologically as a cytoplasmic cup, postulated to “catch” substrates (Erhardt and Hughes, 2010a). Recent research also suggests the C-ring plays a key role in allowing the T3S apparatus to assemble and substrate docking (Erhardt and Hughes, 2010b).

1.5.1.2 Hooks, Caps and Junctions

The flagellar hook structure is cylindrical like the shape of the rod and filament. Structural insights in to the flagellar architecture have shown that all three parts share a similar pattern of construction and subunit packing. The result is that the central channel formed in the flagellum is structurally conserved from the proximal rod up to the flagellar filament tip. The hook consists of approximately 120 copies of FlgE (Samatey *et al.*, 2004). The unique feature of the hook is its flexibility. Its flexibility in all flagellar systems generates the necessary “give” to rotate the filament and to allow for a change in rotational direction due to chemotaxis. In multi-flagellated bacteria the flexibility of the hook also enables the flagellar filaments to form a bundle from different positions on the cell. Hooks of many bacterial species have an optimal length of 55 nm on average. Hook length is controlled by the secretion apparatus proteins, FlhB and FlhA and the hook length determinant FliK, (Hirano *et al.*, 1994).

To assemble the hook a second cap protein is utilised, FlgD. Interestingly in the majority of flagellar systems three cap proteins exist, a rod cap FlgJ, a hook cap, FlgD and a filament cap FliD. After rod completion, FlgJ is replaced by FlgD allowing for hook assembly to begin.. Conversely on completion of the Hook FlgD is then replaced with FliD to allow for filament assembly. All three caps are not thought to drive subunit incorporation but play more of a guiding role to show the next subunit where to enter the growing flagellar structure.

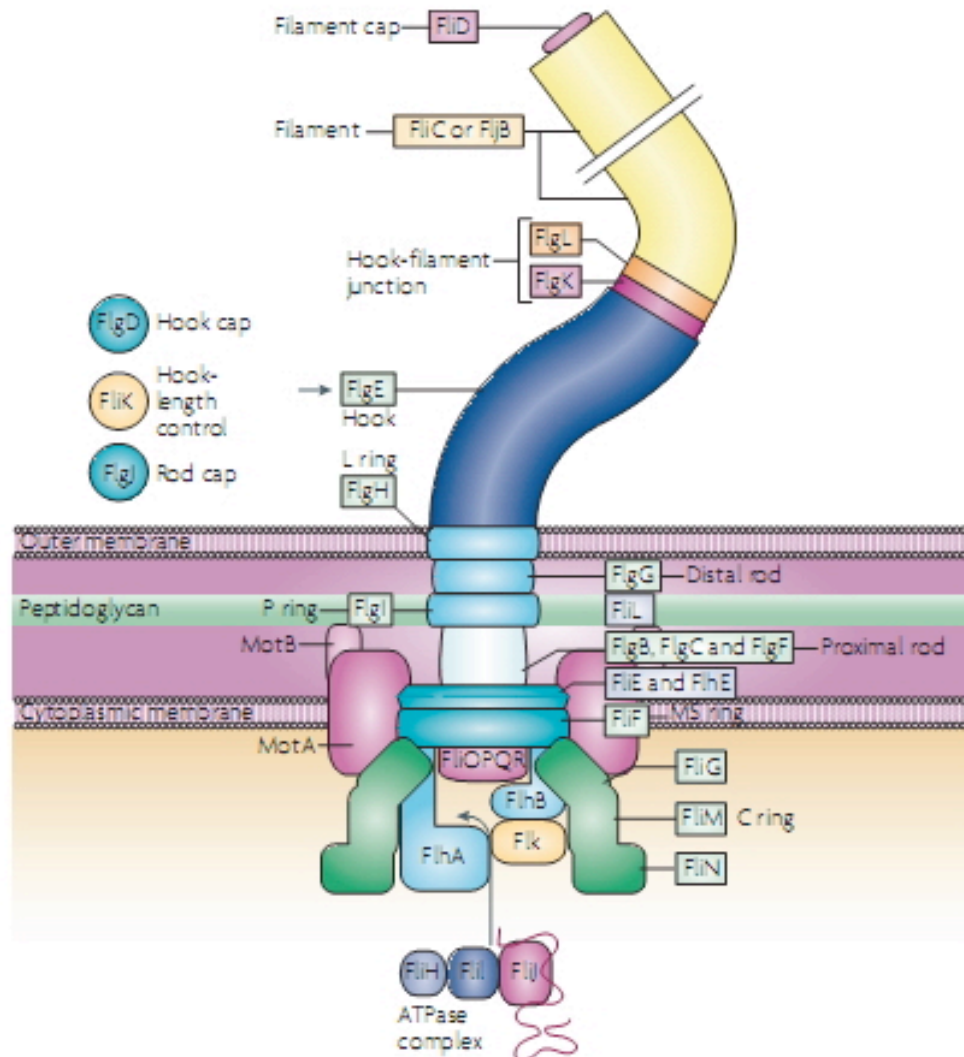


Figure 8: Flagellar components of *Salmonella enteric* serovar typhimurium

The figure shows the structure of the bacterial flagellum embedded in its membrane. Each component is clearly labelled with a name of assembled proteins and/or its common name. The main structural parts consist of a basal body (embedded in the membrane), the hook junction (small flexible part protruding from the basal body) and the flagellar propeller or the extending long filament. In addition, the structure of flagellar type 3-secretion is included in this picture with the assistance of soluble cytoplasmic components, FliH-FliL-FliJ of the ATPase complex. (Taken from Chevance & Hughes, 2008)

After the hook obtains its mature length, the hook cap is replaced by three successive proteins that includes FliD, FlgK and FlgL. These three proteins function as a structural adaptor between the universal joint and the propeller / filament. The first hook-filament junction protein is FlgK on to which the second hook-filament junction protein FlgL assembles. It is on to FlgL that FliD assembles however exactly when FliD replaces FlgD is still not clear, whether it is after FlgL or before FlgK (Homma & Iino, 1985, Homma *et al.*, 1986, Ikeda, 1985, Ikeda *et al.*, 1987) (**Figure 8**). Stoichiometric analysis of junction proteins suggested that 11 FlgK, 11 FlgL (Samatey *et al.*, 2004) and 5 FliD, are assembled to form the hook-filament junction (Imada *et al.*, 1998).

1.5.1.3 The flagellar propeller

The flagella filament is a hollow, long, thin cylindrical structure and helical shape with 20 nm in thickness and a maximum of 10-15 µm in length (Macnab, 1977; Macnab, 2003). Based on the packing of the FliC of *Salmonella* into a filament, it is estimated that an average filament consists of up to 20,000 flagellin subunits (Auvray *et al.*, 2008). Two flagellins, FliC and FljB, are utilised by the majority of *S. enterica* serovars to form a filament. However, only one flagellin is ever utilized due to phase variation (Pearce and Stocker, 1967; Aldridge *et al.*, 2006b). The use of multiple flagellins is a common theme across approximately 45% of all known flagellar systems. Many of these systems utilise all flagellins encoded by their genomes while *S. enterica* is rare in the way it exploits phase variation to use FliC and FljB. *E. coli* is also able to undergo a type of phase variation, however, in this case it is not reversible like that of *S. enterica*. *E. coli* can acquire different *fliC* genes and by an undefined mechanism switch flagellins.

The filament has no direct length-control mechanism, which is not similar to the assembly of the hook. As a result, a broad range of filament length exists and might be important for good motility. Assembly of the filament is achieved via the self-assembly of flagellin into the tip of the filament under its cap protein, FliD (Maki *et al.*, 1998). When the filaments are broken, the ability of re-growing filaments was observed with the continuous export of capping protein (Homma & Iino, 1985). FliD

(see later) generates a gap at the tip of the filament promoting efficient insertion of flagellin into the filament.

1.6 Type 3 secretion

1.6.1 General principles

Type 3 secretion (T3S) systems are prevalently used by many bacterial species to secrete virulence factors and structural components of the flagellum.

The virulent T3SS are structurally related to the flagellum. Both structures have an inner membrane anchor and rod spanning the periplasmic space (Yip & Strynadka, 2006) (**Figure 9**). A key feature of all T3SS is that the substrates are not processed during secretion and they are transported directly from the cytoplasm to the external environment. The N-terminus of all secreted proteins is necessary for secretion. The N-termini of T3S substrates do not exhibit any direct similarity. However, they do possess a number of common features such as the presence of disordered structure and an increase in amphipathic amino acids (Aizawa *et al.*, 1990, Daughdrill *et al.*, 1997).

T3S substrates are required to be either partially folded or unfolded monomers in order to be secreted through the small central channel of the flagellum and virulent T3SS. Secretion efficiency is promoted by a group of secretion chaperones. The T3S chaperones are responsible for bringing the substrates to the secretion apparatus with their exposed signal but also preventing premature degradation prior to secretion and coupling gene expression to the secretion process.

1.6.2 The flagellar T3S apparatus

According to the purpose of this study, the following description of the T3S apparatus will focus on the flagellar system. Nine proteins: FliH, FliI, FliJ, FlhA, FlhB, FliO, FliP, FliQ, and FliR, are defined as the flagellar export apparatus (Minamino & Macnab, 2000). All except the soluble cytosolic FliI, FliH, and FliJ proteins, are integral membrane proteins forming a proton driven export gate within a central pore in the MS-ring (Minamino *et al.*, 2008a). The proposed structure formed by FlhA,

FliH, FliO, FliP, FliQ, and FliR facilitates the preparation and translocation of T3S substrates into the central channel. The soluble components FliH, FliI and FliJ facilitate the delivery of substrates to the export gate (Minamino *et al.*, 2008b) (**Figure 9**).

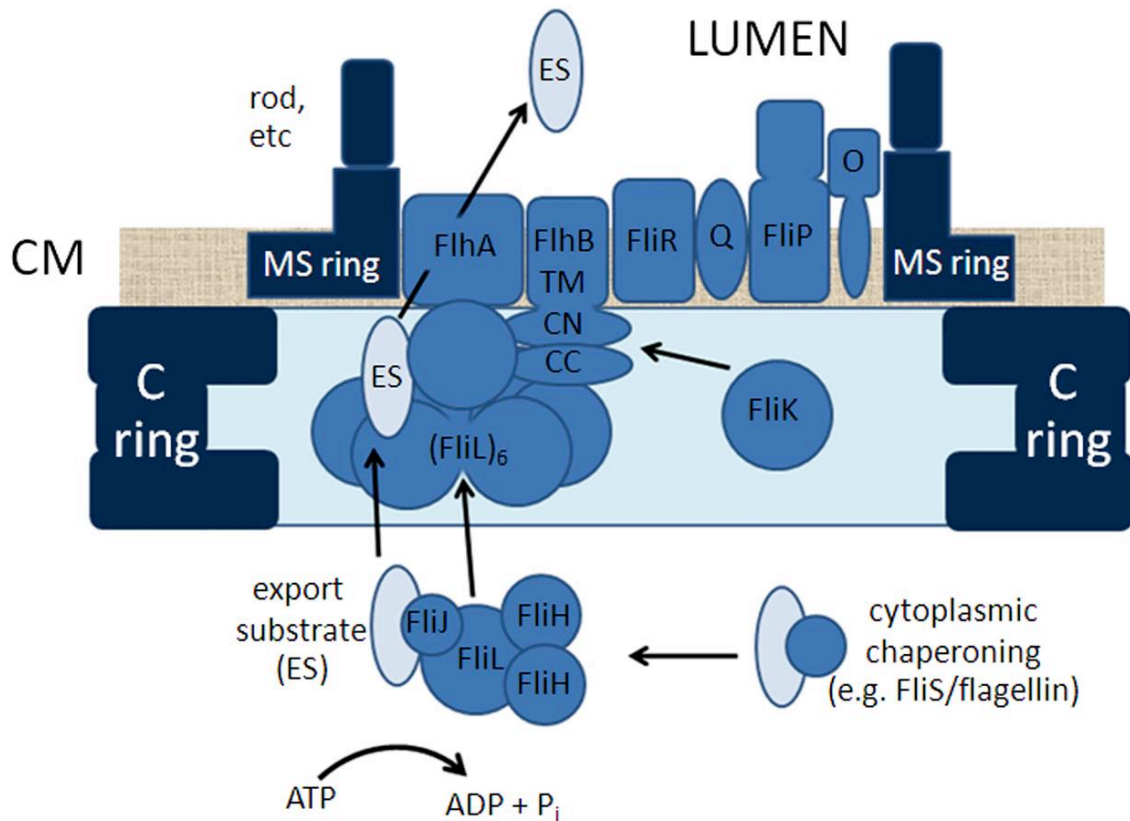


Figure 9: Illustration of the flagellar T3S apparatus

Components grouped within the frame of the MS and C ring embedded in the bacterial membrane, and the complex of soluble proteins (the FliH/I/J complex). The export substrate (ES, pale blue) is thought to be protected from degradation within the cell by cytoplasmic chaperones. The route of the secretion possibly begins with the transfer of substrates to the FliH/I/J complex upon delivery to FliA by rearrangement of the FliH/I/J complex (possibly to a hexameric form of FliI)₆. The cytoplasmic region of FliB undergoes spontaneous cleavage to form CN and CC domains which are necessary for substrate specificity within the export apparatus with the cooperation of FliK, which is exported too. The substrates of both unfolded terminals subsequent to translocation are placed in the lumen and diffuse to their assembly target at the distal end. (**Modified from Macnab, 2004**)

1.6.2.1 T3S energy provision

FliI shows structural similarities to ATPase and therefore is classified as an ATPase (Fan & Macnab, 1996). Based on this observation it has been assumed that ATP hydrolysis drives T3S secretion. FliI retains its full ATPase activity when it assembles into a homohexamer ring *in vitro*. The hexameric ring is also able to interact with the export gate (Claret *et al.*, 2003).

FliH reduces the ATPase activity of FliI by inhibiting the formation of a hexameric ring structure by forming a FliH₂-FliI complex (Minamino & Macnab, 2000). FliH₂-FliI complexes can also interact with the third component FliJ. The FliHIJ complex can dynamically interact with the large cytoplasmic C-terminal domains of FliA and FliB (FliA_c and FliB_c) (Thomas *et al.*, 2004), reflecting a pattern of substrate recruitment and translocation.

The ATPase activity of the FliI complex is not essential for protein export but it helps increasing the efficiency of the secretion process. One investigation that demonstrated this found that a $\Delta fliHI$ mutant could regain motility when a point mutation was introduced into *fliB* (Minamino & Namba, 2008b). This led Minamino *et al* (2008b) and Paul *et al* (2008) to propose that the export process is dependent on the PMF (Proton Motive Force). The role played by ATP hydrolysis has thus been proposed to play a role in substrate delivery instead, helping the substrate release from their chaperone and the unfolding process (Galan, 2001, Akeda & Galan, 2005). Therefore, the primary role of the FliHIJ complex is to present substrates to the T3S system in an unfolded configuration.

1.6.2.2 The T3S substrate-specificity switch

The substrate-specificity switch employs T3S components to mediate the secretion preference for particular substrates in the right sequence for flagellar assembly. The key process of the switch mechanism is the role played by FliK (Minamino *et al.*, 1999). FliK can be secreted through a growing HBB, however, it has been shown that the N-terminal domain is exported while the C-terminal domain remains in close contact with the hydrophilic C-terminal of FliB (FliB_c). The

interaction between FliK and FlhB causes a conformational change of FlhB required for the specificity switch (Minamino & Macnab, 2000). The FlhB_c domain is divided into two subdomains, i.e., FlhB_{cn} and FlhB_{cc}. The cleavage of the FlhB_c between FlhB_{cn} and FlhB_{cc} is necessary for its proper function based on the fact that a mutation in its linker region prevents switching (Fraser *et al.*, 2003). This is an autocatalytic process that will occur in the absence of FliK (Ferris & Minamino, 2006). FliK acts in this case like a molecular ruler to control the length of the hook of approximately 55 nm (Moriya *et al.*, 2006). Moreover, the interaction of its C-terminal region with FlhB_c may repress hook substrate (FlgE) production (Bonifield *et al.*, 2000). These events are essential to regulate the optimum length of the hook and induce filament-associated secretion substrate secretion (Minamino *et al.*, 1999).

Thus the substrate-specificity switch defines the completion of the HBB allowing the last steps of flagellum assembly to begin, including the secretion of the anti- σ^{28} factor FlgM (Hughes *et al.*, 1993) and the production of filament subunit FliC.

1.6.2.3 Flagellar T3S Chaperones

Three flagellar specific T3S chaperones (T3SC), FlgN, FliS and FliT bind the C-terminal region of the substrates; the hook filament junction proteins (FlgK and FlgL), flagellins (FliC and FljB), and the filament capping protein (FliD), respectively.

In addition to their functions, some chaperones act as transcriptional or translational regulators unless bound to their cognate substrate (Miller, 2002). Having dual functions as chaperones or regulators, they possess the ability to couple gene expression with the assembly or secretion process by feedback regulation. The FlgN, the T3S chaperone for the hook-associated proteins FlgK and FlgL (FlgKL) (Fraser *et al.*, 1999), delivers FlgKL to the secretion gate and prevents their aggregation prior to secretion (Bennett *et al.*, 2001). However, FlgN is not essential for FlgKL secretion (Aldridge *et al.*, 2003). The FlgN is also a translational regulator of *flgM* from the class 3 transcription but not class 2 (Karlinsey *et al.*, 2000). In addition, FlgN controls *flgM* translation prior to as well as during HBB assembly. FlgN regulates the translation of *flgM* unless it is bound to FlgKL. FlgKL can therefore be defined as anti-FlgN factors. The interaction between FlgN and FlgK or FlgL is able to sense the actual stage of flagellar assembly.

FliS is the T3S chaperone of FliC binding the flagellin at its C-terminal, has been demonstrated *in vitro* to prevent polymerization of the FliC (Auvray *et al.*, 2008). Concerning the diameter of a flagellar channel being only 20 Å⁰ (Yonekura *et al.*, 2003), the FliC has to be in an unfolded conformation to pass this channel and to assemble at the tip of the filament. As a result, FliS may assist the preparation of an unfolded FliC passes through a secretion channel or prevent filaments assembling in the cell prior to the secretion of FliC. FliT interacts with filament cap FliD monomer with a 1:1 stoichiometry (Fraser *et al.*, 1999, Imada *et al.*, 2010). FliT inhibits P_{class 2} activity by interacting with FliH₄C₂ (Kutsukake *et al.*, 1999).

1.7 The general principles of transcriptional regulation

Gene expression in all bacteria is tightly controlled at the level of transcription initiation, regarded as a principal point of gene regulation. Comprehensive studies showed that transcriptional regulation in *E. coli* is based on a complex network of transcription factors that control approximately 1800 transcription units in response to environmental changes (Karp *et al.*, 2007).

1.7.1 Transcriptional regulation by Sigma Factors (σ)

One type of transcriptional factor that controls bacterial gene expression is the group of proteins known as σ factors. σ factors regulate transcription by allowing RNA polymerase to recognise promoter sequences and initiate transcription. The σ activity itself can also be regulated by internal and external cues.

RNA polymerase holoenzyme is composed of a configuration of core subunits ($\alpha 2\beta\beta'$). The σ subunit is required for recognition of the promoter sequence. In a promoter, two short sequences, -35 & -10, confer binding specificity of RNA polymerase, and σ factors. In the core enzyme complex, the β subunit contains the catalytic activity while β' binds to DNA non-specifically and the α subunit acts as a linker of the (two large) subunits (Hughes and Mathee, 1998). There are additional 5' sequences that are frequently known as upstream activating sequences, which contribute to promoter recognition. These regions are often targeted by transcriptional activator or repressor proteins that can interact with the holoenzyme or

σ factors to increase or decrease promoter recognition under specific conditions (Hughes and Mathee, 1998).

Simple promoters are recognized by the holoenzyme and σ^{70} but some specific promoters need additional factors for transcription initiation (Ishihama, 1988, Ishihama, 1993). The involvement of various regulatory proteins means protein-protein interactions play a crucial role in gene regulation. The structure of functional transcription units specified for accurate initiation also differs to some degree among promoters. Each promoter region is therefore designed differently according to the various combinations of σ -factors and transcription factors responsible for regulating transcription.

The presence of multiple σ factors provides bacteria the sophisticated mechanism to control different subsets of genes simultaneously. The functional differentiation of RNA polymerase by replacement of the σ factor provides bacteria with an effective way to obtain differential gene expression. Seven species of the σ subunit have been identified in *E. coli* by their molecular weight (Hughes, & Mathee, 1998).

- σ^{70} (RpoD) - the "housekeeping" σ factor that transcribes most genes in growing cells.
- σ^{54} (RpoN) - the nitrogen-limitation σ factor
- σ^{38} (RpoS) - the starvation/stationary phase σ factor
- σ^{32} (RpoH) - the heat shock σ factor that is turned on when bacteria are exposed to heat
- σ^{28} (RpoF, FliA) - the flagellar specific σ factor
- σ^{24} (RpoE) - the extracytoplasmic/extreme stress σ factor
- σ^{19} (FecI) - the ferric citrate σ factor that regulates the *fec* gene for iron transport

The σ^{70} -holoenzyme is active at nearly all states of bacterial growth. It is responsible for transcribing many important genes encoding proteins or enzymes for common activity especially in cellular metabolism as shown in **Table 1** (Helmann *et al.*, 1988a).

Table 1: $E\sigma^{70}$ regulates many enzymes responsible for important cell activities.

Proteins or enzymes encoded by genes regulated through $E\sigma^{70}$	
<i>Biosynthesis</i>	amino acids
	nucleotides
	enzyme
	cofactors
	cell wall
	membrane components
<i>carbon source catabolism</i>	The glycolysis pathway
	The pentose phosphate shunt
	The TCA cycle

Heat shock proteins are transcribed by the combination of core enzyme and the alternative σ factor (σ^{32}) under stress conditions. An alternative σ^{28} is responsible for the regulation of flagellar-chemotaxis genes. A single σ factor can co-ordinately activate a group of genes if their promoter sequences are very similar. An additional layer of transcriptional regulation exists for the σ factor activity, which can be inhibited by the presence of proteins defined as an anti- σ factor. An anti- σ factor is capable of preventing the interaction of the σ factor with core RNA polymerase or promoter sequences and thus inhibiting transcription initiation. The mechanisms can also involve anti-anti- σ factors to actively inhibit their specific anti- σ factor or the anti- σ factor is exported out of the cell.

1.7.2 Other regulatory proteins

Other regulatory proteins also influence transcription initiation through protein-protein and protein-DNA interactions. Their behaviours can range from being highly specific transcriptional factors such as the lactose operon repressor, which controls only one transcription unit, through to global regulatory proteins. One example of a global regulator is the cAMP-CRP complex. The Cyclic AMP receptor protein (CRP) controls the expression of nearly 200 genes (Hollands. *et al.*, 2007). The CRP is a homodimer, whose N-terminal can bind to cAMP while the C-terminal binds DNA. If allosterically activated by cAMP, the CRP is selectively bound to DNA units by a helix-turn-helix (HTH) motif. The binding of cAMP-CRP to DNA causes DNA bending and recruits RNA polymerase to initiate transcription.

The nucleoid-associated proteins, which are required for maintaining chromosome folding and compaction, also play an important role in global transcriptional regulation (Dorman, 2003). For example, the histone like nucleoid protein, H-NS, consists of two distinct domains, the N-terminal domain responsible for protein oligomerisation, and the C-terminal DNA binding domain. H-NS is often described as a non-specific DNA binding protein (Grove & Saavedra, 2002, Schroder & Wagner, 2002). H-NS is generally accepted as a negative regulator of gene expression, although it is a positive regulator of $FlhD_4C_2$, the flagellar master regulator expression (Soutourina *et al.*, 2002). An interaction of architectural proteins with DNA might play a key role in understanding the regulation through

environmental signals on promoter architecture, and then transcription, which effects gene expression in bacteria (Jordi *et al.*, 1997).

1.7.3 Post-transcriptional regulation

Gene expression is regulated not only at the level of transcription but also during translation or post-translationally. Translational regulation can regulate both mRNA stability and the physical process of translation. This suggests that there is a control of a protein's amount dictated through the process of translation. Alternatively the level of protein available for a given task can be dictated via post-translational regulation. The most frequently observed mechanisms of post-translational regulation include protein degradation or chemical modification of the protein. Chemical modification such as phosphorylation, glycosylation, methylation, acts like an on-off switch to a process of the protein involved. One example of chemical modification already discussed is the activation of CheY by phosphorylation. In this case the protein levels can be maintained but the protein only becomes active when a signal is perceived and transmitted to CheY via phosphorylation.

1.8 Flagellar regulon

1.8.1 The regulon's architecture (*fla* regulons)

The early definition for describing mutants in bacterial genes relating to their motile behaviour was divided into three phenotypic categories; motile (Mot), flagellated but not motile (Fla) and lacking chemotactic responsiveness (Che). The corresponding genes and their operons were subsequently defined as the "*fla* regulon". The distinctive characteristic that defines a regulon is a common regulatory pattern of a group of genes under the control of the same regulatory protein (Neidhardt, F.S. and Savageau, M.A., 1996.). There are at least 60 genes in *E. coli* and *Salmonella* belonging to the *fla* regulon and clustered into 17 operons.

The *fla* regulon exhibits a surprising level of organization and regulatory features. The *fla* genes have been recently classified into three classes: early, middle, and late, according to when required in the assembly process similar to the

organization of bacteriophage genes (Chilcott & Hughes, 2000) (**Figure 10**). The *fla* genes are transcribed by 3 promoter classes: P_{class1} , P_{class2} , and P_{class3} . The P_{class1} drives early gene expression, P_{class2} middle gene expression and P_{class3} late gene expression. In general, this results in specific genes being expressed at the right time in the assembly pathway. However, the expression of some late *fla* genes are transcribed from both P_{class2} and P_{class3} promoters. Importantly, the main characteristic feature of the *fla* regulon is its ability to couple flagellar gene expression to the assembly pathway. As a result the cascade that controls flagellar promoter activity can be classed as a transcriptional hierarchy of P_{class1} leading to P_{class2} leading to P_{class3} activation.

1.8.2 Activation of the transcriptional hierarchy

The master regulatory protein FlhD₄C₂ is encoded by the early genes *flhDC*. The P_{class1} of the *flhDC* master operon confers the first decision for flagellar synthesis. The P_{class1} promoter is the only promoter of this class. The regulation of transcription from P_{class1} can often be seen as a unique sub-field of flagellar research. A long list of factors can feed their input into P_{class1} allowing the cell to decide whether to initiate or deter flagellar synthesis. The *flhDC* operon is only found in the enteric gamma-proteobacteria and the beta-proteobacteria. Most of our understanding of *flhDC* transcription from the P_{class1} focuses on *S. enterica* and *E. coli*. An extensively large list of factors directly or indirectly regulates the expression and activity of FlhD₄C₂ through the P_{class1} promoter (**Table 2 and Figure 11**). The P_{class1} is not a simple bacterial promoter. The P_{class1} promoter region contains six transcriptional start sites the list of transcriptional regulators can be subdivided based on the transcriptional start sites that are utilised (Yanagihara *et al.*, 1999). *flhDC* transcription is subjected to a wide range of environmental and internal signals including temperature, osmolarity, pH and flagellar assembly (**Table 2 and Figure 11**). Global regulatory proteins such as H-NS and the cAMP-CRP complex exert a positive influence on *flhDC* transcription, however, the majority of regulatory inputs are negative (Wozniak & Hughes, 2008). Other than regulating the activity of the P_{class1} promoter, the RNA binding regulator CsrA controls the stability of *flhDC* mRNA (Wei *et al.*, 2001).

The P_{class2} flagellar promoters are activated by the FlhD₄C₂ complex, in consort with σ^{70} (Liu & Matsumura, 1994, Kutsukake *et al.*, 1990). The FlhD₄C₂ complex assists the binding of RNA polymerase through the interaction with the C-terminal region of its α subunit (Liu and Matsumara, 1995). The FlhD₄C₂ binding sites of P_{class2} are between -30 and -80 (Liu and Matsumara, 1994). The specific sequences, TTATTCC n₁₀₋₁₂ GCAATAA are found in all FlhD₄C₂ binding sites (Stafford *et al.*, 2005).

P_{class3} promoters (late genes) are activated by the flagellar specific σ factor σ^{28} (Ikebe *et al.*, 1999a, Ikebe *et al.*, 1999b, Ohnishi *et al.*, 1990, Helmann *et al.*, 1988b). The activity of σ^{28} is dictated by the presence of its anti- σ factor FlgM. FlgM activity is sensitive to the flagellar assembly pathway as it is secreted after Hook completion. This description of the hierarchy only takes into account its activation. A series of feedback loops sensitive to flagellar assembly are able to influence the activity of each tier of the hierarchy. The protein FlhT, the subject of this thesis, controls one of these feedback loops.

1.8.3 The FlhD₄C₂ component in the circuit

Mutations in *flhD* or *flhC* render cells non-motile. The crystal structure revealed FlhD₄C₂ to be a heteromeric complex (Wang *et al.*, 2006). Wang *et al.*, 2006, proposed a structural model of the FlhD₄C₂ complex bound to DNA. They suggested FlhD (13.3 kDa) and FlhC (21.5 kDa) are predominantly alpha-helical structures (Wang *et al.*, 2006) (**Figure 12**). The FlhC structure revealed an unrecognized zinc-binding domain in which the ion is ligated between four cysteine residues in a distinct tertiary fold (Wang *et al.*, 2006). FlhD molecules form a dimer containing two flexible arms. At the end of each flexible domain, a putative helix-turn-helix (HTH) suggests the presence of DNA binding domain (Campos & Matsumura, 2001). However, the FlhD protein alone is not capable of binding to DNA or activating transcription, only in the presence of FlhC (Liu & Matsumura, 1994). Other proteins capable of interacting with FlhD may influence the conformation and the specificity of DNA binding via the H-T-H motif (Campos & Matsumura, 2001). The purified FlhC on its own was shown to bind specifically to the promoter region of *flhB* gene but FlhD could not bind unless it combined with FlhC. This leads to the proposal that FlhD helps increase the

specificity of DNA recognition by FlhC and also stabilizes the protein-DNA complex (Claret & Hughes, 2000). However, on solving the structure Wang et al. proposed FlhD to be bound onto a bent DNA molecule. The complex of FlhD and FlhC (FlhD₄C₂) is a positive trans-acting transcriptional activator recognizing a highly conserved region in a 28-88 bp upstream region of the transcriptional start sites of its target genes (Liu & Matsumura, 1994, Liu & Sanderson, 1996). As a result, this overlaps with the -35 promoter element of *flhDC*-dependent genes (Liu & Matsumura, 1994, Liu & Sanderson, 1996). The FlhD₄C₂ binding site was revealed as a 17-18 bp imperfect reverted repeat (Stafford *et al.*, 2005, Claret & Hughes, 2002). The FlhD₄C₂-activated σ^{70} promoter has also been found in association with other non-flagellar genes (Stafford *et al.*, 2005, Frye *et al.*, 2006). Once bound to DNA, FlhD₄C₂ interacts with the C-terminal domain of RNA polymerase α subunit, and therefore stabilizes σ^{70} E complex at P_{class2} (Liu *et al.*, 1995, Wang *et al.*, 2006).

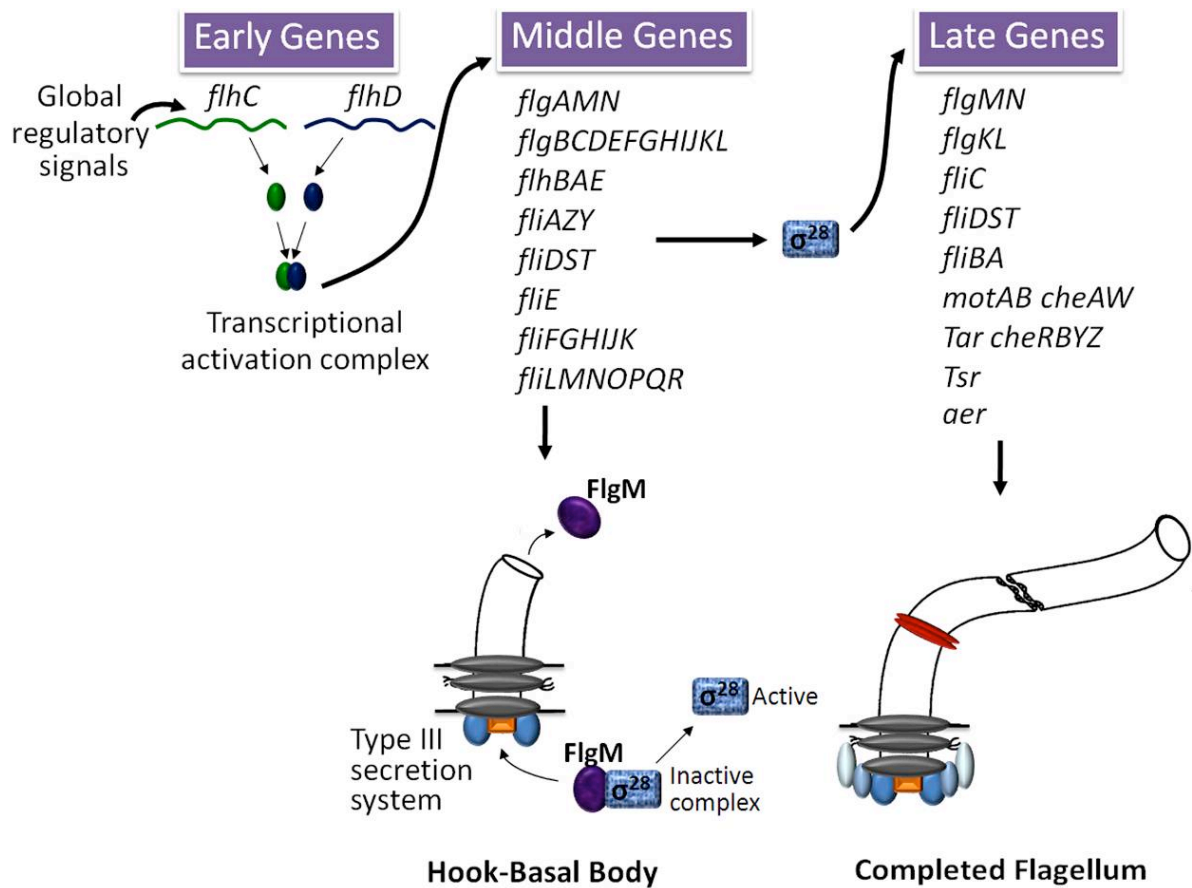


Figure 10: Flagellar genes are expressed in an organized order corresponding to the sequence of flagellar assembly

The *flhDC* operon receives signals from global regulators and is activated prior to class 2 and 3 activation in a defined temporal order. The class 2 and class 3 operon and corresponding products are displayed in a corresponding temporal manner. The inner membrane (IM), peptidoglycan (PG) and outer membrane (OM) are shown. Transcriptional regulation of late genes is shown to be dependant upon secretion of the anti- σ factor FlgM, which inhibits its chaperone - the class 3 σ factor FliA (σ^{28}). Completion of the Flagellar type III secretion System (TTSS) leads to secretion of FlgM and release of FliA. (Modified from Karlinsey *et al.*, 2000)

Table 2: Several factors affect FlhD₄C₂ activity

Factors affect FlhD ₄ C ₂ activity			
Factors	Positive	Negative	Reference
DnaK, DnaJ, and GrpE (temperature)		+	Li <i>et al.</i> , 1993 Shi <i>et al.</i> , 1992
OmpR (osmolarity)		+	Shin and Park, 1995
H-NS (pH)	+		Soutourina <i>et al.</i> , 1999
cAMP-CRP (carbon source)	+		Kutsukake, 1997
FliZ	+		Kutsukake, 1999 Saini <i>et al.</i> , 2008
ClpXP		+	Tomoyasu <i>et al.</i> , 2003
FliT		+	Kutsukake, 1999 Yamamoto & Kutsukake, 2006
Quorum sensing	+		Atkinson <i>et al.</i> , 2008
cell cycle control	+		Pruss & Matsumara, 1997
CsrA	+		Wei <i>et al.</i> , 2001

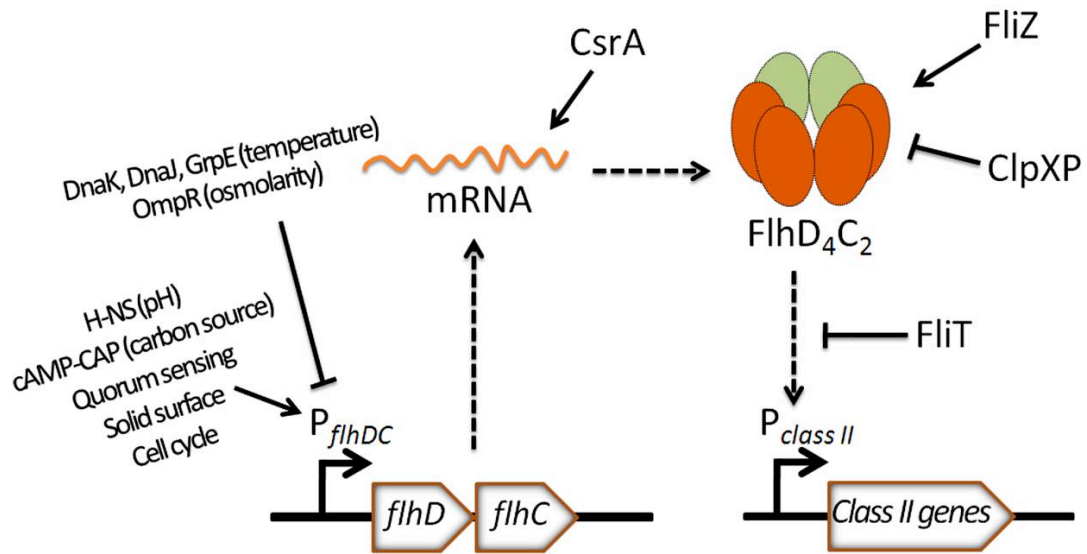


Figure 11: Regulation of flagellar master regulator $FlhD_4C_2$

Expression of *flhDC* is influenced by different regulatory proteins in response to various environmental cues. The stability of the mRNA for *flhDC* is subjected to a variety of regulators. $FlhD_4C_2$ activity upon class II genes is positively and negatively regulated by various proteins such as FliT, ClpXP, and FlhZ. Positive effects are labelled with arrowheads and negative effects with blunt-ends. (Modified from Smith, T. G. and Hoover, T. R, 2009)

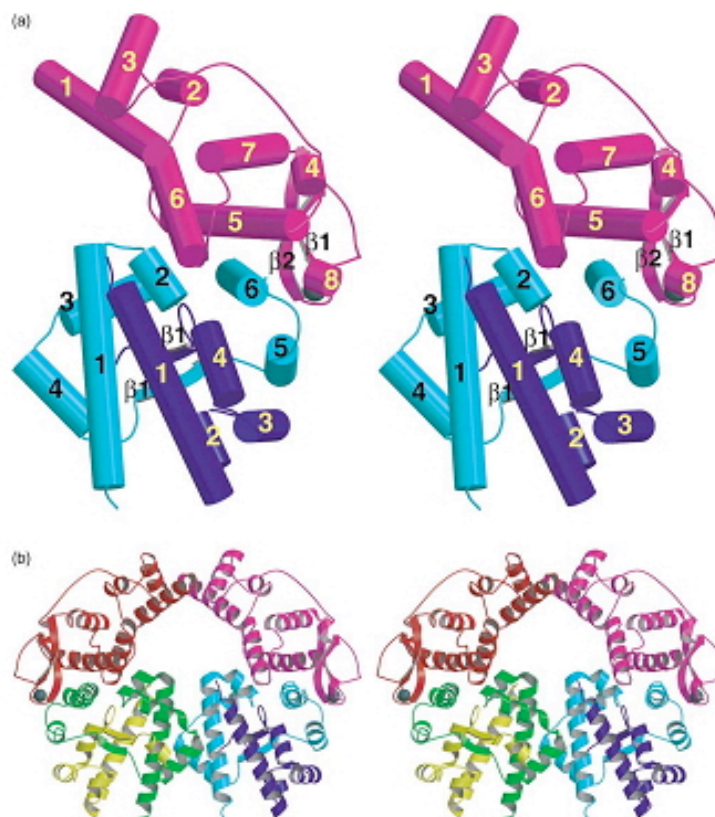


Figure 12: Structure of the FlhD₄C₂ complex

(a) Structural view shows one FlhC protomer and two FlhD protomers forming an FlhD₂C₁ subunit. Helices are shown as numbered cylinders. The colour of FlhD chains A is blue and B is cyan while FlhC is shown in pink. Two FlhD₂C₁ subunits further represent the functional FlhD₄C₂ complex **(b)** Stereo view illustrates ribbon diagram of FlhD₄C₂ complex with two subunits of FlhD₂C₁ joined together. The colours of FlhC and FlhD molecules on the left protomer are represented differently as red for FlhC and as yellow and green for each FlhD while the protomer on the right remains the same as in (a). **(Taken from Wang *et al.*, 2006)**

1.8.4 The HBB assembly Checkpoint and flagellar gene expression

Temporal expression of flagellar genes begins with the expression of the early genes encoding the master regulator, FlhD₄C₂. FlhD₄C₂ then activates the expression of middle genes. Middle genes mostly encode for structural components of the HBB but also the filament junction proteins FlgK and FlgL as well as the filament cap, FlhD. A number of regulators are also encoded by middle genes including *fliA*, *flgM*, *fliT* and *fliZ*. *fliA* encodes the flagellar specific alternate sigma factor, σ^{28} , needed for late gene expression. *flgM* encodes the anti σ^{28} factor, FlgM, that couples the late gene expression to the completion of Hook Basal Body (HBB). FlgM ensures that the expression of late genes occurs after the HBB intermediate structure is ready to continue the final process of flagellar synthesis (**Figure 10**).

1.8.4.1 σ^{28}

A null mutation in the *fliA* gene can prevent all late gene expression and is thus non-motile (Kutsukake *et al.*, 1990, Komeda, 1986). The promoter consensus regions for σ^{28} have been revealed and classified as -35 (TAAAGTTTT) N11 -10 (GCCGATAA), these are very different from σ^{70} -dependent promoters or P_{class2} that need FlhD₄C₂ as the transcriptional regulation (Chilcott & Hughes, 2000). The *fliA* gene is located in the *fliAZY* operon and can be transcribed by P_{class2} or P_{class3} (Ikebe *et al.*, 1999a, Mytelka & Chamberlin, 1996). *fliZ* encodes a positive regulator of FlhD₄C₂ (Kutsukake, 1999 & Saini *et al.*, 2008) while *fliY* has no resolved function during flagellar assembly. σ^{28} is a lot smaller σ^{70} 28 kDa versus 70 kDa but still belongs to the σ^{70} superfamily (Liu *et al.*, 1995, Arnosti & Chamberlin, 1989, Ohnishi *et al.*, 1992). σ^{70} is defined as possessing 4 regions (1 to 4). Region 1 is the largest region that is thought to play some kind of regulatory role of σ^{70} 's own activity. Regions 2, 3 and 4 are within the C-terminal region of σ^{70} and are responsible for -10 and -35 recognition (Lonetto *et al.*, 1992). σ^{28} lacks the large N-terminal domain found in σ^{70} possessing just regions 2, 3 and 4 (Chadsey *et al.*, 1998, Iyoda & Kutsukake, 1995).

1.8.4.2 FlgM

The clue to the coupling between the late gene expression and flagellar assembly came from the discovery of the negative regulator FlgM (Gillen & Hughes, 1993). FlgM is 97-amino-acids (Gillen & Hughes, 1993, Iyoda & Kutsukake, 1995) and can bind to σ^{28} and a RNA polymerase σ^{28} complex, σ^{28} E (Chadsey *et al.*, 1998, Jishage & Ishihama, 1998). Using an *in vitro* transcription assay, σ^{28} was inhibited by the presence of FlgM and can be dissociated from σ^{28} E by FlgM (Chadsey *et al.*, 1998). This characterization therefore classified FlgM as an anti- σ factor (Ohnishi *et al.*, 1992). The K_d of either FlgM to σ^{28} or σ^{28} -holoenzyme is in pM range (Chadsey and Hughes, 2001), and the approximate FlgM concentration in a cell is in the nM range (Karinsey *et al.*, 2000). Core RNA polymerase concentration is in excess to σ^{28} in the cell, thus very little free σ^{28} is found within the cell in the presence of FlgM. FlgM mutagenesis indicated that the amino acid region 42 – 86 was required for anti σ^{28} activity. Under physiological conditions, free FlgM is mostly in an unfolded state (Daughdrill *et al.*, 1997). When bound to σ^{28} , however, FlgM attains a folded conformation with the N-terminal 40 amino acids in an unorganized form either in the presence or absence of σ^{28} . The protein stability of FlgM can also be correlated to the presence of σ^{28} (Aldridge *et al.*, 2006a). FlgM turnover results from the activity of the Lon protease (Barembuch & Hengge, 2007). Structural analysis has shown that FlgM binding rearranges the conserved σ^{28} domains extensively so that they are tightly packed with FlgM wrapped around the outside (**Figure 13**) (Sorenson *et al.*, 2004).

The binding of FlgM to σ^{28} increases the stability of σ^{28} while the presence of the σ^{28} :FlgM complex facilitates FlgM secretion. Like *fliA*, *flgM* is also expressed from both a P_{class2} (*flgAMN*) and P_{class3} (*flgMN*) promoter. P_{class2} produced FlgM is mainly found in the cytoplasm while P_{class3} FlgM is predominantly secreted (Karinsey *et al.*, 2000). It is possible to assume that during HBB assembly, the P_{class2} FlgM is destined to inhibit σ^{28} activity. In contrast P_{class3} FlgM is more readily available for secretion and modulates σ^{28} activity (Karinsey *et al.*, 2000 & Saini *et al.*, 2008) After HBB completion, the expression of FlgM from its class 3 transcript has been proposed to be coupled with its secretion from the cell in a co-translational model. However, direct evidence for such a mechanism is still lacking.

1.8.4.3 The σ^{28} : FlgM switch

The HBB completion is the major structural intermediate of the assembly pathway. Apart from being the foundation of bacterial propeller, HBB hosts all the T3SS components needed for T3S. The HBB and its completion is a fundamental intermediate during flagellar synthesis as it couples gene expression to the pathway. Sensing the completion of the HBB is through the capability of FlgM to be exported by the T3S apparatus (Hughes *et al.*, 1993). The secretion signal of FlgM appears to be its N-terminus and the deletion of this part significantly decreases its cellular level (Chilcott & Hughes, 1998, Iyoda & Kutsukake, 1995). σ^{28} itself facilitates the FlgM secretion and is classified as the FlgM T3S chaperone (Aldridge *et al.*, 2006a). At this checkpoint, bacteria can sense the satisfactory progression of the growing structure morphologically and couple that progression (completed HBB) with the temporal expression of late genes. After dissociating from FlgM and facilitating its secretion, free σ^{28} can start to interact with RNA polymerase and transcribe flagellar P_{class3} .

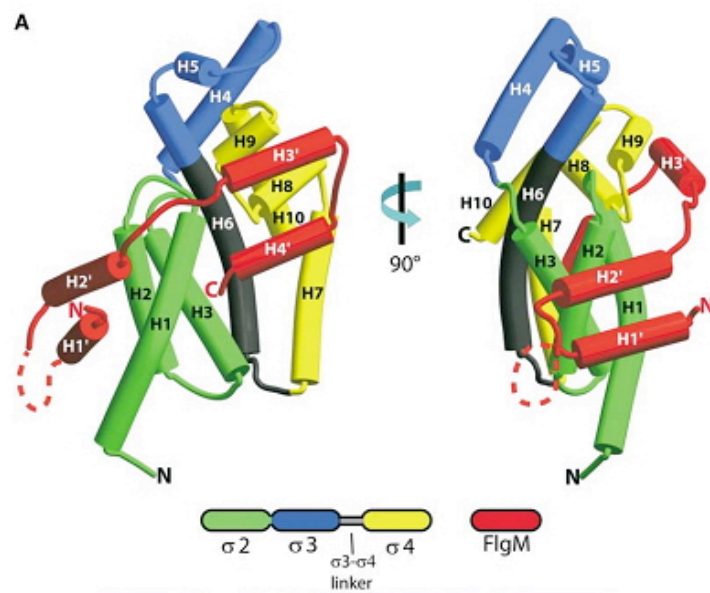


Figure 13: Structure of the *A. aeolicus* σ^{28} / FlgM Complex

The figure illustrates the σ^{28} / FlgM complex in two views (90° phase difference). Shown as coloured cylinders, helices are labelled H1-H10 in σ^{28} and H1'-H4' in FlgM. Under the picture are linear structures of the two proteins with corresponding colours as the picture above. (Taken from Sorenson *et al.*, 2004)

1.9 FliT

The FlgM : σ^{28} complex reflects the dual functionality of a T3S chaperone, σ^{28} , facilitating both secretion efficiency and transcriptional regulation. The dual roles played by members of the flagellar T3S chaperone family is not a unique to just σ^{28} , other members of this family also couple flagellar gene expression to assembly. Another example of a dual role T3S chaperone is FliT, that regulates FlhD₄C₂ activity and interacts with the flagellar secretion substrate FliD (Yamamoto *et al.*, 2006).

FliT is encoded by the *fliT* gene, which forms part of the *fliDST* operon. The *fliT* and *fliS* genes were first described together during the characterization of *fliD* in *E. coli* (Kawagishi *et al.*, 1992). The *fliD* operon, like *fliAZY* and *flgMN*, is transcribed from both P_{class2} and P_{class3} promoters. Primer extension analysis has revealed that the promoters overlap in the promoter region of *fliD* (Kutsukake *et al.*, 1990). Therefore, *fliA* mutations cannot eliminate the expression of the *fliDST* operon. In contrast, a mutation in the *flhDC* operon eliminates *fliDST* expression (Kutsukake *et al.*, 1990).

Fraser *et al.* (1999) proposed FliT as the FliD T3S chaperone. A *fliT* mutant showed a significant decrease in the FliD secretion (Bennett *et al.*, 2001). FliT has also been described to regulate *fla* gene expression. The activity of P_{class3} significantly increased in a *fliT* mutant, with the observation of more FlgM export compared with wild-type (Yokoseki *et al.*, 1996). The concept of a regulatory role for FliT was subsequently shown to negatively regulate P_{class2} transcription. A *fliT* mutant subsequently has increased almost double the number of flagella compared with the wild-type strain (Yokoseki *et al.*, 1996). *fliT* mutants are motile suggesting it is not essential for FliD secretion. This is similar to σ^{28} for FlgM and FlgN for FlgK and FlgL all of which can be secreted without their cognate T3S chaperone albeit inefficiently (Aldridge *et al.*, 2003, Aldridge *et al.*, 2006a).

FliT is a small 14 kDa soluble protein localized in the cytosol. Previous reports suggested a dimer (Bennett *et al.*, 2001). FliT binds the C-terminal helical domain of FliD and prevents oligomerization before FliD secretion (Fraser *et al.*, 1999). FliT supports the FliD export through the flagellar channel, yet it is not essential.

As a regulator, FliT is involved in modulating FlhD₄C₂ activity (Yamamoto & Kutsukake, 2006). FliT activity can be classified as a negative feedback mechanism to turn off or to slow down the expression of middle genes. The binding target of FliT is FlhC in the FlhD₄C₂ complex. Yamamoto and Kutsukake (2006) proposed that binding to FlhD₄C₂ prevents its interaction with P_{class2} (Yamamoto & Kutsukake, 2006). As a result, a regulation loop has been proposed between FliT, FliD and FlhD₄C₂ to fine-tune P_{class2} activity in response to flagellar developmental stages. Before hook-basal body completion, FliT binds to a pool of free FliD in the cytosol, and therefore enabling transcription of the middle genes by FlhD₄C₂. FliD export is mediated by FliT once the hook-basal body completion has occurred and FliT is then free to interact with FlhD₄C₂ to inhibit expression of the middle gene expression (**Figure 14**). This regulation involves protein-protein and protein-DNA interactions, its architecture is very similar to that of FlgM/ σ^{28} . FliD in this circuit is proposed to act as an anti-anti-FlhD₄C₂ factor because of its limited interaction towards FliT only; however, direct evidence for this activity is lacking.

The recent crystal structure of FliT revealed an asymmetric dimer. The FliT molecule contains four α helices ($\alpha 1$, $\alpha 2$, $\alpha 3$, $\alpha 4$), three of which ($\alpha 1$, $\alpha 2$, $\alpha 3$) form an anti-parallel alpha-helical clustered structure (Imada *et al.*, 2010) (**Figure 15**). Hydrophobic interactions participate in the main structure with a flexible C-terminal α helix ($\alpha 4$). Helix- $\alpha 4$ is proposed to play an important regulatory role in FliT function.

Corresponding to the earlier observation (Bennett *et al.*, 2001), the FliT region responsible for FliD binding lies on the $\alpha 2/\alpha 3$ helices, which is hidden by the C – terminal region. Site-directed mutagenesis and pull down assays narrowed down FliD binding to be around amino residue 79 (Imada *et al.*, 2010). With respect to FliD export, FliT binds two soluble components of the T3S secretion apparatus, FliI and FliJ (Evans *et al.*, 2006, Thomas *et al.*, 2004). The binding region is shown to be different from the FliD binding region (Imada *et al.*, 2010).

FliT without the C-terminal $\alpha 4$ region (FliT94) was able to inhibit swarming motility stronger than wildtype FliT. This last α -helix was suggested to therefore autoregulate the activity of FliT. Interestingly deletion of $\alpha 4$ not only increases inhibition of FlhD₄C₂ but also altered the binding characteristics of FliT to FliI and FliJ. In both cases FliT94 bound better to FliI and FliJ than did a full-length FliT protein.

This data seems to suggest that FliT while coupling FlhD₄C₂ activity to flagellar assembly regulates its own activity to prevent either too strong a down regulation of flagellar gene expression or too much FliD being secreted.

1.10 FliD

FliD is the filament cap structure that is believed to act as a guide for the incorporation of flagellins into the bacterial filament. FliD is often defined as HAP2 (hook-associated protein 2), although here it is only referred to as FliD. FliD is a 466 amino acid protein with a molecular mass of 49.8 kDa. The role of FliD in filament assembly dates back to the initial observation that isolated flagellins could form a filament only in a $\Delta fliD$ mutant. Mutation of *fliD* renders cells non-motile. *fliD* mutants secrete flagellin to the culture medium without forming a typical long ordered filament (Homma & Iino, 1985, Homma *et al.*, 1984). A $\Delta fliD$ mutant produces a HBB-FlgK-FlgL substructure with short disordered filament extensions. However, flagellin would stop “leaking” and a filament of longer length and ordered structure would grow when purified FliD was added to the medium (Ikeda *et al.*, 1993). Adding isolated FliD was able to restore a given level of motility to the mutant. This observation indicates that the HBB-FlgK-FlgL complex can serve as an active nucleus for flagellin polymerization, albeit inefficiently (Homma *et al.*, 1986). The rate of filament growth facilitated by FliD was predicted to be approximately 30 nm/min, which corresponded to the addition of one flagellin monomer per second (Ikeda *et al.*, 1993).

In solution FliD has been found to exist as a decamer (Imada *et al.*, 1998). Electron microscopy analysis of the decamer identifies 2 pentameric structures linked together at the tip of feet-like projections in an hourglass formation (**Figure 16**). A monomer to decamer shift depends on pH and salt concentration (Imada *et al.*, 1998). Low pH tends to stabilize the decamer structure, while increasing pH promotes a decamer shift back to the monomer state. The structural transition is most sensitive at pH 8-8.5, which may be a physical regulatory factor. This would provide bacterial cells with a mechanism of preventing decamer formation in a cell maintaining a preferred monomeric form for secretion (Imada *et al.*, 1998). Alternatively this may also play a role during filament assembly.

The cap has been observed by electron microscopy to be a pentameric complex shape of FliD at the tip of filaments (Yonekura, K., S. Maki-Yonekura & K. Namba, 2001) (**Figure 16**). The pentamer configuration is the combination of a pentagonal plate and five protruded leg domains (**Figure 16**). This pentagonal plate-like is placed upon the distal end of the filament in five symmetric positions through its five protruded domains. Separated from one another, the five domains create five gaps with different sizes and shapes between the plate and the filament end (**Figure 17C**). One prominent large gap exhibits an L shape and has been suggested to be the site of flagellin incorporation. This opening is proposed to be the only space large enough to accommodate the newly arriving flagellin subunit thus guiding its insertion into the filament next to the previous flagellin (Yonekura, 2000). Every insertion of a flagellin subunit is proposed to rotate the cap to accommodate the new incoming flagellin subunit in the next position. Theoretically this process will continue as long as flagellins are secreted.

The FliD monomer also interacts with FliT whose function is to prevent FliD oligomerization prior to its export through the flagellar specific T3S apparatus (Bennett *et al.*, 2001). FliD interacts with FliT to form a stable complex through an interaction between the C-terminal half of FliT and a C-terminal region of FliD (Bennett *et al.*, 2001, Fraser *et al.*, 1999). Thus FliT was defined as a T3S chaperone specific for FliD. Interestingly, FliT is not strictly required for secretion for FliD, for example $\Delta fliT$ mutants are motile. Despite being a structural component, FliD was reported to possess another role as a regulatory component in the FliT-FlhD₄C₂ regulatory circuit as it binds to FliT. The argument follows a similar concept as seen for FlgM/s28 that FliD in the cell prevents FliT to interact with FlhD₄C₂ (Yamamoto & Kutsukake, 2006). However, data showing that this is in fact the case is lacking. Importantly, the proposed interactions between FliT and FliD and the net output of this interaction suggests that FlhD₄C₂ activity is sensitive to the assembly status of the flagella through FliD secretion. The central hypothesis of this thesis predicts this proposed model to be correct and aims to test the roles of FliT and FliD on regulating FlhD₄C₂ using in vivo and in vitro biochemical assays.

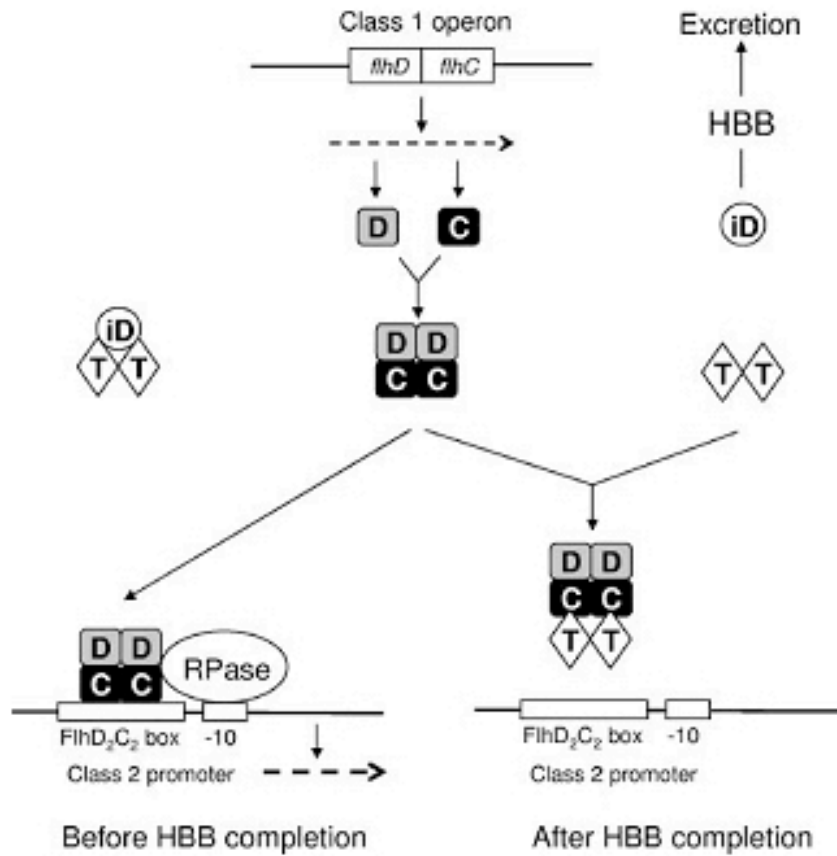


Figure 14: The proposed circuit of FliT negative regulation upon the gene expression of the flagellar Class 2 operon

The function of FliT is to prevent FlhD₂C₂ from binding to P_{class2} promoters. Another factor in this circuit, FliD binds to FliT (acting as a secretion chaperone) and prevents its interaction with FlhD₂C₂, thus freeing functional FlhD₂C₂ to initiate the transcription of P_{class2} genes until completion of the hook-basal-body (HBB) when FliD can be secreted. The horizontal line and broken arrow represent DNA and mRNA, respectively. Abbreviation used: C, FlhC; D, FlhD; iD, FliD; T, FliT; RPase, σ^{70} -RNA polymerase holoenzyme; -10, pribnow box; HBB, hook-basal body. **(Taken from Yamamoto & Kutsukake, 2006)**

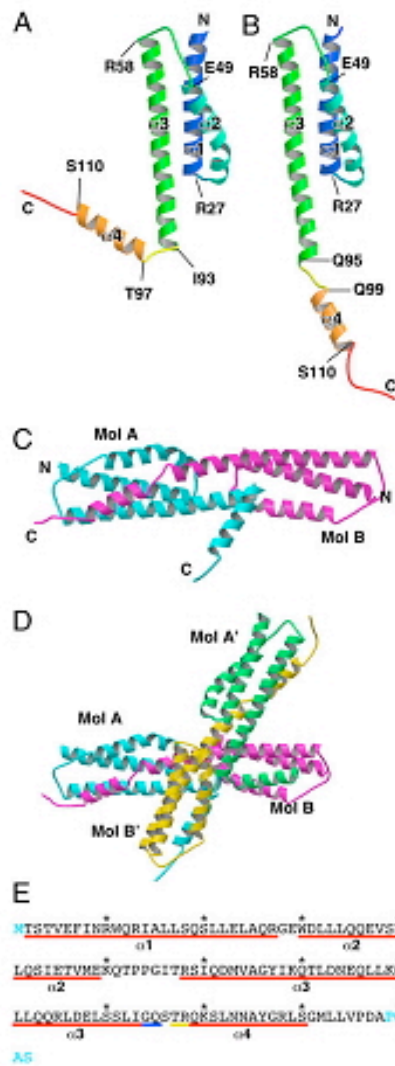


Figure 15: Molecular structure of FliT

Two configurations of FliT, Molecule **(A)** and **(B)**, are shown in a colour-coded ribbon drawings from the N-terminus (blue) to the C-terminus (red). The two structures are indicated to be involved in forming a dimer **(C)** and a tetramer **(D)**. The dimer structure of FliT shows an exposed C-terminus in one molecule (Mol A, cyan colour). The exposed alpha helix at the C-terminal is predicted to play a key role in protein interactions **(C)**. The tetramer structure of FliT shows an exposed C-terminal region resulting from dimer/dimer interactions **(D)**. Note that the structure revealed from the crystal is in a tetramer form. **(E)** Amino acid sequence of FliT is compared between Mol A and Mol B with the underscored regions representing alpha helix: red line, alpha helix in both Mol A and Mol B; yellow line, only in Mol A. The labels $\alpha 1$ - $\alpha 4$ correspond to those in A and B. The terminal residues coloured cyan are missing in the atomic model. **(Taken from Imada *et al.*, 2010)**

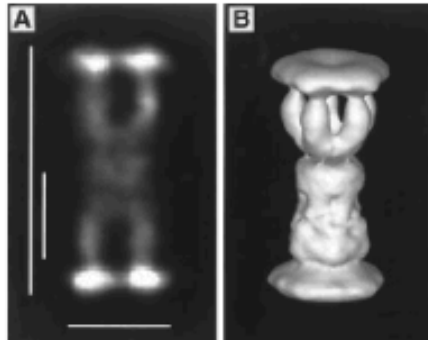


Figure 16: The configuration of FliD decamer in solution

(A) Image of negatively strained particles, revealing the bipolar arrangement of the two pentamers with indicated scale bars: left long, 290 Å; left short, 100 Å; bottom, 120 Å. **(B)** Solid surface reconstructed image of the three-dimensional density map. Two pentamer caps are inversely connected (top and bottom), each containing a plate and five legs. The tentamer connects with legs' domain of each pentamer, conferring a significant flexibility at the centre of the structure. **(Taken from Yonekura, 2000)**

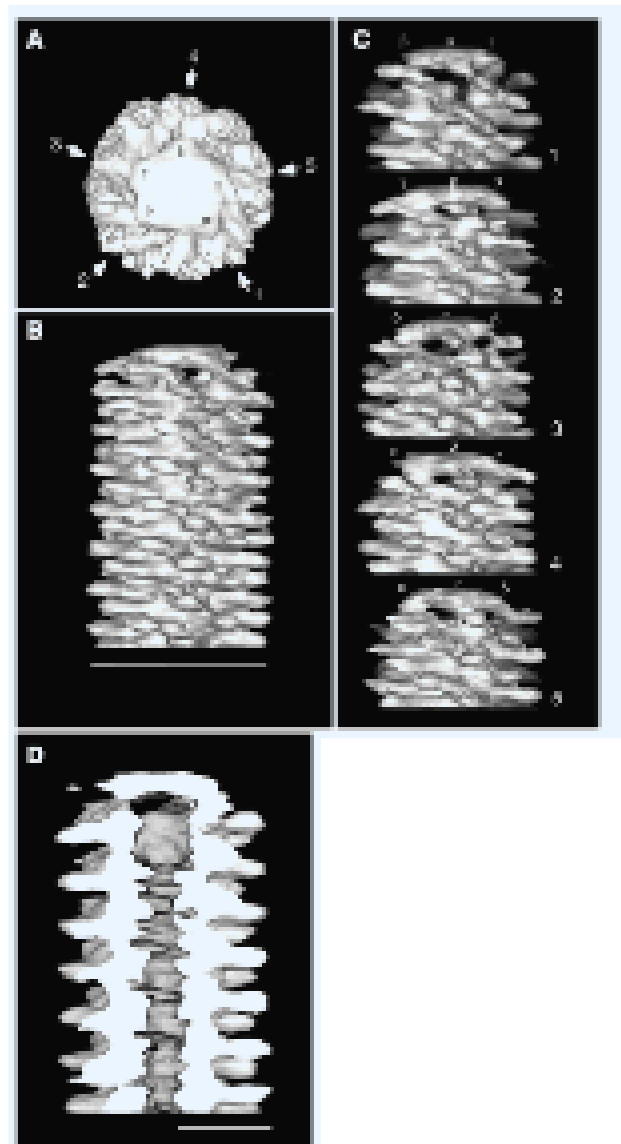


Figure 17: Three-dimensional density map of the cap-filament complex

(A) A pentagonal domain of the cap is shown on the top of a growing filament with five vertices labelled with Greek letters, α to ϵ . The arrow with a number indicates the different orientation showing the pentagon (shown in the side view in (C)). (B) The side view of the filament shows the helical structure of flagellin subunits and the plate domain of the cap. (C) Gaps from five side views' orientation, 1 to 5, are indicated with side views' section perpendicular to the corresponding numbers in (A). Notice that the gap from view 1 is significantly larger than that of the rest and predicted to be the assembly site for newly arriving flagellar subunit. (D) The cap-filament complex is vertically cut revealing the continuous hollow tube from bottom to top structure (Taken from Yonekura, 2000)

Chapter 2

Aim

2 Aims

Flagellar synthesis is an organized process precisely regulated to couple gene expression, protein secretion and flagellar assembly. A significant step of flagellar synthesis utilizes the FlgM – σ^{28} circuit to sense when the Hook Basal Body structure is completely finished before initiation of the expression of class 3 genes. The circuit efficiently explains the synthesis of a single flagellum. However, *S. enterica* possesses multiple flagellar in a peritrichous arrangement. To sense and control the processes of multiflagellar synthesis requires another level of regulation. The FlhD₄C₂ protein, a class 1 protein, is known to initiate the flagellar synthesis. Protein interactions with FlhD₄C₂ have been discovered that present an effective mechanism to control multiflagellar synthesis. FliT is able to prevent the flagellar synthesis by interacting with FlhD₄C₂. FliT-FlhD₄C₂ interaction is supposed to be an inactive complex incapable of inducing class 2 genes expression. However, the outcomes of FliT-FlhD₄C₂ interaction are still unknown. FliD-FliT interaction is strong due to those proteins being a secretion substrate (FliD) and T3S chaperone (FliT). FliT shows inhibitory effect of flagellar synthesis by inhibiting FlhD₄C₂ activity through protein-protein interaction. FliD is supposed to cancel the inhibitory effect of FliT by forming the FliT-FliD complex. This research focuses on exploring the mechanism of FliT toward FlhD₄C₂ in molecular detail under the hypothesis that FliT interacts with FlhD₄C₂ preventing flagellar synthesis uniquely at the first and crucial step in order to decide the proper number of flagella. From the hypothesis, this research was set to have specific targets as followed:

1. To explore the detail of protein-protein interactions: FliT-FliD, FliT-FlhD₄C₂ *in vitro* by using classical and advanced biochemical techniques revealing important biochemical details such as the pattern of interaction, the outcome of the interactions and the stoichiometry of identified interactions.
2. To analyse FlhD₄C₂ DNA binding capability by introducing FliT and it's mutated variants.
3. To use the bacterial two hybrid system (B2H) and test if FlhC or FlhD interacts with

FliT and if FliD can interact with FlhC or FlhD and whether this assay can be used to identify interaction mutants.

4. To determine whether the FliT regions that bind to FlhD₄C₂ or FliD overlap and if so how they influence the regulatory circuit.

5. To assess FliT, FliD and FlhD₄C₂ levels in a bacterial population by immuno blot

Statement: Aspects of this thesis have been included in the publication Aldridge et al 2010.

Chapter 3

Materials

3 Materials

3.1 Bacterial strains and Plasmids

The strains and plasmid used in this study are provided in **Table 1** and **Table 2** respectively. For analysis, the *E.coli* strain BL21 is used for the amplification and purification of proteins. The XL1B strain is used for harbouring cloned genes of Bacterial Two Hybrid System (B2H experiment). The BTH101 strain is used for analysis purpose of B2H.

Table 3: Bacterial strain table

Bacterial strain	Genotype	Reference
<i>E.coli</i> BL21	F- ompT hsdSb(rb-mb-)gal(DE3)	Promega
XL1B		
DH5	Phi-80d lacΔm15 endA1 recA1 hsdR17 supE44 thh-1 gyrA96 relA ΔlacU169	New England Biolabs
BTH101	F-, <i>cya</i> -99, <i>araD</i> 139, <i>galE</i> 15, <i>galK</i> 16, <i>rpsL</i> 1 (<i>Str</i> r), <i>hsdR</i> 2, <i>mcrA</i> 1, <i>mcrB</i> 1.	EUROMEDEX
<i>Salmonella</i> LT2	<i>Salmonella</i> (wide type)	TPA 1

Table 4: Plasmid table

Plasmid Name	Vector	Genotype	Reference
Protein expression			
pPA152	pET28a-mod	<i>fliT</i>	TPA 348
pPA158	pET28a-mod	<i>flhDC</i>	TPA 642
pPA159	pET28a-mod	<i>fliD</i>	TPA 620

Bacterial Two Hybrid (B2H)

pUT18C	pUC19	Amp ^R cloning vector <i>cyaA</i> (225-399)	EUP-18C
pUT18	pUC19	Amp ^R cloning vector <i>cyaA</i> (225-399)	EUP-18N
pKT25	pSU40	Kan ^R cloning vector <i>cyaA</i> (1-224)	EUP-25C
pKNT25	pSU40	Kan ^R cloning vector <i>cyaA</i> (1-224)	EUP-25N
pKT25- <i>zip</i>	pSU40	Kan ^R	EUP-25Z
pUT18C- <i>zip</i>	pUC19	Amp ^R	EUP-18Z
pBluescriptKS		Amp ^R cloning vector	Stratagene
pFliT	pBK	Amp ^R <i>fliT</i> ⁺	(this study)
pFliD	pBK	Amp ^R <i>fliD</i> ⁺	(this study)
pFlhC	pBK	Amp ^R <i>flhC</i> ⁺	(this study)
pUT18c- <i>fliD</i>	pUT18c	Amp ^R <i>fliD</i> ⁺	(this study)
pKT25- <i>fliT</i>	pKT25	Kan ^R <i>fliT</i> ⁺	TPA 2443 (this study)
pKNT25- <i>fliT</i>	pKNT25	Kan ^R <i>fliT</i> ⁺	TPA 2617 (this study)
pUT18- <i>fliT</i>	pUT18	Amp ^R <i>fliT</i> ⁺	TPA 2622 (this study)
pUT18c- <i>fliD</i>	pUT18c	Amp ^R <i>fliD</i> ⁺	TPA 2445 (this study)
pUT18- <i>fliD</i>	pUT18	Amp ^R <i>fliD</i> ⁺	TPA 2642 (this study)
pKNT25- <i>fliD</i>	pKNT25	Kan ^R <i>fliD</i> ⁺	TPA 2619 (this study)
pKNT25- <i>fliT</i>	pKNT25	Kan ^R <i>fliT</i> ⁺	TPA 2617 (this study)
pUT18c- <i>flhD</i>	pUT18c	Amp ^R <i>flhD</i> ⁺	TPA 2604 (this study)
pKNT25- <i>flhC</i>	pKNT25	Kan ^R <i>flhC</i> ⁺	TPA 2616 (this study)
pKT25- <i>flhC</i>	pKT25	Kan ^R <i>flhC</i> ⁺	TPA 2608 (this study)
pUT18- <i>flhC</i>	pUT18	Amp ^R <i>flhC</i> ⁺	TPA 2620 (this study)
pUT18c- <i>flhC</i>	pUT18c	Amp ^R <i>flhC</i> ⁺	TPA 2606 (this study)
pKNT25- <i>flhDC</i>	pKNT25	Kan ^R , <i>fliCD</i> ⁺	TPA 2610 (this study)
pKT25- <i>flhDC</i>	pKT25	Kan ^R , <i>fliCD</i> ⁺	TPA 2615 (this study)
pUT18- <i>flhDC</i>	pUT18	Amp ^R , <i>fliCD</i> ⁺	TPA 2612 (this study)
pUT18c- <i>flhDC</i>	pUT18c	Amp ^R , <i>fliCD</i> ⁺	TPA 2613 (this study)
pKT25- <i>fliT</i> (N74A)	pKT25	Kan ^R , <i>fliT</i> ⁺ (N74A)	TPA (this study)
pKT25- <i>fliT</i> (N74D)	pKT25	Kan ^R <i>fliT</i> ⁺ (N74D)	TPA (this study)

pKT25- <i>fliT</i> (W11R)	pKT25	Kan ^R <i>fliT</i> ⁺ (W11R)	TPA (this study)
pKT25- <i>fliT</i> (k79A)	pKT25	Kan ^R <i>fliT</i> ⁺ (k79A)	TPA (this study)

Mutated FliT protein expression

pGEX6p-1		GST expression plasmid	Stratagene
pMMT002	pGEX6p-1	<i>fliT94</i> [pGEX- <i>fliT</i> (2-94)]	Imada <i>et al.</i> (2010)
pMMT002(I68I)	pGEX6p-1	<i>fliT94</i> (I68A)	Imada <i>et al.</i> (2010)
pMMT002(L72A)	pGEX6p-1	<i>fliT94</i> (L72A)	Imada <i>et al.</i> (2010)
pMMT002(N74A)	pGEX6p-1	<i>fliT94</i> (N74A)	Imada <i>et al.</i> (2010)
pMMT002(E75A)	pGEX6p-1	<i>fliT94</i> (E75A)	Imada <i>et al.</i> (2010)
pMMT002(K79A)	pGEX6p-1	<i>fliT94</i> (K79A)	Imada <i>et al.</i> (2010)
pMMT002(L81A)	pGEX6p-1	<i>fliT94</i> (L81A)	Imada <i>et al.</i> (2010)
pMMT002(L82A)	pGEX6p-1	<i>fliT94</i> (L82A)	Imada <i>et al.</i> (2010)
pMMT002(Q83A)	pGEX6p-1	<i>fliT94</i> (Q83A)	Imada <i>et al.</i> (2010)

Over expressed FliT

pSE380			Invitrogen
pSE- <i>fliT</i>	pSE380	<i>fliT</i>	TPA

3.2 Media, agar plates and antibiotics

Table 5: Antibiotic and supplement stock including working concentrations

Antibiotic or supplement	Solute	Stock concentration	Working concentration
Ampicillin	dH ₂ O	20 mg.ml ⁻¹	100 µg/ml
Kanamycin	dH ₂ O	10 mg.ml ⁻¹	50 µg/ml
IPTG	dH ₂ O	1 M	1mM
DTT (fresh)	dH ₂ O	1 M	1mM
X-gal	DMF	2% w/vol	0.5%

3.3 Primers for PCR reaction

Table 6: Primers used in B2H and Quick change

Gene	Forward Sequence name and number	Reverse Sequence name and number	Experiment
<i>fliD</i> -C	GGCggatccCatggctcaatttcattag fliD+1BamF (445)	CCGAGCTCCTCGCGGTGTACATGGTGAC fliD+1431RSac (134)	B2H
<i>fliT</i> -C	ggcGGATCCcATGACCTCAACCGTGGAG fliT+397KpR (444)	GGCggtaccGAAGAATTTTCATACGAGAC fliT+397KpR (446)	B2H
<i>flhC</i> -C	ggcggatccATGATAATGAGTGAAAAAGCAT TGTTTCAGG flhC+1Bam (448)	CCGAGCTCCGCTGCTGGAGTGTGTTGTCC flhC+616RSc (127)	Protein expression
<i>flhC</i>	ggcggatcccATGATAATGAGTGAAAAAGCAT TGTTTCAGG flhC+1B2HBm (457)	CCGAGCTCCGCTGCTGGAGTGTGTTGTCC flhC+616RSc (127)	B2H
<i>flhC</i> -N	ggcggatccaATGATAATGAGTGAAAAAGC flhCB2HF (478)	ggcgagctcaaAACAGCCTGTTTCGATCTGTT CAT flhCB2HR (479)	B2H
<i>fliT</i> -N	ggcggatccaATGACCTCAACCGTGGAGTTTA fliTB2HF (476)	ggcgagctcaaTGAGGCGCCAGGCGCATCT GGCACGAGTAA fliTB2HR (477)	B2H
<i>fliD</i> -N	ggcggatccgATGGCTTCAATTTTCATCATTA fliDB2HF (474)	GgcgagctcGACTTGTTTCATAGCTGTAAATT GCTG fliDB2HR (475)	B2H
<i>flhD</i> -N	ggcggatccgATGGGAACAATGCATACA flhDB2H(n)F (530)	ggcggatccaTCATGCCCTTTTCTTACG flhDb2hrev-c-kpn (541)	B2H
<i>flhC</i> -N	ggcggatccaATGATAATGAGTGAAAAAGC flhCB2HF (478)	ggcgagctcaaAACAGCCTGTTTCGATCTGTT CAT flhCB2HR (479)	B2H
<i>flhC</i> -C	ggcggatccaATGATAATGAGTGAAAAAGC flhCB2HF (478)	ggcggatccaTTAAACAGCCTGTTTCGATCT flhCB2H(c)R (535)	B2H
<i>flhCD</i>	ggcggatccgATGGGAACAATGCATACA flhDB2H(n)F (530)	ggcgagctcaaAACAGCCTGTTTCGATCTGTT CAT flhCB2HR (479)	B2H
<i>flhCD</i>	ggcggatccgATGGGAACAATGCATACA flhDB2H(n)F (530)	ggcggatccaTTAAACAGCCTGTTTCGATCT flhCB2H(c)R (535)	B2H
<i>fliT</i> (N74A)	Catcaaaaaacgctggagctgagcagctcctgaaaggg N74A (556)	Cccttcaggagctgctcagcgtccagcgtttgttgatg N74A_antisense (557)	Quick change
<i>fliT</i> (K79A)	Caatgagcagctcctggcagggtgctgcaacag K79A (558)	Ctgttgagcagccctgccaggagctgctcattg K79A_antisense (559)	Quick change
<i>fliT</i> (N74D)	Tcaaacaacgctggagctgagcagctcctgaaa N74D (560)	Ttcaggagctgctcatcgtccagcgtttgttgga N74D_antisense (561)	Quick change
<i>fliT</i> (W11R)	Caacctggagtttatcaacctagcagcgtattg W11R (562)	Caatagctgcctacggtgataaactccagcgttg W11R_antisense (563)	Quick change

3.4 DNA Preparation and cloning

PCR machine

- Thermocycler T3000 Biometra

Kits, enzymes

- Proteinase K 20 g/1L
- Bacterial Genomic DNA KIT GenElutetm (Sigma)
- HP plasmid Midiprep kit GenElutetm (Sigma)
- HP plasmid Midiprep kit GenElutetm (Sigma)
- PCR Clean Up Kit GenElutetm (Sigma)
- Gel Extraction Kit GenElutetm (Sigma)
- QuickChange Site-Directed Mutagenesis kit
- Restriction enzyme (Fermentus)
- Primers
- INTEGRATED DNA TECHNOLOGIES INC (IDT)
- www.idtdna.com
- T4 ligase 3U/μl (promega)
- High fidelity enzyme (HF) (Roalab)
- Moltaq Thermostable enzyme (MolzymbGmbH & Co.kg)
- PfuTurbo DNA polymerase conc 2.5U/μl (Stratagene)
- DpnI conc 10U/μl (Stratagene)

3.5 Protein Preparation

Sonicator

Branson (digital sonifer)

Liquid Chromatography System

- AKTA prime plus (GE Healthcare)

Plotter

- REC112 (GE Healthcare)

Protein purifying Columns

- Hiload 16/60 superdex 200 GE prep grade (GE Healthcare)
- Histrap_{tm} Chelates HP column 5 ml (Amersham Biosciences)
- Histrap_{tm} Heparin HP column 5 ml (GE Healthcare)

Protein concentrator

- Vivaspin 20 10,000 CO (Vivaspin)

Glutathione Sepharose 4 Fast Flow 25 ml

3.6 DNA and protein analysis

Gel-doc

- Ingenius syngene bioimaging (Syngene)
- Power pac 300 (Biorad)

Agarose and Acrylamide gel

Developer

- SRX-101A (KonicaMinolta)
- ImageQuant LAS 4000mini (GE Healthcare)

ECL plus western Blotting Detection system

- Amersham Hyperfilm ECL High performance (GE Healthcare)
- Chemiluminescence film (GE Healthcare)

Blot paper

- Amersham Hyperbond-P (GE Healthcare)

seeBlue@plusz Prestrained standard

(Invitrogen)

1 kb DNA Ladder (G5711)

2% x-Gal in DMF

3.7 Analytical instrumentation

- Analytical Ultracentrifugation (AUC)
- Isothermal calorimeter (ITC)
- Surface Plasma Resonance (SPR) (Biacore,Biorad)

Chips for SPR experiment

- SA- chip sensor chip (GE Healthcare)
- NCL-chip sensor chip (Biorad)

3.8 Others

Centrifuge

- HAWK 15/05 Refrigerated (Sunyo)
- 3-16PK Roter 11180 (Sigma)
- Model Avanti J-26XP (Beckman Coulter)
- Roter JA 25.50 MAX 25000 RPM
Fiberlite F10BCI-6x500Y

Waterbath Static Water Bath

with variable heat control (Grant instrumenta)

UV/visible Spectrophotometer

- Ultraspect 1000 UV/visible (Pharmacia Biotech)

Filter membrane

- MFtm Membrane filters 0.45 μ M (Millipore)

Western tank

(Amershan Biosciences)

pH meter

(JENWAY 3510)

Weight

- Model PB602-s/FACT (Mettler Toledo)
- Model EG620-3NM (KERN EG)

Aspirator**Microscope**

- Vickers Magnifier (40/0.65) (Vickers England)

Deep freezer

- -80 Ultralow (vip series -80°C) (Sanyo)

Water system

- PURELAB FLEX (ELGA)

Computer software

Chapter 4

Methods

4 Methods

4.1 Bacterial growth

Growth of *S. enterica* and *E.coli* strains was conducted in Luria Bertani (LB) broth at 37°C with continuously shaking. Appropriate antibiotics and growth supplement were added (**Table 4**) Monitoring growth was performed by measuring optical density (OD at 600 nm) using a spectrophotometer. For obtaining cells at log phase, the culture started growing from diluted overnight culture ($OD_{600} = 0.05$) and then cultivate when the OD_{600} reached 0.6-0.8. For long term storage, strains were frozen at -80°C with DMSO as a cryoprotectant added to a final concentration of 15% w/v. For growing bacteria in solid media, 1.5% agar was used. In motility assays, 0.3% agar was used.

4.2 DNA manipulation procedure

4.2.1 Sigma Bacterial Genomic DNA KIT

E. coli strains were inoculated in 3 ml of LB broth with the needed antibiotic and left overnight at 37°C with continuous shaking. The cells were collected by centrifugation at 12,000 rpm for 2 mins. The supernatant was discarded leaving the cell pellet to be resuspended in 180 µl of Lysis Solution (DNA KIT). Isolation of genomic DNA then followed the manufactures protocol. The chromosomal DNA was eluted by adding 200 µl of the Elution Solution or water to the columns and left at room temperature 5 minutes before performing a final centrifugation (9,000 rpm for 1 minute at 4°C). The genomic DNA was kept at -20°C for further usage.

4.2.2 Isolation of plasmid DNA

4.2.2.1 Crude plasmid DNA extraction

Three to five millilitres of overnight culture from single colony grown in LB with selective antibiotic was performed at 37°C was harvested by centrifugation (1 mins; 12,000 rpm; 4°C) into microfuge tubes. The supernatant was discarded and the pellet homogenously resuspended in 300 µl of solution I (50 mM Glucose, 25 mM Tris HCl

pH 8.0, 10 mM EDTA pH 8, 0.5% RNase A). Then 600 µl of freshly made solution II (200 mM NaOH, 1% SDS) was applied to the resuspended pellet with gently shaking. The solution was incubated in room temperature 5 minutes before adding 250 µl of Solution III (3 M Potassium acetate, 11.5% v/v Glacial acetic acid) with agitated shaking. Upon centrifugation (12,000 rpm for 10 minutes at 4°C), the pellet was left undisturbed, while the supernatant was transferred to a new tube. The plasmid DNA was precipitated by adding 600 µl isopropanol, plasmids were subsequently pelleted by centrifugation (12,000 rpm for 20 minutes at 4°C). The supernatant was carefully discarded without disturbing the colorless pellet at the bottom of the tubes. To wash the pellet, 500 µl of 70% ethanol was added to the tubes and spun down (12,000 rpm for 5 minutes at 4°C). After aspiration and drying the pelleted DNA in a speed vac (10 minutes), the plasmids were resuspended in 25-50 µl according to the copy number of the plasmids.

4.2.2.2 Sigma PLASMID MINI-PREP KIT

A single colony of *E. coli* strain harbouring the plasmid was inoculated in 3-5 ml of liquid LB broth with the appropriate antibiotic and left to grow over night at 37°C in a shaking incubator. Centrifugation of 1.5 ml culture (12,000 rpm for one minute) was performed in a microfuge tube. Plasmid DNA was then isolated according to the manufacturers protocol. Before elutions a final centrifugation of the empty column (12,000 rpm for 1 minutes at 4°C) to ensure all residual liquid had been removed. The eluted plasmids was quantified and kept in 20°C for further experiments.

4.2.3 Restriction endonuclease digestion of DNA

4.2.3.1 Simple Test Digests

DNA (50 ng/ml) of each clone was prepared for a 20 µl reaction. Adding together, 10 µl of DNA, 0.5 µl Bovine Serum Albumin (BSA) and 2 µl of 10X restriction buffer, was mixed in a microfuge tube. 0.5 µl of each endonuclease was needed for each reaction, of which the total volume was adjusted to 20 µl by the addition of ddH₂O. The reactions were incubated at 37°C for one hour. The total samples were run on 0.8% agarose gel and checked for the right size of DNA fragments under UV light.

4.2.3.2 Cloning Experiments

Sigma plasmid preparation was desirable for obtaining the purer quality of plasmids. For cloning experiments 1-2 µg of vector DNA was digested in a 50 µl reaction; 5 µl of 10X compatible restriction buffer, 1-2 µl (12 U/µl) of each restriction endonucleases, with water adjusting the final volume to 50 µl in total. If DNA inserts were derived from PCR reaction, a PCR products were purified with a SIGMA kit before digestion in a 50 µl volume. All reactions were incubated at 37°C for 3 Hours. An aliquot of each reaction 5 µl was checked by 0.8% agarose gel electrophoresis. If only one clear band was observed on the gel, the DNA was prepared for the next ligation step. In case of multiple bands, entire reactions were run on a gel before using a Sigma Gel Extraction Kit to extract only the desirable fragments of DNA. For vectors, DNA precipitation was carried out and resuspended in 20 µl dd water.

4.2.4 Ligation of DNA fragments

After purifying the digested DNA inserts and vectors, 20 µl ligation reactions were prepared following the experimental criteria using excess molar amounts of insert to vector. 1µl of vector (50 ng/µl) and 1-16 µl of insert DNA were ligated in a 20 µl reaction with the further addition of 2 µl (10X ligation buffer), 1 µl of T4 ligase and adjusted to 20 µl with ddH₂O. The reactions were incubated either at room temperature for one hour or at 4°C overnight

4.2.5 Heat shock transformation of *E. coli* cells

4.2.5.1 Preparation and storage of competent cell

A 5 ml LB overnight culture grown at 37 °C with constant shaking was evaluated at OD₆₀₀. 200 ml LB with the appropriate antibiotic was inoculated to have OD₆₀₀ = 0.05. The prepared culture was incubated at 37°C with constant shaking until the OD₆₀₀ of the culture reaching 0.1-0.2. Pelleting cells from the culture was conducted using sterile containers to be centrifuged for 10 minutes at 4°C, 8000 RPM. The supernatant was then discarded carefully and the pellet resuspended homogenously in 40 ml pre-chilled sterile 100 mM CaCl₂ solution. The solution was kept on ice for 40 minutes and then centrifuged 10 minutes at 4°C, 8000 RPM to collect the pellet. The pellet was resuspended in 1 ml pre-chilled sterile 100mM CaCl₂ solution and

sterile 100% glycerol to provide the final concentration of 10% v/v. 100 µl of the solution was transferred to sterile microfuge tubes and subsequently submerged into liquid nitrogen (Shock-freeze). The competent cells were stored at -80°C.

4.2.5.2 Heat shock transformation

Ready prepared *E.coli* competent cells in tubes from -80°C were kept on ice 30 minutes before 50 ng DNA was added and the solution vortexed. The tubes were incubated on ice further 10 minutes, after which it was heat-shock by exposing tubes for 50 seconds to 45°C water or a heat block. Immediately after the tubes were transferred to ice for 2 minutes and the cells suspended in 0.9 ml LB media. The solution was incubated at 37°C with constant shaking for 1 hour before plating the solution with diluted series on selective LB agar plates.

4.2.6 Oligonucleotides as primers

Primers were designed manually by using sequences from the NCBI databases. Primers quality was analysed figuratively in terms of creating; self dimer, self end dimer and informing; TM, GC percent and 3' end stability by Amplifix program. The functional primers were then ordered from IDT (Integrated DNA Technologies).

4.2.7 Polymerase Chain Reaction (PCR)

PCR reactions were performed to amplify desired DNA fragments with selected primers. The 50 µl reactions were set up containing approximately 50-100 ng template, 20 pM of both forward and reverse primers, the four dNTPs each at a final concentration of 2.5 µM, PCR reaction buffer compatible with polymerase, and 1 U of polymerase. In some cases, DMSO at a final concentration of 1 % was added to improve PCR efficiency. The reactions were then placed in a PCR machine following cyclic steps of denaturation, primer annealing and DNA extension. The detail of each step, time and cycle, can be set and kept in the machine as an automatic program (**Appendix H**).

4.2.8 Purification of a PCR fragment (DNA Precipitation)

4.2.8.1 Ethanol precipitation

For a 50 µl PCR reaction, 0.1 volume of 3M Sodium Acetate (5 µl) and 2.5 volume of 100% ethanol (125 µl) were added to the reaction. The PCR DNA was precipitated by storing the solution -80°C for 30 minutes before spinning at 13,000 rpm, 4°C for 15 minutes. After gently discarding the supernatant, the pellet was rinsed with 500 µl of 70% ethanol and centrifuge at 13,000 rpm, 4°C for 10 minutes. Again the supernatant was gently discarded before drying the pellet in the speed vac for 5-10 minutes. The washed pellet was resuspended to the desired volume of buffer or ddH₂O and kept at -20°C.

4.2.8.2 Sigma PCR Clean-Up Kit

To clean PCR products for downstream experiments a PCR clean-up kit was used. The protocol used was according to the manufactures instructions. To elute DNA from the membrane, 50 µl ddH₂O was added to the columns and the columns centrifuged (12,000 rpm for 1 minutes at 4°C). The eluted DNA was stored at -20°C ready for further usage.

4.2.9.3 Sigma Gel Extraction Kit

Extracting DNA, PCR fragments or plasmids, from agarose gel was necessary when multiple bands of DNA fragments were observed on the gel or purified DNA needed. The right band of DNA was observed and selected under UV light and then excised from the agarose gel with a sharp scalpel. The weigh of gel slice was recorded. The DNA was extracted from the agarose according the kits instructions. After the final wash the column was transferred into a new tube and 50 µl of ddH₂O added. The column was centrifuged (12,000 rpm for 1 minutes at 4°C) to elute the bound DNA. The eluted DNA was quantified and kept in 20°C for further experimentation.

4.2.9 Quantitation of DNA

DNA can be quantified by measuring absorbance at 260 nm with a nanodrop machine. The machine can analyzes the concentration of DNA using a defined

protocol returning the concentration as ng/μl and indicating its purity by automatically measuring the 260/280 ratio.

4.2.10 Agarose gel electrophoresis

Electrophoresis on agarose gel is the method for separating different sizes of DNA by the natural electrical property of DNA against electrical field. All agarose gels used in this study included 1X TAE buffer. DNA was visualised by adding 8 μl of Ethidium Bromide 1 mg/ml to 150 ml of melted agarose. Samples were prepared prior to loading by adding stop buffer to a final concentration 1X, which included glycerol to increase the density of the samples allowing them to deposit at the bottom of the wells. The 1 kb DNA marker (Promega) was loaded along with the samples. Voltage was then typically applied using 10 V/cm. The DNA fragments in an agarose gel were observed on a transilluminator using UV light (300 nm). Following the visualization of the resolved DNA fragments, the dimensions of the fragments of DNA were assessed by comparing of the bands with the reference standard DNA marker.

4.3 DNA mutagenesis (QuickChange Site-Directed Mutagenesis kit)

The QuikChange® site-directed mutagenesis kit allows the introduction of a site-specific mutation in double-stranded plasmids. This rapid four-step procedure creates point mutation in order to identify the functioning region of proteins. The QuikChange site-directed mutagenesis method is performed using *PfuTurbo*® DNA polymerase to replicate both plasmid strands with high fidelity beyond the designed primers' region. Incorporation of the designed primers to each strand of plasmids creates mutated plasmids with staggered nicks. Following temperature cycling, the product is digested with endonuclease *Dpn* I, which target only the parental DNA template containing, methylated and hemimethylated DNA. The mutated DNA strand newly synthesized is resistant to *Dpn* I cleavage and once transformed into competent cells the blunt-end ligation of circularized plasmids can be recovered. (**Figure 18**) The colonies containing the vector DNA containing the desired mutations are expected.

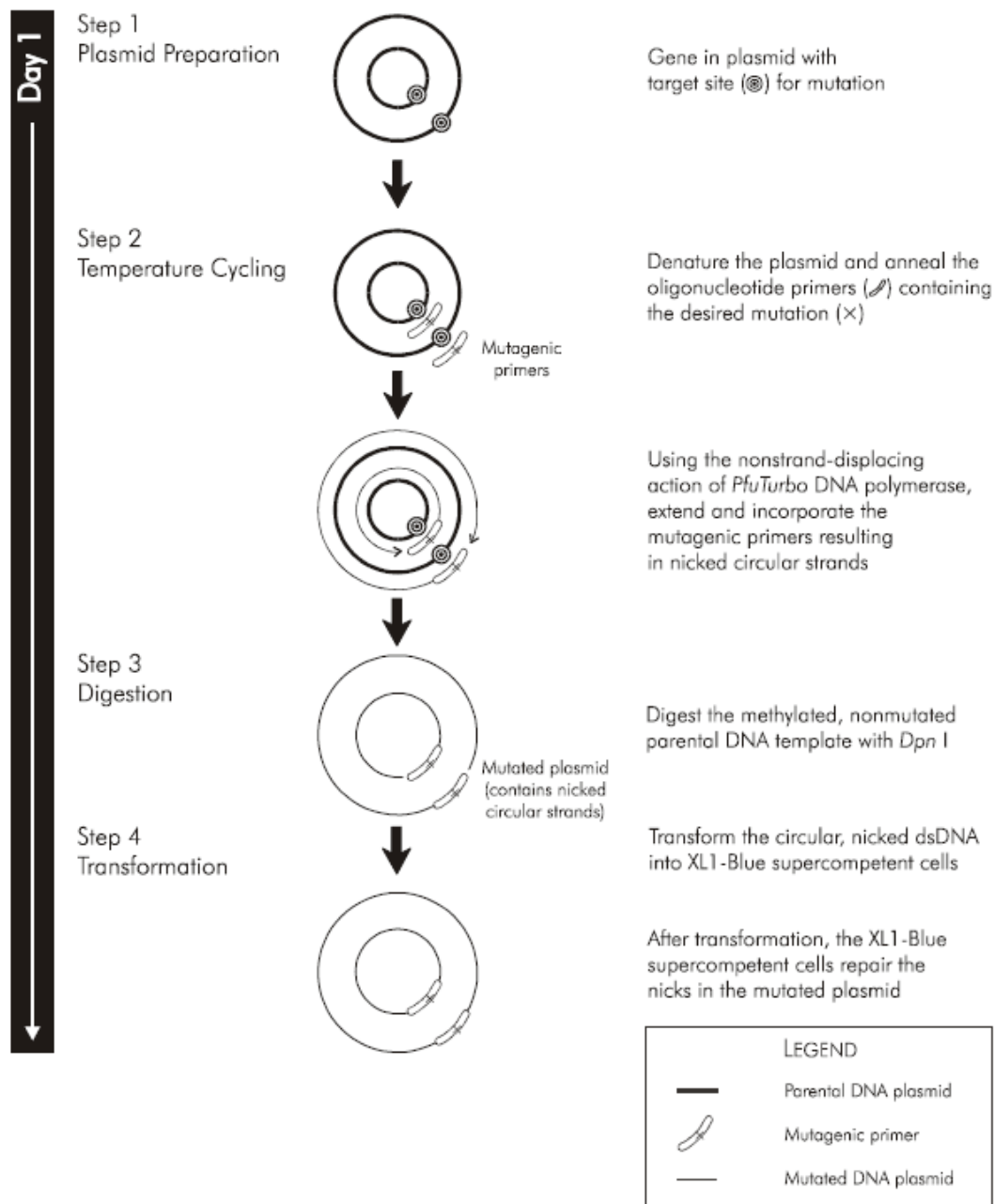


Figure 18: Processes of the QuikChange® site-directed mutagenesis method.

Four steps are in practical experimental explanation; step 1 Plasmids with mutation targets, step 2 desired primers were used with *Pfu Turbo* DNA polymerase to extend the primers creating the nicked circular plasmids, step 3 digest the methylated parental strand with *Dpn* I, step 4 transform the nicked plasmid to be repaired in XL 1-Blue. **Taken from QuikChange® Site-Directed Mutagenesis, INSTRUCTION MANUAL (Stratagene)**

The mutagenic primers were designed individually based on the desired mutated sequence following the criteria as first both of the mutagenic primers must contain the desired mutation and second they have to anneal to the same sequence on opposite strands of the plasmid. A 50 µl PCR reaction was prepared using *PfuTurbo* as DNA polymerase (2.5 U), 125 ng of both primers, 30 ng of plasmids, 2 µmole of each 4 dNTP and 1X final concentration of *PfuTurbo* buffer. The PCR reaction conditions were set as described (**Appendix H**) mainly following the strict manufacture' instruction: 18 cycles of amplified cycle and 1 minute/kb of plasmid length of extension time. After PCR reactions were completed, 10 U of DpnI was added to the reactions incubated for approximately 1 hour at 37 °C. The whole reaction was immediately transformed in to 200 µl of XL1B competent cells. The plasmids of positive clones were extracted (Sigma Prep) and sent to check their mutated sequence.

4.4 Bacterial two hybrid system (B2H)

This *in vivo* technology tests for protein-protein interactions. In this project the BACTH system from Euromedex was supplied by Richard Daniel (CBCB). Cloning of genes into the pUT18(c) and pKT25 vectors was designed as described in the Bacterial Two Hybrid manual (EuroMedex). Correct plasmids were purified and their concentration adjusted to be 50 ng/µl. For identification of interactions 2 µl of each plasmid was co-transformed in to BTH101 using heat-shock transformation. Transformations were plated on LB-agar plates containing kanamycin, ampicillin and X-Gal. Plates were incubated at 37°C and the developing of blue colonies was observed at 24, 48 and 72 Hrs.

4.4.1 *B-galactosidase activity assay*

To quantify the level of β-galactosidase activity encoded by the *lacZ* gene of the *lac* operon, the ability of β-galactosidase to enzymatically cleave the synthetic compound o-nitrophenyl-β-D-galactoside (ONPG) producing a yellow color was used. A 5 ml LB culture of colonies to be tested was incubated at 30°C with constant shaking. Colonies were fresh transformants that had grown only for 24 hours. The density of cells using the OD₆₀₀ was monitored periodically. When the culture's OD₆₀₀ was in the region of 0.6-0.8, cells was spun down, resuspended in 3 ml Saline and kept

tubes on ice. Z-buffer (**Appendix A**), needed to lyse cells and release the enzyme was always freshly prepared. 0.55 ml of the solution was added to a new test tube of which the number corresponds to the samples plus two negative controls before adding 0.1 ml chloroform. For quantifying activity of B2H strains, 500 μ l of saline cell suspension was always used. The 500 μ l of the cells was mixed with the prepared Z-Buffer by vortexing the solution and incubated at 30°C with constant shaking. 0.2 ml of the substrate, ONPG in Z-buffer 4 mg/ml, was added to the solution while timing the reaction exactly 10 minutes and possibly observing the yellow color of the solution. To stop the reaction 0.5 ml of 1M Na₂CO₃ was added. The OD₄₂₀ and OD₅₅₀ of the reaction's solution were measured while the OD₆₀₀ of the Saline solution at room temperature. The β -galactosidase activity in Miller unit was then calculated.

4.5 DNA sequencing

DNA sequence was performed by GATC Biotech Company. High quality plasmid or PCR DNA was prepared using the respective Sigma kit. The DNA concentration was measured using a Nano drop. The concentration range needed for sequencing plasmids was 30-100 ng/ μ l and 10-50 ng/ μ l for PCR products.

4.6 Protein purification procedure

4.6.1 Cell Culture and Preparation

Strains from -80°C glycerol store were plated on LB plates with appropriate antibiotic. A single colony was inoculated to 25 mL LB + required antibiotic and left overnight at 37°C. The 25 ml overnight culture was inoculated to 1L of LB + the antibiotic. The culture was kept at 37°C with shaking until the absorbance of the culture reached OD₆₀₀ = 0.6. IPTG (1M) was added to a final concentration of 1 mM and further incubate at 30°C for 3 Hrs. Cell pellets were then collected by centrifuging at 8000 rpm for 10 min at 4°C and stored at -80 °C. For expression of *flhDC* the plasmid pPA158 was freshly transformed in to BL21 each time by heat shock transformation.

4.6.2 Cell Disruption

The cell pellet from -80°C was defrosted on ice and resuspended in 20 ml of an appropriate loading buffer. The resuspended solution was sonicated with the increasing power 20, 25, 30, 35 sequentially for 30 secs interrupted with 30 secs pause on ice. The suspension was then centrifuged at 30,500 rpm at 4°C for 30 min to remove cell debris. The supernatant was then used immediately for the purification process.

4.6.3 Purification of bacterial proteins

4.6.3.1 His tag isolation of FliT and FliD

His-tag column purification is the first step for purifying His-tag FliD and His-tag FliT. The crude protein samples was loaded on to pre-calibrated His-tag column (5 column volume of loading buffer) at the rate 2 min/ml. Loading buffer was continuously running until the protein monitoring system (OD₂₆₀) reached baseline. Proteins were eluted by passing the gradient (1%/min) of elution buffer. Two millilitre fractions were collected, labelled and kept on ice. To observe the quality of the purified proteins, 16.5% tricine gel electrophoresis of fractions was performed.

4.6.3.2 Heparin isolation of FlhD₄C₂

Instead of using a His-tag column, FlhD₄C₂ was purified using a heparin column calibrated with heparin loading buffer as the yield was ten-fold higher than using the His column. The crude protein sample was applied to the column at the rate 1ml/min and Loading buffer continuously run until the protein monitoring system (OD₂₆₀) reached baseline. Unspecific bound proteins were washed off with a constant 20% elution buffer washing step. Proteins were eluted by applying a continuous gradient (1%/min) of elution buffer from 20% to 100%. Fractions with protein were collected (2 ml/ fraction), labelled and kept on ice. The quality of the purified FlhD₄C₂ was confirmed by 16.5% Tricine gel electrophoresis.

4.6.3.3 GST-protein isolation

GST fusion proteins were isolated using glutathione sepharose beads (Glutathione Sepharose 4 Fast Flow (GE Healthcare)). The amount of slurry used for purification varied according to culture volume. In general, 1 mg of fusion protein approximately from 400 ml culture needs 400 μ l of a 50% slurry suspension (200 μ l sepharose bed volume). Glutathione beads were prepared by adding 5 ml of filtered (0.45 μ m) PBS to 1 ml of slurry. Beads were sedimented by centrifugation at a slow 500 g spin for 5 minutes and decanting the supernatant. Washing steps were repeated three times. Cell lysate from 400 ml cell culture pellet was prepared in 20 ml 1X PBS and filtered through 0.45 μ m filter (Referred cell disruption). The cell lysate was added to the prepared beads in the blue cap 50 ml Falcon tube and incubated at room temperature for 1 hrs. The solution was transferred to a small column that can trap beads but allow the supernatant (flow-through), which is saved for further SDS-PAGE analysis, discarded out of the column by gravity flow. The beads were washed three times by adding 5 ml of PBS and the supernatant collected. Next, 0.5 ml elution buffer, freshly prepared by adding reduced glutathione powder to 20 mM Tris HCl solution pH 8.0 was added to the column. The elution step was performed two or three times. To observe the presence and quality of the purified proteins from the elution, Tricine gel electrophoresis was performed.

4.6.3.4 Gel filtration of FlhD₄C₂, FliT and FliD

Gel filtration step is necessary for achieving high quality of proteins. After performing SDS-PAGE (Tricine 16.5%), His-tag (FliD and FliT) or Heparin (FlhD₄C₂) purified protein fractions containing a high amount of protein were concentrated to 2.5 ml by using a protein concentrator (vivaspin) with the appropriate kDa cut off. The equilibration of S200 gel filtration column was first conducted by passing 3 Column volumes through of a suitable gel filtration buffer at the rate of 1 ml/min or 0.2 ml/min overnight before starting purification step. The concentrated protein was injected to the column by using 2.5 ml injection loop. Fractions were collected (1 ml/fraction), labelled and kept on ice. 16.5% Tricine gel electrophoresis was performed to identify the fractions containing proteins.

4.6.4 The measurement of protein concentration

The presence of aromatic side chain along protein chain allows protein to be capable of absorbing UV light (280 nm). The absorbance is proportional to the protein concentration following the simplified equation $A = xC$, which A = Absorbance, C = Concentration and x = coefficient. Many factors contribute to the value of “ x ” such as the proportion of aromatic amino acid in protein and the length of the solution light pass through the solution. The figure “ x ”, which is distinctive to different protein, can be obtained by the prediction of protein sequence (NCBI website). As a result, the 280 nm absorbance assay provided the predicted concentration of an interested protein. Diluting a protein sample was needed if the OD_{280} value is more than 1. Using gel filtration buffer as a blank solution, OD_{280} of the sample was measured and need some calculations the protein concentration (**Appendix C**).

4.6.5 Thrombin digestion

Recombinant fusion proteins with a polyhistidine-tag or His-tag residue at their C terminal provide an effective way for protein purification. In many expression plasmids, thrombin recognition sequence is encoded and usually located between the cloning sites and polyhistidine-tag sequence. The proteolytic removal of His-tag residue from the expressed target protein can be performed by Thrombin digestion. Before performing the experiment, thrombin concentrations, temperatures and incubated times were assessed by a small scale optimisation. Working concentration of enzyme ranging from 1 U/10 mg to 0.01 U/10 mg were usually tested in a 50 μ l reaction. All reactions were carried out at room temperature. To monitor the cleavage, 5 μ l of the reactions were aliquoted to 1.5 tube at different incubated time of 0, 15, 30, 60, 120, 240 minutes and overnight. Adding 2.5 μ l of 2X SDS-buffer to each reaction, the samples were boiled for 5 minutes and 16.5% Tricine SDS-PAGE was performed. The pattern of digested protein process was monitored.

Performing a large-scale protein digestion was conducted using the data from the small scale optimisation. Gel purified quality His-tagged proteins were first prepared. Protein (1 mg) was diluted in 5 ml of gel filtration buffer and digested with Thrombin (often 0.1 U) at room temperature for four hours. The digested solution was purified by gel filtration again to separate the His-tag moiety and the proteins.

Fractions containing the protein were collected and pooled together. If needed the proteins were concentrated by protein concentrator (vivaspin) with the selected kDa cut off. The concentrated proteins were kept at -4°C.

4.6.6 Cell lysate preparation for western blot

A colony of a bacterial strain was incubated in Luria Bertani (LB) broth overnight at 37°C with continuous shaking. Selective antibiotic was also added with appropriate concentration (**Table 5**). To obtain the OD₆₀₀ of overnight culture, the absorbance of 1:10 diluted culture was measured prior to calculating back to the functional OD₆₀₀ value. For cultivating cells at the log phase, the culture (OD₆₀₀ = 0.05) was prepared and harvest cells when OD₆₀₀ of the growing culture reached 0.6. To predict the approximate amount of cells, colony forming unit (CFU) was performed. Cells from 1 ml of culture were spun down and the supernatant discarded. The cells were suspended in 2X SDS-buffer and resuspended vigorously prior to boiling for 3 minutes. The solution was kept at -20 °C for further analysis

4.6.7 Protein gel electrophoresis (PAGE)

The qualitative analysis of proteins can be achieved effectively by performing polyacrylamide gel electrophoresis (PAGE). It is essential for providing the information of purified proteins such as purity and size of protein. Analyzing preparative proteins by using denatured or SDS-PAGE is quite accurate and reliable. Protein samples were denatured to individual fragments and separated according to their size. An estimate of the true conformation of protein complexes or interactions can be obtained with Native Gel Electrophoresis to which nondenaturing conditions are applied.

4.6.7.1 Native gel electrophoresis

The experiment used 10% native acrylamide gels without a stacking gel (**Appendix A**). When placed into the electrophoresis tank, the assembly was completely filled with native buffer. The comb was gently removed and native buffer used to rinse the wells thoroughly to remove debris. A maximum volume of 20 µl of sample was loaded into individual wells using 1% albumin solution as a maker. The gel was run at the

fixed current (5 mA / gel) at 4°C for between 4-6 Hrs. Gels were immersed into comassie staining solution for at least one hour or overnight before destaining to observe bands.

4.6.7.2 SDS Protein gel electrophoresis

The majority of SDS-PAGE performed in this study used 16.5 % gels due to the size of FliT, FliC and FliD. Sometimes however 12% gels were used for better resolution of FliT:FliD mixed fractions. To run gel electrophoresis the inner chamber was filled with 1X cathode buffer. To remove debris, a syringe with cathode buffer was used to rinse wells. A maximum volume of 20 µL of sample and 5 µl of molecular weight marker were loaded into individual wells using a gel loading pipette tip. 1X anode buffer was filled outside the chamber to cover the bottom of the gel cassette assembly. Gels were run at the fixed current at 25 mA / gel for the stacking gel and 40 mA / gel for the separating gel at room temperature. The gel was run until the dye front reached the bottom of the gel. Visualisation of proteins was achieved by comassie staining

4.6.8 Western blot analysis

Gels were laid into a blotting cassette with an appropriate membrane on the positive side. The blotting cassettes were submerged in CAPS transfer buffer and a fixed voltage of 200 V was applied for 120 minutes. Removing the blot from the assembly, the membrane was incubated with PMT (1X PBS (pH7.4), 5% Milk, 0.1% Tween) overnight with constant shaking at 4°C. The blot was washed 4 times, 5 minutes each, with PMT. The desired primary antibody, was added at a concentration obtained from a trial run along with new PMT and then incubated for 2 Hrs at RT with constant shaking. The membrane was washed 4 times in fresh PMT and then secondary antibody, Goat-α-Rabbit IgG coupled to horseradish peroxidase (Gibco BRL), was diluted 1:10,000 into 5 ml PMT and added to the membrane for 60 minutes at RT with constant shaking. The membrane was washed 4 times with 1X PBS at RT. 3 ml of Lumigen PS-3 Detection Reagent Solution A with 75 µl of Lumigen PS-3 Detection Reagent Solution B was then incubated on the membrane for 5 minutes at RT with constant shaking. The membrane was dried and

fluorescence emittance detected by exposing to a sheet of Amersham Hyperfilm ECL (GE Healthcare).

4.7 Protein analysis procedure

To further characterise the native configuration of a protein subunit, its stoichiometry as well as assembly and disassembly mechanisms of biomolecular complexes, several high-technology machines were used to collect the different sets of information.

4.7.1 Analytical Ultracentrifugation (AUC)

AUC analyses soluble macromolecules by means of applying a centrifugal force with the direct real-time observation of the redistribution of the macromolecule. In addition, the technique requires no label or any chemical modification of proteins for detection and there is no interaction with any matrix or surface as required for a gel filtration. A key feature of the technique is for the characterization of weak or transient interaction. For non-interacting proteins, the molar mass, shape, and the heterogeneity of the sample can be revealed. The latter includes the analysis of the forming oligomers in solution. To plan an analysis, at least three different concentrations of a sample, covering as wide a concentration as possible, are needed to acquire an information-rich data set, which is highly effective in the analysis of the properties of proteins in solution, in particular, their interactions. Interacting components may have sizes ranging from peptides to very large multiprotein complexes. The analysis was performed by Analytical Ultracentrifugation facility (ICAMB, Newcastle University). The sample of protein solution (2 mg/ml) was sent to the service unit along with its working buffer.

4.7.2 Isothermal calorimeter (ITC)

Two interested proteins were purified to the range of 30-300 μM in 5 ml, this large amount of protein needed for FlhD₄C₂: 6 litres give FlhD₄C₂ and FliT: 3 litres of culture. The purification step follows the same protocol except that 2 mM DTT was used in gel filtration buffer. The assays were then performed with Christine Aldridge and Helen Lamb according to standard ITC protocols.

4.7.3 Surface Plasma Resonance (SPR)

An advantage of SPR is the small amount of the protein needed for the assay compared to AUC and ITC (nM). The SPR protocols define one protein as a “ligand” normally attached to the surface of a sensor chip, where a protein-protein interaction occurs. The second protein or “analyte” is then passed over the surface via a microfluidic system. If the analyte interacts with ligand, the refraction index at the surface of the chip changes and is viewed in real time as an increase in signal. “Resonance units” are termed for the increase of the signal. A linear relationship between the mass on the chip and the resonance unit is observed as $1 \text{ RU} = 1 \text{ pg/mm}^2$ (Schuck, 1997). Following the change of signal, a molecular interaction between analyte and ligand happens through the association and dissociation phase. The increasing RUs figure reflects the more amount of the protein actually on the chip while the association – dissociation pattern of a graph determine the kinetic behavior of the interaction (**Figure 19**). All SPR experiments were carried out in BIAcore 2000 or Bio-Rad Proteon XPR36 machine. The experiment was carried out as the following outline.

- **Prepare or activate a selected chip (SA)**

For DNA-protein interaction experiments, SA or neutravidin coated sensor (GE Healthcare and Bio-Rad) was selected. To prepare a chip prior to immobilization process, 1 M NaCl and then 0.05 M NaOH were injected over all flow cells for 60 s at a flow rate 10 ml/min for three consecutive times to ensure removing all unspecific bound compounds.

- **Prepare experimental DNA fragments**

The experimental selected fragments of DNA was as a 80 bp double-stranded oligonucleotide, with a 5' biotinylated forward strand of the *flgB* and *flhB* binding sites of FlhD₄C₂ (**Table 7**) (Stafford *et al.*, 2005). Negative control of DNA was an intergenic region of *fliC* (**Table 7**). DNA was prepared by using PCR machine to anneal each forward and reverse strand of each gene. Two steps were needed for the annealing; 94°C for 2 min and, cooling to 25°C over 45 min. Experimental DNAs were kept at 4°C until use.

Typical Interaction Assay Sensorgram

A "sensorgram" is a plot of the SPR signal vs. time.

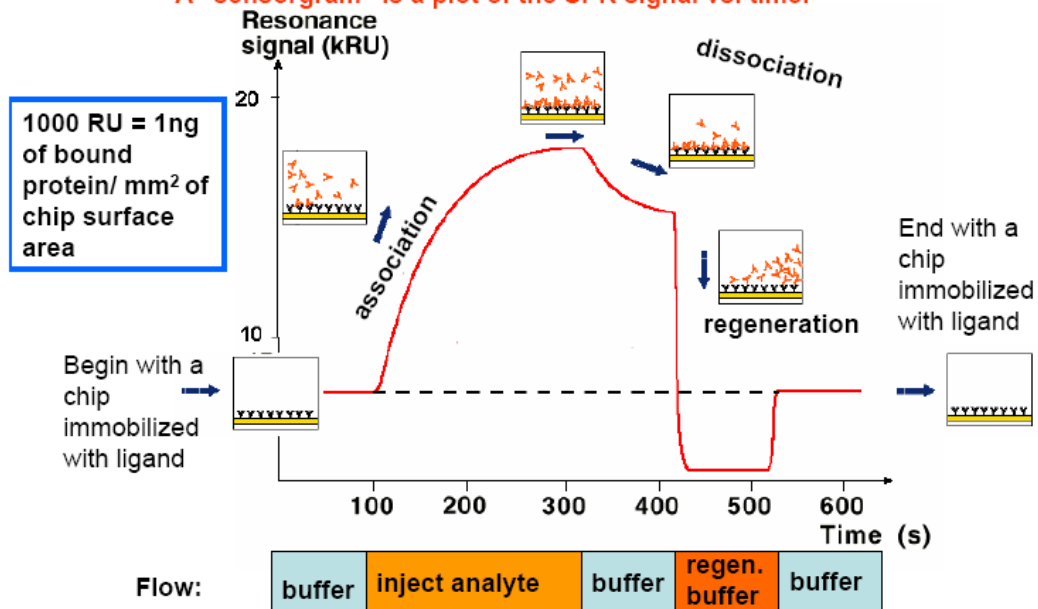


Figure 19: A sensorgram of one cyclic experiment with molecular interaction detail on the chip.

A sensorgram is created by the change of SPR signal through time. For all experiments, buffer flow is always run before the experimental cycle (Light green box, under the graph). Then, the injection of analyte begins with limited time to reach the acceptable and reproducible RU unit (Orange box, under the graph). At the point, the increase of the signal reflects the association or interaction of analyte-ligand complex. Following this step, buffer flow is injected again for showing a behavior of the complex disassociation though time. Finally, all bound proteins are detached by the introduction of regenerate buffer (Red box, under the graph) and buffer flow prepare the chip for next experiment. All molecular interactions' presentation are displayed in rectangular box along the responding signal.

João Paulo. (2006). Brown University, Division of Biology and Medicine,

Available: http://biomed.brown.edu/epscor_proteomics/JPBiacorePresentation.pdf.

Last accessed 10th Nov 2010.

Table 7: DNA sequences used for SPR analysis.

Name	Sequences
<i>P_{flgB}</i>	CCCGTGTGAAGCAAGCATCA AACGCAATAAATAGCG ACGCATTTT GCGTTATTCCGGCG ATAACGCGCGCGTGAAGGCAT
<i>P_{flhB}</i>	CGTATCCGGCTATCTCTATT AACGCCATAAACCCCG CCTTTTTTAC GCTTACTCTGCCT ATTGGCGTAAAGCGGTTCTG
<i>fliC</i>	TACGGGGGGAACTGGTAAAGATGGCTATTATGAAGTTTCCGTTGATAAGACGAACGGTGAGGTGACTCTTGCTGGCGGTG

a. The FlhD₄C₂ inverted repeat as defined by Stafford *et al.* (2005) is shown in bold.

- **Immobilisation of the DNA to the chip**

DNA fragments were injected to the chip incrementally until the signal reaching the required RUs. Biotinylated DNA was immobilized on the chip for 365 RUs (Biacore 2000), and 100 RUs (Bio-Rad). An empty cell is classified as a negative control for background subtraction. The running buffer used for all experiments is phosphate-buffered saline (PBS).

- **Bind FlhD₄C₂ to the bound DNA chip.**

FlhD₄C₂ protein was injected to the system for 60 s over all flow cells to bind the DNA on the chip. Before the next experiment, a regeneration buffer, 6M guanidine-HCl, was injected for 10 s to detach bound FlhD₄C₂ and other nonspecific proteins.

- **Protein-protein interaction analysis**

FliT, as an analyte, was injected over Bound FlhD₄C₂ protein was challenged by different concentrations of FliT reflecting the level of FlhD₄C₂ still bound through the changing of signal.

4.7.4 Protein Crystallography

The concentration of protein solution was adjusted to 5 μ M. The protein solution was centrifuged 12000 rpm 30 min 4°C and the supernatant was kept on ice. Three special 96- wells plates for crystallisation screening were used for a trial test by filling each well with 75 μ l of different screening conditions: Classics, JCSG and PACT suits (Qiagen). The protein solution was mixed with each screening solution and transferred to a special hole besides each well by a special machine (Mosquito TTP Labtech). The mixed solution was saturated with the vapour from a corresponding solution beside by sealing the plates with transparent cover. Three plates containing 288 different screening conditions were incubated at 25°C.

4.7.4.1 The Optimisation of crystallisation conditions

Optimised conditions were designed by varying pH (3.5-5.0) and PEG1500 (17%-27%) with constant 0.1 M MMT. A 24- wells plate was filled with 750 μ l of the designed optimised condition and labelled properly. The hanging drop technique was performed. The protein solution was mixed with each condition and placed on a cover slit. Gel was applied around the edge of the cover slit. The cover slit was then placed over the hole of a well letting the mixed solution hanging against an optimised condition. The plate was kept at 25°C.

4.7.5 Matrix-assisted Laser Desorption/Ionization-time of flight Mass Spectroscopy (MALDI-TOF)

Proteins was first run on a 16.5% Tricine gel, the expected bands were cut and sent to PINN@CLE (Proteomics Investigation @Newcastle) Lab, a Newcastle University service, to run trypsin digestion overnight and MALDI-TOF mass spectroscopy.

Chapter 5

Investigation of FliT/FliD Interaction

Chapter 5 Investigation of FliT / FliD interaction

FliD is an essential structural component of the functional flagellum, acting as the flagellar cap protein. FliT is the FliD T3S chaperone and their interaction assists the export of FliD through the flagellar T3S apparatus. FliT has been described as a negative regulator of flagellar synthesis. On the other hand, FliD plays a positive regulatory role according to the proposed model of Yamamoto & Kutsukake (2006). FliT acts directly on FlhD₄C₂ (the flagella master regulator), while FliD exerts its positive regulatory effect indirectly, because whenever bound to FliT it prevents the latter from interacting with FlhD₄C₂. FliD is therefore classified as an anti-FliT factor or an anti-anti-FlhD₄C₂ factor due to its capability to bind FliT.

The FliT:FliD interaction has been studied in detail (Fraser *et al.*, 1999). The interaction was clearly demonstrated by affinity blotting assays, which indicated that FliT selectively binds to FliD at the C-terminal region. Gel filtration analysis showed that FliT and FliD in mM range (20 mM Tris-HCl, pH 7.4, 500 mM NaCl) could *in vitro* generate a stable complex composed of a FliT homodimer and one FliD (Bennett, 2001). However, knowledge of all the protein interactions in the regulatory circuit among FliT, FliD and FlhD₄C₂ has been lacking.

Our first investigation concentrated on understanding the FliT and FliD interaction. The aim of the study was to confirm their interaction and to determine the stoichiometry based in the μ M range using the interaction analysis conditions after slight modification to the gel filtration buffer (20 mM Tris-HCl, pH 7.9, 300 mM NaCl) of Bennett (2001). This condition was then employed for all further investigations. We assumed that the FliT:FliD interaction would behave in the same way as reported by Bennett (2001) even though the concentration of proteins and buffer conditions had been modified. Our studies included isolation of the FliT:FliD complex and analysis of its properties, such as stoichiometry and possibly its configuration based on our preliminary analysis. Experiments performed included native gel-electrophoresis, gel filtration, analytical ultracentrifugation (AUC) and protein crystallography.

5.1 Purification of FliT and FliD

In order to investigate the FliT:FliD interaction, protein expression and purification of FliD and FliT were performed. Full length *fliT* and *fliD* flanked with His-tag residues at the N-terminus were constructed using the expression vector pET28amod and *E.coli* BL21. Protein expression was induced using 1 mM IPTG, yielding soluble heterologously expressed proteins under standard growth conditions. In order to achieve high yield and purity of each recombinant protein for further analysis, two purification steps were performed: Nickel-Affinity purification column for polyhistidine-tag protein and gel filtration chromatography.

The theoretical molecular weight of FliT and FliD are 14 kDa and 49.8 kDa respectively, which corresponded to the size of the band obtained from protein-containing fractions analyzed by SDS-PAGE for FliT (**Figure 20**) and FliD (**Figure 21**) respectively. FliT purified over the Ni-affinity column was contaminated with a number of high molecular weight proteins, while purification of FliD produced higher purity (**Figures 20A and 21A** respectively). A superior level of purity was achieved with gel filtration, which dramatically increased the purity of FliT (**Figure 20B**) and FliD (**Figure 21B**). An intense single SDS-PAGE band (10 kDa) of FliT was obtained. Although some fractions showed a faint band at around 25 kDa, whose molecular weight corresponded to FliT dimer, the dominant form present in gel filtration buffer condition (Bennett *et al.*, 2001). FliD purification gave a large amount of protein with high purity for further analysis (**Figure 21B**). Gel filtration could decontaminate some of the high molecular weight species (Imada *et al.*, 1998).

After purification of FliT and FliD, the investigation of the FliT:FliD interaction was conducted by performing interaction assays in order to confirm their stoichiometry, behaviour of interaction, and detailed 3-dimensional structure. The analyses were performed using native gel-electrophoresis, gel filtration, and analytical ultracentrifugation (AUC).

It is to be noted that the various amounts of proteins needed for each analysis dictate the number of fractions collected. Native gel-electrophoresis requires a considerably larger amount of protein; therefore, a wider range of fractions was collected, whereas a small amount of proteins is needed for AUC and SPR analyses, and thus only the fraction showing a single protein band in SDS-PAGE were collected.

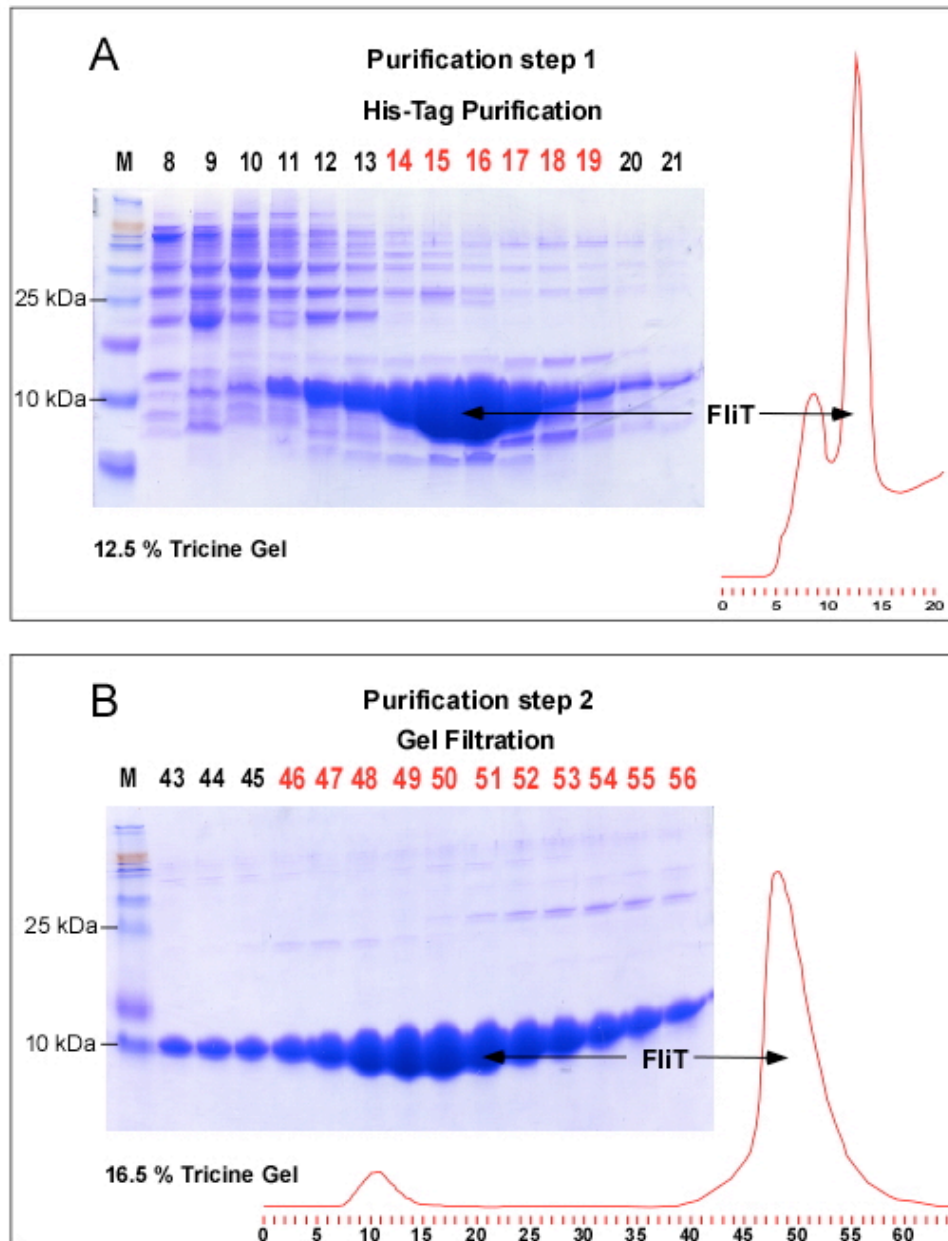


Figure 20: Purification of FliT

FliT purification was performed in two steps. **(A)** The first step of FliT purification used a His-Tag column. The elution profile showed the presence of high molecular weight proteins and a large FliT peak; the fraction numbers are labeled (right), and sodium dodecyl sulfate polyacrylamide gel electrophoresis (SDS-PAGE) of the fractions (left) shows purified FliT of approximately 10 kDa present in fractions 14-19 (red). These fractions were then subjected to a gel filtration purification step. **(B)** Gel filtration of FliT from **(A)** showed the removal of contaminating high molecular proteins. Nevertheless, a protein of approximately 25 kDa co-eluted with the later fraction of FliT (explained in text). SDS-PAGE of the fractions (red) showed the existence of homogeneous FliT, which was used for further analysis. Fractions 46-56 were pooled, concentrated and used in subsequent analysis.

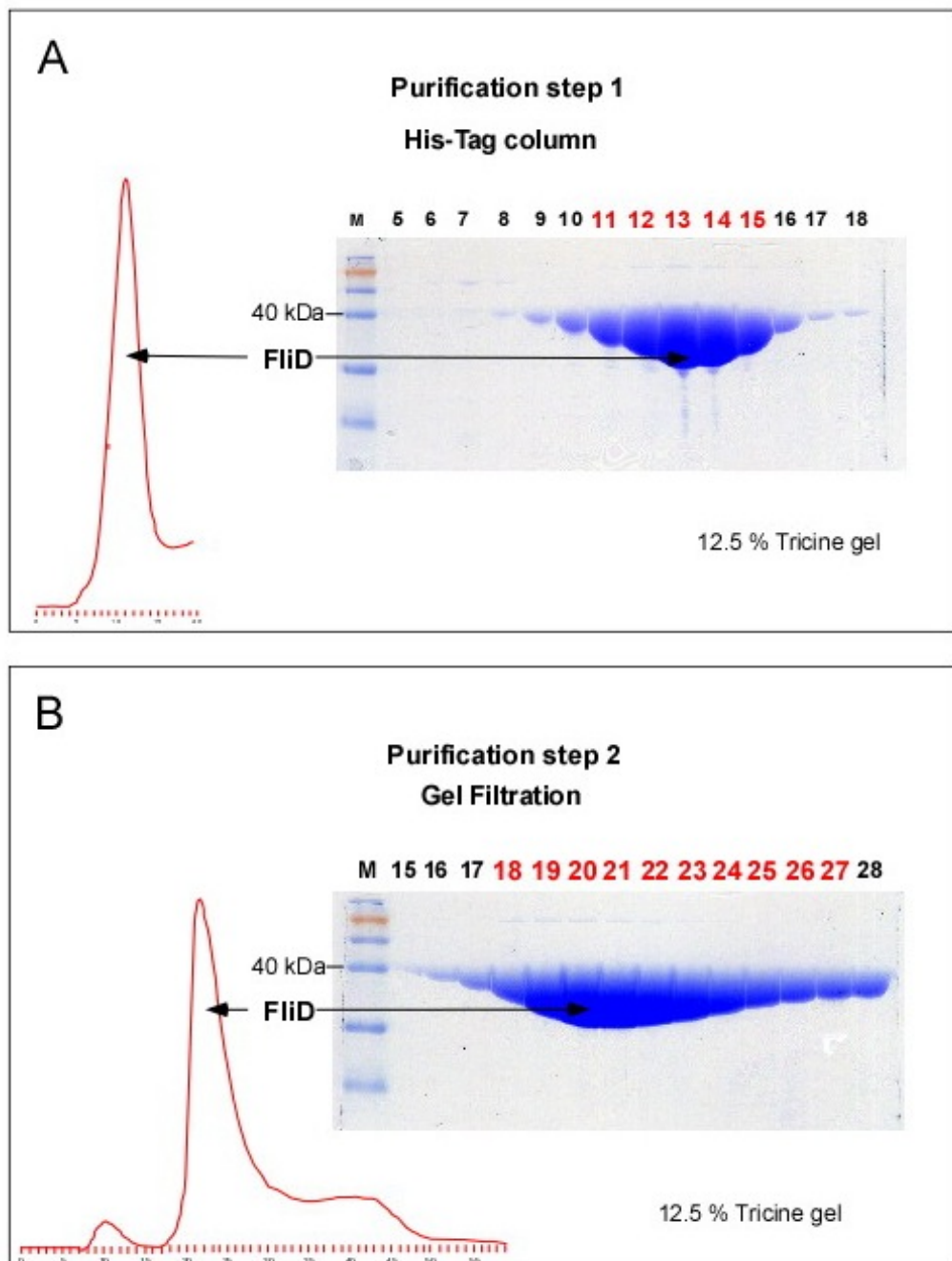


Figure 21: Purification of Flid

Flid purification was performed in two steps. **(A)** The first step of Flid purification used a His-Tag column. The elution profile showed only one peak of Flid peak (left); the fraction numbers are labeled (right), and SDS-PAGE of the fractions (right) showed the majority of Flid (of approximately 40 kDa) present between fractions 11-15 (red). Fractions 11-15 were then subjected to a gel filtration purification step. **(B)** SDS-PAGE of gel filtration of the protein from **(A)** showed one prominent peak of Flid (left). Fractions 18-27 (red) were then pooled, concentrated and used in subsequent analysis.

5.2 Analysis of FliT:FliD interaction by native gel electrophoresis

FliT, a negative regulator of FlhD₄C₂, is counteracted by its interaction with FliD (Yamamoto & Kutsukake, 2006). The binding stoichiometry of FliT:FliD complex has been previously predicted to be 2:1 molar ratio based on gel filtration (Bennett *et al.*, 2001).

We chose to employ native gel-electrophoresis to study the FliT:FliD stoichiometry over a lower range of protein concentrations (μ M). We assumed that the FliT:FliD stoichiometry will be proportional to the changes in FliT/FliD band intensity and amount of free FliT. Thus, we can define the protein molar ratio when there is no free FliT left to form the complex.

Different protein ratios were used together with both FliT and FliD alone as controls. Native gel-electrophoresis (10% acrylamide) of FliT showed that the protein migrated through the matrix, but FliD could not penetrate the gel (**Figure 22A**). One explanation for the lack of FliD migration is that the decamer form of FliD is dominant in the buffer used (Imada, 1998). This decameric FliD may not enter the gel matrix due to its size and possibly charge. Mixing FliT and FliD resulted in reduced FliT intensity rather than creating a new band in the gel. We interpreted this as being due to the formation of a FliT:FliD complex that is not capable of penetrating the acrylamide gel matrix. At the initial FliT:FliD molar ratio of 1:1 the FliT band in the acrylamide gel disappeared, but was still present at higher FliT:FliD ratios (**Figure 22**). These data are not consistent with those of Bennett *et al.* (2001). The concentration of FliT used in Bennett *et al.* (2001) studies to form the FliT:FliD complex was in the mM range, while in our conditions, a μ M range was employed. The formation of a FliT dimer is pH independent (Imada *et al.*, 2010). We surmised that formation of a FliT:FliD complex is dependent on the FliT concentration and thus our results are at odds with those of Bennett *et al.* (2001) but in agreement with those of Imada (2010). Thus, native gel electrophoresis of FliT in the μ M range revealed the putative stoichiometry of FliT:FliD as 1:1.

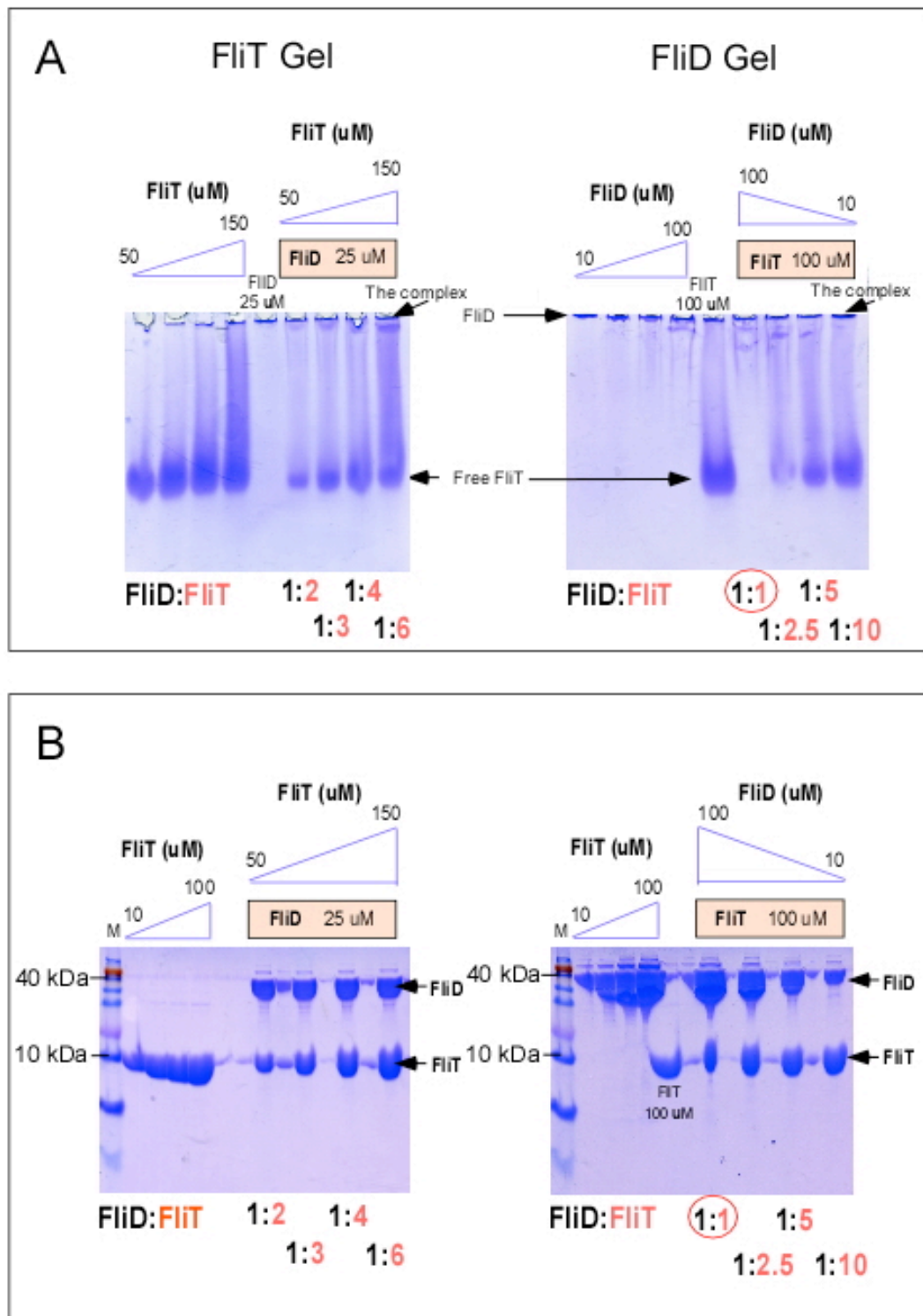


Figure 22: Native gel-electrophoresis of *FliT*:*FliD* complex

(A) Native gel-electrophoresis (10% acrylamide) of *FliT* (left panel) or *FliD* (right panel) both as single proteins and as a mixture with fixed concentration of *FliD* or *FliT* protein. Molar ratios varied from 1:1 to 1:10. *FliT*:*FliD* (1:1) molar ratio is formed (red circle) when there is no *FliT* observed in the gel. It is assumed that the complex cannot enter the gel. (B) SDS-PAGE of the corresponding samples used in (A).

5.3 Analysis of FliT:FliD interaction by gel purification

In order to explore the properties of FliT:FliD complex in more detail, isolating the complex was conducted with gel filtration. The native gel-electrophoresis result suggested a 1:1 molar ratio of the complex. It was therefore assumed that the complex would show a distinct peak on gel filtration distinguishable from the free FliT dimer and FliD decamer. This would allow for the isolation of the complex from its components.

FliT and FliD were first prepared by His-tag affinity chromatography and their concentrations were quantified by a spectrophotometric method using their extinction coefficient from NCBI database. Proteins were mixed together at a 1:1 molar ratio at room temperature and subjected to (uncalibrated) gel filtration chromatography (Hiload 16/60 superdex 200 prep grade). Gel filtration of the mixture revealed a new peak located between the peak of FliD and FliT (**Figure 23A**). SDS-PAGE of the fractions from this peak showed the presence of both FliT and FliD (**Figure 23C**). From the assumption of 1:1 stoichiometry of FliT:FliD, the predicted molecular mass should be 51 kDa (FliD of 37 KDa and FliT 14 KDa). The FliD peak was located at a higher molecular mass as it is mainly in the decamer form with a predicted molecular mass of 400 kDa (Bennett *et al.*, 2001 and Imada *et al.*, 1998), whereas that of FliT was approximately 28 kDa due to its existence as a dimer at the concentration used (**Figure 23A**). However, a more rigorous analysis of these proteins obtained from gel filtration was needed to support the above-mentioned assumptions.

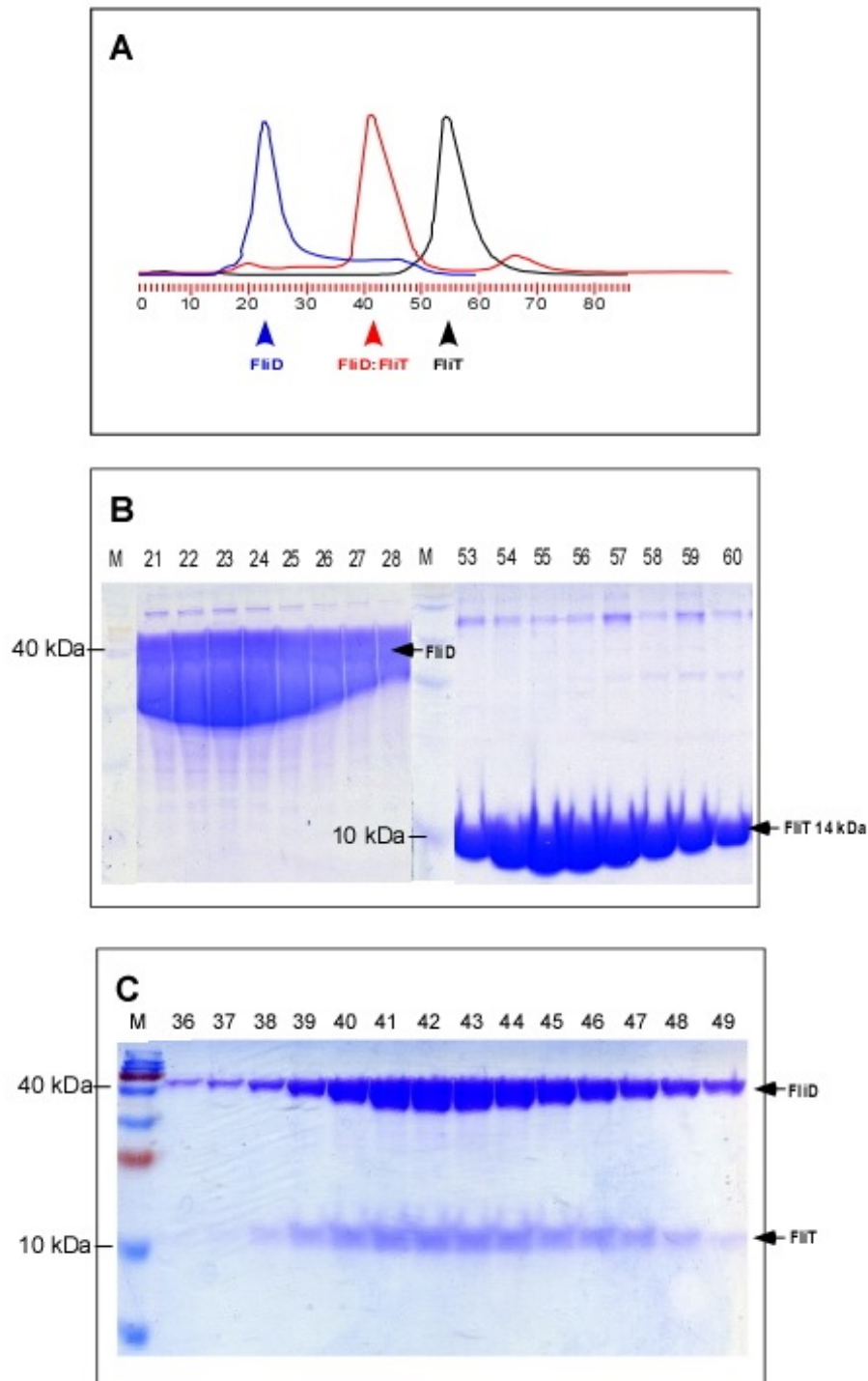


Figure 23: Gel filtration profile of the *FliT*:*FliD* complex

Gel filtration (Hiload 16/60 superdex 200 prep grade) profiles with indicated separate peaks of the *FliT* dimer, *FliD* decamer and a *FliT*:*FliD* 1:1 complex (**A**); with fraction numbers indicated. Each peak was located separately; thus, the complex can be isolated for further analysis. (**B**) SDS-PAGE of purified *FliD* (left) and *FliT* (right (**B**) and (**C**) a gel showing the complex obtained from their respective gel filtration fractions.

5.4 Analytical ultracentrifugation (AUC) of FliT: FliD complex

The isolation of the FliT:FliD complex was successfully accomplished by gel filtration. In order to analyze its properties in more details, such as exact mass and configuration, the complex, FliT and FliD alone were subjected to AUC analysis.

For the study of protein interactions, AUC provides information regarding the behaviour directly of proteins in solution, which gives more details than gel filtration analysis. Having no possible interaction with a matrix as in gel filtration, which could give rise to artifactual results and thereby misleading interpretation, AUC provides information of only the protein-protein interactions in solution. The protein interaction can be monitored in real time from measurement of protein absorbance at 280 nm, and consequently, the information of the protein interaction can be obtained at any time during analysis. Additionally, as the formation of the complex reversibly disassociates and re-associates during the experiment, fast or transient interactions can be revealed.

AUC provides the sedimentation velocities of the proteins in the sample, which are considered to be the raw data of each separated component. Other information of the proteins, such as molecular mass and concentration used, is processed with a specific software program to generate the sedimentation coefficient (S), which is unique to each protein and also different for a particular protein configuration. Interpretation of the S value includes analysis of self-association, which causes proteins to form dimers or larger oligomers (Perugini *et al.*, 2000). For practical purposes, the S value is expressed as $S_{20,w}$, the sedimentation coefficient corrected for the viscosity and density of the solvent, relative to that of water at 20 °C. This value is used to compare information of proteins concerning the various aspects of changes in molecular aggregation, shape and size. $C(s)$ is the sedimentation distribution coefficient, which reflects protein concentration due to different diffusion properties of each protein (Schuck, 1997). An AUC profile is presented with $C(s)$ values plotted on the y-axis and $S_{20,w}$ on the x-axis.

The design of the AUC experiment was to show the oligomeric status of FliT, FliD, and FliT:FliD complex. Such results can provide information regarding the natural configuration of FliT and FliD before their interaction as well as the configuration of the complex under our experimental conditions. The AUC results of FliT or FliD alone share some similarity; both proteins exist in solution in oligomeric state: FliT (9.21 $\mu\text{g/ml}$) mostly as a dimer but also as tetramer (**Figure 24A**), and the majority of FliD (7.26 $\mu\text{g/ml}$) as a decamer (**Figure 24B**). No evidence of aggregation or degradation was found for FliT and FliD in solution, confirming that all the proteins were solubilised. At a 1:1 molar mixture of FliT and FliD in our conditions AUC analysis showed only one oligomeric state with absence of FliD decamer and FliT dimer peaks of FliT (**Figure 24C**). This suggests the complex, which is composed of one molecule each of FliT and FliD, is formed due to strong binding between FliT and FliD and producing only one type of complex across several test concentrations (below 3.6 $\mu\text{g/ml}$). The binding property and its stoichiometry are consistent with results obtained from both native gel-electrophoresis and gel filtration experiments.

For comparison of the three profiles, the AUC profiles of the three protein preparations were combined into one profile (**Figure 25**). The molecular mass of FliT:FliD complex was calculated to be 53.8 kDa. The peak of the complex appears at the same location of FliT tetramer (56.0 kDa) and, surprisingly, that of FliD monomer (predicted molecular mass of 37 kDa). The explanation lies on the fact that FliD in solution normally exists as a pentamer or decamer; thus, in the monomeric state FliD may fold into a more compact conformation than that of that expected (possibly to avoid exposing hydrophobic surface(s) present when forming oligomer) and hence producing a higher than expected dense particle. That the molecular mass of FliT:FliD 1:1 complex (predicted molecular mass of 53 kDa) is slightly smaller than the calculated value possibly comes from induced change in conformation arising from the formation of the complex. The AUC results clearly show that the complex contains one molecule each of FliD and FliT only at approximately $S_{20, w}$ of 3.5. Thus this preparation is suitable to perform subsequent analysis, especially x-ray crystallography.

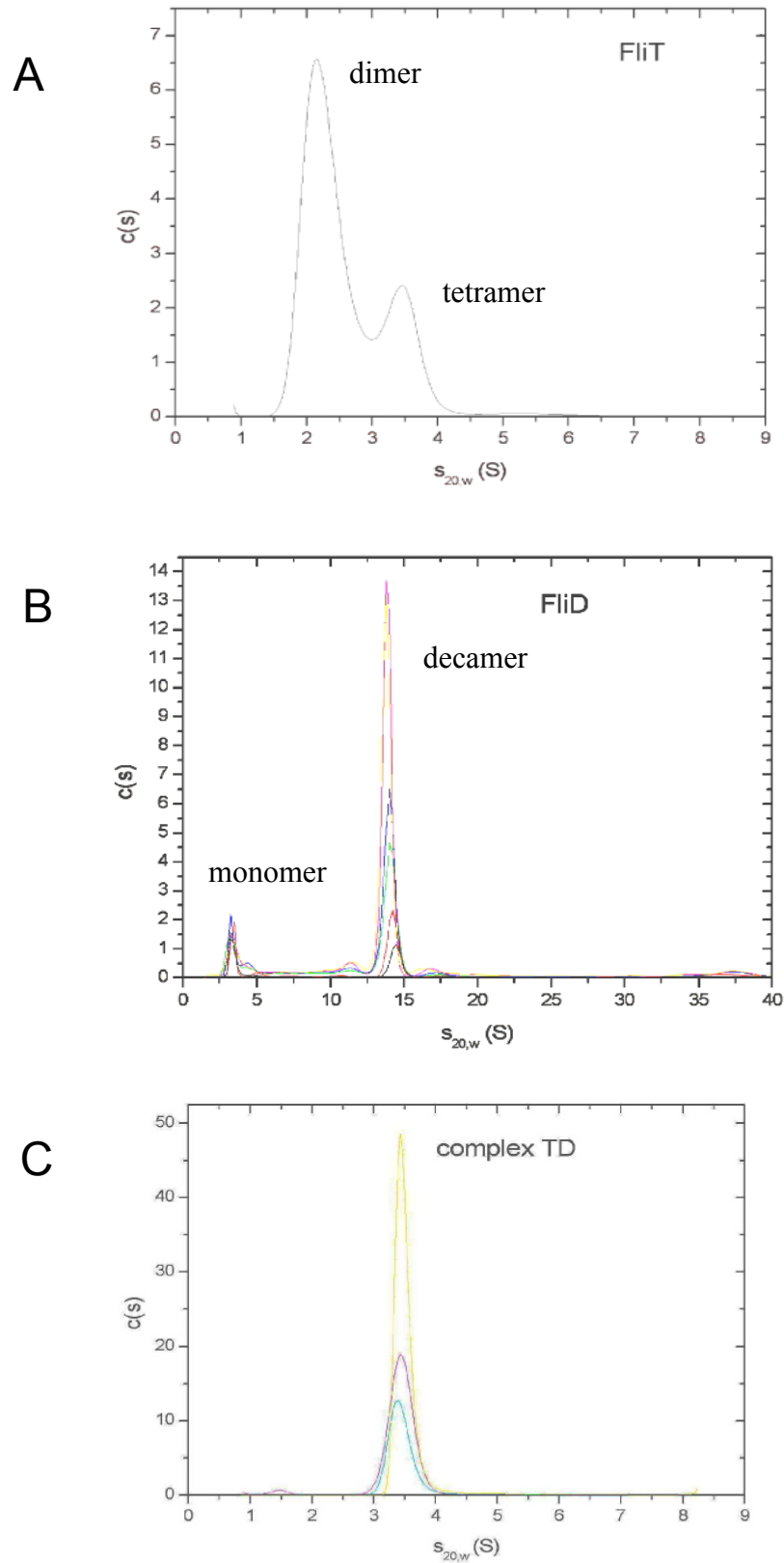


Figure 24. AUC analysis of *FliT*, *FliD* and the *FliT*:*FliD* complex.

The complex shows only one molecular form in gel filtration buffer (300 mM NaCl, 20 mM Tris).

(A) *FliT* alone (9.2 $\mu\text{g/ml}$) shows two forms with dimer predominating. **(B)** *FliD* (7.26 $\mu\text{g/ml}$) presents two forms with the decamer predominating. **(C)** The complex shows only one form at all concentrations tested (from 3.6 $\mu\text{g/ml}$).

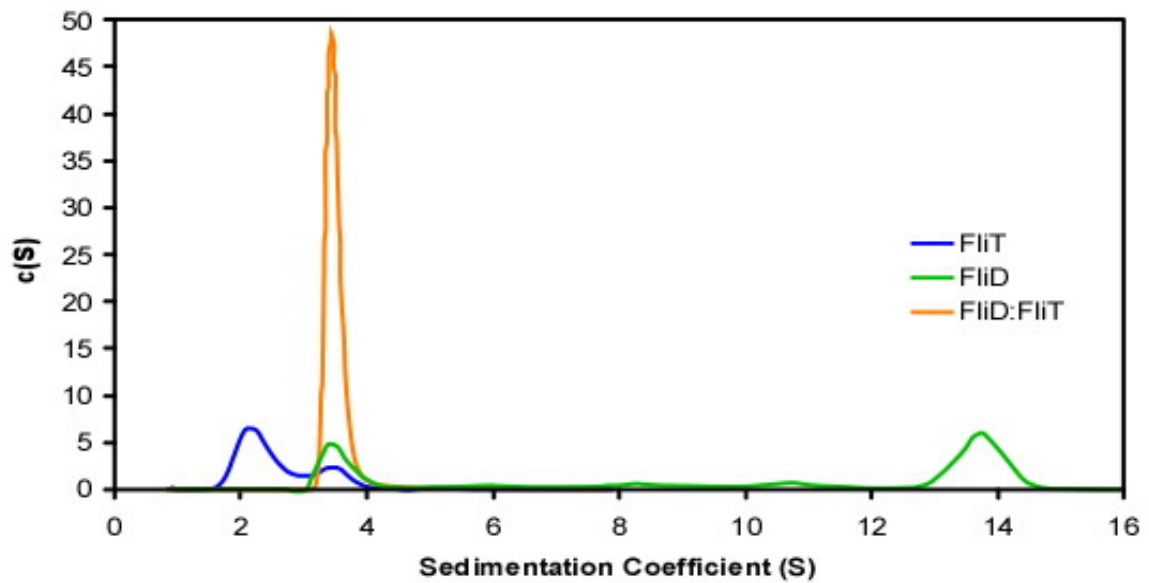


Figure 25. Composite AUC profiles of FliT, FliD, and the FliT:FliD complex.

AUC profiles from the individual proteins and complex have been combined into one graph. The complex (3.6 $\mu\text{g/ml}$ gel filtration buffer) (yellow line) shows a sharp peak suggesting only one form exists in solution. However, FliT (9.2 $\mu\text{g/ml}$ of the same buffer) and FliD (7.26 $\mu\text{g/ml}$ of the same buffer) exist in more than one form. The majority of FliT is a dimer together with a smaller amount of tetramer, while FliD exists mainly as a decamer and a small fraction as monomer. (In collaboration with Solovyova, Alexandra; Newcastle University, Institute for Cell and Molecular Biosciences)

5.5 Isolation of FliT:FliD crystals

The stable nature of FliT:FliD complex in solution indicates it should be possible to obtain crystals for subsequent x-ray crystallography in order to gain 3-dimensional structural information at the atomic level. The isolated complex from gel filtration was therefore subjected to a variety of protein procedures. From 300 different buffer conditions tested, protein crystals formed in a solution containing 0.1 MMT pH 4.0, 25% PEG 1500 (w/v) produced promising crystals for X-ray diffraction. A large-scale preparation of crystals was thus prepared using this solution with minor variations (pH of 3.5, and 19% w/v PEG 1500). Large crystals were generated, (**Figure 26**) but unfortunately they produced only X-ray diffraction patterns of low resolution, and so no further experimentations were pursued, especially in the light of publication of the FliT structure (Imada *et al.*, 2010).

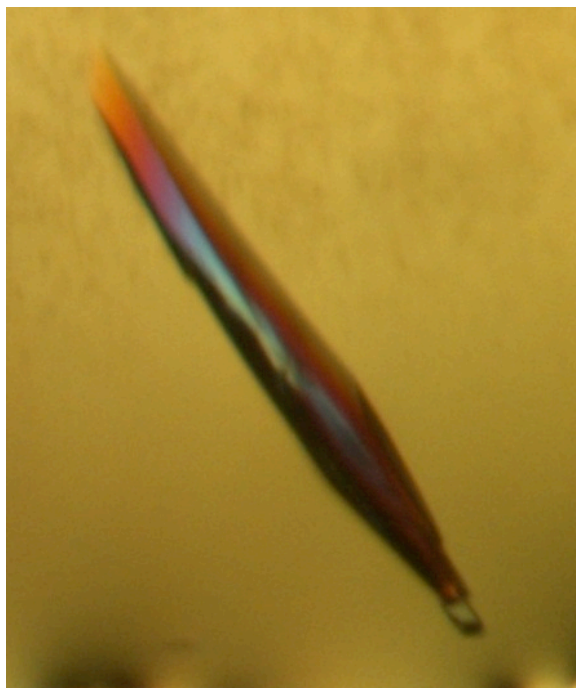


Figure 26: Crystals of FliT:FliD

Crystals of FliT:FliD complex were obtained from a solution of 0.1 MMT pH 4.0, 25% PEG 1500 (w/v). The crystal shows a rod shape of sufficient thickness to perform X-ray diffraction studies.

5.6 Discussion

The ability to isolate FliT and FliD as soluble proteins was achieved allowing studies of their interaction. Native gel-electrophoresis suggested a 1:1 interaction of FliT:FliD in our conditions (1.5 M glycine buffer, pH 8.3); nevertheless, the complex could not be visually shown as a unique band in the gel matrix (10% acrylamide), possibly due to the bound FliD neutralizing the charge of FliT, which is located at the region where FliD binds to FliT (Imada, 2010), and renders the complex having no net charge leaving only free FliT to move into the gel. In comparison, native gel-electrophoresis was successfully performed to show FliI/FliH complex as a unique band from the interaction between FliI (51 kDa) and FliH (26 kDa) (Minamino, 2000).

In our case, further analysis employing gel filtration allowed isolation of a complex when a 1:1 molar ratio mixture of FliT and FliD was used, generating a unique peak eluting from the column. This purified component was further characterized by AUC, which indicated a calculated molecular mass of 53 kDa, suggesting a stoichiometry of one molecule of FliD (37 kDa) to one molecule of FliT (14 kDa), which corresponded to the theoretical molecular mass of 51 kDa. These data are inconsistent to previous findings (based on gel filtration) of a trimer composed of 2 molecules of FliT (30 kDa) and one molecule of FliD (50 kDa) forming the complex of 90 kDa (Bennett *et al.*, 2001). In those studies, FliT concentration was in the mM range, while we used μ M concentrations. Imada *et al* (2010) demonstrated that FliT exists in solution in equilibrium between a dimer and higher oligomers and this is concentration but not pH dependent. Thus FliT concentrations used in different experiments could possibly play a critical role in determining the final stoichiometry of FliT:FliD complex existing in solution. Consistent with our findings Imada *et al* (2010) reported a 1:1 stoichiometry of FliT:FliD complex, similar to many other T3S protein:cognate molecular chaperone interactions.

Chapter 6

Investigation of FliT/FliD₄C₂ interaction

Chapter 6 Investigation of *FliT* & *FliH₄C₂* interaction

FliH₄C₂ is a master regulator of the *Fla* regulon, activating flagellar synthesis. Its expression is controlled by various internal and external factors. Internal regulation is defined as endogenous control of the *Fla* regulon by itself; in contrast, external regulation is defined as environmental or cellular regulation of *fliHDC* expression/activity. Nutrient availability in the medium controls the number of flagella present per cell (Adler & Templeton, 1967). A cytoplasmic protein, *FliT*, has been reported to exhibit a negative regulatory effect towards *FliH₄C₂* through its binding with *FliH* (Yamamoto & Kutsukake, 2006). The regulatory effect of *FliT* upon *FliH₄C₂* has not been deeply investigated despite the fact that the regulatory model was proposed. The underlying hypothesis is that *FliT* in cells acts as a regulator of *FliH₄C₂* which also cooperates with the other component, *FliD*, to create a regulatory feedback loop. The net outcome of this circuit is proposed to be a change in *FliH₄C₂* activity, which significantly impacts the rate of flagellar synthesis.

FliT is the utmost key protein in the regulatory loop due to its capability to bind both *FliD* and *FliH₄C₂*. Strong interaction of *FliT* and *FliD* at the 1:1 stoichiometry was previously shown (**Chapter 5**). Further analysis here focuses on the *FliT* and *FliH₄C₂* interaction. Yamamoto *et al* (2006) previously proposed interaction mechanism hints to us that *FliT* binds *FliH₄C₂* to prevent its DNA binding capability. However, the resulting outcome of the *FliT*:*FliH₄C₂* interaction has not been investigated in detail. This leads us to the purification of the *FliH₄C₂* complex and to analyze its interaction with *FliT* *in vitro*. The experimental objective is to analyze *FliT* and *FliH₄C₂* interaction *in vitro* under the same conditions and methodology used for the *FliT*/*FliD* analysis; native gel, gel filtration and AUC to determine the behaviour of the protein interactions. The interaction of *FliT* and *FliH₄C₂* can shed light on the regulatory mechanism of the target of *FliT*, the crucial master regulator *FliH₄C₂*, in order to control flagellar synthesis. This also aims to determine if the mechanism of interaction for *FliT* can explain how multiflagellated bacteria regulate their flagellar synthesis to achieve a distinct number of flagella.

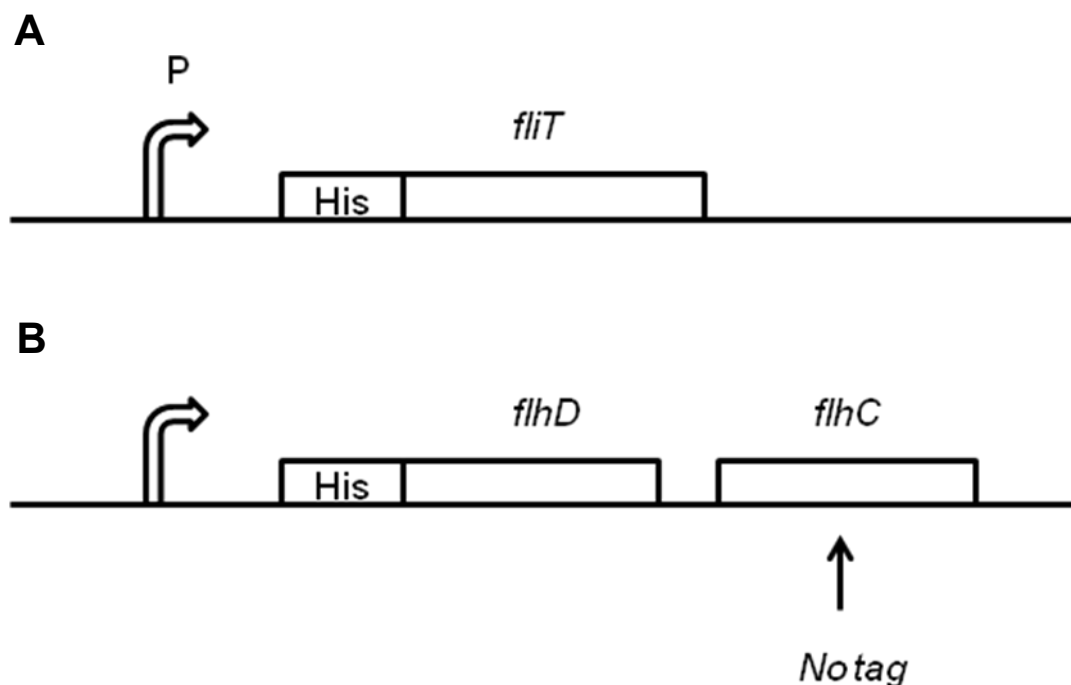


Fig. 27. FliT and FlhD expressed with His Tags (except FlhC).

FliT (A) and *FlhD* (B) are expressed with a His Tag moiety at the N terminus. No tag is required for the expression of *FlhC* (B). His Tag purification was performed with *FliT* while *FlhD₄C₂* purification was performed using Heparin purification (Method 4.6.3). Expression of *flhD* and *flhC* create an *FlhD₄C₂* with His Tag flanking only at N- terminus of *FlhD*

6.1 Purification of FliH₄C₂ for further analysis

The investigation of the interaction between FliT and FliH₄C₂ was performed by using full length FliT and FliH₄C₂ flanked with His-tag residues at the N-terminus with an IPTG inducible promoter. Only FliH of FliH₄C₂ exhibited a His-tag (**Figure 27**). Purification of FliT was established as described in Chapter 5. In order to obtain a high yield of FliH₄C₂, the plasmid (pET28a-mod) containing *fliHDC* was isolated and freshly transformed into BL21 competent cells for the expression of FliH₄C₂ as a soluble complex was isolated under standard conditions consistent with previous studies (Wang *et al.*, 2006) using a Heparin column instead of a His-tag column. The ability of FliH₄C₂ to bind Heparin (which mimics one strand of the DNA helical structure) was initially performed to purify FliH₄C₂ through its capability to bind DNA (Liu & Matsumura, 1994). The His Tag moiety at the N-terminal of FliH is possibly buried in the FliH₄C₂ complex, reducing purification yields (data not shown).

The heparin column was used to purify the FliH₄C₂ complex in the first step. In order to reduce other nonspecific DNA binding proteins, a 20% solution of elution buffer (0.1 M NaCl) was used to wash the loaded column until the profile reached baseline, prior to a 20-100% continuous gradient elution pattern (0.1 to 0.5 M NaCl in buffer) to collect FliH₄C₂ fractions. Two intense bands of FliH and FliD were observed at the molecular weight of 13 kDa and 25 kDa respectively. However, after the first purification by Heparin column, FliH₄C₂ was contaminated with a large amount of other proteins (**Figure 28A**). The contaminated proteins were reduced significantly after performing gel filtration (**Figure 28B**).

FliH₄C₂ *in vivo* is reported to be an unstable protein with a short half-life (Claret & Hughes, 2000). FliH₄C₂ easily precipitated out of solution if its concentration was above 25 µM. A stable, soluble solution of FliH₄C₂ was kept for 48 hrs if 300 mM NaCl and 1 mM DTT was added to the buffer. Due to the instability of FliH₄C₂, even in this buffer, analysis was always performed using freshly prepared FliH₄C₂ complexes.

6.2 Analysis of FliT:FliH₄C₂ interaction by native gel electrophoresis

Interaction between FliT and FliH₄C₂ was demonstrated by using native gel electrophoresis similar to that performed for FliT and FliD. FliT can migrate through the matrix, while like FliD, FliH₄C₂ cannot (**Figure 29**). The inability of FliH₄C₂ to migrate through the matrix is possibly due to its large size (93 KDa). Addition of FliT resulted in no new bands although a smear pattern of the sample migration did appear (**Figure 29A**). Compared with FliT alone at the same concentration, the reduced intensity of the FliT band (10 μ M – 60 μ M) in the mixed samples was consistent with the interaction between FliT and 10 μ M FliH₄C₂ (**Figure 29A**). Corresponding SDS-PAGE of the same samples showed that FliH₄C₂ was observed. The contaminating proteins became evident when the fractions of FliH₄C₂ from gel filtration were concentrated to the desired concentration used in the experiment. From the mixed samples native gel analysis of the FliT:FliH₄C₂ interaction suggests a stoichiometry of 1:1 or 2:1. Any higher ratio showed excess of FliT not bound to FliH₄C₂ (**Figure 29A**). The data also suggest that in solution FliH₄C₂ exists and interacts as a complex with FliT in preventing FliT migration in to the matrix.

The result suggests a larger amount of FliT is possibly needed to interact with FliH₄C₂. Other sets of FliT/FliH₄C₂ interactions were conducted at various molar ratios of FliT to FliH₄C₂. High (25 μ M) and low (10 μ M) concentrated FliH₄C₂ was mixed with different ranges of FliT concentrations (**Figure 30**). FliT disappeared from the gel suggesting all FliT remained on the top of the gel when FliT:FliH₄C₂ (2:1) was applied (**Figure 30**). A consistent result of both experiments was found and suggested the stoichiometry between FliT:FliH₄C₂ as 2:1. However, no evidence of new products was revealed. This is a preliminary result which needs more conclusive analysis to reveal the behaviour of the interaction and possibly to observe the FliT/FliH₄C₂ complex.

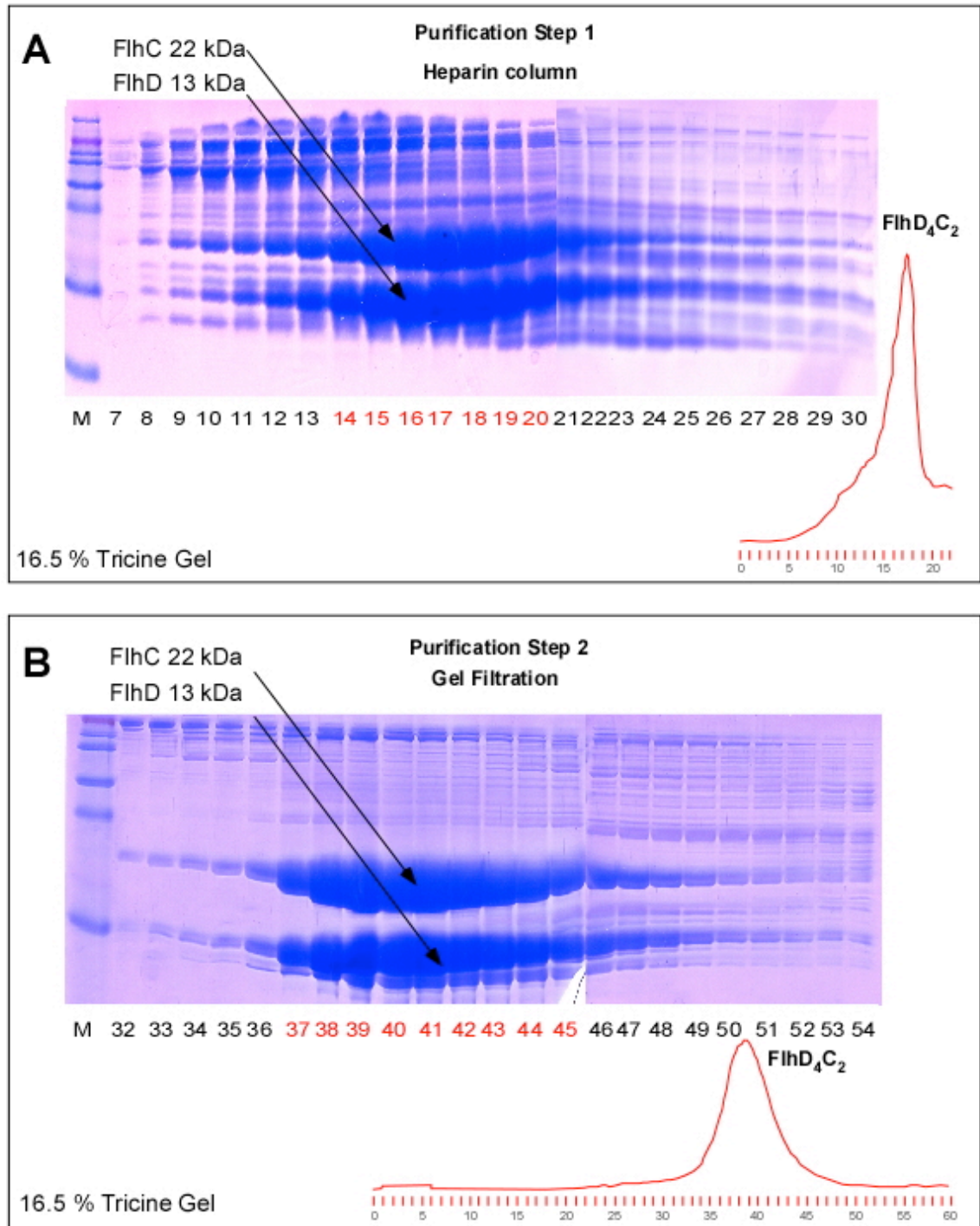


Figure 28. Purification of FliH₄C₂

FliH₄C₂ purification was performed in two steps prior to analysis **(A)** The first step of FliH₄C₂ purification utilized a Heparin column. The SDS-PAGE of the labelled fractions shows the majority of FlhC and FlhD at approximately 22 kDa and 13 kDa respectively. Fractions 14-20 (red) were then subjected to a further purification step. **(B)** Gel filtration of FliH₄C₂ from **(A)** shows the removal of many high molecular weight contaminating proteins. The gel of the defined fractions shows higher purified FliH₄C₂ and the selected fractions 37-45 (red) were then pooled, concentrated and used in subsequent analysis.

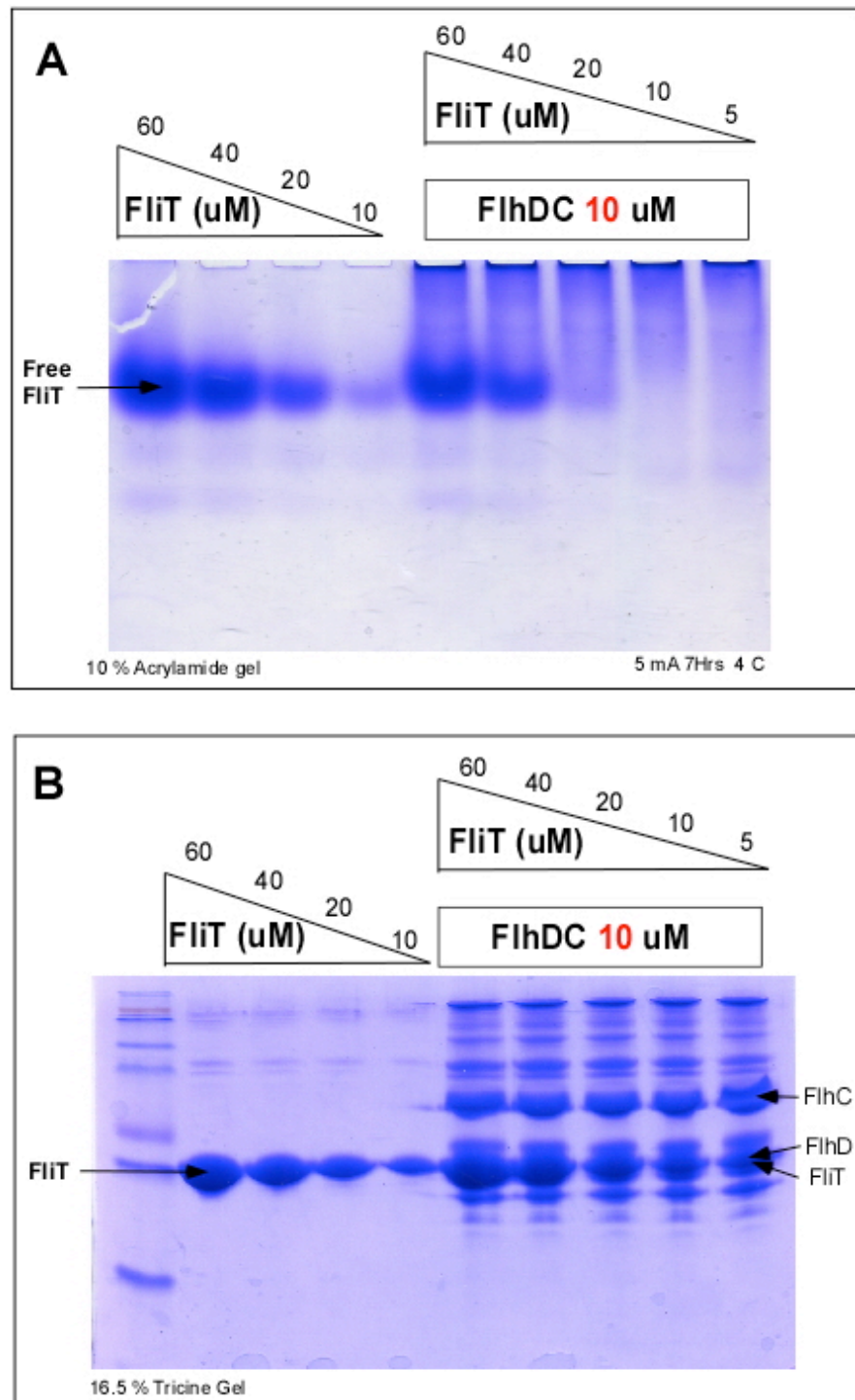


Figure 29. Native gel analysis of *FliT: FlhD₄C₂* interaction with the corresponding SDS-PAGE.

(A) Native gel assay showing decreasing *FliT* levels on the left and decreasing levels of *FliT* with a constant (10 μ M) level of *FlhD₄C₂* on the right side. Addition of *FlhD₄C₂* reduced *FliT* band intensity and generated the smear pattern along the path of their migration. The *FliT* band disappeared completely at a *FliT:FlhD₄C₂* 1:1 molar ratio. **(B)** The corresponding SDS-PAGE of the same samples. The *FliT* / *FlhD₄C₂* solution contains other contaminated proteins and the intense band of *FlhD₄C₂* and *FliT*.

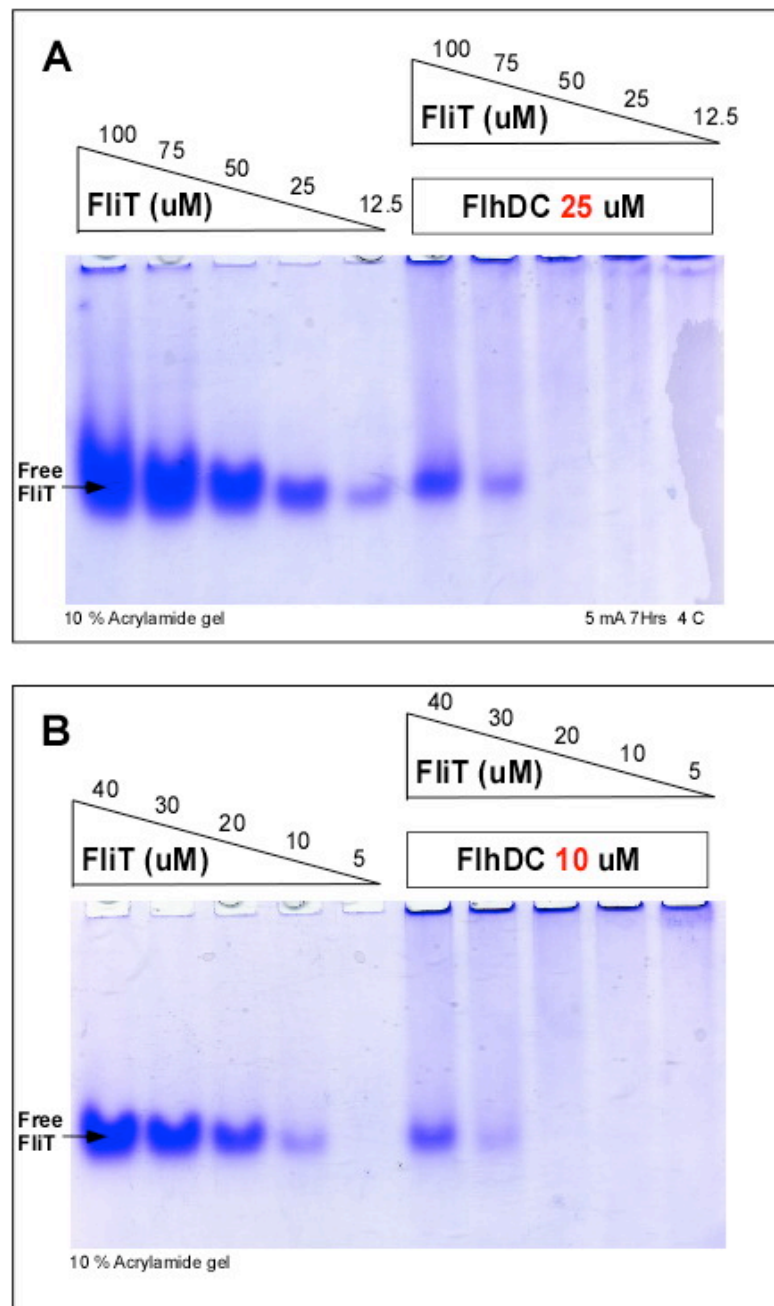


Figure 30. Native gel analysis showing the effect of increased FlhD₄C₂ concentrations.

(A) Native gel assay showing a decreasing concentration series of FliT on the left and the same with addition of a constant 25 μ M level of FlhD₄C₂ the right. Addition of FlhD₄C₂ reduced FliT band intensity and generated a smear pattern along the path of their migration. The FliT band disappeared completely at the FliT:FlhD₄C₂ 2:1 molar ratio. **(B)** Native gel assay showing a decreasing concentration of FliT on the left with addition of constant levels of 10 μ M FlhD₄C₂ on the right. The decrease of each protein concentrations in all mixed samples was performed to retain the same FliT: FlhD₄C₂ molar ratio as in (A). Addition of FlhD₄C₂ reduced FliT band intensity.

6.3 Analysis of *FliT*:*FlhD₄C₂* interaction by gel purification

Native gel analysis suggests the interaction between *FlhD₄C₂* and *FliT*, strongly supporting the proposed interaction of *FliT* with *FlhC* (Yamamoto and Kutsukake, 2006). After the success of isolating a stable *FliT*:*FliD* complex, the subsequent objective was to isolate the *FliT*:*FlhD₄C₂* complex for further analysis, as gel filtration was successful in obtaining a *FliT*:*FliD* complex the same technique was exploited for *FliT*:*FlhD₄C₂*.

To determine if a distinct peak of a *FliT*:*FlhD₄C₂* complex could be generated, gel filtration with two molar ratios of 1:5 (*FliT*:*FlhD₄C₂*) and 1:1 was performed (**Figure 31**). In contrast to the observed behaviour of *FliT*:*FliD* interactions, no distinct peak was observed. Nevertheless, the gel filtration showed the disappearance of the *FliT* peak from its usual region of elution. This result itself further strengthens the other evidence to suggest that *FliT* participates in protein-protein interactions with *FlhD₄C₂*. An interesting observation when comparing the elution profiles was a slight distortion of the *FlhD₄C₂* peak (**Figure 31**). In the presence of *FliT* a slight but noticeable right shoulder produced an asymmetrical peak. *FliT* controls confirmed an expected behaviour of *FliT* without *FlhD₄C₂* (data not shown). The lack of a new peak when *FliT*:*FlhD₄C₂* were allowed to interact was somewhat of a surprise. As *FliT* alone disappeared, the data suggests that a new complex might have a similar molecular weight as *FlhD₄C₂* or this new species behaves in a similar manner to *FlhD₄C₂* during gel filtration. This leaves the question how does the *FliT*:*FlhD₄C₂* interaction change the configuration of the *FlhD₄C₂* complex?

The SDS-PAGE analysis of the *FlhD₄C₂* control peak shows a symmetrical distribution (**Figure 31 B**). After increasing *FliT* concentration, more protein at the right side (smaller mass) emerges and produces an asymmetrical peak for the fractions associated with *FlhD₄C₂* (**Figure 31 A**). In addition, there was a consistent but slight shift of the *FlhD₄C₂* and *FliT* peak from fraction 39 to 40/41 compared with the *FlhD₄C₂* control. In order to examine the effect of *FliT*, increasing ratios were used with the concentration of *FliT* increased to 3 μ M, creating a 1:1 molar ratio. As a result, the right shoulder of the *FlhD₄C₂* peak was larger with a long tail of proteins at the *FlhD₄C₂*/*FliT* region. This result suggests the protein interaction does not only

follow a simple protein binding mechanism but at least there should be a distinct peak of the complexes. In addition, at both concentrations of *FliT* (0.6 and 3 μ M), the *FlhD₄C₂* peak shows a shift to the right suggesting a smaller mass, contrary to the prediction of a larger *FliT*:*FlhD₄C₂* complex as a product. Moreover, the SDS PAGE could not differentiate *FliT* or *FlhD* in the gel; hence, the *FlhD₄C₂* complex would generate the same gel profile as the *FliT*:*FlhD₄C₂* complex. However, even though being consistent with previous studies and the native gel analysis the question of complex existence and *FliT* disappearance still remained.

Taken all together, the sensible assumption is that adding *FliT* to *FlhD₄C₂* does not simply generate a complex but produces an altered complex from the *FliT*/*FlhD₄C₂* interaction. One explanation is that *FliT* interaction generates a smaller complex than a complete *FliT*:*FlhD₄C₂* complex. In doing so, the new complex behaves very similar to *FlhD₄C₂* in gel filtration. The next experiment was performed using higher concentrations of *FliT* in order to assess whether the isolation of a high molecular weight *FliT*:*FlhD₄C₂* complex was possible with *FliT* in excess or whether a smaller complex became the dominant species of the interaction.

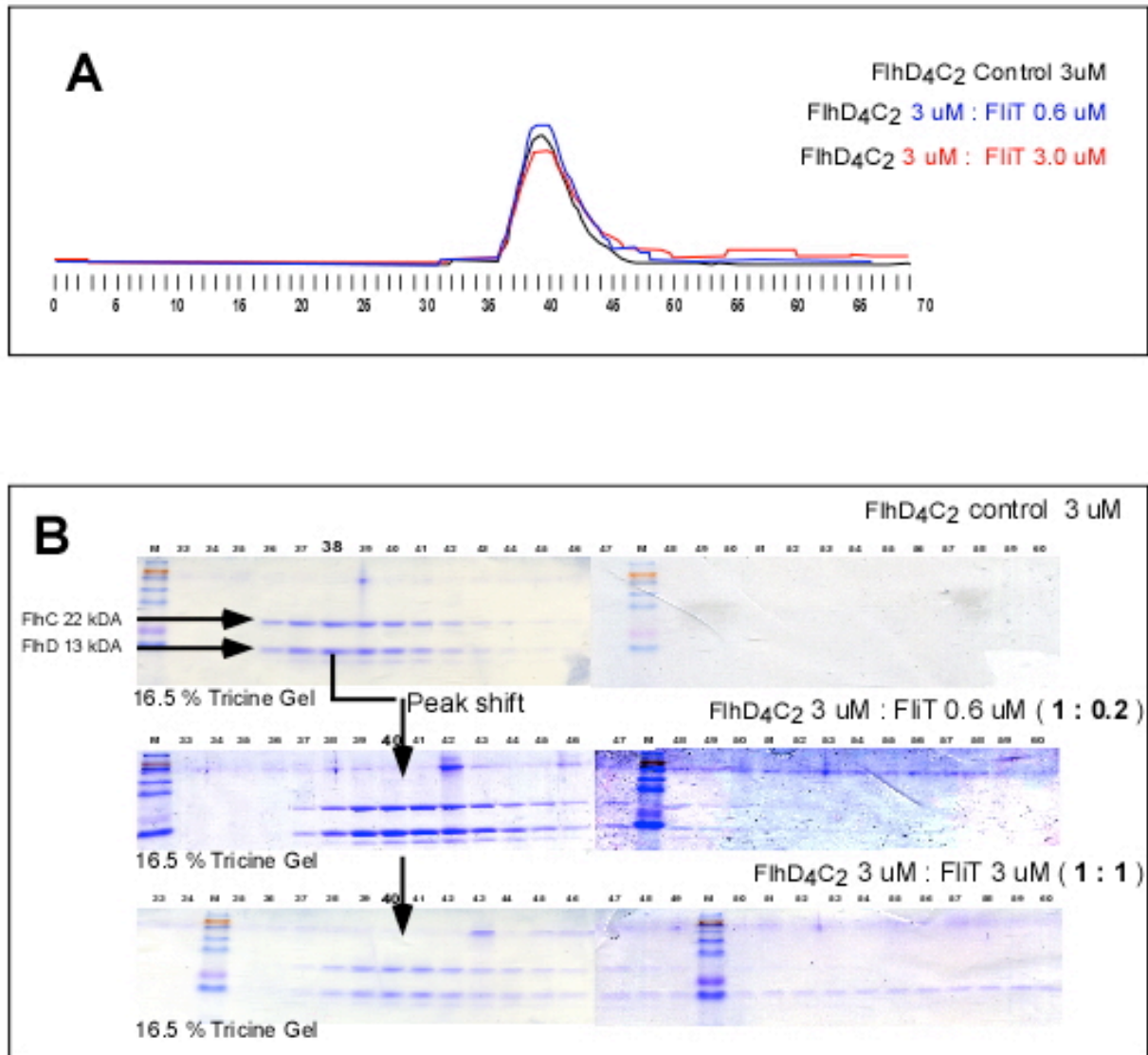


Figure 31. Gel filtration analysis revealed no new peak of the *FliT: FlhD₄C₂* complex but the original *FlhD₄C₂* peak shifted to the right side.

(A) Gel filtration assay indicates the effect of *FliT* towards *FlhD₄C₂* in producing no new peak. The elution profile graphs show 3 μM *FlhD₄C₂* control (black line), with the addition of 0.6 μM *FliT* (blue line), and with the addition of 3 μM *FliT* (red line). The introduction of *FliT* to *FlhD₄C₂* generates the disturbance of gel profiles on the right side which renders the peak slightly asymmetric. Note that the *FliT* control revealed a single peak at fraction 56 (not shown). **(B)** The corresponding SDS-PAGE from the region covering *FlhD₄C₂* and *FliT* as labelled shows the effect of the addition of *FliT* as the relocation of the main peak to the right (smaller mass), and the presence of additional bands at the same size.

To attempt to isolate the FliT:FliH₄C₂ complex increased amounts of FliT were used to observe whether any collectible complex of protein interaction was produced. For this purpose, either 6 μ M or 30 μ M FliT and a fixed 6 μ M FliH₄C₂ concentration were subjected to gel filtration (**Figure 32**). Still, no distinct peak emerged at a greater mass than FliH₄C₂ alone. Our focus was the FliH₄C₂ peak after FliT introduction. Our attempt to find a FliT:FliH₄C₂ complex by gel filtration was not successful even after increasing FliT concentration. Although, the charts suggested a right sided FliH₄C₂ that made the FliH₄C₂ peak even more asymmetrically when a 5:1 FliT:FliH₄C₂ ratio was analysed. Consistently, the SDS-PAGE analysis revealed no evidence of bands in fractions 28-34 where a complex larger than FliH₄C₂ would be expected. Instead a consistent pattern with a peak shift to fraction 40/41 was observed for both ratios analysed (**Figure 33**). Our main assumption therefore still holds that the FliT:FliH₄C₂ interaction produces a complex that behaves similar to FliH₄C₂ alone. We therefore assume FliT could interact with FliH₄C₂ subunits in an unknown mechanism producing an unidentified configuration of the complex but further assessment of the interaction was needed to confirm this.

One issue remains is the whereabouts of FliT. Only in the 5:1 mix was FliT alone observed where a dimer peak usually forms. We predict the peak at fraction 40/41 is considered the main product of the interaction and that it behaves in a similar manner to native FliH₄C₂, when subjected to gel filtration. If this holds true, FliT should be in the FliH₄C₂ region and thus further analysis was required to determine whether FliT was in fact in this region.

Therefore at this point we assume that the function of FliT is not to associate with the FliH₄C₂ complex but to substitute itself for either FliH or FliC in the FliH₄C₂ complex in an unidentified configuration. The subsequent experiments were designed to prove this working hypothesis and the existence of FliT in the main peak.

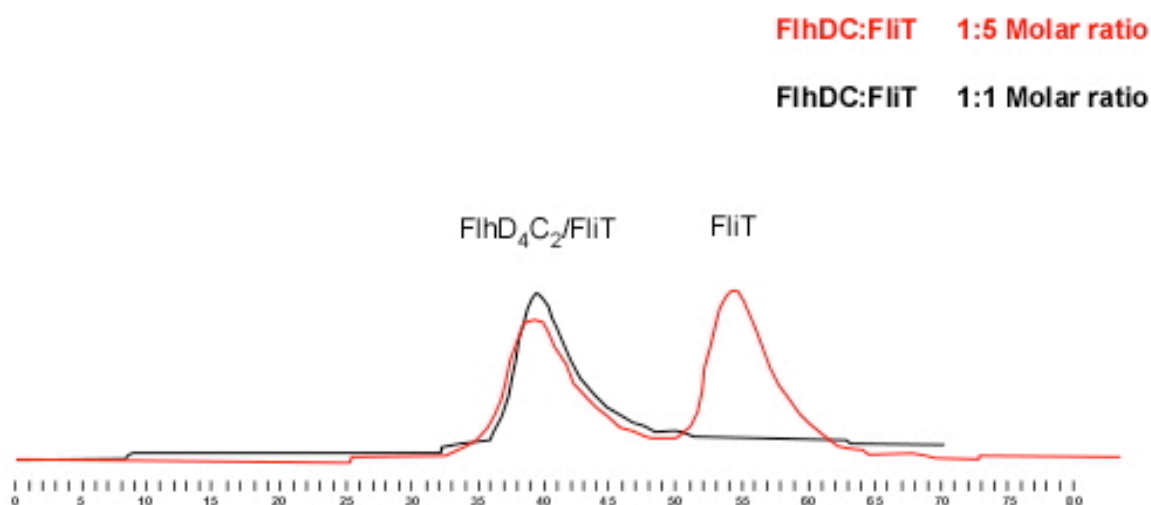


Figure 32. FliT interacts with FliD₄C₂ in generating a FliT/FliD₄C₂ complex the size of FliD₄C₂.

Gel filtration profiles of a 1:1 FliT:FliD₄C₂ (black) and 5:1 FliT:FliD₄C₂ (red). That FliT peak disappears in the 1:1 FliT:FliD₄C₂ profile indicating a FliT interaction with FliD₄C₂. Highly concentrated FliT affects the FliD₄C₂ peak by heightening the peak and broadening the FliD₄C₂ shoulder to the left. The contribution of FliT to become the FliT:FliD₄C₂ complex is not noticeable as a distinct peak. Still, the majority of FliT interaction is predicted to reside on the main peak in an unidentified configuration of FliT/FliD₄C₂. FliT concentration exerts its effect significantly at the main peak, which evidently shows its capability of creating the FliT/FliD₄C₂ complex having roughly the same mass as the FliD₄C₂ complex. This behaviour of the reaction led to the assumption that FliT possibly substitutes itself for some components of the complex through an unidentified mechanism or possibly disrupts the whole FliD₄C₂ complex and rearranges its subunits again before binding FliT to create a product having the same size as FliD₄C₂ alone.

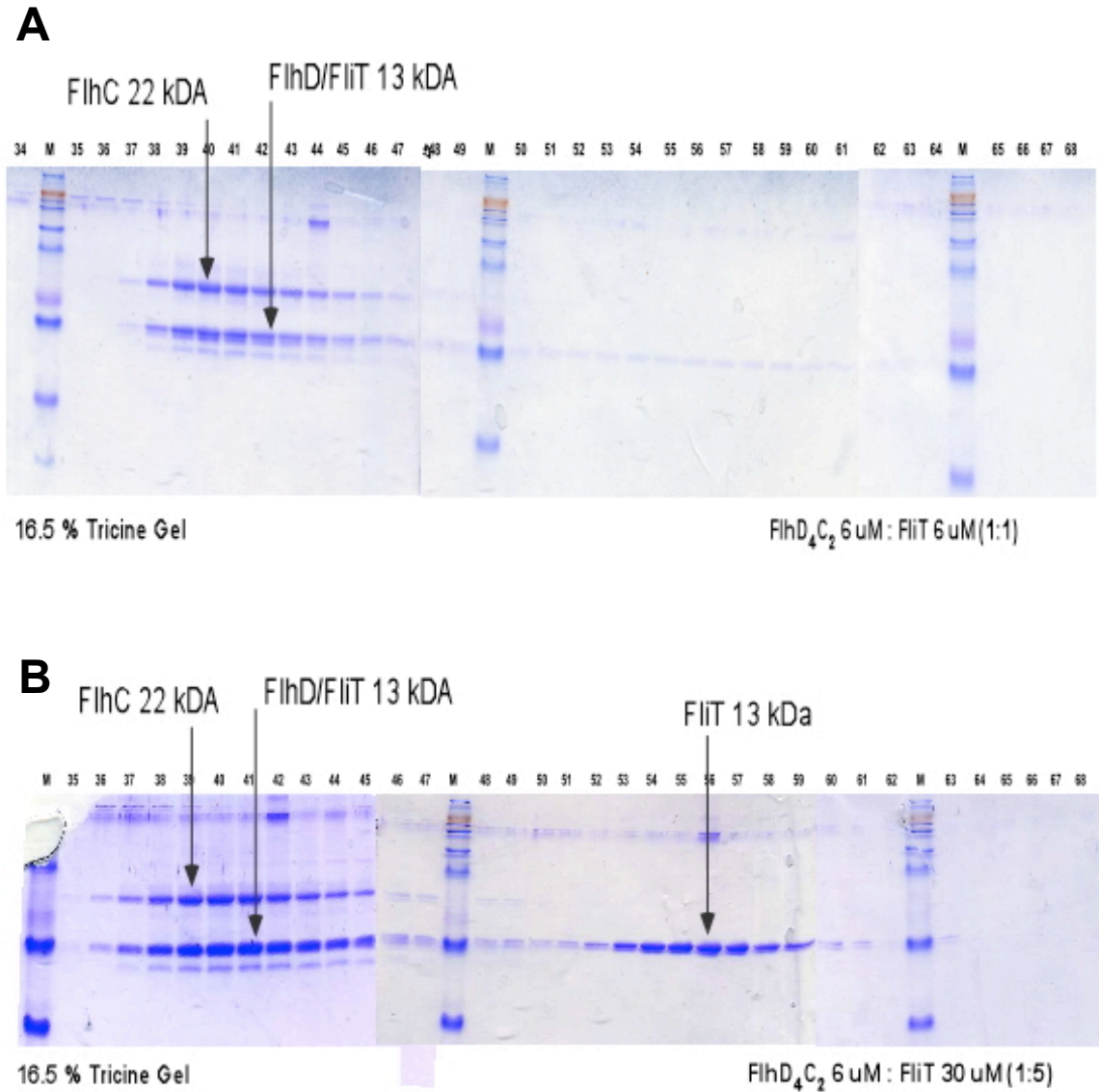


Figure 33. SDS-PAGE of gel filtration all indicates the main peak at FliH₄C₂ region while 1:1 FliT:FliH₄C₂ ratio, smaller complex (FliT/FliH) and excess FliT ,larger complex (FliT: FliH₄C₂).

(A) The 1:1 FliT:FliH₄C₂ ratio shows the presence of the faint continuous bands at FliH/FliT region revealing protein interaction in creating smaller products derived from combination of mainly FliT and FliH rather than simple binding from two proteins. **(B)** Five times FliT concentration to FliH₄C₂ shows strong unreacted FliT bands and the main bands (FliT/ FliH₄C₂) connecting with smaller subunits (FliT/FliH/FliH) but still there was no evidence of the larger complex (FliT/FliH₄C₂).

6.4 MALDI-TOF MS Analysis of FliT incorporated in the products of the FliT:FliH₄C₂ interaction

Gel filtration experiments showed that FliT disappeared when mixed with equal amounts of FliH₄C₂. In nearly all experimental conditions, no new peak was found unless excess amounts of FliT were added. Faint peaks emerged with very high concentrations of FliT (data not shown). These peaks were assumed to be transient complexes possibly generated from nonspecific binding between FliT and FliH₄C₂ due to the amount used. For this reason, the only strong peak from the FliH₄C₂ region is the only possible candidate of being a FliT:FliH₄C₂ complex. If the assumption is true, we expect the relocation of FliT to the FliH₄C₂ fractions due to FliT binding to FliH or FliC.

In our SDS-PAGE analysis, it is difficult to discriminate between FliT and FliH, as both are approximately 13 kDa and thus are superimposed to each other. Therefore the presence of FliT should be detected with FliH at the 13 kDa band (**Figure 33**). To confirm our prediction, Matrix-Assisted Laser Desorption / Ionization-Time Of Flight Mass Spectrometry (MALDI-TOF MS) (**Figure 34**), was used to analyse the protein species on the gel. (**Figure 33**).

Our experimental approach collected fraction 39 from the peak of FliH₄C₂ alone as well as fraction 40 from the peak of a (1:1) FliT: FliH₄C₂ mix. Firstly, SDS-PAGE of both fractions was performed. The lower and upper bands were cut out. Each band of both fractions was digested with trypsin, whose target is exclusively on peptide bonds of the C-terminal of the amino acids lysine and arginine resulting in effective fragmentation of protein in the preferred mass analyzed by mass spectrometry (MS) (Olsen *et al.*, 2004). MALDI-TOF analysis showed that proteins from the control fraction of 39 (FliH₄C₂ control) are FliC (**Figure 35A**) and FliH (**Figure 35B**) while in fraction 40 ((1:1) FliT: FliH₄C₂ mix), consistent with our prediction, the upper band was FliC (**Figure 36A**) while the lower band is FliH plus FliT (**Figure 36B**).

According to this result, the product of the FliT:FliH₄C₂ interaction has the same gel filtration profile as the FliH₄C₂ control. The data confirm FliT does not

simply bind to *FliH*₄*C*₂ due to the products having the same or less molecular weight than *FliH*₄*C*₂ itself from gel filtration analysis, instead *FliT* produces a given subcomplex whose products has nearly the same mobility as *FliH*₄*C*₂ itself during gel filtration.

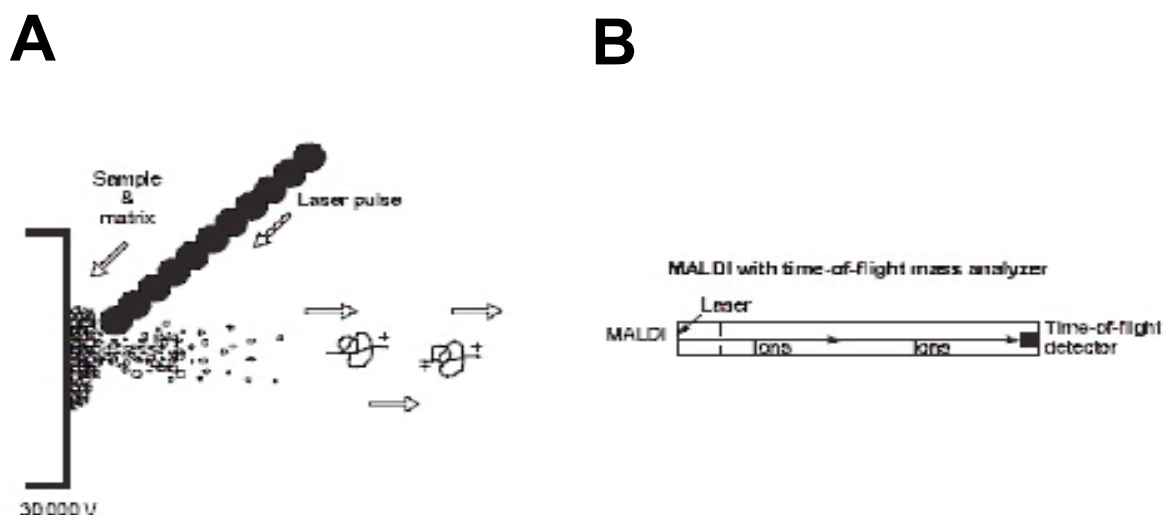


Figure 34 MALDI-TOF illustrated cartoon

(A) MALDI. Protein samples are imbedded into a special matrix and are bombarded with a laser beam. **(B)** The resulting ionized fragments move through an electrical field with a distinctive velocity dependent on their mass: Time Of Flight (TOF).
(Extracted from Lewis, Wei, & Siuzdak, 2000)

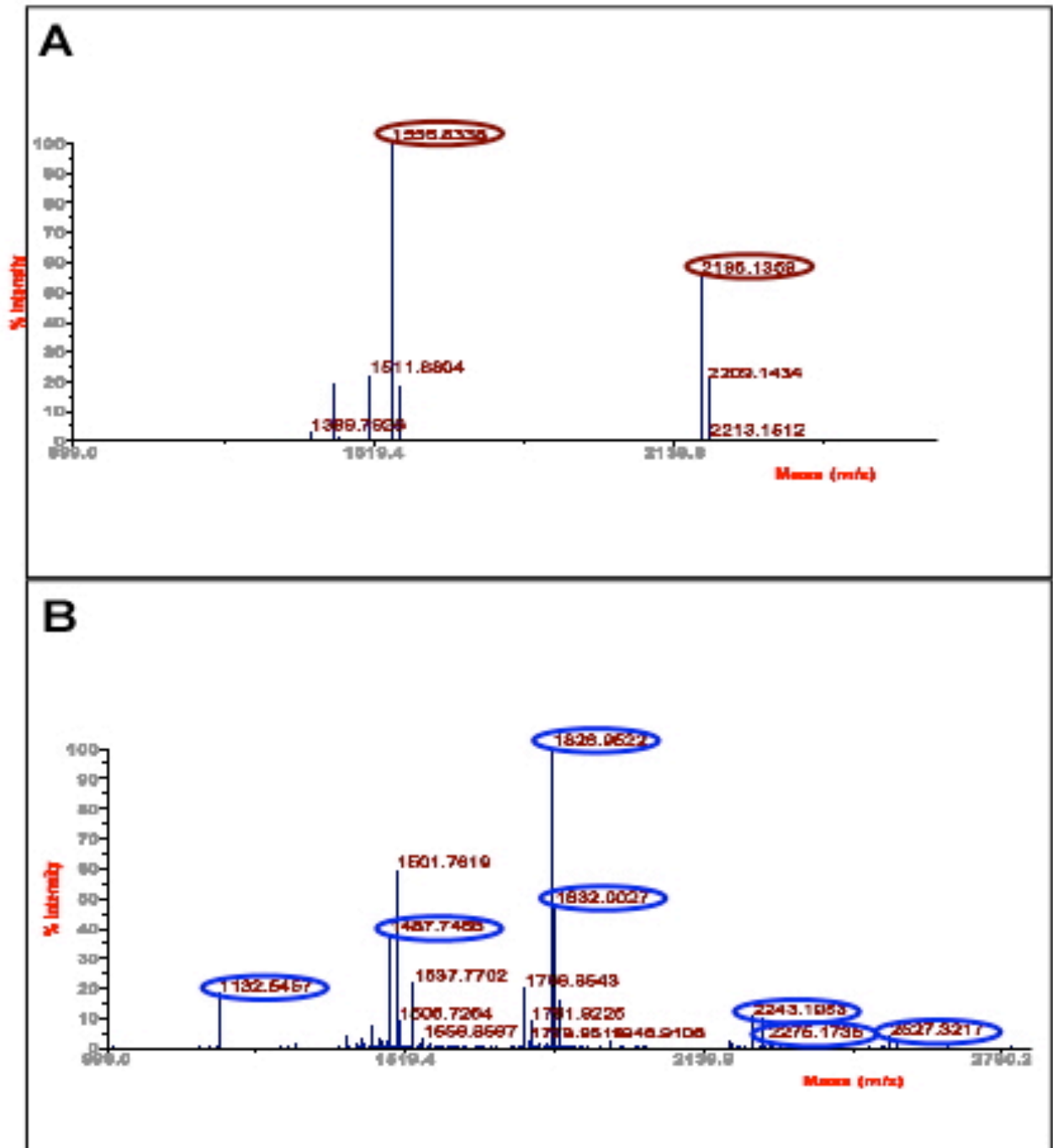


Figure 35. FlhC (A) and FlhD (B) peptide mass fingerprint obtained from MALDI-TOF experiments of FlhD₄C₂ control collected at FlhD₄C₂ peak (fraction 40)

FlhD and FlhC control bands created unique peaks indicating the identity of each protein subunit. In our control, FlhD (B) and FlhC (A) produce unique profiles of peaks due to their difference in amino acid sequence. Protein bands from the SDS-PAGE gel were excised and sent for tryptic digest and MALDI-TOF analysis to determine the protein identity. (A) Peptide mass fingerprint from MALDI-TOF indicates the protein in an upper band, FlhC, with the molecular weight 21.5 kDa. Brown elliptical circles represent the signals originated from FlhC fragments. (B) Peptide mass fingerprint from MALDI-TOF indicates the protein in a lower band, FlhD, with the molecular weight 12.9 kDa based on specific analysis program. Blue elliptical circles represent the signals originated from FlhD fragments.

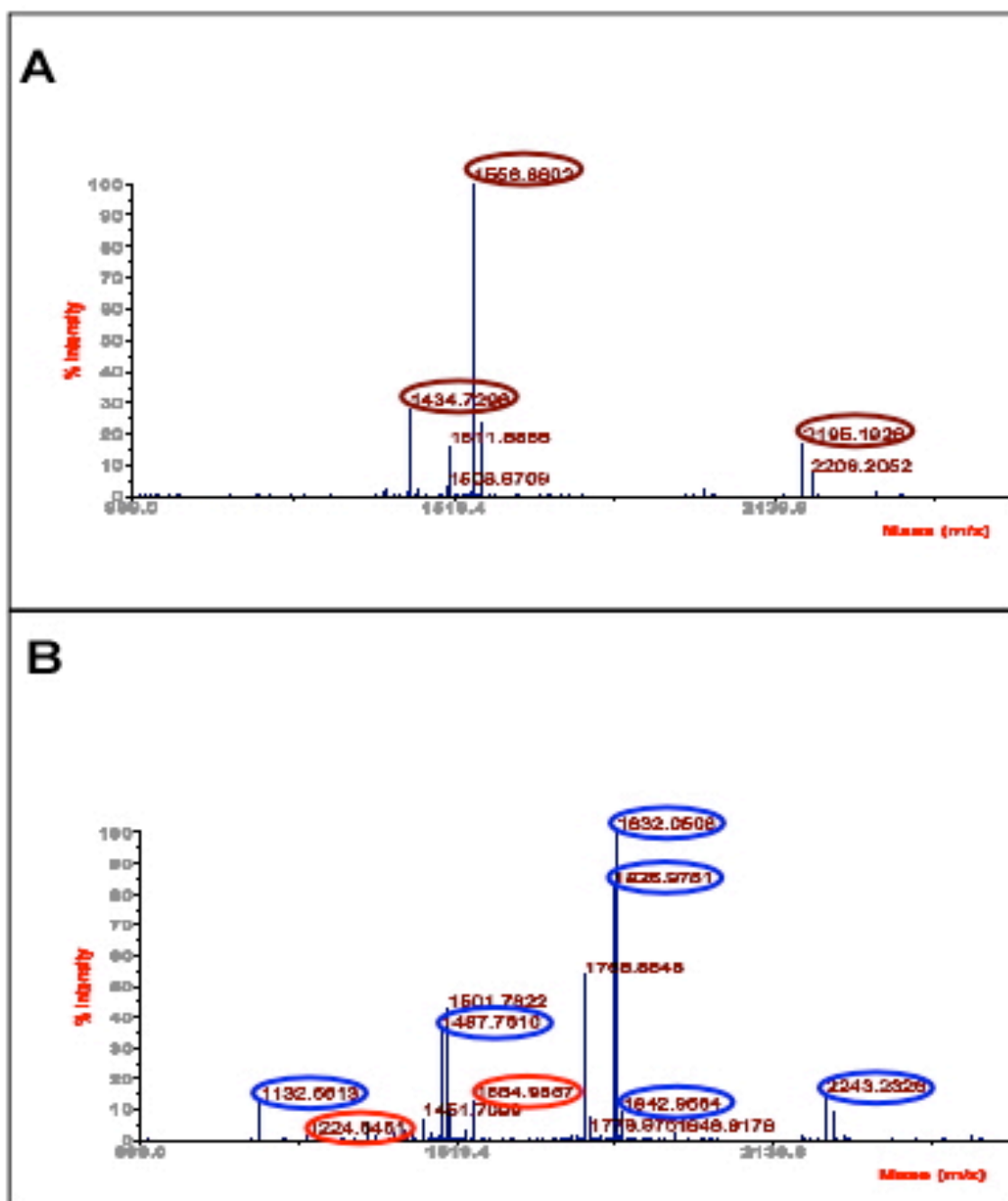


Figure 36. FliH (A) and FliH/FliT (B) peptide mass fingerprint obtained from MALDI-TOF experiments of a FliT: FliH₄C₂ mix collected at the same region (FliH₄C₂ peak, Fraction 39)

FliH (A) and FliH/FliT (B) suggest FliT interacts with FliH₄C₂ from the gel filtration assessments of FliT:FliH₄C₂ mix created the same peak as FliH₄C₂ control. It can be assumed that FliT contributes to the peak. (A) Two strong peaks (brown elliptical circle) indicate FliH peptide mass profile compared with FliH control with the same molecular weight 25 kDa (**Figure 36A**). Together with the profile, one additional strong peak emerges but cannot convince us to identify it as a product because this interaction doesn't involve polypeptide breaking but only subunit binding. (B) FliH peptide mass fingerprint shows almost identical peptide mass fingerprint (blue elliptical circle) and evidence of FliT protein (red elliptical circle). Experimental procedure was performed the same as FliH₄C₂ control (**Figure 36**). The calculated mass based on specific analysis program identified from lower band revealed two proteins coexisting, FliH and FliT, with the molecular weight 13.6 kDa and 12.9 kDa respectively.

6.5 Analysis of the FliT:FliH₄C₂ interaction by Analytical Ultra Centrifugation (AUC)

Analysis of the FliT:FliH₄C₂ interaction was firstly revealed by native gel electrophoresis with the assumption of simple binding between the proteins but the stoichiometry was not identified accurately. Further analysis using gel filtration, confirmed the interaction. However, no evidence of new product of larger mass by simple binding of FliT to FliH₄C₂ was gained. The results from MALDI-TOF analysis confirmed that FliT delocalized to FliH₄C₂ region. However, the results cannot be explained accurately or suggest what FliT does during the interaction. In order to solve this problem, further analytical analysis was introduced.

Our hypothesis was that if we carry out the interaction with a higher resolution experiment, the products of the interaction should be separated from FliH₄C₂ and FliT. It was predicted that the possible products of this reaction could be a subcomplex of FliT:FliH₄, FliT:FliH₃ or a FliT:FliH₄:FliH₃ combination. However, the resolution of gel filtration means that the new complex cannot be separated from the FliH₄C₂ complex. Another method, Analytical Ultra Centrifugation (AUC), was introduced to determine the product identities of FliT:FliH₄C₂ interaction products.

According to the AUC experiment, the different species of protein are indicated by the sedimentation coefficient (S) (**Chapter 5.4**). The FliH₄C₂ control (8 μ M) creates a single peak with a calculated mass of 94.9 kDa (**Figure 37**). The addition of a 1:1 molar ratio of FliT significantly reduced the height of the FliH₄C₂ peak and produced a distorted shoulder towards the left side (smaller mass) of the FliH₄C₂ peak. The FliH₄C₂ peak reduced significantly to form a broad and asymmetrical peak to the left side without the evidence of new species of greater mass. When introducing higher FliT:FliH₄C₂ molar ratios at 5:1 (green line) or 10:1 (dark blue line) this shoulder starts to form a new defined peak but still asymmetrical. This result suggests that FliT functions to disrupt FliH₄C₂. The new peak was calculated to have a mass of 61-63 kDa (**Figure 37**) (Perugini *et al.*, 2000). In fact, the 5:1 and 10:1 ratios look very similar and suggest a complete disruption of FliH₄C₂ requires excess FliT.

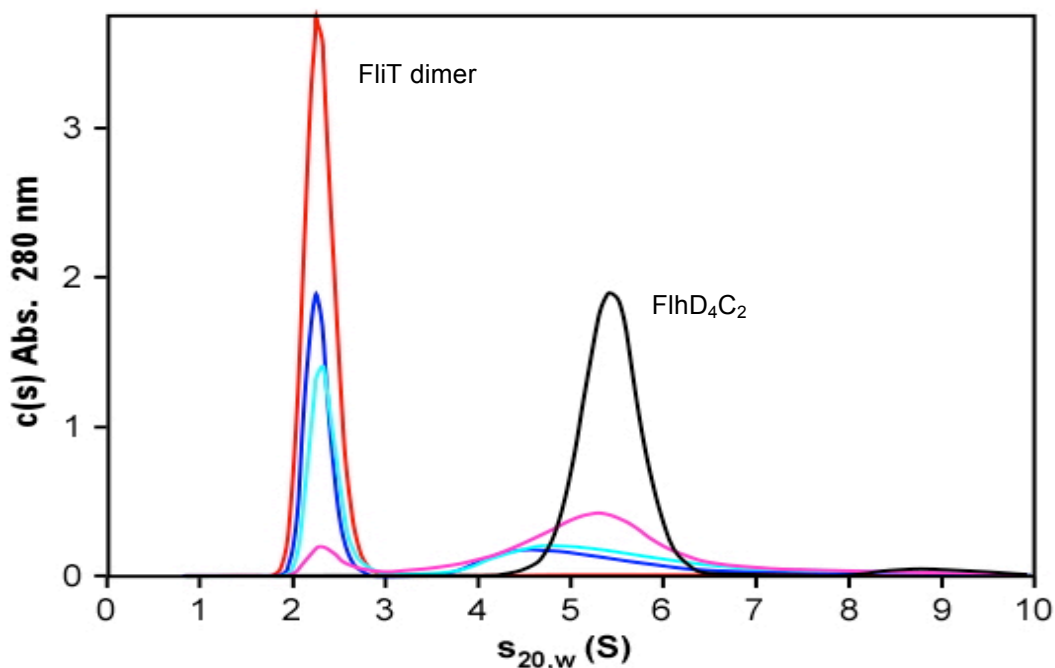


Figure 37. Analytical ultracentrifugation analysis of the interaction of FliT with FliH₄C₂.

FliT (red line) and the FliH₄C₂ complex (black line) were performed as a control. FliT is a dimer with a molecular weight of 28 kDa and the FliH₄C₂ complex has a mass of 94.9 kDa. FliT was added to FliH₄C₂ to achieve a 1:1 molar ratio (pink line). When introducing higher FliT: FliH₄C₂ molar ratios at 5:1 (green line) or 10:1 (dark blue line) this shoulder starts to form a new but still asymmetric peak with a calculated mass of 61–63 kDa. (**Adapted from Aldridge *et al.*., 2010.**)

6.6 Discussion

FliT was reported to bind FlhC and the FlhD₄C₂ complex (Yamamoto & Kutsukake, 2006). In this regulatory circuit, FliT plays a pivotal role in regulating FlhD₄C₂ activity and thus regulates flagellar gene expression. In order to investigate the circuit in more detail, the biochemical properties of the FliT:FlhD₄C₂ protein interactions have been explored. Contrary to Yamamoto's study based on reconstituted FlhD₄C₂, this study relied on the preparation of FlhD₄C₂ complex in a soluble solution. The FlhD₄C₂ purification using heparin column followed by gel filtration in high salt gel filtration buffer (300 mM NaCl, Tris 20mM, pH 7.9) provides a high yield of FlhD₄C₂ complex applied for further analysis.

FliT:FlhD₄C₂ interaction was first explored by native gel analysis to confirm their interaction and to reveal the first evidence about the stoichiometry of FliT:FlhD₄C₂ interaction in a range of 1:1 to 2:1 (FliT:FlhD₄C₂). In addition, native gel analysis suggested the stoichiometry from protein interaction independent of the concentration of FlhD₄C₂ used. According to native gel analysis, protein interaction relied on the FliT band disappearing when added to FlhD₄C₂ as the complex or product was not visible as a unique band on the gel.

In order to explore the interaction in more depth in terms of the products and stoichiometry, gel filtration of a low concentration of FliT (0.6 μ M) mixed with FlhD₄C₂ (3 μ M) was initially performed. This analysis revealed that FliT disappeared and the FlhD₄C₂ peak maxima shifted to the right side (smaller mass) by 1/2 fractions. After increasing the FliT concentration (3 μ M), gel filtration analysis indicated that FliT still disappeared together with the FlhD₄C₂ peak shifted as previous one. Our hypothesis was that FliT interacts with FlhD₄C₂ and then accumulates within the FlhD₄C₂ fractions. Still, no evidence of a large FliT:FlhD₄C₂ complex was observed; instead, SDS-PAGE showed FliT/FlhD bands continues on the right shoulder of FlhD₄C₂ or the expected product peak. From this point, the data suggested that FliT interacts with FlhD₄C₂ possibly in a destructive way in generating various complexes no larger than FlhD₄C₂ complex.

MALDI-TOF analysis confirmed the existence of FliT together with FliH and FliD after the interaction. Previous studies showed FliT interacts with FliH (Claret *et al.*, 2002). Nevertheless, our previous results showed that the interaction isn't simple binding. In addition, the size of the product was still in question as well as its composition. Results from gel filtration revealed that no products larger than the FliH₄C₂ complex was observed except a faint band in excess FliT, which is considered as an artefact from excess FliT. One possible explanation of FliT interaction is that it does not simply bind to the FliH₄C₂ complex but drives the complex dissociation.

Other than the analysis of protein-protein interactions using the methods described in this chapter, an alternative quantitative method is Isothermal calorimeter (ITC). ITC is considered to be a gold standard method for obtaining protein interaction parameters. The principle of this technique is the detection of heat generated when a ligand and analyte interact. ITC is extremely useful when working with simple 1:1 interaction kinetics or when studying the interaction of small molecules with proteins. The feasibility of using ITC to analyse the FliT:FliH₄C₂ interaction was assessed during this work (data not shown). However, the data produced was deemed to be unreliable. After determining the result of the FliT:FliH₄C₂ interaction by AUC we were able to explain why ITC was not a suitable technique. Our reasons for not taking our ITC analysis further was that too many heat generating reactions were occurring when FliT was added to FliH₄C₂. These included: FliT interacting with FliH₄C₂, FliH₄C₂ disassociating and the generation of an as yet undefined complex that included FliT. Unfortunately, a fourth issue with ITC was that at the protein concentrations need to perform ITC, FliT would also transition from a monomer to a dimer (a fourth heat generating reaction). Therefore, even though ITC is an extremely robust technique the nature of the FliT:FliH₄C₂ interaction and the behavior of the proteins themselves deemed this technique unreliable to study the outcomes of this interaction.

As ITC did not produce reliable data we turned to AUC to confirm our hypothesis that behaviour of FliT interaction was to disrupt the FliH₄C₂ complex. In this analysis, the FliH₄C₂ complex significantly disappears when mixed with increasing FliT concentrations. For this reason, the assumption that FliT disrupts the

FlhD₄C₂ complex was then established. The resolution of this technique showed the ability to separate products out of reactants, which was not possible with the other techniques. Moreover, AUC analysis suggests the main product of *FliT*:*FlhD₄C₂* interaction is a complex of proteins having a molecular weight about 61-63 kDa. As we know *FliT* interacts with *FlhC* we propose that this new complex have a core combination of *FliT* and *FlhC*. Our data cannot rule out of *FlhD* inclusion. The exact combination as well as its stoichiometry of the product needs more investigation.

Chapter 7

SPR analysis of FliT:FlhD₄C₂:DNA interaction

Chapter 7. SPR analysis of *FliT*:*FlhD₄C₂*:DNA interaction

The main focus of this project was to investigate the biochemical properties of the *FliT*:*FliD*:*FlhD₄C₂* regulatory circuit. Yamamoto and Kusukake (2006) first showed that *FliT* interacted with *FlhC*. They proposed a model in which *FliT* acted as an anti-*FlhD₄C₂* factor preventing *FlhD₄C₂* binding to DNA. In chapter 6 we have now shown that on interacting with *FlhD₄C₂*, *FliT* disrupts the complex presumably through its interactions with *FlhC*. To effectively see this response we had to introduce excess amounts of *FliT* to the *FlhD₄C₂* complex and were only able to observe the result using analytical ultracentrifugation. This data is consistent with Yamamoto's model but still does not take into consideration the role *FlhD₄C₂* binding to DNA plays.

FlhD₄C₂, being a master transcriptional regulator of flagellar gene expression, is not only involved in protein-protein interactions. To activate transcription *FlhD₄C₂* binds a defined binding site just upstream of the -35 component of class 2 flagellar promoters. The way in which *FlhD₄C₂* interacts with DNA, where its binding sites are located and how it contacts RNA polymerase defines *FlhD₄C₂* as a Type I transcriptional activator (Liu *et al.* 1995). The ability of *FlhD₄C₂* to bind DNA therefore adds a fourth factor to the *FliT*:*FliD*:*FlhD₄C₂* regulatory circuit, the *FlhD₄C₂* DNA binding site.

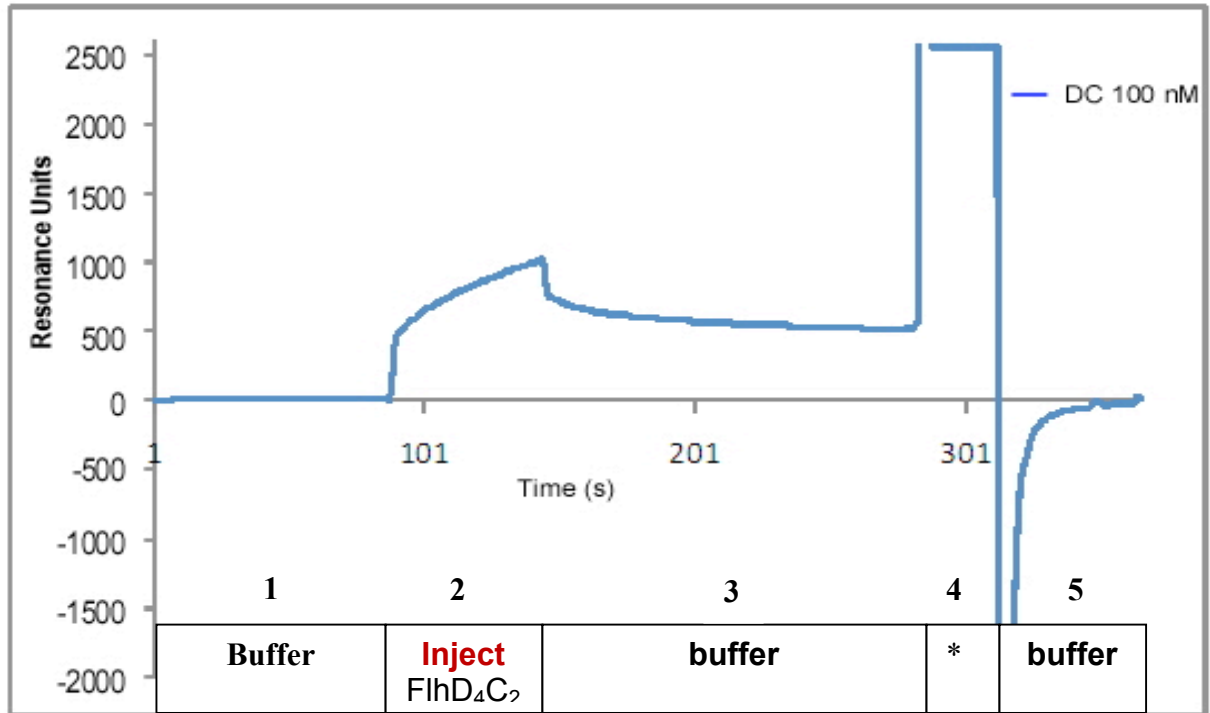
At this point in this project and with respect to the literature the main focus on how this regulatory circuit works has been to investigate the protein-protein interactions. We were therefore interested to ask what role does *FlhD₄C₂* binding DNA play in the regulatory circuit. For example are the protein-protein interactions more important or does the ability to bind DNA play a significant role in defining the dynamics of the regulatory circuit. As we wished to investigate several aspects of the *FlhD₄C₂*:DNA interaction with respect to the circuit we decided to utilise Surface Plasma Resonance (SPR) as our chosen assay method over more conventional DNA shift assays. Surface Plasma Resonance (SPR), is a well-known method for the study of protein-protein interactions for the analysis of binding preference, binding strength and interaction dynamics. This technique uses an optical component called the sensor surface, where a change in the refractive index in response to different

conditions of mobile solutes is the mode of detection. The sensor surface forms a flow cell where aqueous buffers can run through. In order to investigate the analyte:ligand interactions, ligands are first immobilized on the surface and analytes are then run over the bound ligand through the flow cell. If an interaction occurs this is detected in real time by a change in the refractive index and defined using the term resonance units (RU).

An advantage of SPR for this project was that we could first bind *FlhD₄C₂* to its DNA binding site then introduce *FliT* and/or *FliD* to monitor their influence upon the *FlhD₄C₂*:DNA complex as well as their ability to influence the actual *FlhD₄C₂*:DNA interaction. To detect the later we followed changes in *FlhD₄C₂*:DNA binding kinetics when combinations of *FlhD₄C₂*, *FliT* and *FliD* were added to the empty DNA binding site. This chapter describes the data generated using initially two known *FlhD₄C₂* binding sites (*P_{flgB}* and *P_{flhB}*) and what was believed to be a randomly chosen DNA sequence (an internal sequence from the coding region of *fliC*) that would act as a control. As the binding kinetics were very similar for both known binding sites we focussed the majority of analysis on the binding site previously being defined to have the strongest affinity for *FlhD₄C₂* (Stafford *et al.*, 2005).

7.1 *FliT* regulation towards *FlhD₄C₂*:DNA interaction monitored by SPR analysis.

In this study, DNA or promoter regions of *flgB* and *flhB*, and the intragenic region of *fliC* were immobilized separately to a chip and tested for being *FlhD₄C₂* binding sites. To prepare an *FlhD₄C₂* binding surface, a biotinylated DNA fragment form of *flgB* was bound to a streptavidin coated sensor chip. Since the intragenic region of *fliC* was not thought to be an *FlhD₄C₂* binding site, it was selected to be a negative control. The general protocol followed throughout all SPR experiments is summarized in **Figure 38**. Changes in the refractive index are defined as resonance units (RU). Each cycle of the SPR experiment was run consecutively as follows; 1) buffer to generate a baseline correction; 2) the *FlhD₄C₂* was injected for a defined period; 3) buffer injected to measure disassociation; 4) a regeneration injection with NaOH to remove all proteins from the DNA; and finally 5) a final buffer wash to prepare the chip surface for a subsequent experiment.



*Regenerate buffer

Fig. 38 The Sensogram diagram generated by SPR experiment

An analysis of protein interaction was performed using SPR over time. The result of a sensogram displayed resonance number on the Y-axis as the amount of the FlhD₄C₂ that bound to a ligand (DNA; *P_{flgB}*) on a chip. Each SPR experiment's cycle needed baseline adjustment of the buffer (1), duration of FlhD₄C₂ injection (2), washing unspecific protein binding by the buffer and leaving only FlhD₄C₂ that bound to a ligand at approximately 500 RU (3), removing total bound FlhD₄C₂ by regenerating buffer (NaOH) (4) and baseline adjustment using the buffer (5). The capability and the affinity of the FlhD₄C₂ to bind to the ligand were observed mainly in steps 2 and 3. An increase in the slope after injection reflected the ability of the FlhD₄C₂ to bind to the ligand, and the left RU value reflected the protein affinity or the stability of protein after binding. SPR data were interpreted exclusively from graph only in steps 2 and 3. The result could be measured quantitatively for one variable factor.

For simplicity, when presenting the results of SPR experiments the X-axis was defined to include only the whole of step 2 and all or part of step 3 (**Figure 39**). Interestingly, even from this first experiment it is clear that the *FliH*₄*C*₂:DNA complex was rather stable showing an almost straight line after an initial drop when the system was moved to a disassociation buffer injection (**Figure 39: step 3**). This is consistent with previous studies of the *FliH*₄*C*₂:DNA interaction (Claret *et al.*, 2000, Wang *et al.*, 2006).

An initial experiment was to use a given concentration of *FliH*₄*C*₂ and monitor its ability to bind *P*_{*fliG*B}, *P*_{*fliH*B} and *fliC* DNA. We assumed that the *FliC* DNA would act as a negative control showing no binding. To our surprise all three fragments were able to capture *FliH*₄*C*₂ (data not shown). Although not expected, Stafford and Hughes (2005) were able to measure a non-specific interaction of *FliH*₄*C*₂ to DNA in their study when defining the binding site of *FliH*₄*C*₂. Consistent with their study the *fliC* interaction had a different binding curve to *P*_{*fliG*B} and *P*_{*fliH*B} and during experiments to be discussed later the interaction with *FliC* is clearly different from DNA containing a known *FliH*₄*C*₂ binding site.

In order to determine the affinity of *FliH*₄*C*₂ to *P*_{*fliG*B} in our system the isolated *FliH*₄*C*₂ was analysed using concentrations of 50 nM, 100nM, and 200 nM (**Figure 39A**). The binding profile of the *FliH*₄*C*₂ was increased with concentration, which suggested a specific binding. The binding properties of the *FliH*₄*C*₂ could be revealed more deeply through the manual evaluation of *K*_D and *R*_{max} of the data (**Table 8**). *R*_{max} is defined as the maximum level of resonance that the SPR machine could reach. When describing enzyme reactions *V*_{max}, is often defined as the maximum activity that could be reached by the reaction, *R*_{max} can be regarded in a similar light being the maximum level an interaction could theoretically reach if saturation is not achieved during an injection. The *K*_D and *R*_{max} were manually calculated from the binding profiles via fitting to a Langmuir adsorption equation (C. Rao, personal communication). This was performed, as the profiles did not match standard models possible due to the nature of how *FliH*₄*C*₂ interacts with DNA. For example as *FliH*₄*C*₂ could bind the negative control it suggests the complex can first bind DNA loosely and only if a binding site is present a stronger interaction would occur. In SPR this would alter the binding profiles from defined standard models

complicating analysis of the data. For the FlhD₄C₂:DNA interaction the K_D calculated was approximately 10-fold lower than previously described (Stafford and Hughes, 2005). However, encouragingly they were still in the nM range. Such differences between detection techniques are known to be one of the limitations of techniques like SPR.

To investigate the effect FliT had upon the FlhD₄C₂:DNA interaction, mixtures of 1:1 FliT: FlhD₄C₂ were analysed by SPR and the results compared with those from FlhD₄C₂ alone (**Figure 39**). A significant decrease in RU was observed, however, the FlhD₄C₂:DNA interaction was still detectable. Analysis of the K_D and R_{Max} values of the FliT: FlhD₄C₂ mixes suggested that one aspect of the regulatory mechanism employed by FliT was to reduce the availability of FlhD₄C₂ rather than reduce the affinity of FlhD₄C₂ to DNA (Table 8). This can be seen in a significant drop in the R_{max} value but a similar K_D value for both data sets. This observation is consistent with the AUC data in chapter 6 where we show that FliT disrupts the FlhD₄C₂ complex.

The fact that the AUC data was consistent with the SPR profiles of the 1:1 FliT: FlhD₄C₂ combinations led us to determine the concentration of FliT needed to completely inhibit the interaction of FlhD₄C₂:P_{flgB} DNA. The chosen concentration of FlhD₄C₂ (100 nM) was mixed with various concentrations of the FliT, (0 nM, 100 nM, 150 nM, 250 nM, and 400 nM) before performing the sample injection (**Figure 40**). The lowest concentration of the FliT (100 nM) effectively reduced the RU value by nearly half as compared to the FlhD₄C₂ alone (**Table 9**). An increase in the FliT concentration resulted in a decrease in the RU value until it reached nearly the same RU value for 250 and 400 nM of the FliT (**Figure 40 and Table 9**). This suggests that the stoichiometry of the FliT:FlhD₄C₂ interaction resulting in maximum inhibition was greater than 2:1. This is consistent with the AUC data where a strong disassociation of the FlhD₄C₂ complex was only observed with excess FliT. This suggests that to have a significant influence on FlhD₄C₂ activity, FliT needs to be in excess in the cell.

7.2 Motility assay of overexpressed *FliT*

The analysis of the *FliT*:*FlhD₄C₂* interaction by AUC suggested that the mechanism of shutting down flagellar synthesis was through the disruption of free *FlhD₄C₂* complexes by *FliT*. The initial SPR data was consistent with this observation in that a strong inhibition of the *FlhD₄C₂*:DNA interaction. In order to serve as a primer for the synthesis of flagella, the *FlhD₄C₂* complex was supposed to be present in both free form (ready to work) and DNA bound form (working form). As *FliT* is classified as a negative regulator for flagellar synthesis, the protein would be predicted to disrupt the *FlhD₄C₂* complex. Our data suggests this requires excess amounts of *FliT*. This suggests that if we were to artificially increase *FliT* concentrations in the cell we should inhibit flagellar gene expression leading to a non-motile phenotype. Therefore a motility assay of *S. Typhimurium* where *fliT* was overexpressed using motility agar was performed (**Figure 41**). Surprisingly, multicopy overexpression of *FliT* was not able to completely inhibit flagellar gene expression measured via the ability of *S. Typhimurium* to be motile. A valid explanation from the motility data might be that the level of overexpression of *FliT* was not sufficient to destroy all free *FlhD₄C₂* complexes. An alternative explanation is that *FlhD₄C₂* exhibits a given level of resistance to *FliT* disruption. This would result in a given amount of *FlhD₄C₂* free to bind DNA and able to initiate flagellar synthesis.

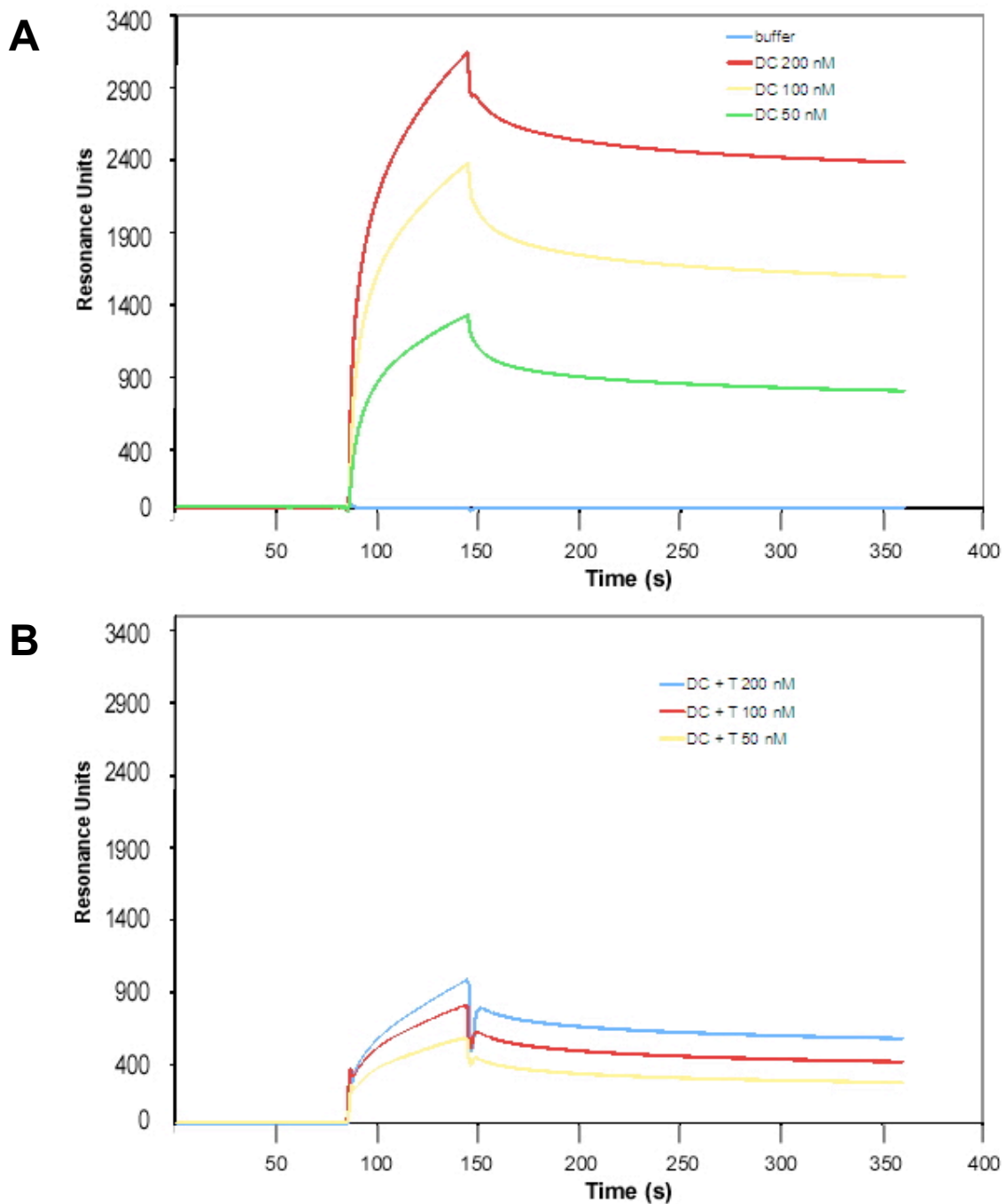


Figure 39. SPR analysis of *FlhD₄C₂* and *FlhD₄C₂/FliT* interaction to *P_{flgB}* (DNA)

(A) The binding profiles of the *FlhD₄C₂* at various concentrations to *P_{flgB}*. Different concentrations of the *FlhD₄C₂* in nM range; 50 (green line), 100 (yellow line) and 200 (red line) were subjected and then bound to *P_{flgB}* in a concentration-dependent manner. The *FlhD₄C₂* showed a high irreversible affinity for DNA at 200s. Buffer alone showed no nonspecific binding. **(B)** An analysis of the *FliT* that inhibited on the *FlhD₄C₂*'s capability to bind to *P_{flgB}*. All individual experiments were performed with several concentrations of 1 to 1 ratio of the *FlhD₄C₂/FliT*, i.e., 50, 100, 200 nM, freshly prepared before injection. The *FliT* mixed with *FlhD₄C₂* at equal amounts could reduce the signal (RU) from *FlhD₄C₂* itself approximately 200%. Results of all experiments done with various concentrations of the mixture at 1:1 ratio of the *FlhD₄C₂/FliT*, i.e., 200 nM (blue line), 100 nM (red line), and 50 nM (yellow line) showed a significant reduction of RU signal. **(Adapted from Aldridge *et al.*, 2010.)**

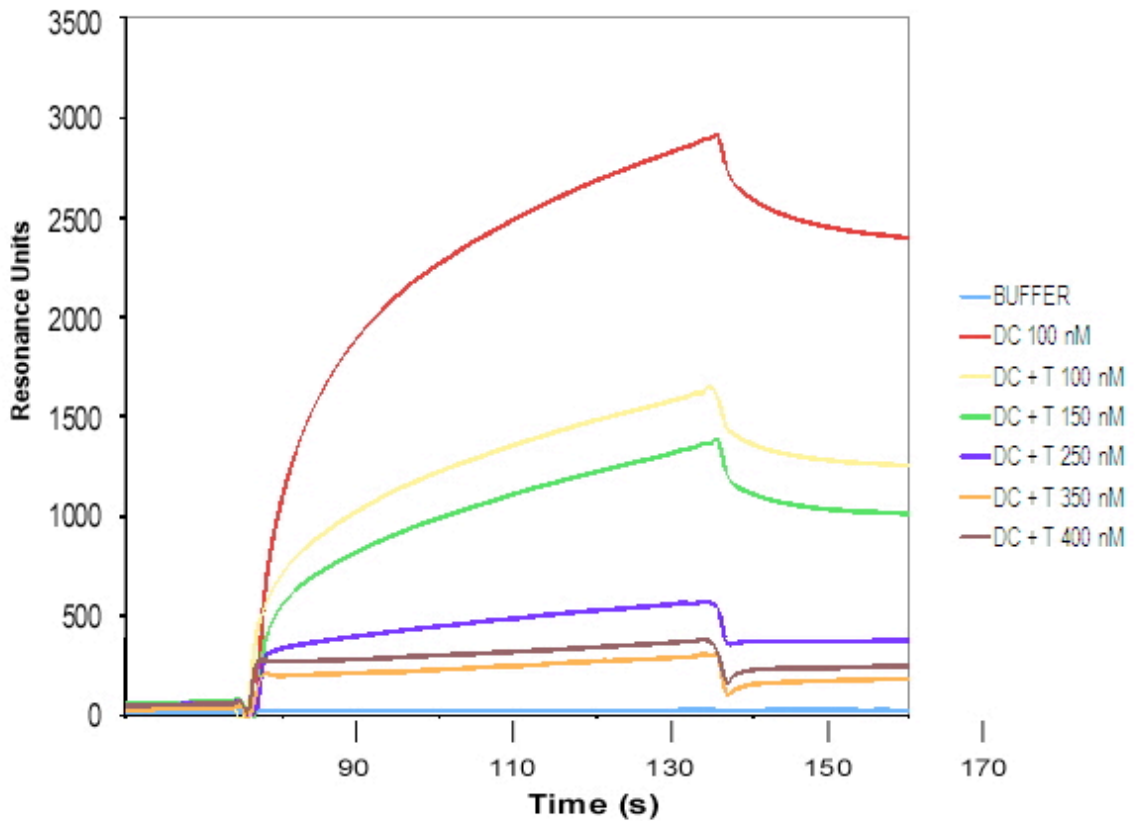


Figure 40. SPR analysis of FliT regulation towards FlhD₄C₂:DNA interaction.

Results of an analysis of the FliT concentrations that are required to inhibit FlhD₄C₂:P_{flgB} DNA complex formation were shown that the binding profiles of the FlhD₄C₂ (red line) when compared with those of the FlhD₄C₂ mixed with various concentrations of the FliT (different colours), freshly prepared before injection. All individual experiments were performed with 100 nM of the FlhD₄C₂. Red line represents No FliT. Yellow represents 100 nM FliT. Green represents 150 nM FliT. Dark blue represents 250 nM FliT. Orange represents 350 nM. Brown represents 400 nM FliT and a buffer control (light blue). The signal reduction nearly reached its saturation or no further reduction at approximately 400 nM or of the FlhD₄C₂ and FliT mixture at 1: 4 ratio, which was supposed to be the stoichiometry of FlhD₄C₂ that was completely interacted with the FliT and inhibited the formation of FlhD₄C₂:DNA complex. (Adapted from Aldridge *et al.*., 2010.)

Table 8: Biochemical Parameters generated by SPR experiment

Biochemical parameter	K _D (nM)	R _{max} (RU)
FlhD ₄ C ₂	175	3933
FlhD ₄ C ₂ + <i>FliT</i>	214	560

Table 9: The SPR data of FlhD₄C₂ signal from various concentrations of *FliT* interaction

Concentration of <i>FliT</i>	Relative reduction in FlhD ₄ C ₂ :DNA interaction
0	1.000
100	0.501
150	0.397
250	0.199
400	0.138

(Analysis was performed in collaboration with C. Rao (University of Illinois, Urbana, IL, USA)

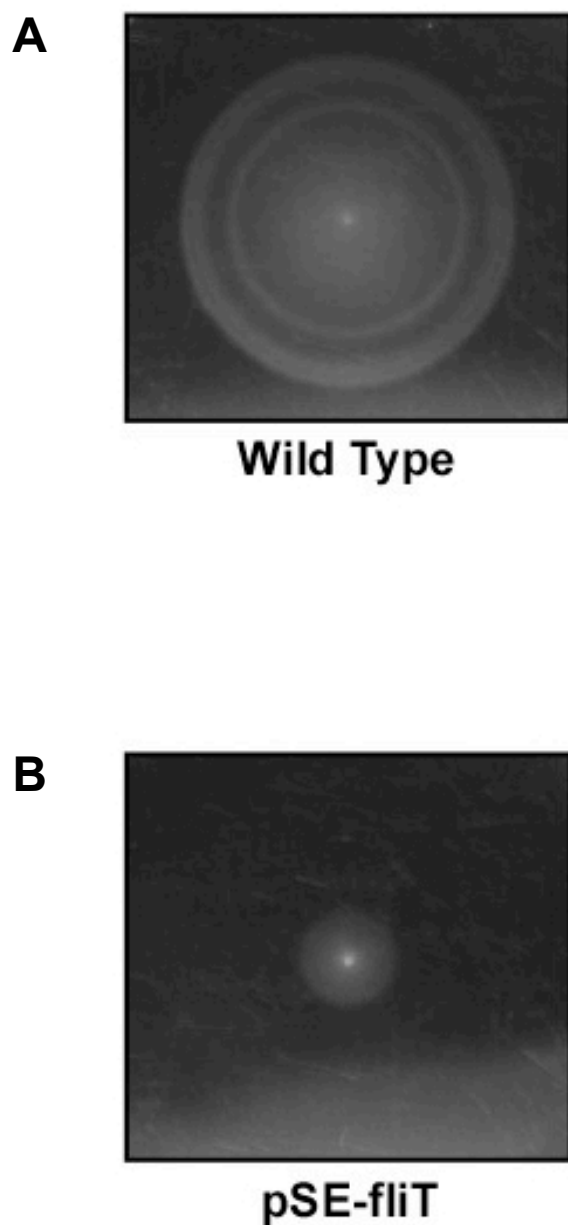


Figure 41. The motility test and swimming pattern of the wild type and the overexpressed *FliT* strain.

The motility of the wild type *S. typhimurium* (**A**) observed in 4 hrs at RT and the reduction of the motility of the overexpressed *FliT* strain (**B**) were compared. An overexpression of the *FliT* strain effectively reduced the motility but it could not render cells non motile.

7.3. An SPR analysis shows resistance of *FlhD₄C₂*:DNA complex to *FliT*.

At this point the *in vitro* and *in vivo* motility data suggests a complicated regulatory interplay between *FliT* and *FlhD₄C₂*. We have shown that excess *FliT* is required to induce the disruption of the *FlhD₄C₂* complex, that excess *FliT* is required to significantly inhibit the *FlhD₄C₂*:DNA interaction, however when overexpressed *FliT* is unable to completely inhibit motility. These observations led us to postulate that some *FlhD₄C₂* is escaping *FliT* regulation and drives the production of flagella. One testable explanation for this observation is the hypothesis that DNA-bound *FlhD₄C₂* would be resistant to regulation of the *FliT*. This hypothesis is a valid option, as we know that *FlhD₄C₂* can bind both its binding site plus non-specifically to DNA.

To test this hypothesis the previous SPR experiments were modified to incorporate two injections, the first *FlhD₄C₂* to generate a *FlhD₄C₂*:DNA complex and then a second injection of either free DNA or *FliT* (**Figure 42**). The addition of free *P_{flgB}* DNA was used as a control for disassociation of *FlhD₄C₂* from the biotinylated sensor chip bound DNA fragment. In effect this control was similar to a standard competition assay where we assumed excess free *P_{flgB}* DNA would compete the bound *FlhD₄C₂* off the immobilised DNA. When establishing the SPR experiments two promoter regions, *P_{flgB}* and *P_{flhB}*, and one intragenic region, *fliC*, were tested to reveal the specific *FlhD₄C₂* binding capability toward DNA. We used all 3 immobilised fragments during the setup of this second assay (**Figure 43**). This allowed us to show the differences in *FlhD₄C₂* binding to these DNA fragments. When free *P_{flgB}* was flowed over *P_{flgB}* a straight line was observed suggesting a 1:1 exchange. However for *P_{flhB}* and *fliC* immobilised DNA a much sharper drop in disassociation was observed when free *P_{flgB}* was used, consistent with our initial assumption and the observations of Stafford and Hughes (2005). This experiment also shows that we are able to disassociate *FlhD₄C₂* from DNA without using an aggressive regeneration step.

The effect of *FliT* on the *FlhD₄C₂*:*P_{flgB}* complex was then tested. The *FlhD₄C₂* complex was first bound to the *P_{flgB}* DNA binding site, this complex was then subjected to the *FliT* at a concentration of 100 nM and compared the response

observed when free P_{flgB} DNA was injected (**Figure 44**). The introduction of FliT to the system could not reduce the RUs of the DNA-bound FlhD₄C₂ (**Figure 44**). Other attempts at higher concentrations of the FliT were also performed with the results shown to be the same (data not shown). In contrast, as in the positive control experiment, 100 nM P_{flgB} injected over the FlhD₄C₂:P_{flgB} complex resulted in departure of FlhD₄C₂ from the immobilised DNA fragment (**Figure 44**).

These results suggested that the FlhD₄C₂:DNA complex protects FlhD₄C₂ from the interaction with FliT. As a result, the FlhD₄C₂-DNA complex could escape the regulation of the FliT, allowing the complex to activate the expression of flagellar genes. Thus our data suggests the net result of the regulation of the FliT is to restrict the availability of functional FlhD₄C₂ in response to flagellar synthesis. Furthermore the fact that we did not observe a FliT: FlhD₄C₂:DNA complex being formed in these experiments suggests that when bound to DNA the complex is unable to interact with FliT. This is consistent with both Yamamoto and Kutsukake (2006) and Claret *et al.*, (2000) as they both show that FliT binds FlhC and it is FlhC that is the major DNA binding component of the FlhD₄C₂ complex.

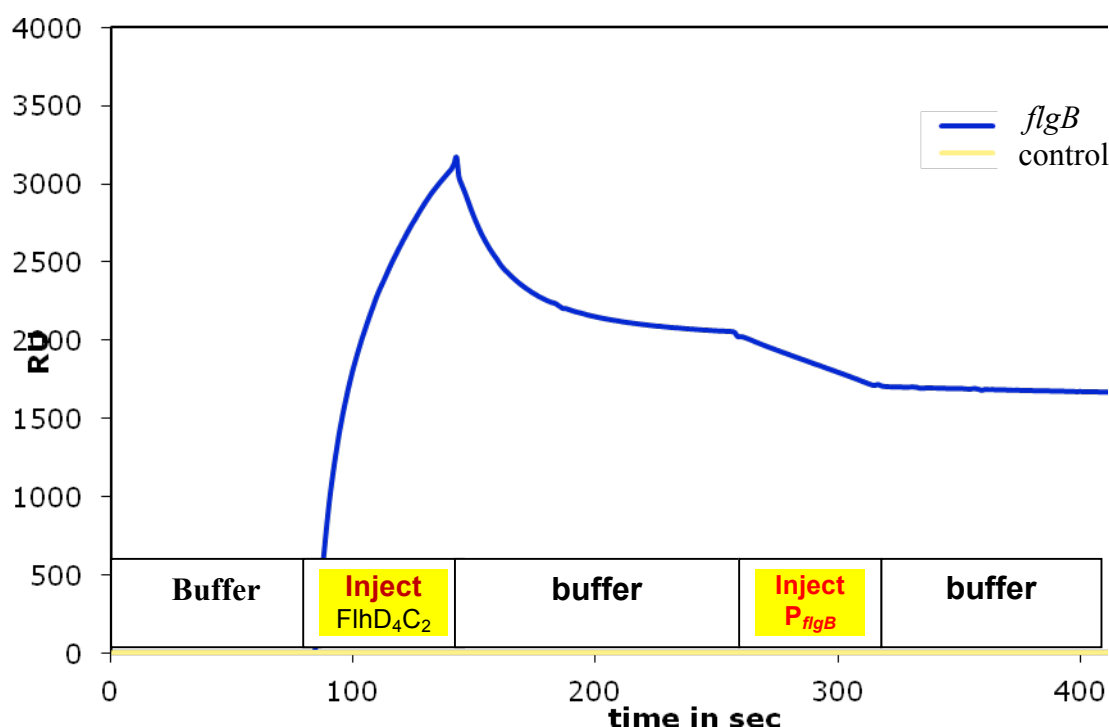


Figure 42. SPR Profile showing the double injection of *FliH*₄*C*₂ and *P*_{*flgB*}, respectively

Results of the analysis of the affinity of analyte to bind to ligand after challenge from an inhibitor. The experiment began with the first injection (freshly prepared *FliH*₄*C*₂; 100 nM) of the DNA-bound *FliH*₄*C*₂, followed by the second injection (*P*_{*flgB*}) in order to study the capability of the *FliH*₄*C*₂ to depart from DNA. Introduction of the *P*_{*flgB*}, (the signal reducing agent), caused significantly reduced levels of the *FliH*₄*C*₂ DNA complex, whereas buffer that replaced the *P*_{*flgB*} induced no change of signal. The *P*_{*flgB*} acted as competitive ligands that were incapable of binding the *FliH*₄*C*₂ to DNA.

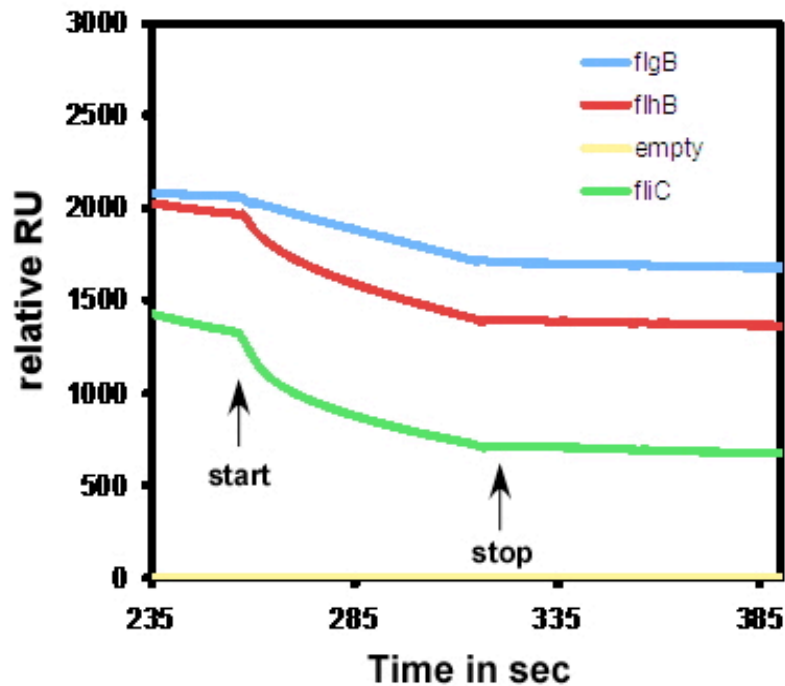


Figure 43. FlhD₄C₂ departure from various FlhD₄C₂:DNA complex by *flgB* challenge.

The SPR profiles showed the ability of DNA pieces in stealing the FlhD₄C₂ from the DNA-bound FlhD₄C₂ on the chip. A first injection of the FlhD₄C₂ was performed to bind the FlhD₄C₂ to the fixed ligands, which labelled in colours on the chip. Results showed that the FlhD₄C₂ had high affinity to bind to the promoter region of *flgB* and *flhB* (2,000 RU), while, in intragenic region of *fliC*, low affinity was detected at 1,500 RU. The second injection of *flgB* that intended to depart the FlhD₄C₂ from its DNA ligands began at start point and finished at stop point, and then continued with the buffer. Results obtained after the introduction of 100 nM *flgB* to DNA pieces, demonstrated that the *flgB* can depart the FlhD₄C₂ from all DNA ligands. It was noted that the *fliC* had some degree of affinity to bind to the FlhD₄C₂. (Adapted from Aldridge *et al.*., 2010.)

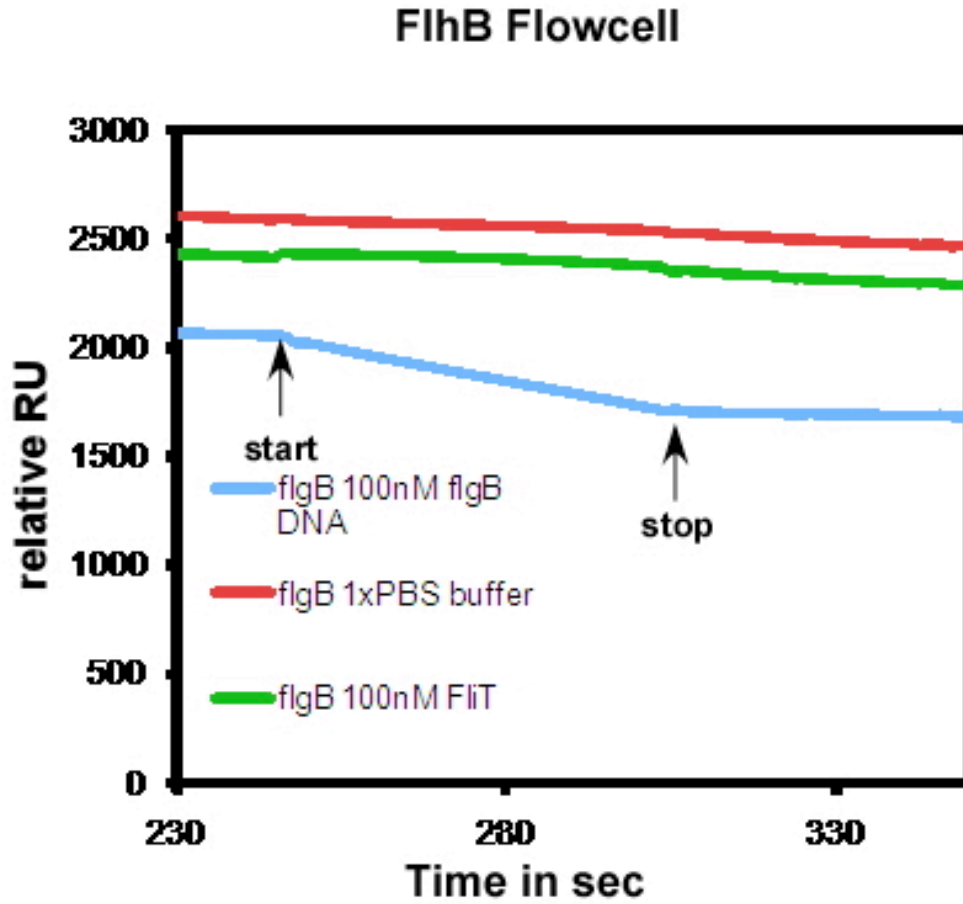


Figure 44. Resistance of *FlhD₄C₂*:DNA complex to *FliT*.

The SPR profile of the introduction of the buffer (red line) or 100 nM of the *FliT* (green line) over the *FlhD₄C₂*:*P_{flgB}* DNA complex revealed similar results when the other DNA species and higher concentrations of the *FliT* were used (data not shown). The arrows indicate the injection start and stop time points. It was shown that the *FliT* and buffer could not depart the *FlhD₄C₂* from the *FlhD₄C₂*:*P_{flgB}* DNA complex, whereas the departure of the *FlhD₄C₂* was found after the introduction of the *flgB* to the system, and the reduction of RU was shown as a blue line. (Adapted from Aldridge *et al.*., 2010.)

7.4 FliD as an anti-anti-FlhD₄C₂ factor

FliD, the flagellar capping protein, was shown to be involved in the FlhD₄C₂ circuit by its capability to bind to FliT (see **Chapter 5**) at the C-terminal region (Imada *et al.*, 2010). FliD was proposed to play a positive regulatory role for the production of flagella by binding to FliT, and inhibited the negative regulatory role of FliT (Yamamoto & Kutsukake, 2006). The mechanism by which FliD exerts this regulation had not yet been studied in detail, only proposed. For this reason, a further study using SPR analysis was performed to observe the effect of FliD toward the regulation of FlhD₄C₂ by FliT. We assumed that if FliD acted as an anti-anti- FlhD₄C₂ factor as proposed by Yamamoto and Kutsukake (2006) introducing FliD with FliT and FlhD₄C₂ would increase the level of FlhD₄C₂:DNA complexes formed.

FliD together with FlhD₄C₂ at a 1:1 molar ratio had no effect on the ability of FlhD₄C₂ to bind DNA (**Figure 45**). As predicted, the binding capability of the FlhD₄C₂ was significantly increased if FliD was injected at a 1:1 molar ratio in solution with FliT and FlhD₄C₂, compared to FliT/FlhD₄C₂ alone (**Figure 45**). Therefore, FliD functions as a positive regulator by interacting with the FliT to form the stable FliT:FliD complex. Accordingly, the availability of FliT to destroy the FlhD₄C₂ complex in the circuit was reduced by the presence of the FliD. The fact that the FliD formed a complex with the FliT with a 1:1 molar ratio identified that the FliT should not be available in the solution and complete recovery of the FlhD₄C₂ signal should be theoretically expected. It was shown that the some free FliT was left in solution that could exert an inhibitory effect on the FlhD₄C₂. This may also be due to the dynamics and stability of the other interactions FliT is involved in (i.e. FliT:FlhC and the stability of the FliT:FliD complex). However with the experimental design used these aspects could not be monitored in detail.

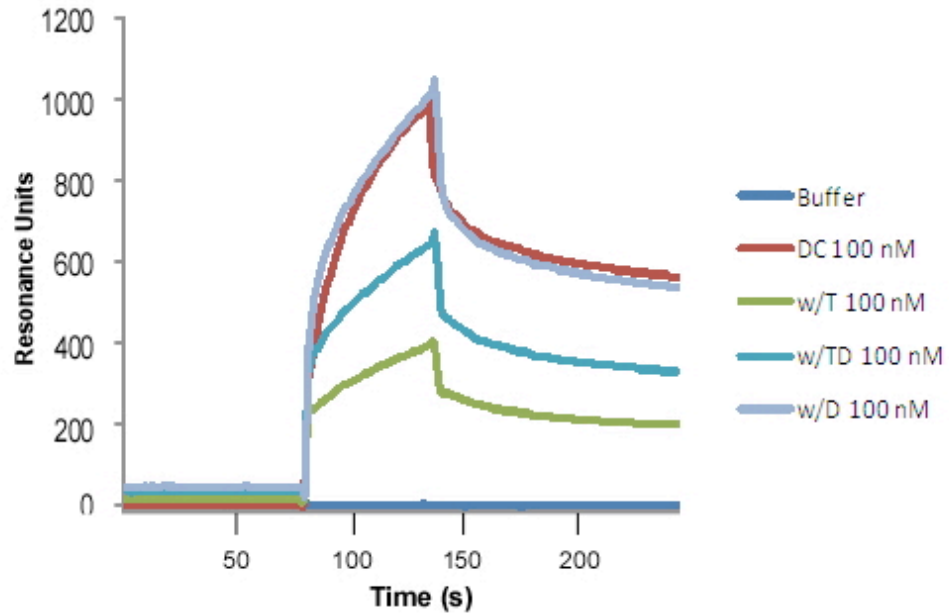


Figure 45. FliD, an anti-anti-FlhD₄C₂ factor.

SPR profiles indicated the effect of the FliD to counteract the inhibitory capability of the FliT toward free FlhD₄C₂ to form the complex with DNA (*P_{figB}*). In all assays, a 1:1 ratio of all components was used with a concentration of 100 nM. Red line: FlhD₄C₂ alone; green line: FlhD₄C₂ + FliT; purple: FlhD₄C₂ + FliD; light blue: FlhD₄C₂ + FliT + FliD and Gray Dark blue: Buffer control. Resonance units are shown in the percentage relative to the maximal RU of FlhD₄C₂ alone. (Adapted from data presented in Aldridge *et al.* , 2010.)

7.5 DISCUSSION

FliT has an important role as it selectively interacts with either FlhD₄C₂ or FliD to control flagellar synthesis. This regulatory circuit has been proposed with FliT being central to the circuit (Yamamoto and Kutsukake, 2006). FliT interacted with FlhD₄C₂ in a destructive manner and produced several components with mass equal to or less than FlhD₄C₂ itself (**chapter 6**). In contrast to Yamamoto and Kutsukake (2006) model our data has explained the regulatory details of the circuit. SPR analysis led us to explore the 4th component of the circuit: FlhD₄C₂ binding DNA. Unexpectedly, FlhD₄C₂ was able to bind the *fliC* DNA fragment. The ability to bind non-specifically to DNA has been observed previously for FlhD₄C₂. Stafford and Hughes also found that FlhD₄C₂ could interact with another non-specific random DNA fragment although not as efficiently as to a DNA fragment containing an FlhD₄C₂ DNA binding site. Using our two injection SPR experiments we were able to show that the interaction with *fliC* DNA was indeed different to P_{flgB} DNA based on the response curves we observed on injection of free P_{flgB} DNA to FlhD₄C₂ bound to each of the three DNA fragments we used (**Figure 43**). As predicted, FlhD₄C₂ binds significantly to the promoter region of *flgB* and *flhB*. When FliT mixed with FlhD₄C₂ was injected over P_{flgB}, only the remaining of undisturbed FlhD₄C₂ complex was available to bind DNA. Calculation to the theoretical R_{max} and K_D values further strengthened the assumption that FliT regulates FlhD₄C₂ by disrupting the complex. The K_D values remained almost equal with or without the addition of FliT while the R_{max} was significantly reduced (**Table 8**). Overall, the products of the FliT/ FlhD₄C₂ interaction lose the capability to bind DNA.

In vivo motility assays suggested excess FliT in cells is incapable of completely inhibiting motility, which indicates a complex interplay between all factors of the FliT:FliD:FlhD₄C₂ circuit. Results of *in vitro* study of the FliT:FlhD₄C₂ interaction suggested that the interaction fundamentally cause the disruption of FlhD₄C₂ and the products were incapable of binding. Aligning *in vivo* results with *in vitro* study suggested that a level of resistance to FliT destruction of FlhD₄C₂ existed. One explanation for this resistance was the hypothesis that when FlhD₄C₂ was bound to its DNA binding sites it was resistant to FliT.

We were able to prove this hypothesis by modifying the SPR experiment to accommodate two injections. We found that while free DNA could compete FlhD₄C₂ off the bound DNA FliT could not. The selectivity of FliT interacting with free FlhD₄C₂ not DNA-bound FlhD₄C₂ was consistent with the explanation for the motility phenotype observed in the presence of excess FliT. The results suggest that FliT acts as an induced inhibitor of FlhD₄C₂ having the net result of slowing down flagellar production but not completely shutting down the process. This is interesting as it suggest the role of the FliT circuit is to tune flagellar gene expression rather than act as a defined switch. In order to expand the circuit by counteracting FliT activity, the addition of FliD to the system was analyzed. According the SPR experiments, FliD positively regulated the availability of FlhD₄C₂ through its interaction with FliT forming a stable FliT:FliD complex. Using a molar ratio of 1:1 we again observed the inability of FliD or FliT to completely inhibit FlhD₄C₂ activity or FliT activity. Our analysis was unable to take into consideration the stability of the FliT:FliD complex or the fate of the disrupted FlhD₄C₂ complexes and the FliT used to instigate its disruption. These are feasible aspects of the circuit that with care can be monitored using SPR, AUC and other interaction techniques such as ITC.

The next questions were whether such binding could occur *in vivo* and to what extent FliT had affinity to each component. For example during this study we were unable to complement SPR analysis of the FliT:FliD interaction with FliT:FlhD₄C₂ interaction data (data not shown). However, the AUC data present an explanation for why this was not possible. In summary, in this chapter we have shown that FlhD₄C₂ exhibits a degree of resistance to FliT if it can bind DNA before generating a FliT:FlhD₄C₂ complex. The general principle of regulation with respect to FliT is that it reduces FlhD₄C₂ availability to bind DNA. Finally as previously proposed we determined that FliD can be defined as an anti-anti- FlhD₄C₂ factor.

Chapter 8

The analysis of FliT:FliD:FlhD₄C₂ interaction by B2H

Chapter 8. The analysis of *FliT*:*FliD*:*FliH*₄*C*₂ interaction by the Bacterial Two-Hybrid system

The regulatory mechanism that dictates the output of the *FliT*:*FliD*:*FliH*₄*C*₂ circuit was established through *In vitro* experiments (Chapter 5-7). While the biochemical data identified the proposed interactions and a possible mechanism, how these proteins communicated with each other *in vivo* is still unknown. The complicated environment in cells could change the results obtained from the *in vitro* experiments, and thus, nullify the proposed hypothesis. In the previous chapter we have shown that *FliT* reduces the availability of *FliH*₄*C*₂ rather than altering its affinity to DNA. We also showed that *FliH*₄*C*₂ bound to DNA was resistant to *FliT* regulation. However, we were unable to complement this SPR analysis with a similar SPR analysis of the *FliT*:*FliH*₄*C*₂ interaction. An alternative method to using *in vitro* techniques like SPR for protein-protein interaction studies is the use of the bacterial two-hybrid system (**Figure 46**). In the B2H system the interaction of target proteins leads to the expression of *lacZ* via activation through the activity of adenylate cyclase. By using X-Gal (define X-gal) *lacZ* expressing colonies turn blue on agar plates.

In the B2H-system, two DNA sequences encoding for two separate fragments of the adenylate cyclase have been genetically separated into different plasmids, pUT18/ pUT18c and pKNT25 / pKT25. These plasmids, were designed to monitor a protein interaction generating fusions of genes of interest to either end of the cyclase fragments T18 and T25 (**Figure 47**). Once cloned in to the appropriate vectors pairs of plasmids, one T18 one T25, are co-transformed into the indicator strain BTH101. If the two proteins of interest were able to interact, the right arrangement of adenylate cyclase was created for its functional role in the system. The functional enzyme could then activate the *lac* operon (cAMP) transcription, which in turn produced LacZ to generate a classic X-gal induced blue coloration of the colonies.

An advantage of the B2H-system is that if a positive interaction is detected the generated plasmids can be mutated randomly or through targeted mutagenesis to identify important amino acid residues required for the protein-protein interaction.

Apart from wishing to use the B2H-system to confirm the *FliT*:*FlhD₄C₂* interaction *in vivo*, we also wished to using any positive interaction to then generate mutations in *FliT*, *FliD* and *FlhD₄C₂* that would disrupt the respective interactions. Such mutations could then be analysed using both *in vivo* and *in vitro* assays to determine their impact up the net output of the regulatory circuit, namely flagellar synthesis. However, during the establishment of this system for this project the structure of *FliT* became available through the work of Drs Tohru Minamino and Katsumi Imada (Osaka University) (Imada et al 2010). Therefore, we altered our strategy to utilise our collaborators mutants as well as a number of other mutants isolated previously in our laboratory by Christine and Phillip Aldridge (data not shown).

The structure of *FliT* was recently revealed to contain a configuration of four α helices. The C-terminal α helix (α_4) was flexible and predicted to possess an autoregulatory behaviour (**Figure 48**) (Imada, 2010). This C terminal α_4 -helix was a flexible arm, which was predicted from the structure to allow the interaction of *FliT* monomers. How it interacted across these monomers made it lie in the predicted region for *FliD* and *FlhC* binding. Imada et al (2010) generated a deletion mutant of this C-terminal helix (*FliT94*). Expressing *fliT94* from a plasmid rendered *S. Typhimurium* non-motile compared to a significantly reduced motile phenotype of excess wild type *FliT* (**Figure 41**). The data of Imada et al suggested that the *FliT94* mutant strongly interacted with the *FlhD₄C₂*. Imada *et al* (2010) using site directed mutagenesis of *FliT94* of highly conserved residues found within the region α_4 would interact with a second monomer. In doing so Imada *et al* (2010) were able to show that this conserved region was the preferred binding site of the *FliT* to *FlhC*. The *FliT94* mutant was selected for this analysis due to exaggerated phenotypic change, from non-motile to motile. In light of the structure of the *FliT*, the *FliT94* mutant parenting several point mutations, which was mostly dominated on α_3 region, was used for further experiment using B2H and SPR analysis. Importantly some of the analysis described in this chapter transferred the mutations of Imada *et al* (2010) from *FliT94* to wild type *FliT*. We aimed to use these mutations in the B2H system and further SPR experiments to clarify the regulatory mechanisms driving the *FliT*:*FliD*: *FlhD₄C₂* circuit.

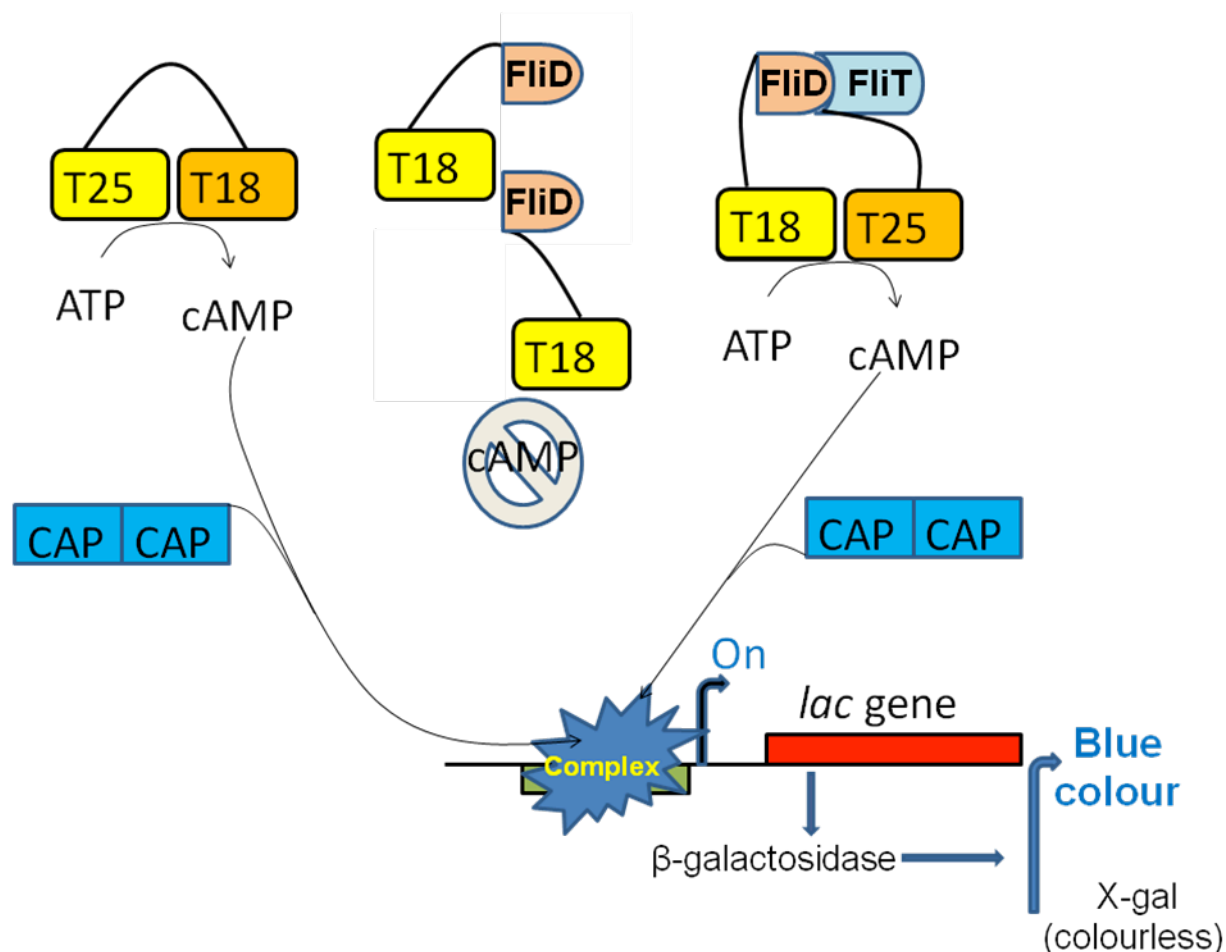
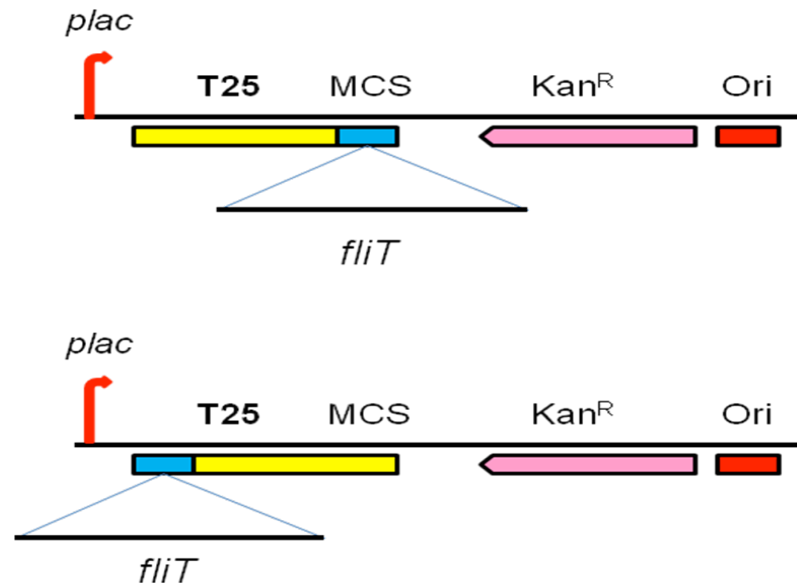


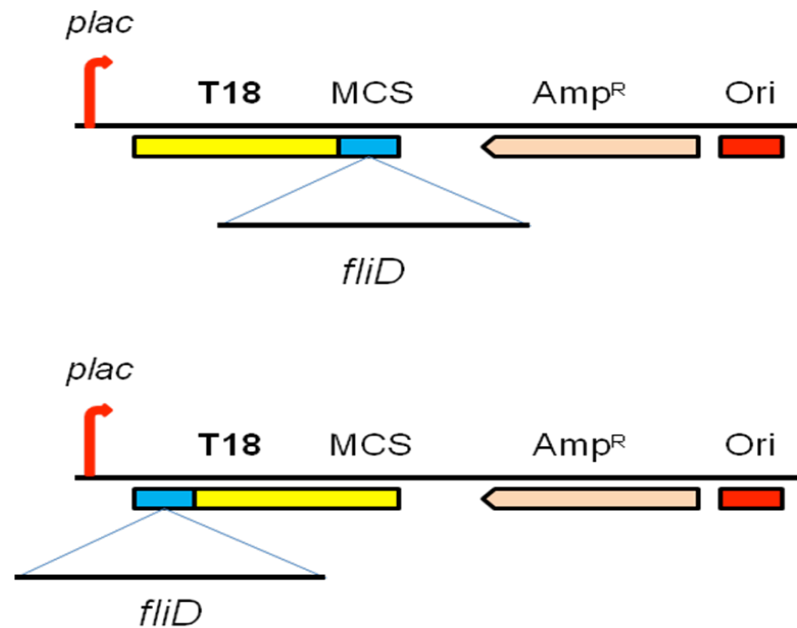
Figure 46. The principle of B2H assay showing *FliT* and *FliD* interaction

The system used *lac* operon to create blue colour that could be observed when two interested chimera proteins (*FliT*, *FliD*) were bound together. T25 (yellow box) and T18 (yellow box) were separated fragments of adenylate cyclase, which was able to function when they were in contact to generate cAMP. To activate *lac* operon, cAMP forms a complex with CAP to activate the expression of *lacZ*. B-galactosidase formed *lacZ* modified X-gal generating blue color on colonies, which could be observed by eyes. Two interested proteins had to be expressed as chimera proteins, which one of them joined to T18 and the other to T25 fragment, separately. Left panel, T25 and T18 linked together as the functional enzyme was able to create cAMP. Illustration on the right, *FliD* joining to T18 fragment while *FliT*, to T25, due to *FliT*:*FliD* interaction, T18 and T25 fragments were capable of generating camp, and then blue colonies were observed on the cells harbouring two plasmids. Illustration in the middle, *FliD* joined to both T18 and T25 but no interaction of *FliD* occurred then T18 and T25 were far apart that unable to generating cAMP and white colonies observed.

A



B



Gene organisation

Figure 47. Different gene organisation in B2H plasmids results in free C or N terminal regions for analysis.

Important parts of B2H plasmids are presented containing antibiotic genes, T25 or T18, a multiple cloning site (MCS), an origin of replication (Ori) and promoter of Lac genes (plac). *fliT* (A) or *fliD* (B) gene cloning at MCS on the right side of T25 creates free FliT C-terminal chimera protein while that on the left creates free N-terminal protein for analysis. FliT or FliD chimera proteins expose either C-terminus or N-terminus for protein interaction analysis.

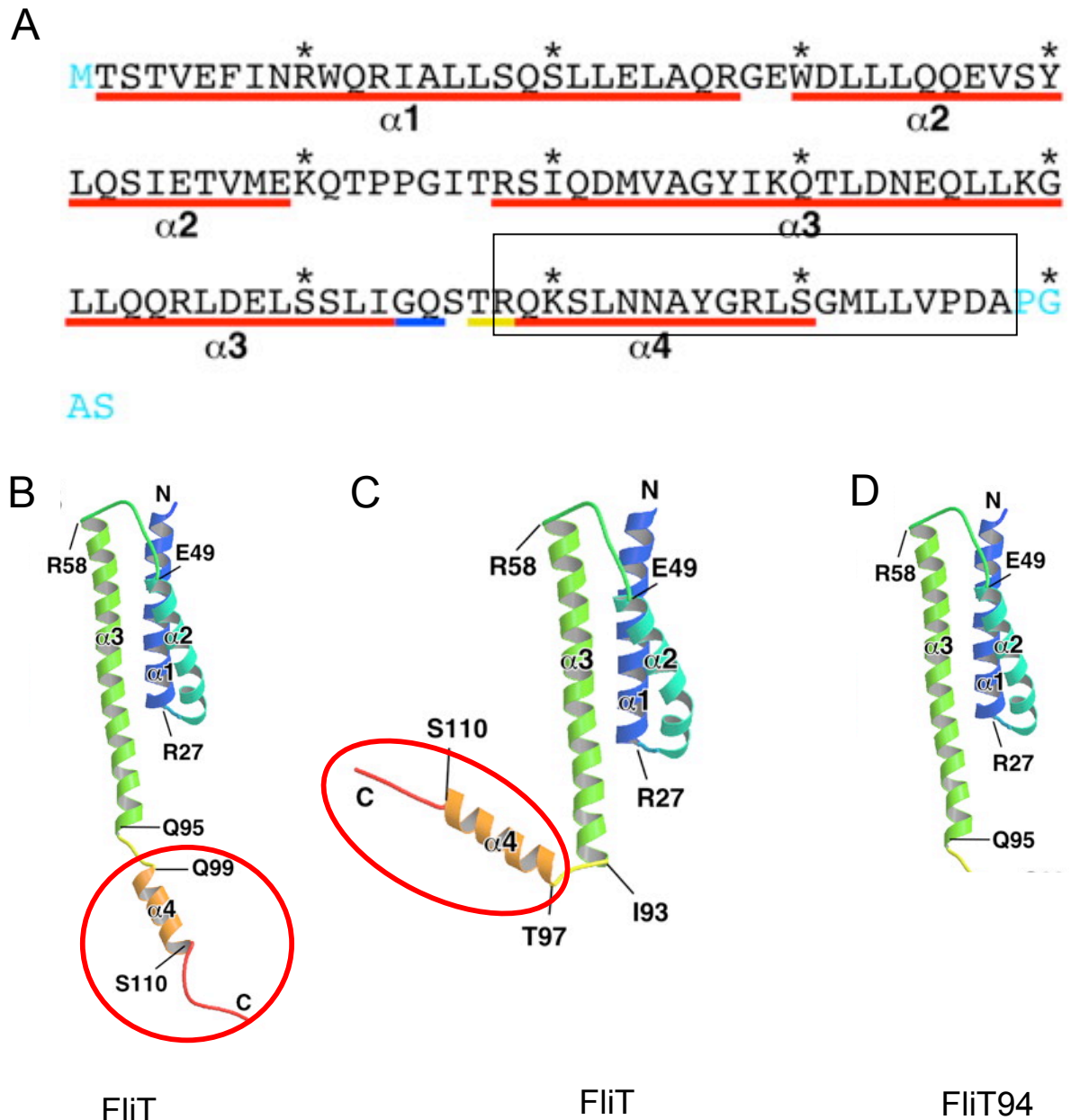


Figure 48. The coding sequence of *FliT* showing four α regions (red underlined) and predicted *FliT* tertiary structure containing flexible region (α 4) at C-terminus, where its deletion creates *FliT94*.

(A) Primary protein sequence of *FliT* (with all α regions underlined) emphasizing on α 4 region at the C-terminus (black box). The colored residues were missing in the predicted model of *FliT* (B, C) Tertiary structure of *FliT* is composed of four α helical structures; α 4 (flexible arm in a black circle), and packed α region; α 1, α 2, α 3. The indicated amino acids identify the boundaries of the α -helices (D) *FliT94* lacks a C-terminus or α 4 region, which is predicted to be the regulatory region controlling *FliT* behaviour. (Adapted from Imada *et al.* 2010)

8.1. *FliT*:*FliD* interaction by B2H

As the interaction between *FliT*:*FliD* had been previously characterised and confirmed in this study, testing the B2H-system for use in this analysis utilised this interaction pair. Both the *fliT* and *fliD* genes were amplified by PCR, and cloned into pBluescript (**Figure 49**). The cloning of *fliT* and *fliD* was performed with pUT18c and pKT25 plasmid. This meant that the C-termini of both *FliT* and *FliD* were freely exposed and available to interact with each other in the cytosol environment. The logics of using these orientations came from previous studies that showed the interaction site of *FliT* within *FliD* was at the extreme C-terminal of *FliD* (Fraser et al 1999). Successfully cloned plasmids were isolated and digested for subsequent subcloning of *fliT* into pKT25, and of *fliD* into pUT18c (**Figure 50**). Each B2H plasmid harbouring the *fliD* and *fliT* genes was then subsequently co-transformed into BTH101 competent cells to analyse the protein interaction. The colonies that containing both chimera *fliT* and *fliD* in appropriate B2H plasmids showed a dark blue colour after incubating at 37 °C for 24 hrs for bacterial growth (**Figure 50E**). Negative controls using only the B2H vectors, and a positive control using pKT25-zip and pUT18-zip behaved as expected (**Figure 50E**). Therefore consistent with previous work and the analysis of *FliT*:*FliD* in chapter 5 the B2H-system was also able to show the interaction between *FliT* and *FliD*. The next step was then to expand the use of the system to include *FliH*₄*C*₂.

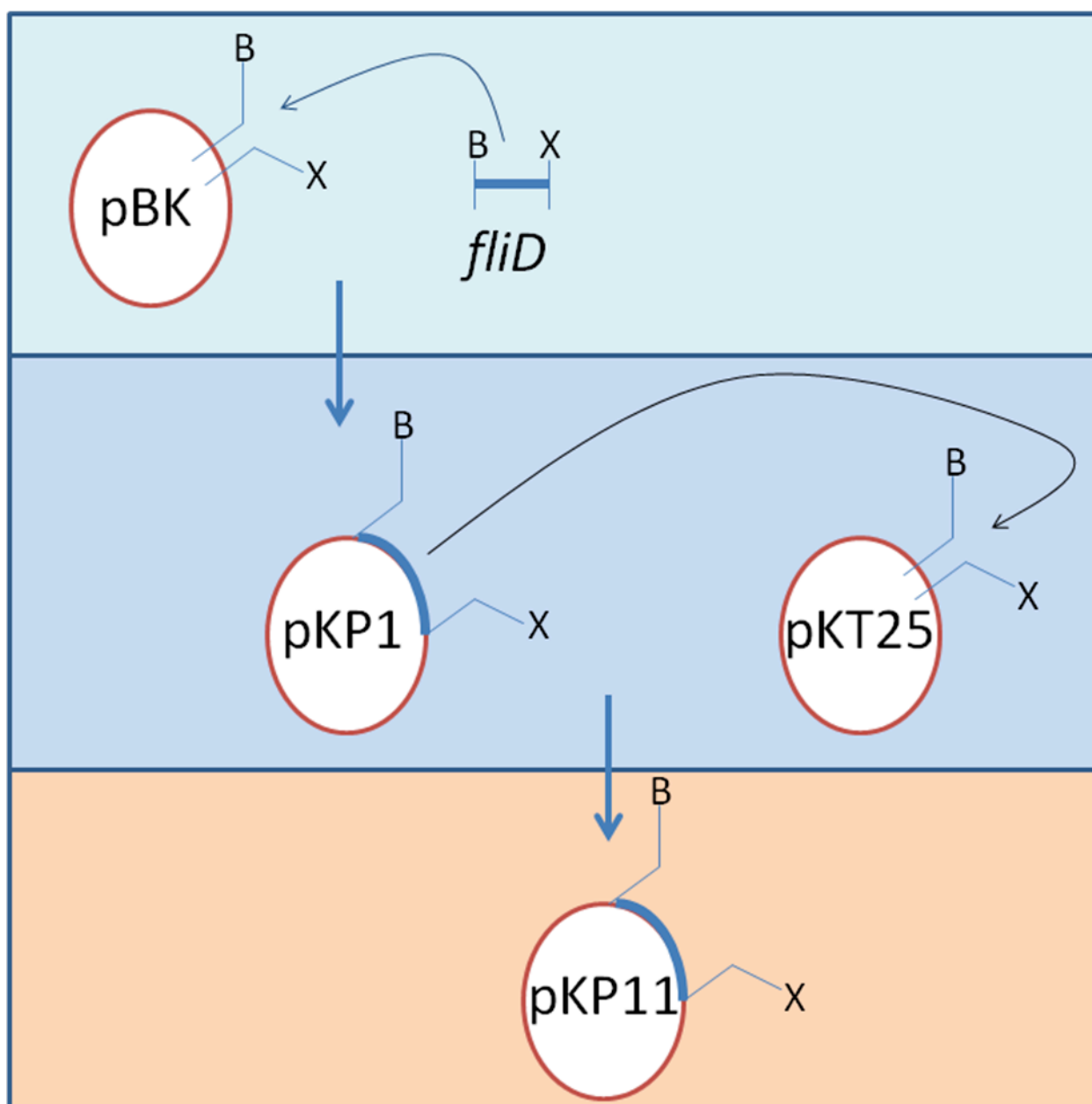


Figure 49. The construction of recombinant plasmids or pUT18 carrying *fliD* gene (pKP11) for B2H analysis requires 2 steps.

First, *fliD* was inserted into the pBK plasmid. The first constructed plasmid containing *fliD* was called pKP1. The *fliD* gene was subsequently subcloned into pKT25, which generated a functional recombinant plasmid (pKP11) for a B2H analysis.

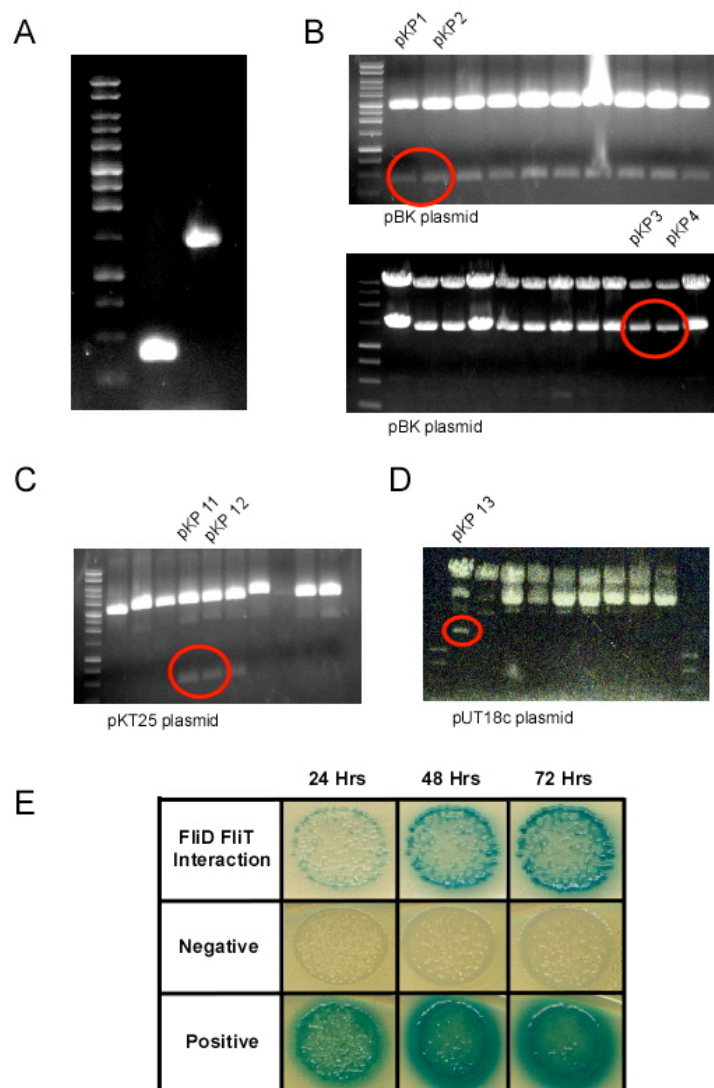


Figure 50. The B2H assay of FliT and FliD interaction.

(A) The PCR amplification of FliD and FliT was performed and the genes were cloned into pBK plasmids (Figure 51). The successful cloning was observed by performing test digests with the extracted plasmids from the transformed clones. (B). Inserted genes were subcloned into plasmids, pKT25 and pUT18c, with the identification of clones harbouring the given genes by performing test digests (C and D). The interaction of proteins between FliT and FliD was shown by blue color of the BTH 101 transformed cells harbouring both recombinant plasmids, *fliT* (pKT25-*fliT*) and *fliD* (pUT18c-*fliD*), which could express both FliT and FliD in the cells and the interaction of the proteins rendered blue colour of the cells (E).

8.2 Expanded combination assay of all proteins in the circuit

The ability to visualise the interaction between *FliT* and *FliD* using the B2H method provided the opportunity to observe other possible interactions among the proteins of the *FliT*:*FliD*:*FlhD₄C₂* circuit. The *flhDC* operon organisation allows for more than the genetic dissection of the *flhC* and *flhD* genes in the B2H system. As they form a natural operon it was decided to investigate the protein interactions via the B2H system to cover *fliT*, *fliD*, *flhC*, *flhD*, and an *flhDC* complex generating 15 clones within the timeframe of this study (**Table 10**). Using this set of 15 clones fifty-six specific combinations were transformed into the indicator strain BTH101 (**Appendix D**) by matching appropriate recombinant plasmids (**Figure 51 and Appendix D** (complete image)). Three different zones of the matrix were divided in order to represent the results of analysed interactions, which were the combinations of *FliT* with *FliD* (**Figure 51A**), *FliT* and *FliD* interacting with *FlhC* or *FlhD* or *FlhD₄C₂* (**Figure 51B**) and interactions between *FlhD* or *FlhC* (**Figure 51C**). Positive reactions (blue colonies) were observed in all three zones however those between *FliT*:*FliD* (**Figure 51A**) and *FlhD* or *FlhC* (**Figure 51B**) were, visually, significantly more than those in the cross interaction zone between all four proteins (**Figure 51B**). These results were consistent with our understanding of the interaction belonged to *FliT*, *FliD* and *FlhD₄C₂*. Although difficult to quantify these results suggest that *FliT* displayed a strong binding preference to *FliD* and *FlhD₄C₂* when compared to *FlhC*.

The results of the interaction for *FliT*/*FliD* did not show any particular preference with respect to which terminal was fused (**Figure 52**). This observation can be explained that we know that the last helix (α_4) is not needed for either interaction of *FliT* with *FliD* or *FlhD₄C₂*. However a weak binding for the *FliT*'s dimer could be detected when comparing the negative control to the permissive *FliT*:*FliT* combination (**Figure 51A**).

It was predicted that the *FliT* should interact with *FlhC* and *FlhD₄C₂*. Results suggested, however, that the *FliT* interacted with both *FlhD* and *FlhC* (**Figure 51B**). Although a stronger binding preference to *FlhC* was more consistent with the work of Yamamoto and Kutsukake (2006) and Imada et al (2010). In contrast, the *FliT* interacted strongly with *FlhD₄C₂* especially when T25 was fused to the N-terminal of

FliT, leaving *FliT*'s C-terminal free. From our previous results, *FliT* disrupts *FlhD₄C₂* into smaller components (Chapter 6). Interestingly using the *flhDC* clones it could have been plausible discrimination between T18/T25 fused to either *flhC* or *flhD* was feasible. However, all combinations showed a relative similar interaction strength based on blue colony color. Therefore, these results only confirmed the *FliT*:*FlhD₄C₂* interaction. Importantly, *FliD* showed no preference to *FlhC*, *FlhD* or *FlhD₄C₂* combinations. Only one *flhC* clone showed very weak interaction or no interaction to any combination. Even though the sequence of this clone was correct (data not shown) from the rest of the profiles we could not explain why this one combination of *FlhC* in the B2H-system did not behave in a predictable manner (**Figure 51C**).

8.3 Analysis of *FliT* point mutations (B2H)

The interactions of proteins in the *FlhD₄C₂* circuit were positively observed from all expected interactions including *FliT*:*FliD*, *FliT*:*FlhC*, *FlhC*:*FlhD* and *FliT*:*FlhD₄C₂*. These results were consistent with previous observations (Yamamoto *et al.*, 2006). The *FliT*:*FliD* interaction was observed and predicted to be strong following the intense blue colour of colonies. The interaction of *FliT*:*FlhC* was subsequently shown that a weak interaction occurred by based on a lighter blue colour. As the system produced a consistent assessment of the circuit the next question asked was whether putative interaction mutants could be identified using the B2H system.

This analysis included two mutants W11R and N74D that had been isolated in a genetic screen using random mutagenesis of *fliT* in this laboratory (Aldridge and Aldridge unpublished). The second of these (N74D) was chosen as it had been identified by Imada *et al* (2010). From the work of Imada *et al* (2010) two alanine substitutions were chosen for testing in our B2H-screen N74A and N79A. Importantly, W11R and N74D mutants were from a functional screen prior to the structure being known while N74A and N79A, were from site directed mutagenesis based on structural information. Mutants, N74A, N74D, N79A, and wild type, *FliT*, interacted with *FliD* and *FlhD₄C₂* significantly but the interaction with *FlhC* was significantly weaker (**Figure 53**). W11R, did not show any interaction with both *FliD* and *FlhC* but still retained some *FlhD₄C₂* interaction but only after 72 hours of

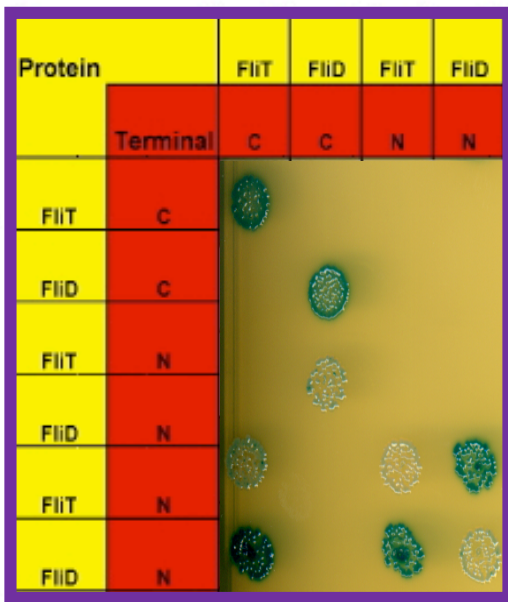
Table 10. Detail of plasmids and their pairings used in the B2H experiment

Number	TPA ¹	Plasmid	Protein expression	
			Protein	Free terminal
1	2443	pKT25- <i>fliT</i>	<i>FliT</i>	C-terminus
2	2445	pUT18c- <i>fliD</i>	<i>FliD</i>	C-terminus
3	2617	pKNT25- <i>fliT</i>	<i>FliT</i>	N-terminus
4	2619	pKNT25- <i>fliD</i>	<i>FliD</i>	N-terminus
5	2622	pUT18- <i>fliT</i>	<i>FliT</i>	N-terminus
6	2624	pUT18- <i>fliD</i>	<i>FliD</i>	N-terminus
7	2604	pUT18c- <i>flhD</i>	<i>FlhD</i>	C-terminus
8	2616	pKNT25- <i>flhC</i>	<i>FlhC</i>	N-terminus
9	2620	pUT18- <i>flhC</i>	<i>FlhC</i>	N-terminus
10	2608	pKT25- <i>flhC</i>	<i>FlhC</i>	C-terminus
11	2606	pUT18c- <i>flhC</i>	<i>FlhC</i>	C-terminus
12	2610	pKNT25- <i>flhDC</i>	<i>flhDC</i>	N-terminus
13	2622	pUT18- <i>flhDC</i>	<i>flhDC</i>	N-terminus
14	2615	pKT25- <i>flhDC</i>	<i>flhDC</i>	C-terminus
15	2613	pUT18c- <i>flhDC</i>	<i>flhDC</i>	C-terminus

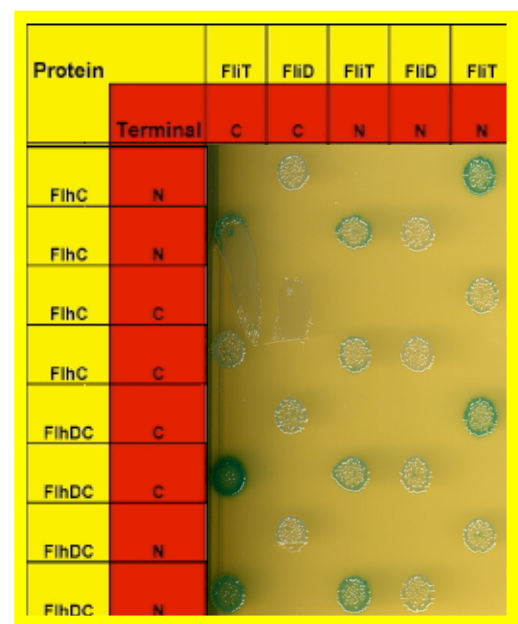
TPA	2443 ²	2445	2617	2619	2622	2624	2604	2616	2620	2608	2606	2610	2612	2615	2613
2443	X														
2445		X													
2617			X												
2619				X											
2622					X										
2624						X									
2604							X								
2616								X							
2620									X						
2608										X					
2606											X				
2610												X			
2612													X		
2615														X	
2613															X

1. TPA Numbers: The lab strain collection uses the nomenclature TPAxxxx. Here for simplicity the TPA numbers are used to describe the plasmids.
2. The lower grid of this table indicates the TPA pairings used the B2H test the results are shown in **Figure 51**. Colors relate to Fig. 51A, 51B and 51C

A



B



C

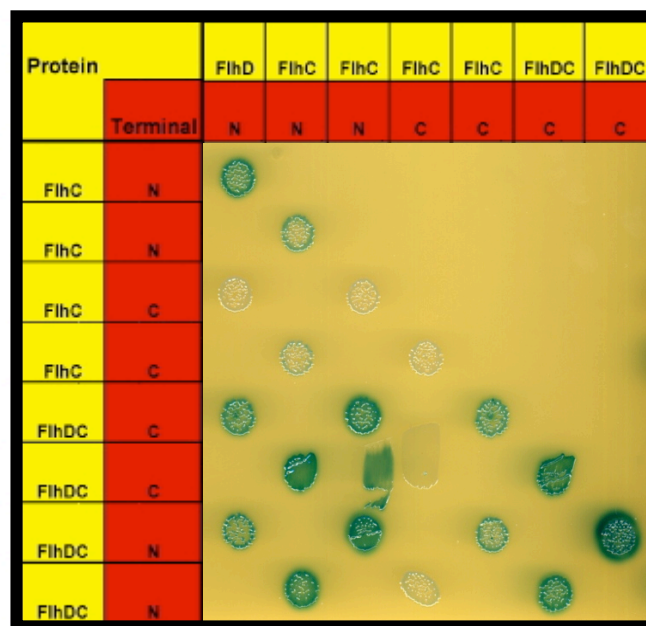


Figure 51. The actual result on big square agar plate representing B2H experiments from different protein interaction with either C or N terminal free.

The name of proteins of an interaction of all combinations was displayed within a yellow box and a free protein terminal (red box) of which the crossing line generated from a horizontal box against a vertical one represented each different combination of a protein interaction. Each combinations were tested for protein interaction. Big blue box (Upper, left) focused on the result of the interaction between *FliT* and *FliD*, yellow box (Upper, right) between *FliH*C and *FliT*, and black box (Bottom, center) between *FliH*C and *FliH*₄*C*₂. The observed colour was seen roughly in three levels of blue colour, dark, moderate blue, and very pale blue or white (negative result). Dark blue represented the strong interaction of two given genes while the moderate blue suggested the weak interaction was assumed. Positive and negative controls were also displayed in two separated pairs. Incubational time for this experiment was 48 Hrs.

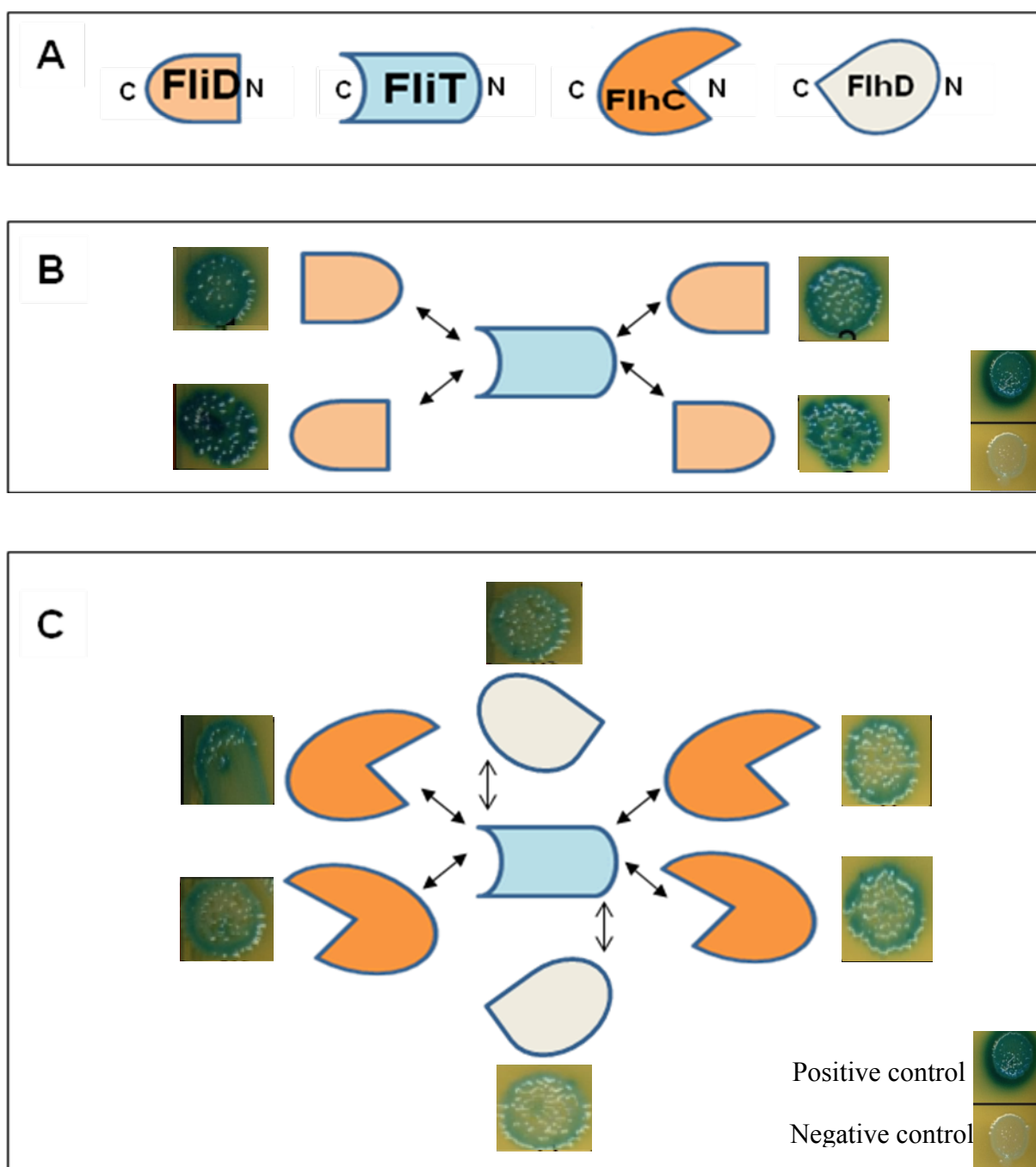


Figure 52. Cartoon presentation showing interaction of FliT/FliD/FlhD and FlhC specifying C and N terminal and their corresponding B2H results.

(A) FliT (blue symbol), FliD (light brown), FlhD (Gray) and FlhC (orange) are represented with distinctive shape of C and N terminal. (B) FliT/FliD interaction is shown in that FliT is in the middle processing both C and N terminal, of which each one can strongly interact with both C and N terminal of FliD. (C) FliT is able to bind FlhC and FlhD in different direction but rather weaker than FliT/FliD interaction. Positive and negative control are located at the lower right of a box.

incubation. These results suggest that W11R may have lost all its ability to interact with all partners and maybe a non-functional mutant of *FliT*. In contrast the interaction changes seen for N74D, N74A and N79A compared to the biochemical data may reflect the fact that these were all used in full length *FliT* constructs for this analysis. N74A and N79A had primarily been characterised using the deletion mutant *fliT94*, missing the last α -helix. However, this knowledge further strengthens the proposed role of the last helix in autoregulating the activity of *FliT*. Results of analysis from B2H could provide the functional assay for mutants although visual colour interpretation limited the power of this assay to scale the strength of protein interaction.

8.4 SPR analysis of *FliT94* mutants

The structure of the *FliT* revealed by Imada *et al.* (2010) demonstrated that it comprised of 3 packed alpha helices ($\alpha 1$, $\alpha 2$, $\alpha 3$) with one flexible alpha helix ($\alpha 4$) (**Figure 48**). The *FliT94* mutant was a *FliT* variant that lacked of $\alpha 4$ helix region with an increased interaction toward *FlhD₄C₂*. *S. Typhimurium* harbouring *fliT94* showed a non-motile phenotype (**Figure 54A**). Several point mutations of the *FliT94* mutant were constructed in order to observe the correlation between phenotypic change (motility assay) with *FlhD₄C₂* and *FliT* interaction behaviour (**Figure 54B**). These experiments came from the collaboration between Katsumi Imada, Tohru Minamino and the Aldridge Lab.

Alanine-substituted mutagenesis of the *FliT94* mutant was performed creating 8 *FliT94* mutants, i.e., I68A, L72A, N74A, L81A, Q83A, E75A, K79A, and L82A (Imada *et al.*, 2010). The mutants were tagged with GST protein (Imada *et al.*, 2010). Analysing their phenotype with respect to a motility assay (**Figure 54A**) found that some mutations could suppress the non-motile phenotype (I68A, N74A, E75A, K79A, and L82A). In contrast some still retained the nonmotile phenotype (L72A, L81A, and Q83A). *In vitro* pull down assays conducted with some selected mutants determined their binding capability for *FlhC* in crude extract (Aldridge *et al* (2010)). These results were consistent with the suppression of the non-motile phenotype (**Figure 41**). E75A showed the strongest binding capability to the *FlhD₄C₂*, which was similar to that of

the wild type, while the others displayed the strong reduction in *FlhD₄C₂* binding (**Figure 54**).

As these mutants lay within a conserved region of *FliT* and that they colocalised to where *FliD* (Imada et al (2010)) would also interact suggests that the binding sites for *FlhC* and *FliD* overlap. We were therefore interested to determine how these mutations would influence the ability of *FlhD₄C₂* to interact with DNA. Our B2H-system data with 2 of these mutants suggest that when introduced in to full length *fliT*, these mutations could still lead to a detectable interaction using a *flhDC* B2H clone. The GST-*FliT*94 derivatives N74A, E75A, K79A and L82A were compared to GST-*FliT*94 using our SPR *FlhD₄C₂*:DNA interaction assay (**Figure 56**). We decided to focus on the format of the SPR assays which used a constant concentration of *FlhD₄C₂* and increasing GST-*FliT*94 concentrations of 1:1, 1:2 and 1:4.

In these SPR assays GST-*FliT*N74A was found to loose some ability to inhibit the *FlhD₄C₂* interaction although a concentration dependent change was still visible (**Figure 55A**). This was consistent with its motility phenotype being one of the two weaker suppressors used in this analysis. In contrast to N74A, the other 3 mutations used showed a stronger change in the inhibition ability. GST-*FliT*94(K79A) had the weakest inhibitory effect only starting to show inhibition of *FlhD₄C₂* at a 1:4 ratio of *FlhD₄C₂*:*FliT* (**Figure 55C**). The last two mutants E75A and L82A behaved surprisingly similar (**Figure 55B and D**). Inhibition was still evident at a 1:1 and 1:2 ratio however much weaker than GST-*FliT*94. Interestingly, the 1:4 ratio profiles were very similar for E75A, K79A and L82A. This is consistent with our data on full length *FliT* that best results at disrupting *FlhD₄C₂* and inhibiting the *FlhD₄C₂*:DNA interaction were always observed when *FliT* was in excess. This also suggests that these mutations do still possess some affinity to the *FlhD₄C₂* complex. This proposal is also consistent with our B2H-system data when N74A and K79A were introduced into full length *fliT*.

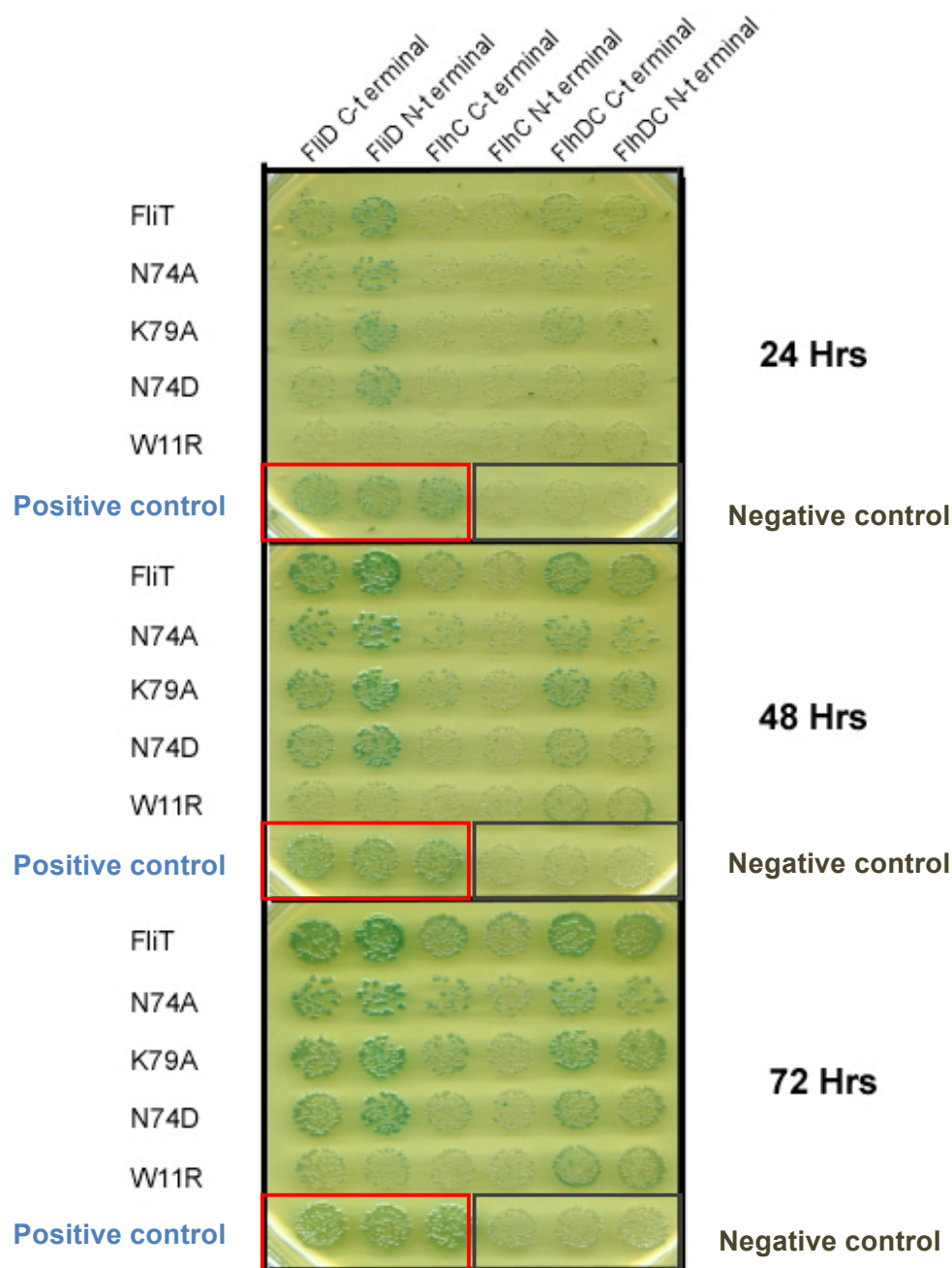


Figure 53. The protein interaction test (B2H) of mutant producing different specified single amino acid substitutions of *FliT* protein at different location against wild type producing *FlhD*, *FlhC*, and *FlhD₄C₂*.

The interactions of *FliT* and 4 *FliT* mutants against *FlhD*, *FlhC*, and *FlhD₄C₂* protein were tested. The specified mutations of *FliT* at the important amino acid for *FliT* function (Imada, 2010) were generated by performing quick-change method with wild type *FliT* B2H plasmids. The protein interactions of N74A, K79A, and N74D mutants were observed with *FlhD*, *FlhC*, and *FlhD₄C₂* resulted in nearly the same scale (blue color) as *FliT* wild type. The W11R mutant showed no interaction, represented by the very pale blue of colonies from the mutated *FliT* with both *FlhD* and *FlhC* but not *FlhD₄C₂*.

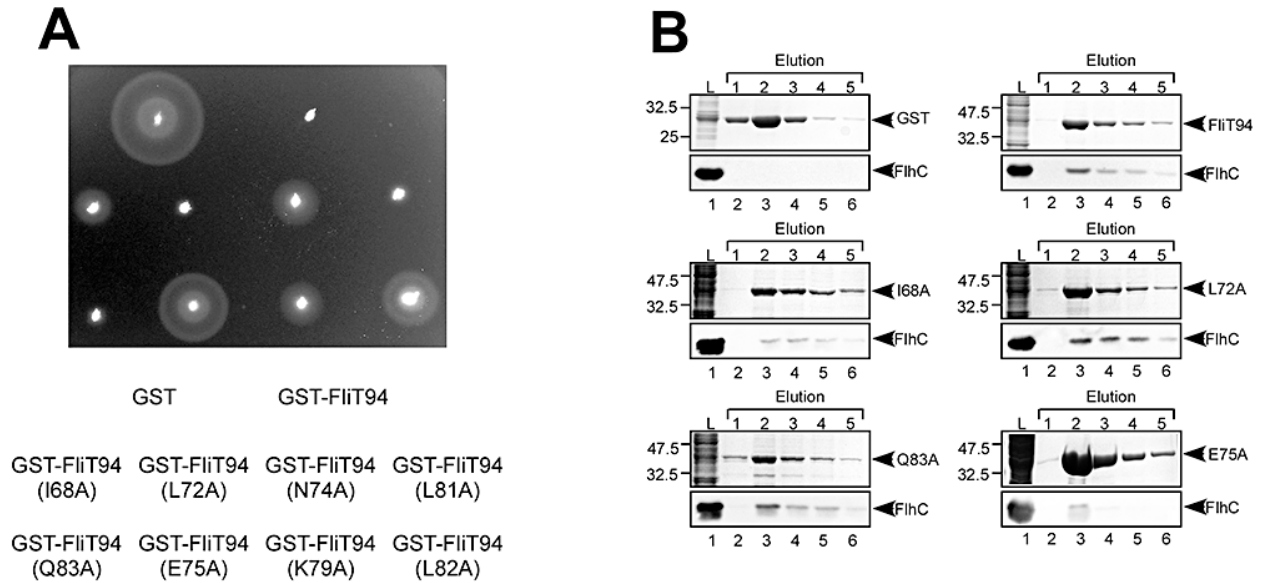


Figure 54. Mutation of FliT (E75A) shows both decreasing FliT inhibition from motility assay and weak interaction to FliH₄C₂.

(A) The motility assay using semi-solid agar to compare the mobility of different alanine substitution mutations present along alpha 3 regions of FliT of the *gst-fliT94*. (B) In *S. enterica*, GST-FliT and its corresponding FliT mutants from the motility assay were expressed and pulled down prior to immunoblotting against FliHc using polyclonal anti-FliHc antibody. In E75A, FliHc was hardly detected compared with other mutants (Adapted from Aldridge et al 2010)

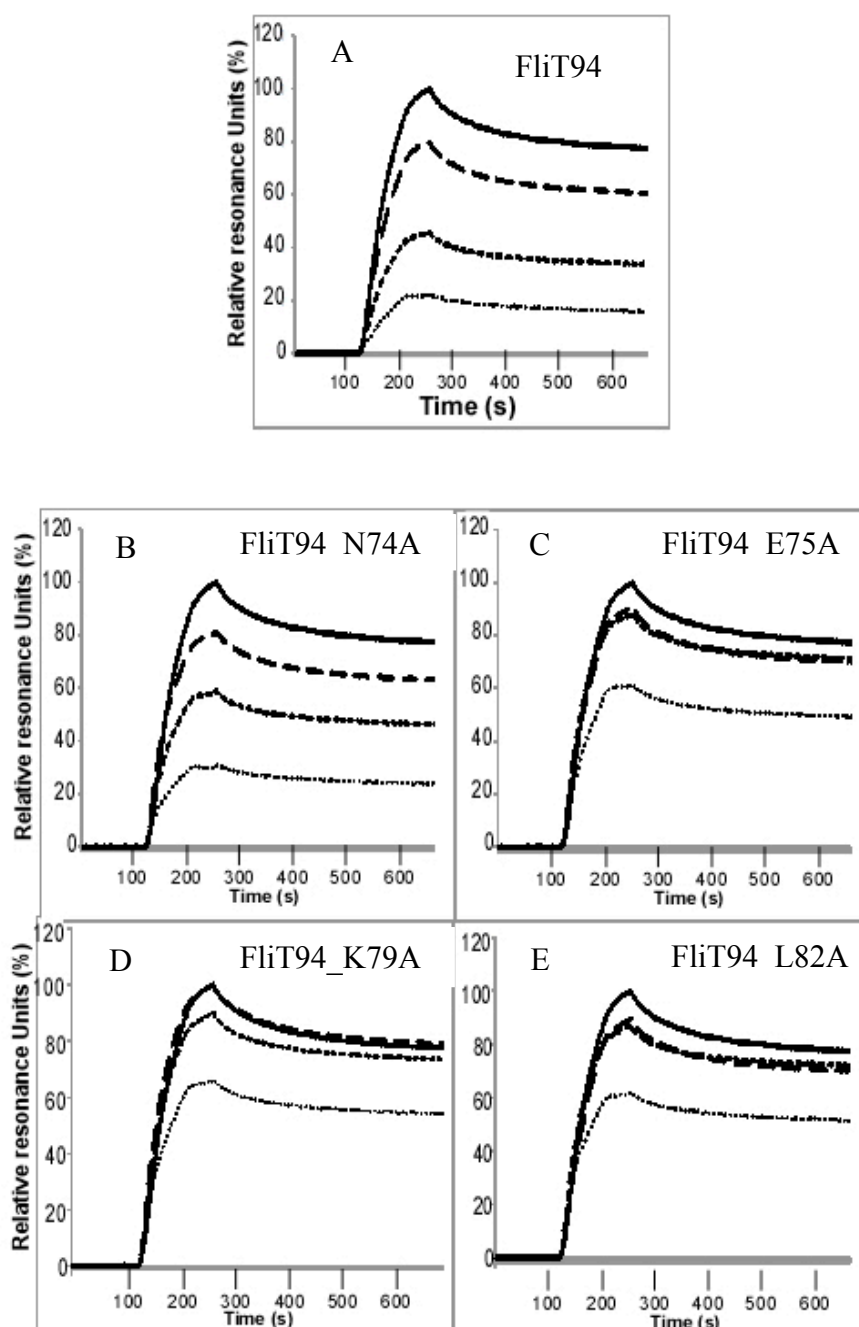


Figure 55. SPR data showed FliT94 mutation renders various inhibitory effect of several mutated FliT to FliH₄C₂

SPR analysis of FliT94 (A) and several FliT mutants with single amino acid substitution, N74A (B), E75A (C), K79A (D) and L82A (E), was displayed to compare the effect of each mutated FliT toward FliH₄C₂. All graphs are represented as Relative resonance units (%) in x axis and Time (s) in y axis (A) 100 nM FliH₄C₂ alone (black line) and with 4 concentrations of mutant FliT are shown; 100nM (long dash bold line), 200nM (short dash bold line), 400 nM (short dash light line), The same line format are applied with all graphs to create the same molar ratio between FliH₄C₂: FliT94 (mutated). The SPR result from E75A showed the most impaired binding capacity to FliH₄C₂ (C), and the impaired capacity was also consistent with the motility assay data in (Figure 26). (Adapted from data presented in Aldridge et al 2010)

Chapter 9

The quantification of the concentration of FliT, FliD, and FlhD₄C₂ by western blot analysis

Chapter 9. The quantification of the concentration of *FliT*, *FliD*, and *FlhD₄C₂* by western blot analysis

The function of the regulatory circuit proteins, *FlhD₄C₂*, *FliT*, and *FliD*, rely on the concentration of each protein in the cell. The availability of the key regulatory protein, *FliT*, could lead to the decision of bacteria to start flagellar synthesis through changes in *FlhD₄C₂* activity. The activity of *FliT* is dictated by its binding preference to *FliD* and *FlhD₄C₂* and their availability. Furthermore, the overlapping binding region in the *FliT* tertiary structure suggests both *FliD* and *FlhD₄C₂* can compete for *FliT*. Therefore, active *FliT* is dependent on the concentration of the *FliD* and *FlhD₄C₂* with respect to its own abundance. The quantification of the concentration of *FliT*, *FliD*, and *FlhD₄C₂* in a population was performed by immuno-blot analysis in order to predict the balance of the circuit in cells.

The quantitative assays were performed on log phase populations predicted to be active for the synthesis of flagella. We assumed for this analysis that the distribution of proteins would be uniform per cell. Analysis of flagellar numbers suggests that at least for wild type a normal distribution of flagellated cells is present (Aldridge *et al.* 2010). As a proportion of the population is found to produce no flagellar, the quantification of the three proteins, *FliT*, *FliD*, and *FlhD₄C₂*, in a bacterial population, was chosen to reveal the average concentrations of each species rather than defining protein concentration per cell. The visualised bands reflecting the amount of proteins in cells were standardized with the bands from actual amounts of the expressed proteins after the His-tag moiety was removed. (Figure 56).

9.1. The quantification of proteins, *FliT*, *FliD*, and *FlhD₄C₂*, in a natural form in a bacterial population.

The standard proteins were purified by gel filtration, and the concentration range of standard protein used was from 2 to 100 nM. The quantification of the proteins' concentration was estimated based on the intensity of the immuno-band analysed by the program "Image J".

In the case of the *FlhD₄C₂*, the His-tag is fused to *FlhD*, therefore we used a *FlhC* antibody to directly quantify *FlhD₄C₂* without thrombin digestion. The protein concentrations used was obtained by calculating OD₂₆₀ using predicted absorption coefficient from NCBI database.

The analysis of the amount of proteins *in vivo* via western blot was conducted by using triplicate independent cell extracts, and were included as three lanes on the right panel of each gel (**Figure 57 - 59**). Standard proteins in nM range were performed on the left hand side ranging from 2 to 100 nM (**Figure 57 - 59**). The quantification was based on a specific antibody to each protein. The cell samples included wild type, $\Delta fliT$, and $\Delta fliD$, whose cells were normalised by both spectrophotometry and colony forming units (CFU).

9.2. *FliT* and *FliD* are more abundant than *FlhD₄C₂*

Using the standard curves produced from isolated forms of *FliT*, *FliD* and *FlhC* an estimate of the average amount of each protein could be obtained for all three proteins (**Figures 57 - 59**). For *FliT* and *FlhC* the standard curves produced a linear regression for 2-50 nM. In contrast, due to the high sensitivity obtained with the *FliD* antibody the standard curve produced a logarithmic regression. In wild type, from each standard curve the average concentration of *FliT*, *FliD* and *FlhC* were calculated to be 24 ± 3 nM, 8 ± 3 nM and 11 ± 2 nM respectively. This suggests that *FliT* is approximately 2-fold in excess of *FlhC* and 3-fold in excess of *FliD*. However, *FliD* is a structural protein that a certain amount of detected protein will be used for flagellar synthesis. Interestingly, only *FliD* (53 ± 8 nM) values changed significantly in $\Delta fliT$ compared to *FlhC* (8 ± 2 nM). A slight drop in *FlhC* was seen 8 from 11 nM but this is very little compared to the 7.5 fold change seen for *FliD*. *FlhC* was undetectable in $\Delta fliD$ possibly as a result of the change in autoregulation of *flhDC* expression inhibited by over active *FliT* (data not shown). *FliT* levels were unaffected by $\Delta fliD$ with a calculated average concentration of 21 ± 4 nM in $\Delta fliD$ compared to a wild type value of 24 nM.

9.3 Discussion

The concentration of proteins, *FliT*, *FliD*, and *FlhD₄C₂*, in a population of cells was not previously assessed before. The biochemical characterisation of the regulatory circuit reveals the relationship between the abundance of these proteins. Being able to correlate their abundance to how they regulate flagellar synthesis, will provide us more insight in to the net output of the circuit. *FliD* is a structural part of a flagellum. However, *FliD* was expected to be in the cytoplasm in order to function in the circuit. The central factor of the circuit, *FliT*, was detected in a large amount (24 nM) compared to others in a wild type population. Both *fliT* and *fliD* are within the same operon but their levels are very different. *FliD* being secreted can explain this. Brown et al (2008) showed that a significant amount of *FliD* is secreted from the cell. Trying to repeat these experiments in mutants unable to secrete *FliD* imbalances the amounts of *FliT* and *FlhC*, so was not considered a valid option.

The *in vitro* data for *FliT* and *FlhD₄C₂* showed that excess *FliT* was required to prevent *FlhD₄C₂* activity. SPR and AUC experiments showed that significant inhibition needed above 2 fold more *FliT*. Here the analysis suggests that *FliT* is 2 fold higher than *FlhC*. Taking into account *FlhC* is a dimer in the *FlhD₄C₂* complex and that the active form of *FliT* maybe a monomer, the detected levels are consistent with *FliT* being important at all times during flagellar synthesis. Especially as the detectable levels of *FliD* are below or equal to *FlhC*. This quantification of western blots has proved to successfully approximate the concentration of all three proteins in the circuit *in vivo*. From the results, the important message is that in wild type, the concentration of $FliT > FlhD_4C_2 \geq FliD$. These levels correlate to what we find *in vitro* to be necessary for *FliT* to regulate *FlhD₄C₂*.

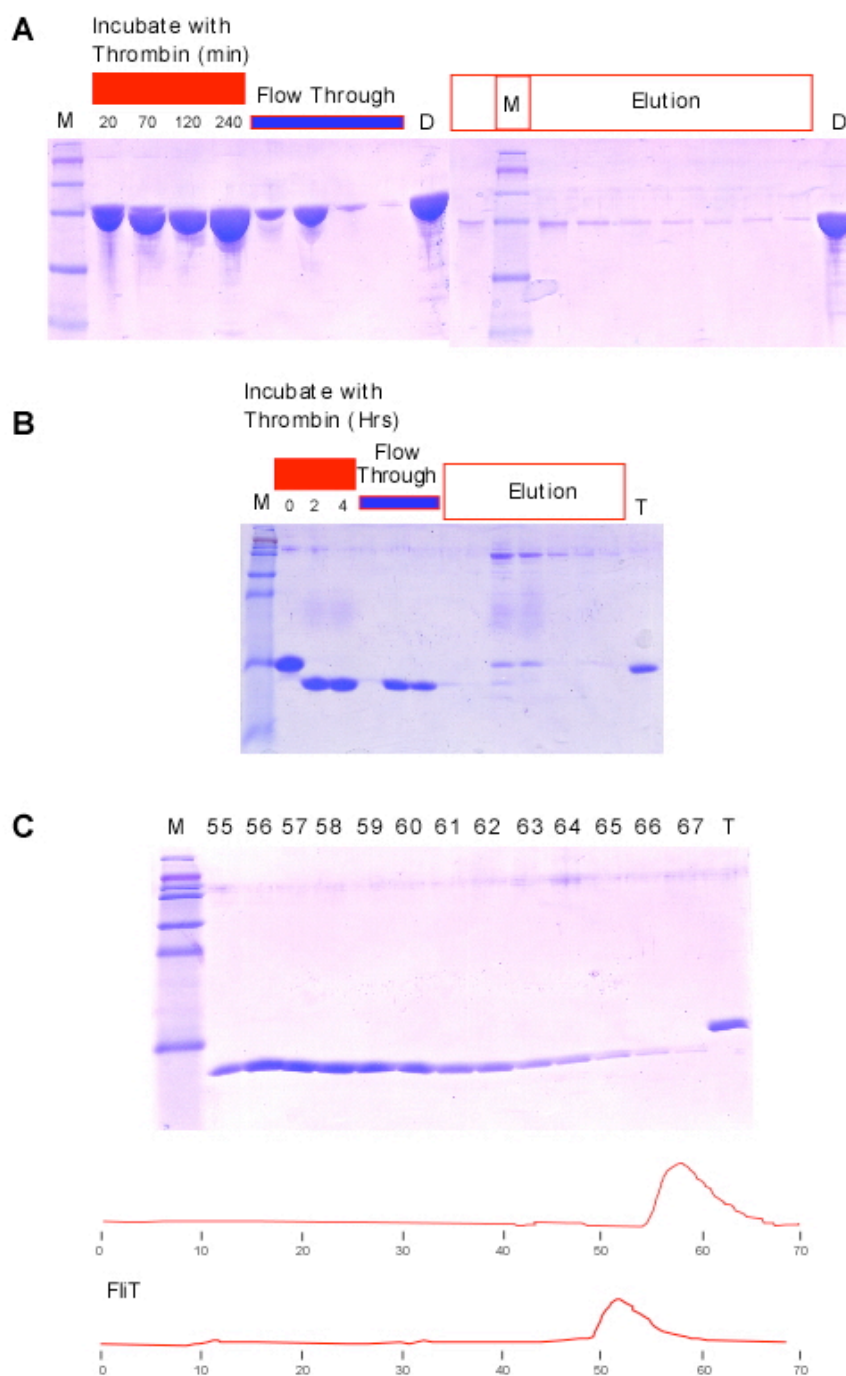
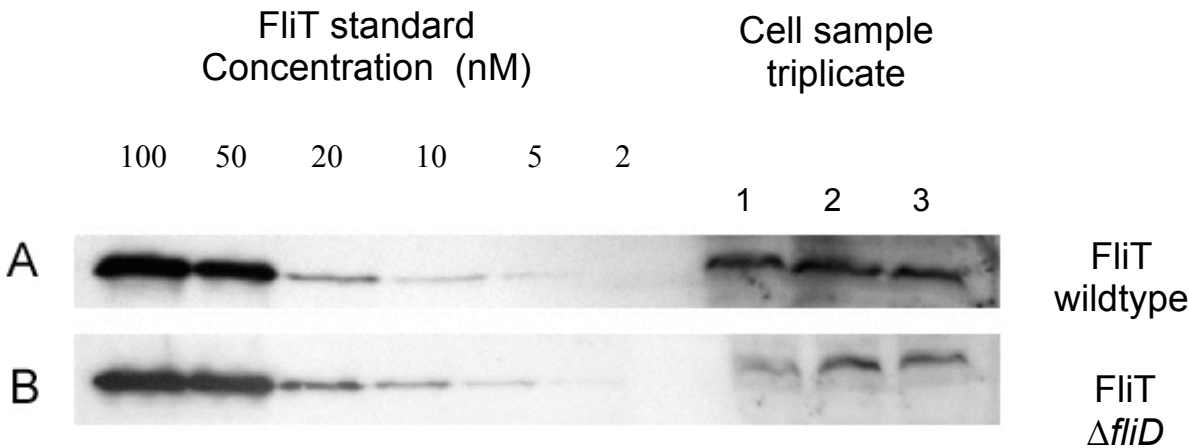


Figure 56: Thrombin digestion of *FliT* and *FliD*

(A) Results of SDS PAGE show *FliD* in each step of Thrombin digestion. The change of *FliD* size is hardly noticed even after 4 Hrs of incubation. The amount of *FliD* reduced significantly in Flow through. (B) *FliT* digestion is evidently observed with its smaller size on the gel and the large amount in Flow through. (C) After Thrombin digestion, gel filtration was performed with the digested proteins to remove any contaminant and retain the proteins in gel buffer and observe the smaller size of *FliT* on the gel.



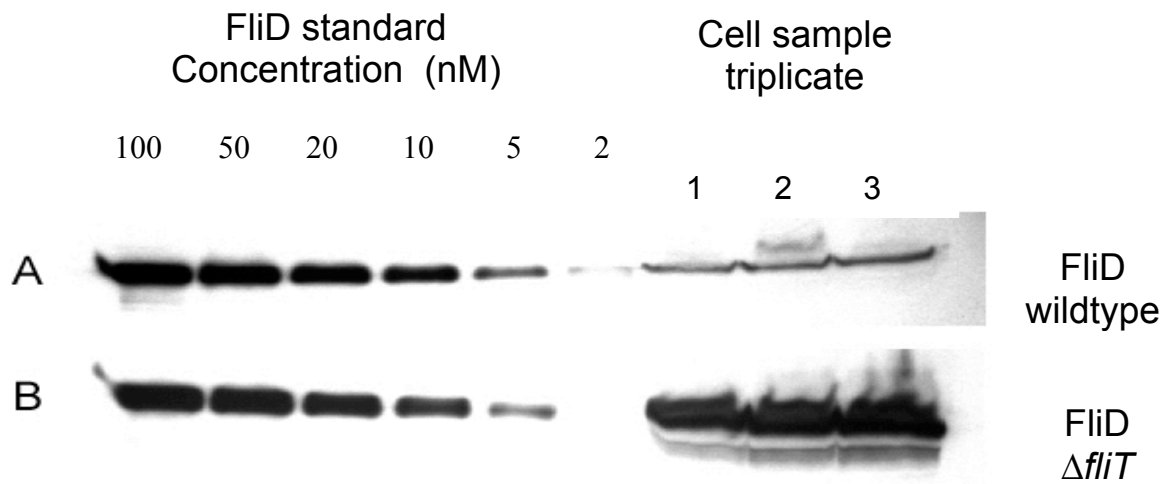
C

FliT Concentration (nM)	Blot A	Blot B	Average
100	3904	4226	4065
50	3322	3849	3585
20	1566	1048	1307
10	459	418	438
5	179	139	159
2	0	26	13

Triplicate cell sample	1	2	3	Average
Blot A wild type	2112	1659	1736	1836
Blot B <i>ΔfliD</i>	1225	1825	1740	1597

Figure 57: FliT quantification

Results of the western blot of FliT and its analytical data. The western blots of FliT **(A)** for wild type and **(B)** for *ΔfliD* strain show the measurable intensity of both samples and FliT standards. **(C)** The table shows FliT's quantified results from protein standard concentration and cell sample bands by image J program..



C

FliD Concentration (nM)	Blot A	Blot B	Average
100	5021	5905	5463
50	4359	5228	4794
20	3832	3476	3654
10	2283	2045	2164
5	762	753	757
2	53	112	83

Triplicate cell sample	1	2	3	Average
Blot A Wild type	1703	1476	2426	1868
Blot B $\Delta fliT$	3971	5209	5417	4866

Figure 58: FliD quantification

Results of the western blot of FliD and its analytical data. The western blots of FliD (A) for wild type and (B) for $\Delta fliT$ strain show the measurable intensity of both samples and FliD standards. (C) The table shows FliD quantified results from the protein standard and of cell sample bands by image J program.

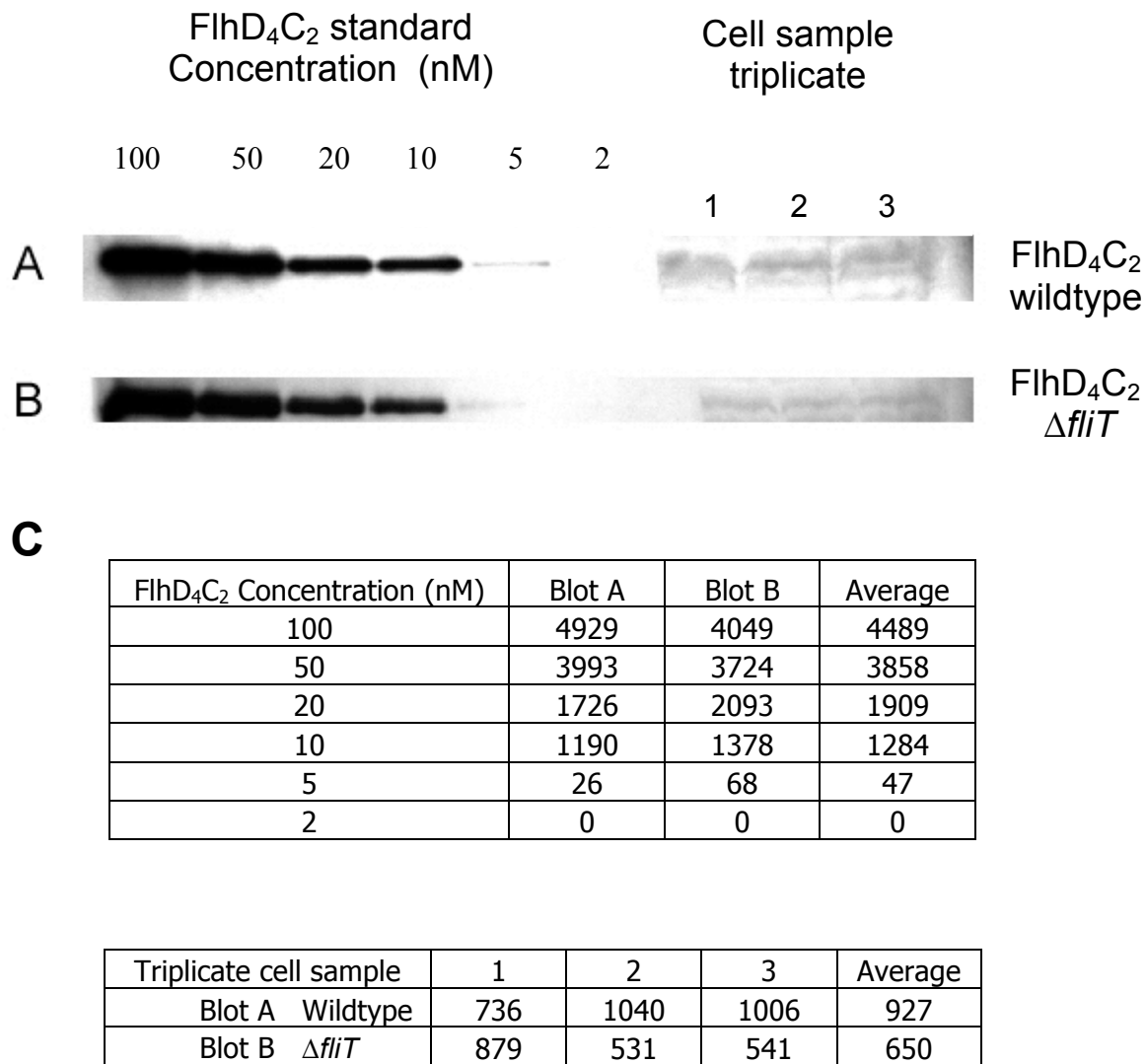


Figure 59: FlhD₄C₂ quantification

Results of the western blot of FlhD₄C₂ and its analytical data. The western blots of FlhD₄C₂ (**A**) for wild type and (**B**) for $\Delta fliT$ strain show the weak bands of samples but strong in FlhD₄C₂ standards. (**C**) The table shows FlhD₄C₂'s quantified results from protein standard and of cell sample bands by image J program.

Chapter 10

Discussion, Conclusion and Future Research

Chapter 10 Discussion, Conclusion and Future Research

10.1 Discussion

A model of protein-protein and protein-DNA interactions has been reported with the interplay among FliT, FliD and FlhD₄C₂ that dictates the decision to express the *fla* regulon (Yamamoto & Kutsukake, 2006). Inhibition of FlhD₄C₂ by FliT is integral to this regulatory circuit especially in multiflagellated bacterial species. The net output is proposed to stop or pause flagellar synthesis, to obtain an optimal number of flagellar per bacterial cell.

The interconnecting regulatory circuits that produce the flagellar regulation system have been schematically related to the FlgM:σ²⁸ circuit. FlgM:σ²⁸ regulation shows the coupling mechanism between flagellar gene expression and flagellar synthesis specifically related to the completion of Hook Basal Body (HBB). Breaking the FlgM:σ²⁸ system, effectively stops gene expression at the middle of flagellar process. In detail, FlgM binding to σ²⁸ prevents further processes until the secretion of FlgM frees σ²⁸ to drive gene expression to complete a flagellum. In comparison to the Yamamoto model, FliT inhibition of FlhD₄C₂ activity during flagellar synthesis follows nearly the same strategy of protein-protein regulation (**Figure 60**).

FlhD₄C₂ exerts its activity at the top of *fla* regulon; therefore, it acts as the key regulator for determining the synthesis of a flagellum. FlhD₄C₂ have been reported to receive influences both from external and internal messages to modulate bacterial flagellation (Soutourina & Bertin, 2003). In our focus, endogenous FliT negatively regulates the activity of FlhD₄C₂ through its binding of the FlhD₄C₂ complex. Forming the complex with FlhD₄C₂, FliT is assumed to prevent FlhD₄C₂ from binding its target DNA and activating P_{class2} expression (Yamamoto *et al.*, 2006). The *in vitro* study of FliT interaction with FlhD₄C₂ was established in this study to explore the mechanism FliT interacts with the FlhD₄C₂ complex and the outcome with respect to regulation. FlhD₄C₂ components, FlhC and FlhD, were separated and analysed previously by Yamamoto *et al* (2006). To explore the FliT effect on FlhD₄C₂ complexes, the preparation of active form of FlhD₄C₂ was established.

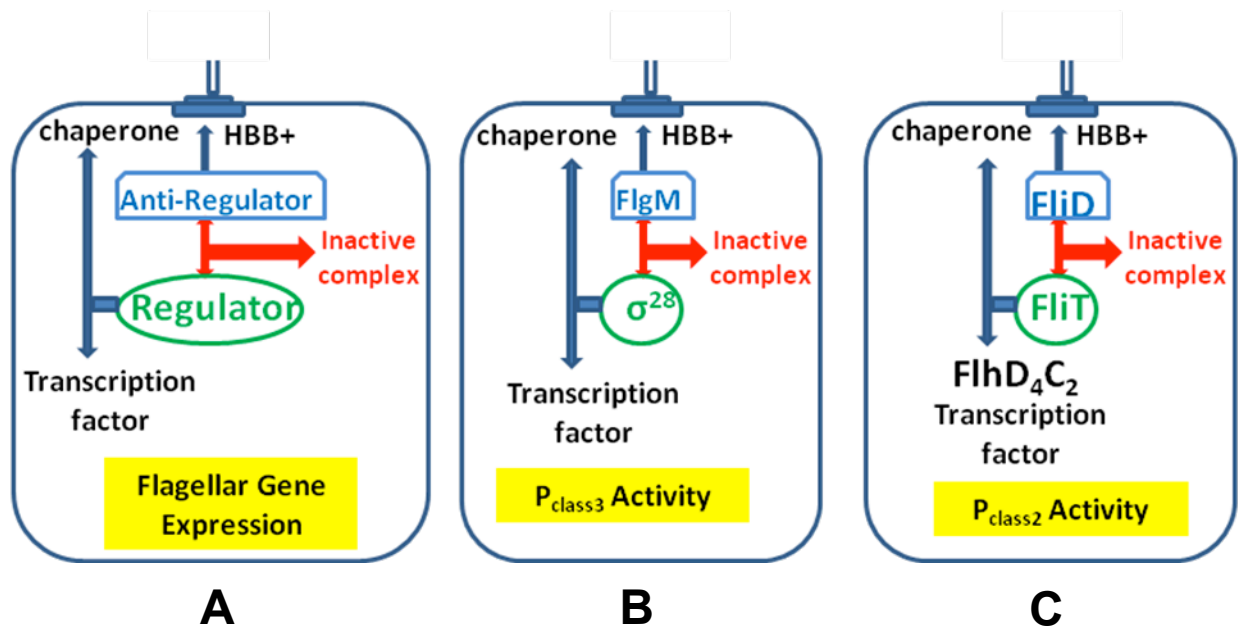


Figure 60: A general mechanism applied to the regulatory circuit used for flagellar gene expression.

(A) A general proposed regulatory strategy that is dominated by protein interactions between a regulator and anti-regulator controlling flagellar gene expression. Dual factions of a regulator are proposed, both as a chaperone and transcription factor. When as a chaperone, flagellar gene expression is inhibited until the secretion of anti-regulator occurs with the assistance of the regulator. (B) The FlgM:σ²⁸ regulatory circuit: FlgM inhibits σ²⁸ before being secreted and then σ²⁸ is able to activate the P_{class3} activity. (C) FliT:FliD:FlhD₄C₂ regulatory circuit, using the proposed mechanism. The FliT inhibition of FlhD₄C₂ dominates the circuit, until FliD interacts with FliT and the activity of FlhD₄C₂ then resumes. The secretion of FliD allows for the inhibitory effect of FliT to FlhD₄C₂. (Brown *et al.*, 2009)

Native gel electrophoresis and gel filtration showed FliT interacting with FliD with a stoichiometry of FliT 1 : FliD 1, which was consistent with Imada *et al* (2010). The FliT:FlhD₄C₂ interaction was shown when mixing two proteins together in a ratio of approximately 2:1 for FliT to FlhD₄C₂. Attempts to isolate a FliT:FlhD₄C₂ complex were unsuccessful when gel filtrated, however, FliT unbound disappeared. MALDI-TOF analysis of the obtained fractions around the FlhD₄C₂ peak suggested FliT interacting with FlhD₄C₂. To define the outcome of the interaction alternative in vitro interaction techniques had to be employed. ITC was tried but produced inconclusive results. As a result our analysis turned to AUC that showed that the FlhD₄C₂ complexes were disrupted by FliT. A product of the interaction was a promising smaller complex at 61–63 kDa (**Figure 37**). From the size of each component this complex could be either a disrupted FlhD₄C₂ complex or a complex of FlhC and FliT or FlhD, FlhC and FliT. Time constraints and the technicalities of using AUC to elucidate the composition of this new species were outside the scope of this project. A working model for FliT:FliD:FlhD₄C₂ regulation is illustrated in **Figure 61**. This model takes into account the protein-protein interactions and their outcomes as defined by the in vitro analysis performed here. Importantly the ability of FlhD₄C₂ to bind to its target DNA sites as a fourth component of the circuit is necessary to correlate the in vitro data with in vivo phenotypes observed.

SPR analysis of the FliT:FlhD₄C₂ interaction reveals that FliT is unable to disrupt DNA bound FlhD₄C₂. This was an unexpected results leads to the proposal that the target of FliT regulation is soluble FlhD₄C₂. In contrast when bound to DNA FlhD₄C₂ is effectively hidden from regulation. This observation is consistent with previous observations that FlhC is the interaction partner of FliT and that FlhC is the main DNA binding component of the FlhD₄C₂ complex (Yamamoto & Kutsukake, 2006, Claret & Hughes, 2000). Our data suggests that the binding interface on FlhC for FliT is either buried in the FlhD₄C₂:DNA complex or is even the DNA binding site itself. This explains how FlhD₄C₂ can escape from FliT disruption by binding to its target DNA. Analysis of the K_D and R_{max} of the FlhD₄C₂:DNA interaction in the absence and presence of FliT further suggests that the role of FliT is to reduce FlhD₄C₂ availability to reach its targets but not its ability to bind its targets. This means that even under negative regulation via FliT some FlhD₄C₂ activity is able to

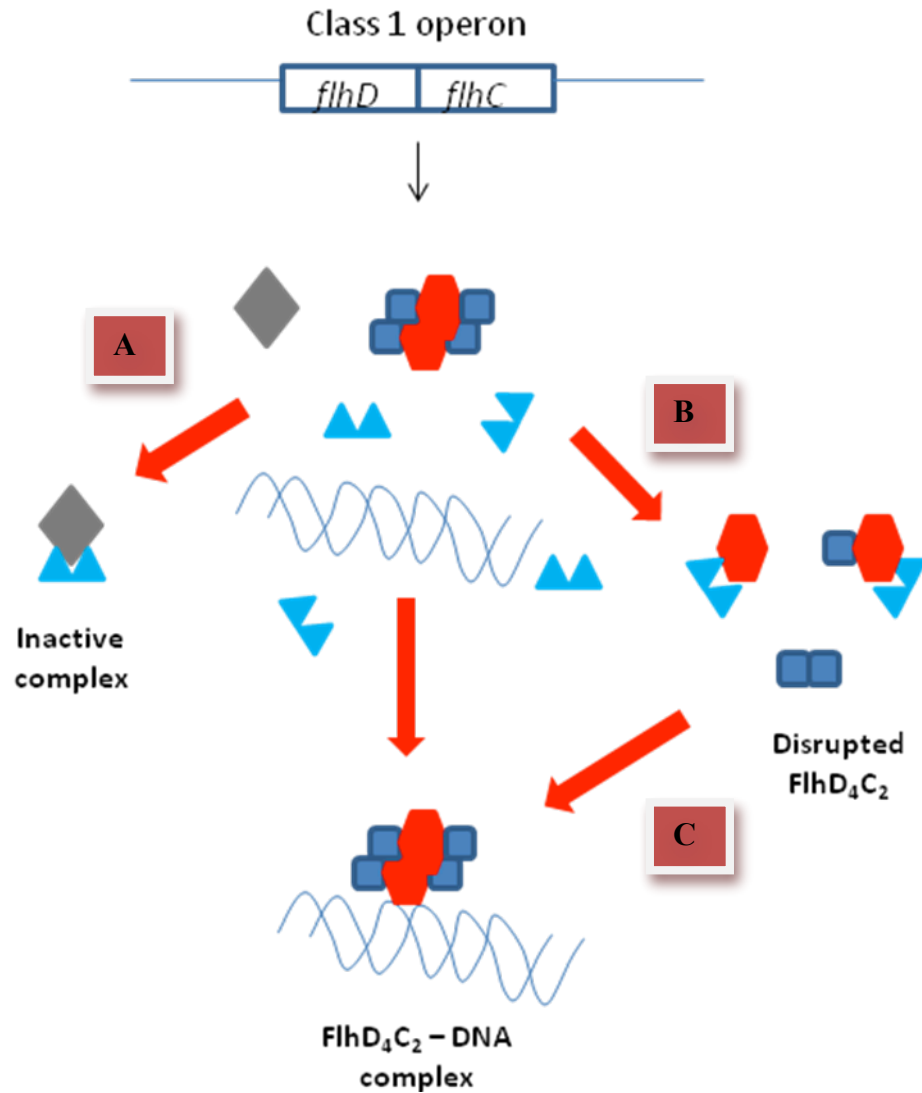


Figure 61: The mechanism of action from each counterpart in the circuit.

FlhD₄C₂ complex; FlhC as red hexagon, FlhD blue rectangular, is expressed from Class 1 operon, *flhD* and *FlhC*. FliT (blue triangle, dimer), FliD (gray diamond) and DNA (P_{class2}). Protein-protein and protein-DNA interactions regulate flagellar gene expression by controlling the amount of FlhD₄C₂-DNA complex. In the presence of FliD, (A) FliT binds to FliD promoting FlhD₄C₂ activity until FliD secreted HBB (Hook Basal Body). (B) FliT effectively prevents FlhD₄C₂-DNA complex by disrupting the free form of FlhD₄C₂ complex. (C) In the presence of FliT, a few of FlhD₄C₂-DNA complexes form and are resistant to FliT disruption. The regulation relies on different amounts of each proteins, we estimate from measuring the average protein levels in a population that FliT is 2-fold in excess to FliD and FlhD₄C₂.

maintain a basal level of flagellar gene expression. With this basal activity, FlhD₄C₂ can assure some flagellation occurs in a population.

The FliT structure shows that C-terminal α helix structural component are crucial for the binding to its counterparts; FlhD₄C₂ and FliD (Imada *et al.*, 2010). An overactive FliT variant existed that had this helix removed generating FliT94. Mutated FliT was analysed based on alanine substitutions in FliT94. FliT94 shows stronger binding with the FlhD₄C₂ complex than wild type. Amino acid substitutions of FliT 94 in α 3 were conducted to evaluate if there is single or a group of amino acids, which affect FlhD₄C₂ binding to FliT. Results suggest a group of FliT94 mutation around the position at 75-82 significantly reduce FlhD₄C₂ destruction. For FliD interaction, the position at 79 in FliT is crucial for its binding. Consequently, the binding site for FlhD₄C₂ and FliD in FliT may also overlap. In a molecular view, it reflects that the dual functions of FliT are separated. Only one role occurs at one time effectively dictated by binding competition between each counterpart.

All data further implies the importance of the availability of all proteins towards the circuit. It suggests FliT selectively functions according to competitive binding of its counterparts for the overlapped binding sites in FliT (Imada *et al.*, 2010). However, from the crystal structure, the α 4 region of FliT can move and mask α 3 from its counterparts. This hints us the movable α 4 region possibly dictating FliT function. To this point, both FliT availability and its conformation contribute to the functionality of the circuit.

Protein- protein interaction in the circuit has been reviewed mostly *in vitro*. As described, the concentration of each counterpart affects the functionality of the circuit. In a cell context, their existing concentrations were assessed. The *in vitro* data suggested that to regulate FlhD₄C₂ activity effectively needs excess FliT. The assay of FliT, FliD, and FlhD₄C₂ levels by immuno detection found a small quantity FlhD₄C₂ ; with surprisingly, FliT was detected in the amount needed to efficiently regulate FlhD₄C₂ activity in a cell. This implies, as an internal factor, FliT is in excess and its influence over reducing FlhD₄C₂ activity to the basal rate of flagellation is key at all points during flagellar synthesis.

Why FliT selectively interacts or disrupt with the only free FlhD₄C₂ complexes rather than the form of FlhD₄C₂ bound DNA? Cells might use this selectivity to give the basal rate of flagellar synthesis rather than completely shut down the process to retain the minimum numbers of flagella needed for their survival. FliT availability is driven by the transcription of both P_{class2} and P_{class3} promoter, which is under the influence of FlhD₄C₂. The insensitive FlhD₄C₂ bound with DNA is able to escape the disruptive effect from a basal level of FliT, which is maintained to counteract to free FlhD₄C₂.

In the previous situation, the regulatory circuit then maintains its basal inhibitory effect of FliT until FliD expression occurs resulting in active flagellar synthesis to reach the average numbers of flagella need for survival. Again, cells would restores the basal level of FliT after FliD secretion and reduce flagellar synthesis. However, on average in the population our data suggests that FliT is in excess of FliD and FlhD₄C₂. Therefore, this kind of regulation is thus considered to be a special case of regulation which doesn't restrict its regulation under only some conditions but is continual and maintains flagellar synthesis at a given rate rather than an on-off switch.

10.2 Conclusion

To control the number of bacterial flagella, regulation of FlhD₄C₂ is critical. This study shows the importance of FliT regulation of that activity during all stages of flagellar synthesis. A framework of the regulatory circuit was studied focusing on protein-protein interactions. Many questions were asked to explain the role and also mechanism of each component in the circuit, FliT, FliD and FlhD₄C₂. This study is predicted to explain another regulatory level of flagellar synthesis dictating the number of flagella in enteric bacteria.

The framework of the circuit is established via the interaction among FliT, FliD, and FlhD₄C₂, and another component, the DNA binding sites of FlhD₄C₂, which is closely associated with FlhD₄C₂. In parallel with the well-known FlgM- σ^{28} regulatory circuit, the actual circuit seems to be conserved. FliT exhibit inhibitory effect through its destructive effect to the FlhD₄C₂ complex but surprisingly not DNA bound FlhD₄C₂. The presence of FliD counteracts the inhibitory effect of FliT though the strong binding. Interestingly, over expressed FliT strain showed much decrease of mobility phenotype but not all inhibited. The result suggests FlhD₄C₂ still functions even in excess FliT. Results show the regulation of the flagellar synthesis is linked to FlhD₄C₂ activity through the FliT circuit.

10.3 Future research

This work has explored the mechanism of the regulatory circuit which is related to interaction among the components. Much molecular and biochemical details were explained focusing on the behavior detail of the circuit *in vitro* analysis. Other work needed to be continued to strengthen the circuit is performing on single cell resolution analysis including first quantifying flagellar gene expression of the proteins in the circuit and second monitoring the expressed proteins in a single cell environment. That would strengthen the role circuit as controlling flagellar number. In addition, those analyses in *FliT* mutants are also studied in the cell context as well.

As being the master regulator of flagellar synthesis, FlhD_4C_2 receive signals from both inside and outside cells. *FliT* is considered to be an internal factor effecting FlhD_4C_2 in the circuit but the extent of external factors contributed on FlhD_4C_2 should be explored in details to couple the bacterial niche to flagellar synthesis and expand factors affecting FlhD_4C_2 expression to reach the level of deeper insight about the control of the number of flagella.

Chapter 11

Reference

Chapter 11 References

- Adler, J. & B. Templeton, (1967) The effect of environmental conditions on the motility of *Escherichia coli*. *Journal of general microbiology* 46: 175-184.
- Aizawa, S. I., F. Vonderviszt, R. Ishima & K. Akasaka, (1990) Termini of *Salmonella* flagellin is disordered and become organized upon polymerization into flagellar filament. *Journal of Molecular Biology* 211: 673-677.
- Aldridge, C., Poonchareon, K., Saini, S., Ewen, T., Soloyva, A., Rao, C. V., Imada, K., et al. (2010). The interaction dynamics of a negative feedback loop regulates flagellar number in *Salmonella enterica* serovar Typhimurium. *Molecular microbiology*, 78 (6): 1416–1430.
- Aldridge, P. D., J. E. Karlinsey, C. Aldridge, C. Birchall, D. Thompson, J. Yagasaki & K. T. Hughes, (2006a) The flagellar-specific transcription factor , 28 , is the Type 3 secretion chaperone factor FlgM. *Genes & Development*: 2315-2326.
- Aldridge, P.D., Wu, C., Gnerer, J., Karlinsey, J.E., Hughes, K.T., & Sachs, M.S, (2006b) Regulatory protein that inhibits both synthesis and use of the target protein controls flagellar phase variation in *Salmonella enterica*. *Proceedings of the National Academy of Sciences of the United States of America* 103: 11340- 11345.
- Aldridge, P., J. Karlinsey & K. T. Hughes, (2003) The type 3 secretion chaperone FlgN regulates flagellar assembly via a negative feedback loop containing its chaperone substrates FlgK and FlgL. *Molecular Microbiology* 49: 1333-1345.
- Akeda, Y. & J. E. Galan, (2005) Chaperone release and unfolding of substrates in type 3 secretion. *Nature* 437: 911-915.
- Alon, U., M. G. Surette, N. Barkai & S. Leibler, (1999) Robustness in bacterial chemotaxis. *Nature* 397: 168-171.

- Arnosti, D. N. & M. J. Chamberlin, (1989) Secondary sigma factor controls transcription of flagellar and chemotaxis genes in *Escherichia coli*. *Proceedings of the National Academy of Sciences of the United States of America* 86: 830-834.
- Atkinson, S., Chang, C.-Y., Patrick, H. L., Buckley, C. M. F., Wang, Y., Sockett, R. E., Cámara, M., *et al.*, (2008). Functional interplay between the *Yersinia pseudotuberculosis* YpsRI and YtbRI quorum sensing systems modulates swimming motility by controlling expression of *flhDC* and *fliA*. *Molecular Microbiology* 69: 137–151.
- Atsumi, T., Maekawa, Y., Yamada, T., Kawagishi, I., Imae, Y., & Homma, M., (1996). Effect of viscosity on swimming by the lateral and polar flagella of *Vibrio alginolyticus*. *Journal of Bacteriology*, 178: 5024–5026
- Attmannspacher, U., B. E. Scharf & R. M. Harshey, (2008) FliL is essential for swarming: motor rotation in absence of FliL fractures the flagellar rod in swarmer cells of *Salmonella enterica*. *Molecular Microbiology* 68: 328-341.
- Auvray, F., Thomas, J., Fraser, G. M., & Hughes, C, (2008) Flagellin Polymerisation Control by a Cytosolic Export Chaperone. *Journal of Molecular Biology* 308: 221–229
- Baker, M. D., P. M. Wolanin & J. B. Stock, (2005) Signal transduction in bacterial chemotaxis. *BioEssays* 28: 9-22.
- Barembuch, C. & R. Hengge, (2007) Cellular levels and activity of the flagellar sigma factor FliA of *Escherichia coli* are controlled by FlgM-modulated proteolysis. *Molecular Microbiology* 65: 76-89.
- Bennett, J. C. Q., J. Thomas, G. M. Fraser & C. Hughes, (2001) Substrate complexes and domain organization of the *Salmonella* flagellar export chaperones FlgN and FliT. *Molecular Microbiology* 39: 781-791.

- Berg, H. C. 2003, *E. coli in Motion*, Springer-Verlag, New York
- Berg, H. C. & D. A. Brown, (1972) Chemotaxis in *Escherichia coli* analysed by three-dimensional tracking. *Nature* 239: 500-504.
- Blair, D. F., (2006) Fine structure of a fine machine. *Journal of bacteriology* 188: 7033-7035.
- Blair, D. F, (1995) How bacteria sense and swim. *Annual Review of Microbiology* 49: 489–522
- Bonifield, H. R., S. Yamaguchi & K. T. Hughes, (2000) The flagellar hook protein, FlgE, of *Salmonella enterica* serovar typhimurium is posttranscriptionally regulated in response to the stage of flagellar assembly. *Journal of Bacteriology* 182: 4044-4050.
- Campos, a. & P. Matsumura, (2001) Extensive alanine scanning reveals protein-protein and protein-DNA interaction surfaces in the global regulator FlhD from *Escherichia coli*. *Molecular microbiology* 39: 581-594.
- Chadsey, M. S. & Hughes, K. T, (2001) A multipartite interaction between *Salmonella* transcription factor σ^{28} and its anti-sigma factor FlgM: implications for σ^{28} holoenzyme destabilization through stepwise binding. *Journal of Molecular Biology* 306: 915-929.
- Chadsey, M. S., J. E. Karlinsey & K. T. Hughes, (1998) The flagellar anti- factor FlgM actively dissociates *Salmonella typhimurium* 28 RNA polymerase holoenzyme. *Genes & Development* 12: 3123-3136.
- Chevance, F. F. V. & K. T. Hughes, (2008) Coordinating assembly of a bacterial macromolecular machine. *Nature reviews. Microbiology* 6: 455-465.

- Chilcott, G. S. & K. T. Hughes, (2000) Coupling of flagellar gene expression to flagellar assembly in *Salmonella enterica* serovar typhimurium and *Escherichia coli*. *Microbiology and Molecular Biology Reviews* 64: 694-708.
- Chilcott, G. S. & K. T. Hughes, (1998) The type III secretion determinants of the flagellar anti-transcription factor, FlgM, extend from the amino-terminus into the anti-sigma28 domain. *Molecular Microbiology* 30: 1029-1040.
- Claret, L., S. R. Calder, M. Higgins & C. Hughes, (2003) Oligomerization and activation of the Flil ATPase central to bacterial flagellum assembly. *Molecular Microbiology* 48: 1349-1355.
- Claret, L. & C. Hughes, (2002) Interaction of the atypical prokaryotic transcription activator FlhD₂C₂ with early promoters of the flagellar gene hierarchy. *Journal of Molecular Biology* 321: 185-199.
- Claret, L. & C. Hughes, (2000) Functions of the subunits in the FlhD(2)C(2) transcriptional master regulator of bacterial flagellum biogenesis and swarming. *Journal of Molecular Biology* 303: 467-478.
- Daughdrill, G. W., M. S. Chadsey, J. E. Karlinsey, K. T. Hughes & F. W. Dahlquist, (1997) The C-terminal half of the anti-sigma factor, FlgM, becomes structured when bound to its target, sigma 28. *Nature Structural Biology* 4: 285-291.
- Dorman, C., (2003) Regulation of gene expression by histone-like proteins in bacteria. *Current Opinion in Genetics & Development* 13: 179-184.
- Elowitz, M. B., M. G. Surette, P. E. Wolf, J. B. Stock & S. Leibler, (1999) Protein mobility in the cytoplasm of *Escherichia coli*. *Journal of Bacteriology* 181: 197-203.
- Erhardt, M. & Kelly T. Hughes, (2010a) C-ring requirement in flagellar type III secretion is bypassed by FlhDC upregulation. *Molecular Microbiology* 75: 376–393

- Erhardt, M., Numba Keiichi & Kelly T. Hughes, (2010b) Bacterial Nanomachines: The Flagellum and Type III Injectiosome. *Cold Spring Harbor perspectives in biology* 2: 1-22
- Evans, L. D. B., G. P. Stafford, S. Ahmed, G. M. Fraser & C. Hughes, (2006) An escort mechanism for cycling of export chaperones during flagellum assembly. *Proceedings of the National Academy of Sciences of the United States of America* 103: 17474-17479.
- Fan, F. & R. M. Macnab, (1996) Enzymatic characterization of Flil. An ATPase involved in flagellar assembly in *Salmonella typhimurium*. *Journal of Biological Chemistry* 271: 31981-31988.
- Ferris, H. U. & T. Minamino, (2006) Flipping the switch: bringing order to flagellar assembly. *Trends in microbiology* 14: 519-526.
- Fraser, G. M., T. Hirano, H. U. Ferris, L. L. Devgan, M. Kihara & R. M. Macnab, (2003) Substrate specificity of type III flagellar protein export in *Salmonella* is controlled by subdomain interactions in FlhB. *Molecular Microbiology* 48: 1043-1057.
- Fraser, G. M., J. C. Bennett & C. Hughes, (1999) Substrate-specific binding of hook-associated proteins by FlgN and FliT, putative chaperones for flagellum assembly. *Molecular Microbiology* 32: 569-580.
- Frye, J., J. E. Karlinsey, H. R. Felise, B. Marzolf, N. Dowidar, M. McClelland & K. T. Hughes, (2006) Identification of new flagellar genes of *Salmonella enterica* serovar Typhimurium. *Journal of Bacteriology* 188: 2233-2243.
- Galan, J. E., (2001) *Salmonella* interactions with host cells: type III secretion at work. *Annual Review of Cell and Developmental Biology* 17: 53-86.

- Gillen, K. L. & K. T. Hughes, (1993) Transcription from two promoters and autoregulation contribute to the control of expression of the *Salmonella* typhimurium flagellar regulatory gene *flgM*. *Journal of Bacteriology* 175: 7006-7015.
- Grove, A. & T. C. Saavedra, (2002) The role of surface-exposed lysines in wrapping DNA about the bacterial histone-like protein HU. *Biochemistry* 41: 7597-7603.
- Hansen-Wester, I. & M. Hensel, (2001) *Salmonella* pathogenicity islands encoding type III secretion systems. *Microbes and Infection* 3: 549-559.
- Helmann, J. D. & M. J. Chamberlin, (1988a) Structure and function of bacterial sigma factors. *Annual review of biochemistry* 57: 839-872.
- Helmann, J. D., F. R. Masiarz & M. J. Chamberlin, (1988b) Isolation and characterization of the *Bacillus subtilis* sigma 28 factor. *Journal of Bacteriology* 170: 1560-1567.
- Hirano, T., S. Yamaguchi, K. Oosawa & S. Aizawa, (1994) Roles of FliK and FlhB in determination of flagellar hook length in *Salmonella* typhimurium. *Journal of Bacteriology* 176: 5439-5449.
- Hollands, Kerry, Stephen J W Busby, & Georgina S Lloyd, (2007) "New targets for the cyclic AMP receptor protein in the *Escherichia coli* K-12 genome." *FEMS Microbiology Letters* 274: 89–94
- Holt, P. S. & L. H. Chabal, (1997) Detection of motility and putative synthesis of flagellar proteins in *Salmonella* pullorum cultures. *Journal of Clinical Microbiology* 35: 1016-1020.
- Homma, M., K. Kutsukake, M. Hasebe, T. Iino & R. M. Macnab, (1990) FlgB, FlgC, FlgF and FlgG. A family of structurally related proteins in the flagellar basal body of *Salmonella* typhimurium. *Journal of Molecular Biology* 211: 465-477.

- Homma, M., T. Iino, K. Kutsukake & S. Yamaguchi, (1986) In vitro reconstitution of flagellar filaments onto hooks of filamentless mutants of *Salmonella typhimurium* by addition of hook-associated proteins. *Proceedings of the National Academy of Sciences of the United States of America* 83: 6169-6173.
- Homma, M. & T. Iino, (1985) Locations of hook-associated proteins in flagellar structures of *Salmonella typhimurium*. *Journal of Bacteriology* 162: 183-189.
- Homma, M., K. Kutsukake, T. Iino & S. Yamaguchi, (1984) Hook-associated proteins essential for flagellar filament formation in *Salmonella typhimurium*. *Journal of Bacteriology* 157: 100-108.
- Hughes, K. T., & Mathee, K. (1998). The anti-sigma factors. *Annual review of microbiology* 52: 231–286.
- Hughes, K. T., K. L. Gillen, M. J. Semon & J. E. Karlinsey, (1993) Sensing structural intermediates in bacterial flagellar assembly by export of a negative regulator. *Science (New York, N.Y.)* 262: 1277-1280.
- Ikebe, T., S. Iyoda & K. Kutsukake, (1999a) Promoter analysis of the class 2 flagellar operons of *Salmonella*. *Genes and Genetic system* 74: 179-183.
- Ikebe, T., S. Iyoda & K. Kutsukake, (1999b) Structure and expression of the *fliA* operon of *Salmonella typhimurium*. *Microbiology (Reading, England)* 145: 1389-1396.
- Ikeda, T., S. Yamaguchi & H. Hotani, (1993) Flagellar growth in a filament-less *Salmonella fliD* mutant supplemented with purified hook-associated protein 2. *Journal of Biochemistry* 114: 39-44.
- Ikeda, T., M. Homma, T. Iino, S. Asakura & R. Kamiya, (1987) Localization and stoichiometry of hook-associated proteins within *Salmonella typhimurium* flagella. *Journal of Bacteriology* 169: 1168-1173.

- Ikeda, T., (1985) "Cap" on the tip of *Salmonella* flagella. *Journal of Molecular Biology* 184: 735-737.
- Imada, K., T. Minamino, M. Kinoshita, Y. Furukawa & K. Namba, (2010) Structural insight into the regulatory mechanisms of interactions of the flagellar type III chaperone FliT with its binding partners. *Proceedings of the National Academy of Sciences of the United States of America* 107: 8812-8817.
- Imada, K., F. Vonderviszt, Y. Furukawa, K. Oosawa & K. Namba, (1998) Assembly characteristics of flagellar cap protein HAP2 of *Salmonella*: decamer and pentamer in the pH-sensitive equilibrium. *Journal of Molecular Biology* 277: 883-891.
- Ishihama, A., (1993) MINIREVIEW Protein-Protein Communication within the Transcription Apparatus. *Journal of Bacteriology* 175: 2483-2489.
- Ishihama, A., (1988) Promoter selectivity of prokaryotic RNA polymerases. *Trends in Genetics* 4: 282-286.
- Islam, M., J. Morgan, M. P. Doyle, S. C. Phatak, P. Millner & X. Jiang, (2004) Persistence of *Salmonella* enterica serovar typhimurium on lettuce and parsley and in soils on which they were grown in fields treated with contaminated manure composts or irrigation water. *Foodborne Pathogens Disease* 1: 27-35.
- Iyoda, S. & K. Kutsukake, (1995) Molecular dissection of the flagellum-specific anti-sigma factor, FlgM, of *Salmonella* typhimurium. *Molecular and General Genetics* 249: 417-424.
- Jishage, M. & A. Ishihama, (1998) A stationary phase protein in *Escherichia coli* with binding activity to the major sigma subunit of RNA polymerase. *Proceedings of*

- the National Academy of Sciences of the United States of America* 95: 4953-4958.
- João Paulo. (2006). *BIACORE T100: An overview of underlying concepts, basic operation, experimental techniques and potential applications*. Available: http://biomed.brown.edu/epscor_proteomics/JPBiacorePresentation.pdf. Last accessed 10th Nov 2010.
- Jones, C. J. & R. M. Macnab, (1990) Flagellar assembly in *Salmonella typhimurium*: analysis with temperature-sensitive mutants. *Journal of Bacteriology* 172: 1327-1339.
- Jordi, B. J., A. E. Fielder, C. M. Burns, J. C. Hinton, N. Dover, D. W. Ussery & C. F. Higgins, (1997) DNA binding is not sufficient for H-NS-mediated repression of proU expression. *Journal of Biological Chemistry* 272: 12083-12090.
- Kamiya, R., S. Asakura, K. Wakabayashi & K. Namba, (1979) Transition of bacterial flagella from helical to straight forms with different subunit arrangements. *Journal of Molecular Biology* 131: 725-742.
- Karlinsey, J. E., J. Lonner, K. L. Brown & K. T. Hughes, (2000) Translation/secretion coupling by type III secretion systems. *Cell* 102: 487-497.
- Karp, P. D., I. M. Keseler, A. Shearer, M. Latendresse, M. Krummenacker, S. M. Paley, I. Paulsen, J. Collado-Vides, S. Gama-Castro, M. Peralta-Gil, A. Santos-Zavaleta, M. I. Penaloza-Spinola, C. Bonavides-Martinez & J. Ingraham, (2007) Multidimensional annotation of the *Escherichia coli* K-12 genome. *Nucleic Acids Research* 35: 7577-7590.
- Katayama, E., T. Shiraishi., K. Oosawa., N. Baba., S. I. Aizawa, (1996) Geometry of the flagellar motor in the cytoplasmic membrane of *Salmonella typhimurium* as determined by stereo-photogrammetry of quick-freeze deep-etch replica images. *Journal of Molecular Biology* 255(3): 458-475.

- Kawagishi, I., V. Muller, a. W. Williams, V. M. Irikura & R. M. Macnab, (1992) Subdivision of flagellar region III of the *Escherichia coli* and *Salmonella typhimurium* chromosomes and identification of two additional flagellar genes. *Journal of General Microbiology* 138: 1051-1065.
- Kihara, M., G. U. Miller & R. M. Macnab, (2000) Deletion analysis of the flagellar switch protein FliG of *Salmonella*. *Journal of Bacteriology* 182: 3022-3028.
- Komeda, Y., (1986) Transcriptional control of flagellar genes in *Escherichia coli* K-12. *Journal of Bacteriology* 168: 1315-1318.
- Kubori, T., S. Yamaguchi & S. Aizawa, (1997) Assembly of the switch complex onto the MS ring complex of *Salmonella typhimurium* does not require any other flagellar proteins. *Journal of Bacteriology* 179: 813-817.
- Kutsukake, K., T. Ikebe & S. Yamamoto, (1999) Two novel regulatory genes, *fliT* and *fliZ*, in the flagellar regulon of *Salmonella*. *Genes & Genetic systems* 74: 287-292.
- Kutsukake, K, (1997) Autogenous and global control of the flagellar master operon, *flhD*, in *Salmonella typhimurium*. *Molecular and General Genetics* 254: 440–448
- Kutsukake, K, (1994) Excretion of the anti-sigma factor through a flagellar substructure couples flagellar gene expression with flagellar assembly in *Salmonella typhimurium*. *Molecular and General Genetics* 243: 605-612
- Kutsukake, K., Y. Ohya & T. Iino, (1990) Transcriptional analysis of the flagellar regulon of *Salmonella typhimurium*. *Journal of Bacteriology* 172: 741-747.
- Lahiri, A., A. Lahiri, N. Iyer, P. Das & D. Chakravorty, (2010) Visiting the cell biology of *Salmonella* infection. *Microbes and Infection*: 1-10.
- Larsen, S. H., R. W. Reader, E. N. Kort, W. W. Tso & J. Adler, (1974) Change in direction of flagellar rotation is the basis of the chemotactic response in *Escherichia coli*. *Nature* 249: 74-77.

- Lee, H. J. & K. T. Hughes, (2006) Posttranscriptional control of the *Salmonella enterica* flagellar hook protein FlgE. *Journal of Bacteriology* 188: 3308-3316.
- Levit, M. N., T. W. Grebe & J. B. Stock, (2002) Organization of the receptor-kinase signaling array that regulates *Escherichia coli* chemotaxis. *Journal of Biological Chemistry* 277: 36748-36754.
- Li, C., Louise, C. J., Shi, W., & Adler, J, (1993). Adverse conditions which cause lack of flagella in *Escherichia coli*. *Journal of bacteriology*, 175(8): 2229–2235
- Liu, S. L. & K. E. Sanderson, (1996) Highly plastic chromosomal organization in *Salmonella typhi*. *Proceedings of the National Academy of Sciences of the United States of America* 93: 10303-10308.
- Liu, X., N. Fujita, a. Ishihama & P. Matsumura, (1995) The C-terminal region of the alpha subunit of *Escherichia coli* RNA polymerase is required for transcriptional activation of the flagellar level II operons by the FlhD/FlhC complex. *Journal of Bacteriology* 177: 5186-5188.
- Liu, X. & P. Matsumura, (1994) The FlhD/FlhC complex, a transcriptional activator of the *Escherichia coli* flagellar class II operons. *Journal of Bacteriology* 176: 7345-7351.
- Lonetto, M., M. Gribskov & C. a. Gross, (1992) The sigma 70 family: sequence conservation and evolutionary relationships. *Journal of Bacteriology* 174: 3843-3849.
- Macnab, R. M., (2004) Type III flagellar protein export and flagellar assembly. *Biochimica et Biophysica Acta* 1694: 207-217.
- Macnab, R. M., (2003) How bacteria assemble flagella. *Annual Review of Microbiology* 57: 77-100.

- Macnab, R., (1984) Bacterial Motility and the Bacterial Flagellar Motor. *Annual Review of Biophysics and Biomolecular Structure* 13: 51-83.
- Macnab, R. M., (1977) Bacterial flagella rotating in bundles: a study in helical geometry. *Proceedings of the National Academy of Sciences of the United States of America* 74: 221-221.
- Maddock, J. R. & L. Shapiro, (1993) Polar location of the chemoreceptor complex in the *Escherichia coli* cell. *Science* 259: 1717-1723.
- Maki, M., Ferenc Vonderviszt, Yukio Furukawa, Katsumi Imada and Keiichi Namba, (1998) Plugging interactions of HAP2 pentamer into the distal end of flagellar filament revealed by electron microscopy. *Journal of Molecular Biology* 227: 771-777
- Miller, V. L., (2002) Connections between transcriptional regulation and type III secretion? *Current Opinion in Microbiology* 5: 211-215.
- Minamino, T., K. Imada & K. Namba, (2008a) Mechanisms of type III protein export for bacterial flagellar assembly. *Molecular bioSystems* 4: 1105-1115.
- Minamino, T., & Namba, K., (2008b) Distinct roles of the FliI ATPase and proton motive force in bacterial flagellar protein export. *Nature* 451(7177): 485–488.
- Minamino, T. & R. M. Macnab, (2000) Interactions among components of the *Salmonella* flagellar export apparatus and its substrates. *Molecular Microbiology* 35: 1052-1064.
- Minamino, T., B. Gonzalez-Pedrajo, K. Yamaguchi, S. I. Aizawa & R. M. Macnab, (1999) FliK, the protein responsible for flagellar hook length control in *Salmonella*, is exported during hook assembly. *Molecular Microbiology* 34: 295-304.

- Moriya, N., T. Minamino, K. T. Hughes, R. M. Macnab & K. Namba, (2006) The type III flagellar export specificity switch is dependent on FliK ruler and a molecular clock. *Journal of Molecular Biology* 359: 466-477.
- Mytelka, D. S. & M. J. Chamberlin, (1996) *Escherichia coli* *fliAZY* operon. *Journal of Bacteriology* 178: 24-34.
- Nambu, T., K. Kutsukake, (2000) The Salmonella FlgA protein, a putative periplasmic chaperone essential for flagellar P ring formation. *Microbiology* 146: 1171–1178.
- Nambu, T., Tohru Minamino, Robert M. Macnab, and Kazuhiro Kutsukake, (1999) Peptidoglycan-Hydrolyzing Activity of the FlgJ Protein, Essential for Flagellar Rod Formation in *Salmonella typhimurium*. *Journal of Bacteriology* 181: 1555-1561
- Neidhardt, F. C. (Ed. in Chief), R. Curtiss III, J. L. Ingraham, E. C. C. Lin, K. B. Low, B. Magasanik, W. S. Reznikoff, M. Riley, M. Schaechter, and H. E. Umbarger (1996) *Escherichia coli* and *Salmonella*: Cellular and Molecular Biology, 1st edn, ASM press, Washington, D.C
- Ohnishi, K., K. Kutsukake, H. Suzuki & T. Lino, (1992) A novel transcriptional regulation mechanism in the flagellar regulon of *Salmonella typhimurium*: an antisigma factor inhibits the activity of the flagellum-specific sigma factor, sigma F. *Molecular Microbiology* 6: 3149-3157.
- Ohnishi, K., K. Kutsukake, H. Suzuki & T. lino, (1990) Gene *fliA* encodes an alternative sigma factor specific for flagellar operons in *Salmonella typhimurium*. *Molecular and General Genetics* 221: 139-147.
- Paul, K., M. Erhardt, T. Hirano, D. F. Blair & K. T. Hughes, (2008) Energy source of flagellar type III secretion. *Nature* 451: 489-492.

- Paul, K., J. G. Harmon & D. F. Blair, (2006) Mutational analysis of the flagellar rotor protein FliN: identification of surfaces important for flagellar assembly and switching. *Journal of Bacteriology* 188: 5240-5248.
- Pearce, U.B., and Stocker, B.A, (1967). Phase variation of flagellar antigens in *Salmonella*: abortive transduction studies. *Journal of General Microbiology* 49: 335-349.
- Perugini, M. A., P. Schuck & G. J. Howlett, (2000) Self-association of human apolipoprotein E3 and E4 in the presence and absence of phospholipid. *Journal of Biological Chemistry* 275: 36758-36765.
- Prüss, B. M., Markovic, D., and Matsumura, P, (1997) The *Escherichia coli* flagellar transcriptional activator *flhD* regulates cell division through induction of the acid response gene *cadA*. *Journal of Bacteriology* 179: 3818–3821
- QuikChange® Site-Directed Mutagenesis (2005), INSTRUCTION MANUAL (Stratagene)
- Rao, C. V., J. R. Kirby & A. P. Arkin, (2004) Design and diversity in bacterial chemotaxis: a comparative study in *Escherichia coli* and *Bacillus subtilis*. *PLoS biology* 2: 239-252.
- Samatey, F. A., H. Matsunami, K. Imada, S. Nagashima, T. R. Shaikh & D. R. Thomas, (2004) Structure of the bacterial flagellar hook and implication for the molecular universal joint mechanism. *Nature* 431: 1062-1068
- Saini, S., Brown, J. D., Aldridge, P. D., and Rao, C. V, (2008) FliZ Is a Posttranslational Activator of FlhD₄C₂ -Dependent Flagellar gene expression, *Journal of Bacteriology* 190: 4979–4988
- Sanna, M. G., R. V. Swanson, R. B. Bourret & M. I. Simon, (1995) Mutations in the chemotactic response regulator, CheY, that confer resistance to the phosphatase activity of CheZ. *Molecular Microbiology* 15: 1069-1079.

- Schroder, O. & R. Wagner, (2002) The bacterial regulatory protein H-NS--a versatile modulator of nucleic acid structures. *Biological Chemistry* 383: 945-960.
- Schuck, P., (1997) Use of surface plasmon resonance to probe the equilibrium and dynamic aspects of interactions between biological macromolecules. *Annual Review of Biophysics and Biomolecular Structure* 26: 541-566.
- Segall, J. E., S. M. Block & H. C. Berg, (1986) Temporal comparisons in bacterial chemotaxis. *Proceedings of the National Academy of Sciences of the United States of America* 83: 8987-8991.
- Shi, W., Zhou, Y., Wild, J., Adler, J., and Gross, C. A, (1992) DnaK, DnaJ, and GrpE are required for flagellum synthesis in *Escherichia coli*. *Journal of Bacteriology* 174: 6256–6263
- Shin, S., & Park, C, (1995) Modulation of flagellar expression in *Escherichia coli* by acetyl phosphate and the osmoregulator OmpR. *Journal of Bacteriology* 177: 4696–4702
- Smith, T. G., & Hoover, T. R. (2009). Chapter 8 - Deciphering Bacterial Flagellar Gene Regulatory Networks in the Genomic Era. *Advances in Applied Microbiology* 67: 257–295).
- Sorenson, M. K., S. S. Ray & S. A. Darst, (2004) Crystal Structure of the Flagellar sigma²⁸/Anti-sigma Complex sigma (28)/FlgM Reveals an Intact σ Factor in an Inactive Conformation. *Molecular Cell* 14: 127-138.
- Sourjik, V. & H. C. Berg, (2002) Binding of the *Escherichia coli* response regulator CheY to its target measured in vivo by fluorescence resonance energy transfer. *Proceedings of the National Academy of Sciences of the United States of America* 99: 12669-12674.
- Soutourina, O. A., E. Krin, C. Laurent-Winter, F. Hommais, A. Danchin & P. N. Bertin, (2002) Regulation of bacterial motility in response to low pH in *Escherichia*

- coli*: the role of H-NS protein. *Microbiology (Reading, England)* 148: 1543-1551.
- Soutourina, O., Kolb, a, Krin, E., Laurent-Winter, C., Rimsky, S., Danchin, a, & Bertin, P, (1999) Multiple control of flagellum biosynthesis in *Escherichia coli*: role of H-NS protein and the cyclic AMP-catabolite activator protein complex in transcription of the *flhDC* master operon. *Journal of Bacteriology* 181: 7500–7508
- Stafford, G. P., T. Ogi & C. Hughes, (2005) Binding and transcriptional activation of non-flagellar genes by the *Escherichia coli* flagellar master regulator FlhD₂C₂ Printed in Great Britain. *Microbiology* 151: 1779-1788.
- Stock, J. B., M. N. Levit & P. M. Wolanin, (2002) Information processing in bacterial chemotaxis. *Sci STKE* 132: pe25.
- Stock, A., S. Clarke, C. Clarke & J. Stock, (1987) N-terminal methylation of proteins: structure, function and specificity. *FEBS Letters* 220: 8-14.
- Thomas, J., G. P. Stafford & C. Hughes, (2004) Docking of cytosolic chaperone-substrate complexes at the membrane ATPase during flagellar type III protein export. *Proceedings of the National Academy of Sciences of the United States of America* 101: 3945-3950.
- Tomoyasu, T., Takaya, A., Isogai, E., & Yamamoto, T, (2003) Turnover of FlhD and FlhC, master regulator proteins for *Salmonella* flagellum biogenesis, by the ATP-dependent ClpXP protease. *Molecular microbiology* 48: 443–52
- Turner, L., W. S. Ryu & H. C. Berg, (2000) Real-Time Imaging of Fluorescent Flagellar Filaments. *Journal of Bacteriology* 182: 2793-2801.
- Wadhams, G. H. & J. P. Armitage, (2004) Making sense of it all: bacterial chemotaxis. *Nature Reviews Molecular Cell Biology* 5: 1024-1037.

- Wang, S., R. T. Fleming, E. M. Westbrook, P. Matsumura & D. B. McKay, (2006) Structure of the *Escherichia coli* FlhDC complex, a prokaryotic heteromeric regulator of transcription. *Journal of Molecular Biology* 355: 798-808.
- Wang, H. & P. Matsumura, (1996) Characterization of the CheAS/CheZ complex: a specific interaction resulting in enhanced dephosphorylating activity on CheY-phosphate. *Molecular Microbiology* 19: 695-703.
- Wei, B. L., a. M. Brun-Zinkernagel, J. W. Simecka, B. M. Pruss, P. Babitzke & T. Romeo, (2001) Positive regulation of motility and *flhDC* expression by the RNA-binding protein CsrA of *Escherichia coli*. *Molecular Microbiology* 40: 245-256.
- Wozniak, C. E. & K. T. Hughes, (2008) Genetic dissection of the consensus sequence for the class 2 and class 3 flagellar promoters. *Journal of Molecular Biology* 379: 936-952.
- Yamamoto, S. & K. Kutsukake, (2006) FliT acts as an anti-FlhD₂C₂ factor in the transcriptional control of the flagellar regulon in *Salmonella enterica* serovar typhimurium. *Journal of Bacteriology* 188: 6703-6708.
- Yamashita, I., K. Hasegawa, H. Suzuki, F. Vonderviszt, Y. Mimori-Kiyosue & K. Namba, (1998) Structure and switching of bacterial flagellar filaments studied by X-ray fiber diffraction. *Nature Structural and Molecular Biology* 5: 125-132.
- Yanagihara, S., S. Iyoda, K. Ohnishi, T. Iino & K. Kutsukake, (1999) Structure and transcriptional control of the flagellar master operon of *Salmonella typhimurium*. *Genes & genetic systems* 74: 105-111.
- Yip, C. K. & N. C. Strynadka, (2006) New structural insights into the bacterial type III secretion system. *Trends in Biochemical Sciences* 31: 223-230.

- Yokoseki, T., T. Iino & K. Kutsukake, (1996) Negative regulation by *fliD*, *fliS*, and *fliT* of the export of the flagellum-specific anti-sigma factor, FlgM, in *Salmonella typhimurium*. *Journal of Bacteriology* 178: 899-901.
- Yonekura, K., S. Maki-Yonekura & K. Namba, (2003) Complete atomic model of the bacterial flagellar filament by electron cryomicroscopy. *Nature* 424: 643-650.
- Yonekura, K., S. Maki-Yonekura & K. Namba, (2001) Structure analysis of the flagellar cap-filament complex by electron cryomicroscopy and single-particle image analysis. *Journal of Structural Biology* 133: 246-253.
- Yonekura, K., (2000) The Bacterial Flagellar Cap as the Rotary Promoter of Flagellin Self-Assembly. *Science* 290: 2148-2152.
- Zhang, P., C. M. Khursigara, L. M. Hartnell & S. Subramaniam, (2007) Direct visualization of *Escherichia coli* chemotaxis receptor arrays using cryo-electron microscopy. *Proceedings of the National Academy of Sciences of the United States of America* 104: 3777-3781.

Appendix A: Growth media and solutions

Sterilisation of solutions

Some Solutions need sterilization, which is normally performed in glassware at 121°C for 30 minutes. When heat destabilising a chemical component, sterilization was performed instead using filtration system. Pouring agar over Petri dishes needs one litter of growth media solution containing agar (all components, 2X concentrated) sterilised in a large conical flask with the other containing the same amount of water. After sterilisation the water was cooled to RT by immersing the flask in a cold-water bath before appropriated antibiotics and growth supplements were added. Required solution was the mixture and immediately poured into Petri dishes and cooled at room temperature for 72hrs then stored at 4°C.

General growth media

Liquid Culture Media

LB- Luria–Bertani

Tryptone	1%	10 g/L
Yeast Extract	0.5%	5 g/L
NaCl	1%	10 g/L

Solid growth Media

Growth Plates

1.5% (15 g/L) of Difco agar was added to the liquid media.

Motility Plates

0.3% (3 g/L) of Difco agar was added to the liquid media.

Plasmid DNA extraction

Solution 1

Glucose	50 mM
Tris.HCl (pH 8.0)	25 mM
EDTA (pH 8.0)	10 mM

Solution 2	(10 ml) fresh
NaOH	2 ml
10 % SDS	1 ml
H ₂ O	7 ml

Solution 3	(100 ml)
5 M Potassium acetate	60 ml
Glacial acetic acid	11.5 ml
H ₂ O	28.5 ml

Agarose gel electrophoresis

10 x Gel loading buffer

Tris Acetate (pH 8.0)	200 mM
EDTA	5 mM
Glycerine	50 %
Bromophenol blue	0.1 %
Xylene cyanol FF	0.1 %
Orange G	0.1 %

50x TAE running buffer

(1 L)

Tris	242 g
Glacial acetic acid	57.1 ml
EDTA	37.7 g

SDS-PAGE

Acrylamide gels for SDS-PAGE, Tricine gels for SDS-PAGE

Separating gel %	16.5 %	12%	10%	Stacking gel (3.96 %)
acrylamide (15 ml)				
Separating acrylamide	5 ml	3.6 ml	3 ml	-
Stacking acrylamide	-	-	-	1 ml
Tricine gel buffer	5 ml	5 ml	5 ml	3.1 ml
50% glycerol	5 ml	5 ml	5 ml	-
H ₂ O	-	1.4 ml	2 ml	8.4 ml
APS (10%)	75 µl	75 µl	75 µl	100 µl
TEMED	7.5 µl	7.5 µl	7.5 µl	10 µl

Tricine gel buffer

Tris pH 8.25	3 M
SDS	0.3 %

SDS-PAGE Loading buffer

Tris.HCl	62.5 mM
Glycerol	10 %
SDS	2 %
β-Mecarptoethanol	5 %
Bromophenol blue	BLUE

Cathode (upper) running buffer

Tris pH 8.25	100 mM
Tricine	100 mM
SDS	0.1 %

Anode (lower) running buffer

Tris pH8.9	200 mM
------------	--------

Coomassie blue stain (per litre)

Methanol	400 ml
Acetic acid	100 ml
H ₂ O	500 ml
Coomassie	1.1 g

SDS-PAGE Destain (per litre)

Methanol	400 ml
Acetic acid	100 ml
H ₂ O	500 ml

Western blot analysis

10x Transfer buffer (1L)

Glycine	144 g
Tris base	30.25 g

1 x Transfer buffer (1 L)

10 x Transfer buffer	100 ml
Methanol	100 ml
H ₂ O	800 ml

10x Phosphate buffer solution (1 L) (pH 7.4)

NaCl	80 g
KCl	2 g
Na ₂ HPO ₄	14.4 g
KH ₂ PO ₄	2.4 g

Membrane blocking solution

PBS	1 x
Milk	5 %
Tween	0.1 %

Native gel electrophoresis

10X Native gel buffer pH 8.3

Glycine	1.5 M
Tris-HCl	250 mM

Native acrylamide gel 10%

ddH ₂ O	13.38 ml
10X buffer	2 ml
40% acrylamide	4.5 ml
10% APS	100 µl
TMED	20 µl

Native loading buffer

Glycerol	30%
1X Native gel buffer pH 8.3	70%
bromphenol blue	Blue

Column gel electrophoresis

His-tag loading buffer pH 7.5, filtered and degassed

Hepes	50 mM
NaCl	150 mM
Imidazol	20 mM

His- tag eluting buffer pH 7.5, filtered and degassed

Hepes	50 mM
NaCl	150 mM
Imidazol	1 M

Heparin loading buffer pH 7.9 filtered and degassed (1L)

Tris	1.21 g
------	--------

Heparin loading buffer pH 7.9 filtered and degassed (1L)

Tris	1.21 g
NaCl	29.22 g

Gel filtration buffer pH 7.9 filtered and degassed**FliT and FlID**

Tris	20 mM
NaCl	150 mM

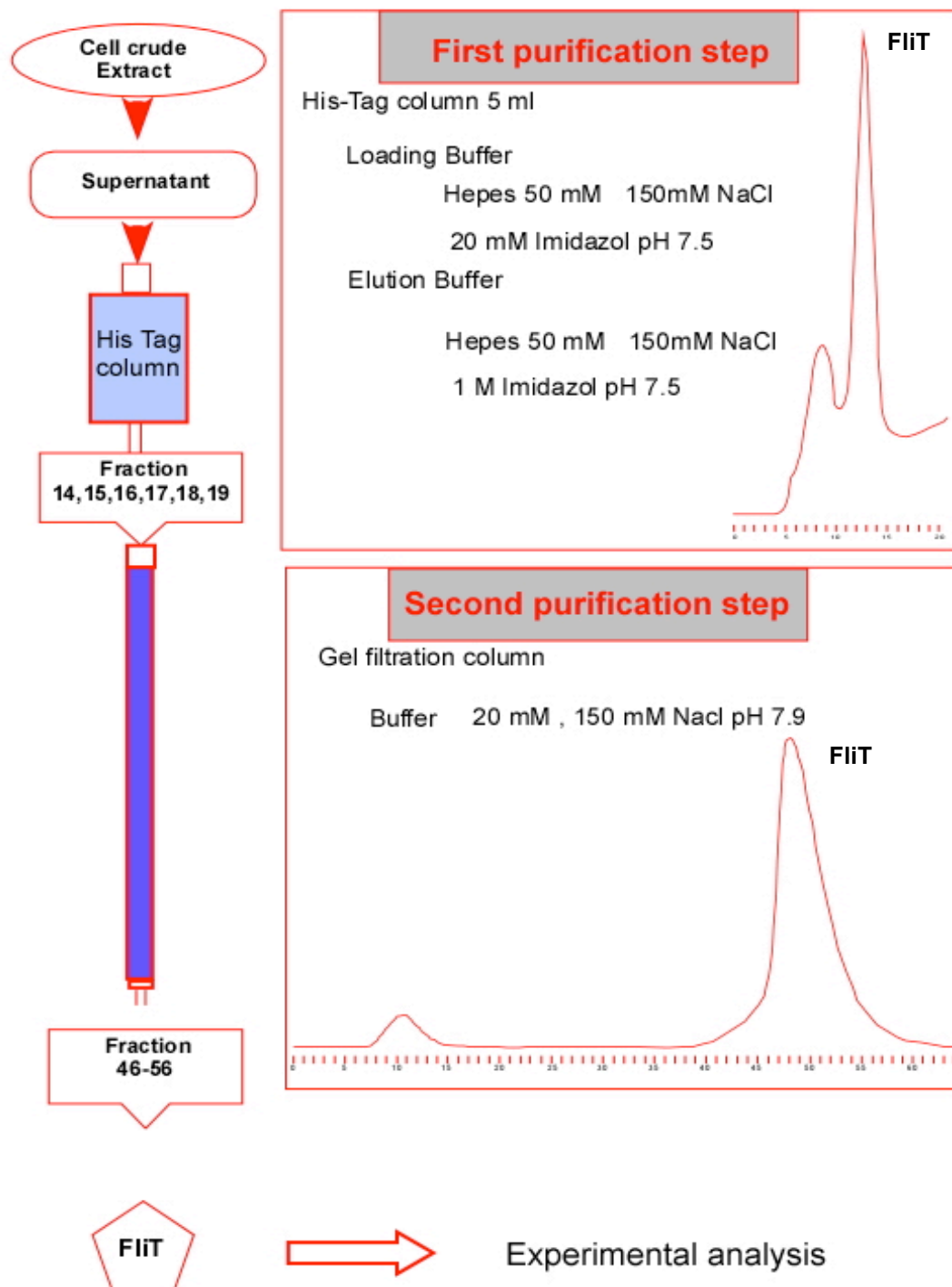
FlhD₄C₂

Tris	20 mM
NaCl	300 mM

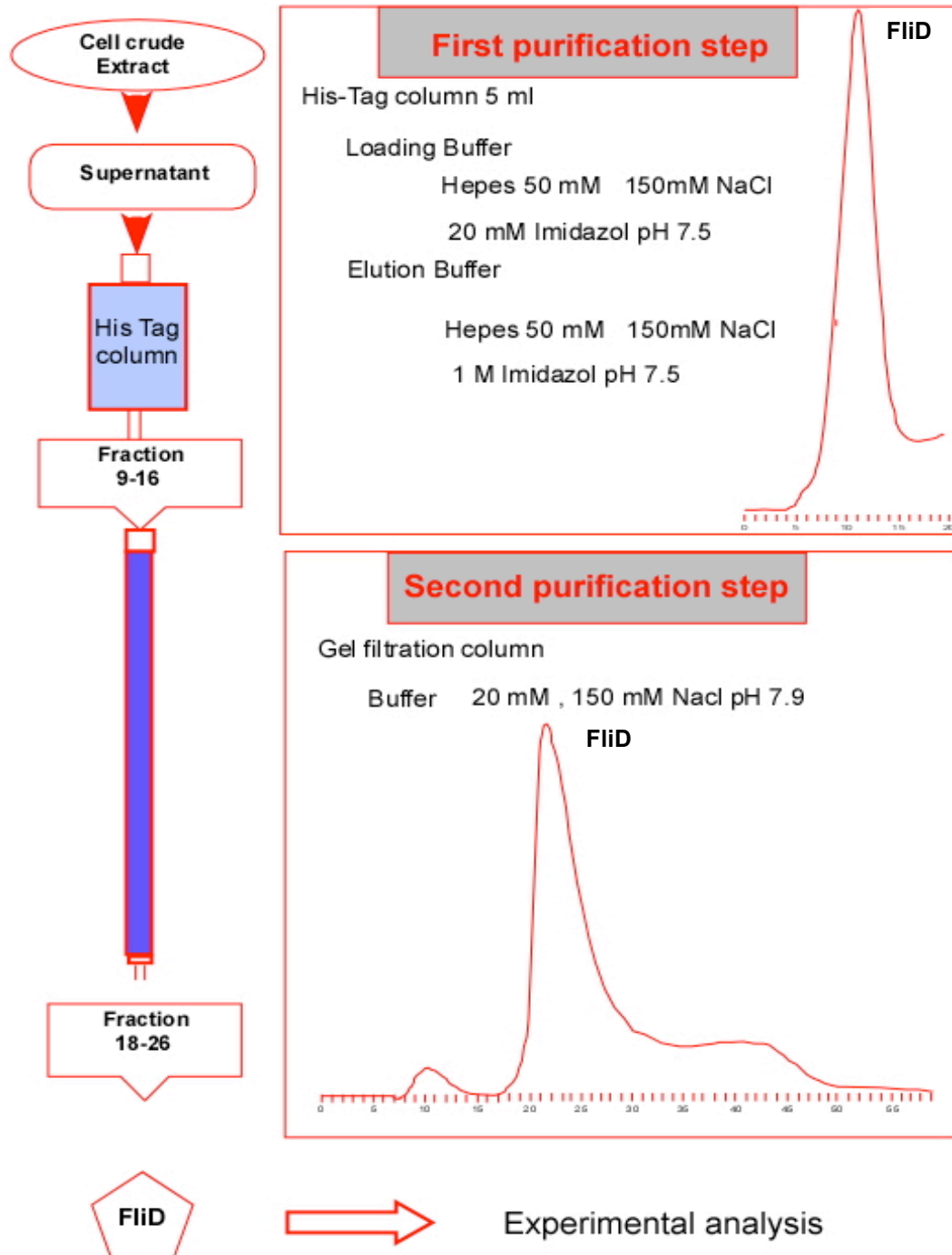
Appendix B: Protein preparation for analysis

Methods Illustrated from crude extract to isolated protein

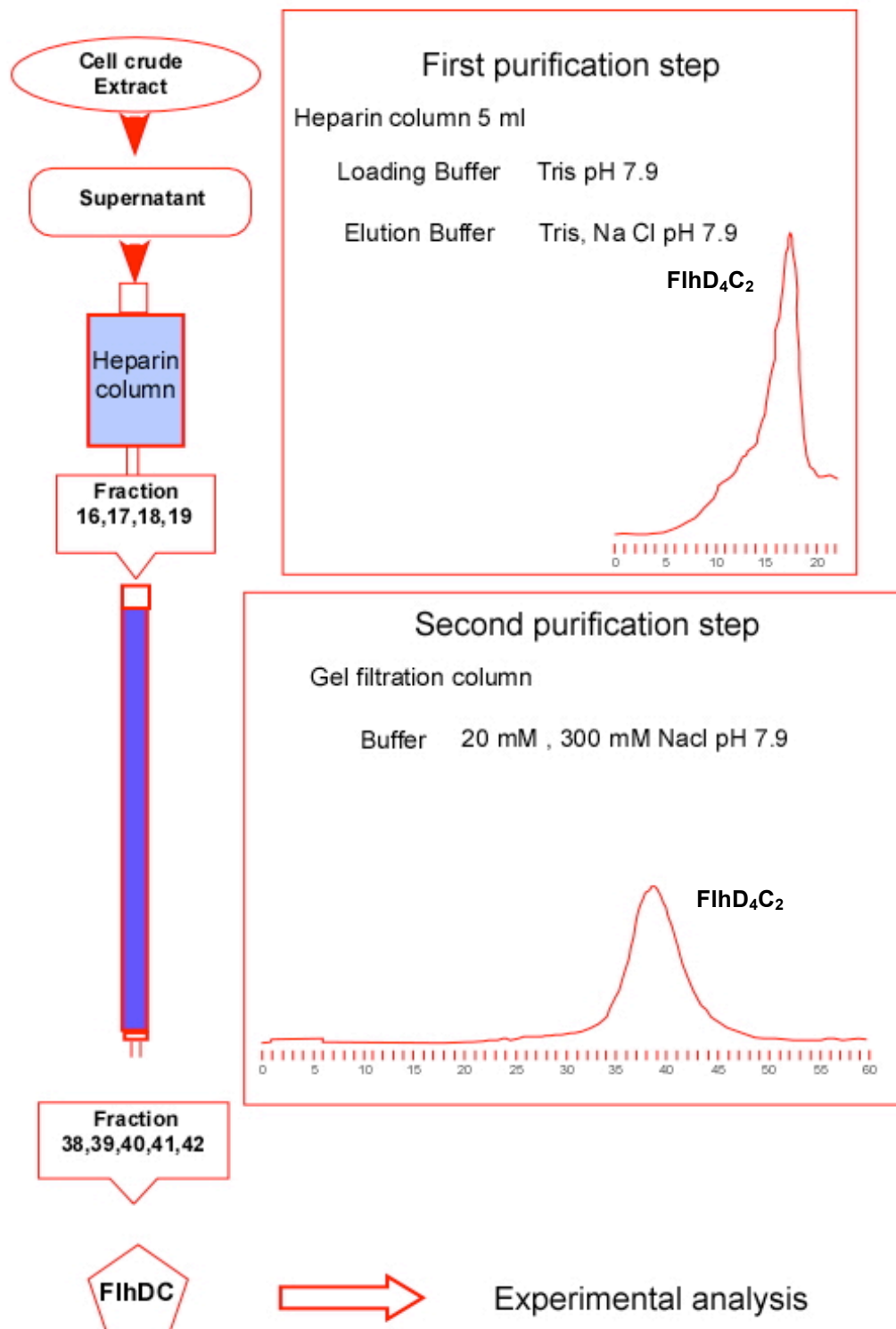
1. FliT purification



2. FliD purification



3. FlhD₄C₂ purification



Appendix C: The prediction of protein concentration

Information needed for the prediction

- Absorbance λ_{280} of protein solution (**A**)
- Extinction coefficient (**E**) predicted from protein sequence (NCBI)

FliT	=	1.129
FliD	=	0.379
FliD:FliT	=	0.541
FliD ₄ C ₂	=	0.670

The equation for predicting protein concentration (mg/ml)

$$C \text{ (mg/ml)} = \frac{A * (\text{dilution factor})}{E}$$

Notice: Dilution factor is the number referring how much protein solution is diluted before measuring absorbance for example diluting 10 times referring 10 as dilution factor.

The equation for predicting protein concentration in Molarity (μM) require

Molecular mass of a protein (**M**) (kDa)

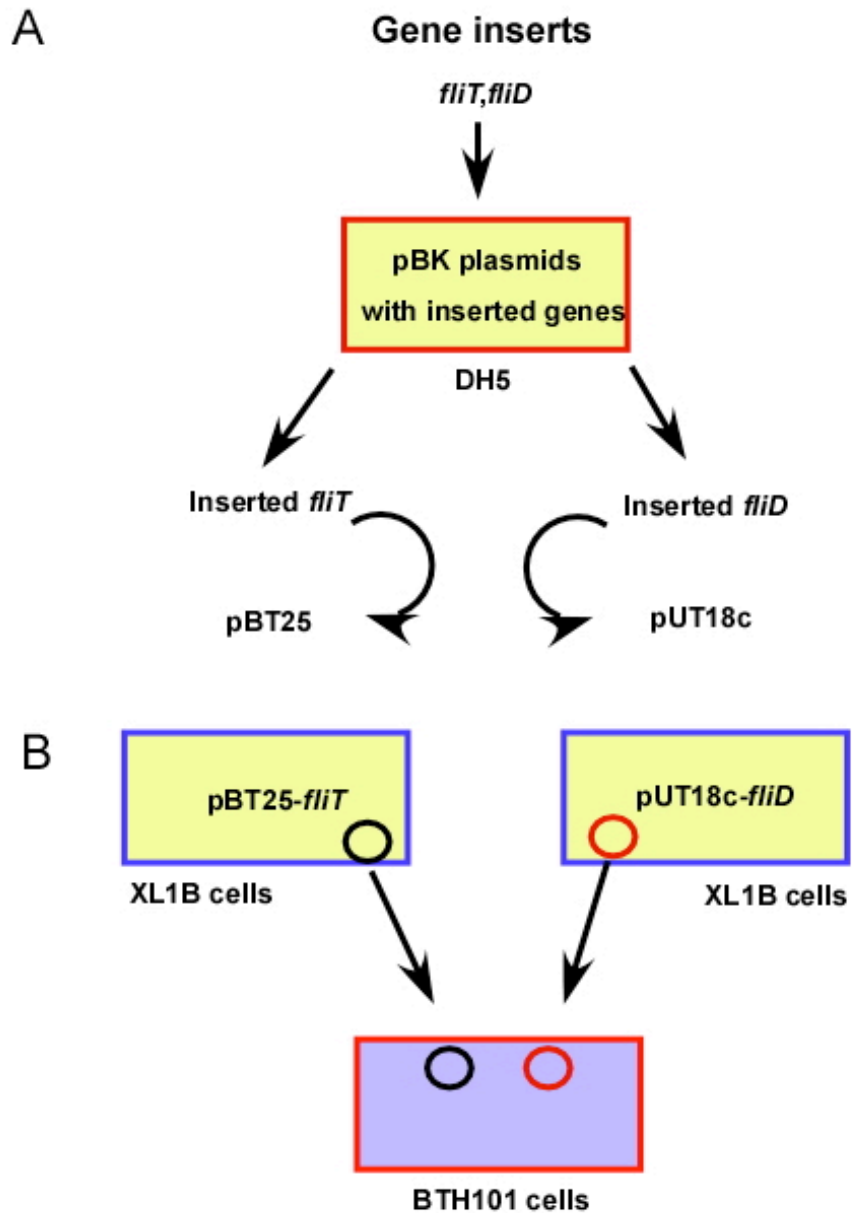
FliT	=	13.7
FliD	=	49.8
FliD ₄ C ₂	=	97.0

The equation for predicting protein concentration (μM)





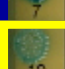
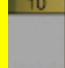
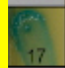
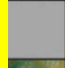
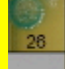
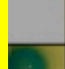
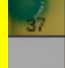

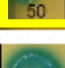












$$C \text{ (}\mu\text{M)} = \frac{C \text{ (mg/ml)} * 1,000}{M \text{ (g/mole)}}$$



Appendix D: Bacterial Two Hybrid system (B2H)



1. Methods Illustrated for protein interaction analysis (FliT and FliD)





2. The actual result on big square agar plate representing B2H experiments from different protein interaction with either C or N terminal free of all 56 combinations.

Protein		FlIT	FlID	FlIT	FlID	FlIT	FlID	FlhD	FlhC	FlhC	FlhC	FlhC	FlhDC	FlhDC	FlhDC
	Terminal	C	C	N	N	N	N	N	N	N	C	C	C	C	N
FlIT	C	X													
FlID	C		X												
FlIT	N			X											
FlID	N				X										
FlIT	N					X									
FlID	N						X								
FlhD	N							X							
FlhC	N								X						
FlhC	N									X					
FlhC	C										X				
FlhC	C										X				
FlhDC	C											X			
FlhDC	C												X		
FlhDC	N													X	
FlhDC	N														X

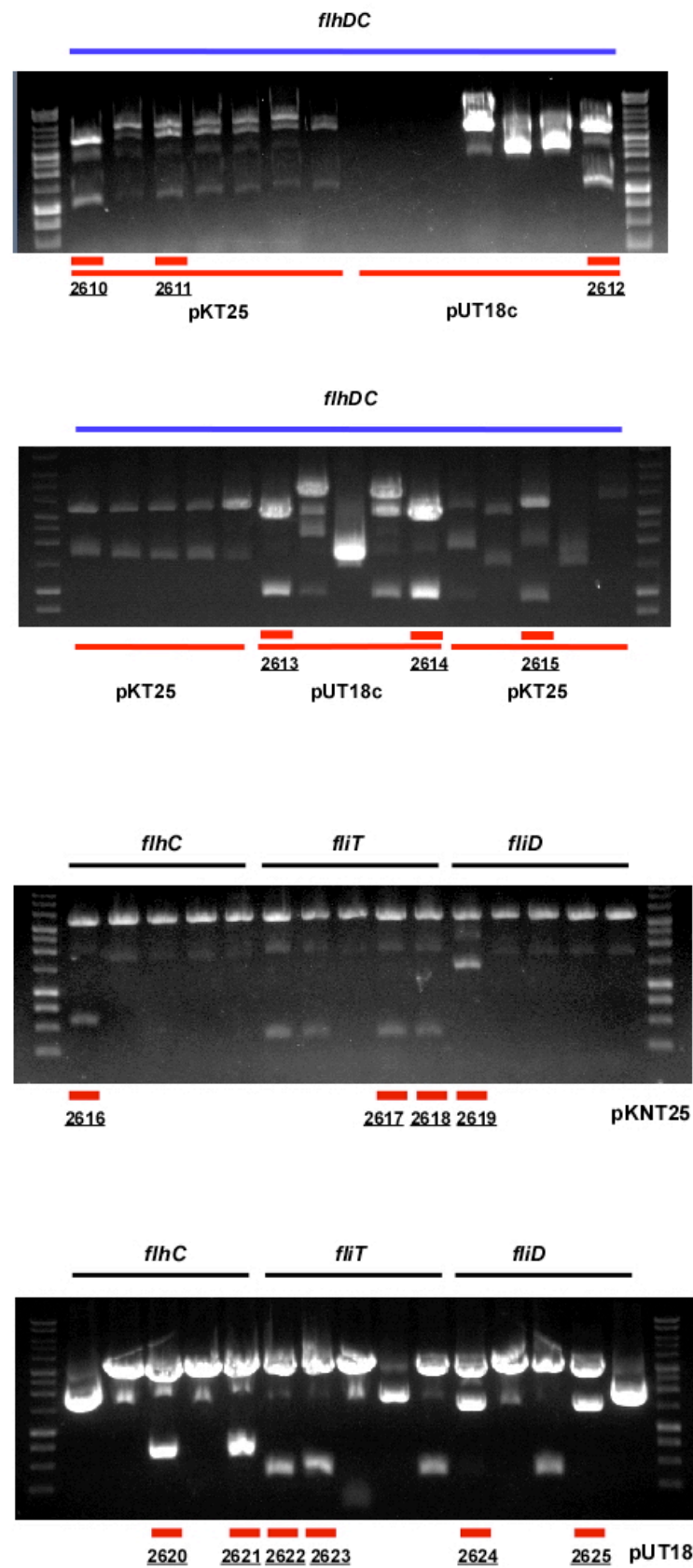


 Positive control
 Negative control



 Positive control
 Negative control



 Positive control
 Negative control

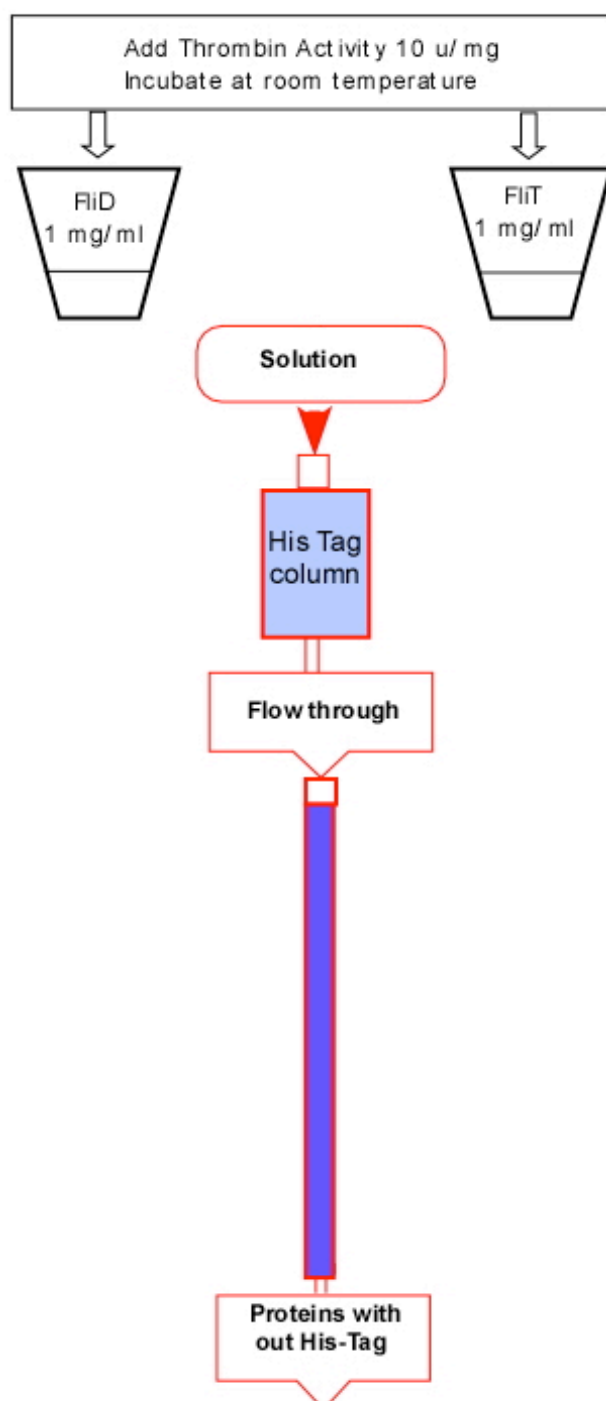
Incubational time for this experiment was 48 Hrs.

3 Test digestion showing gene insert of all 16 clones



Appendix E: Thrombin digestion of proteins

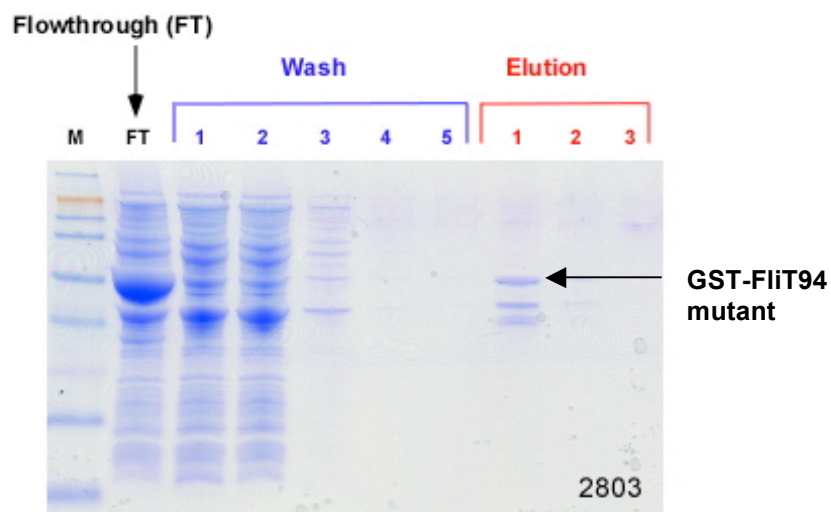
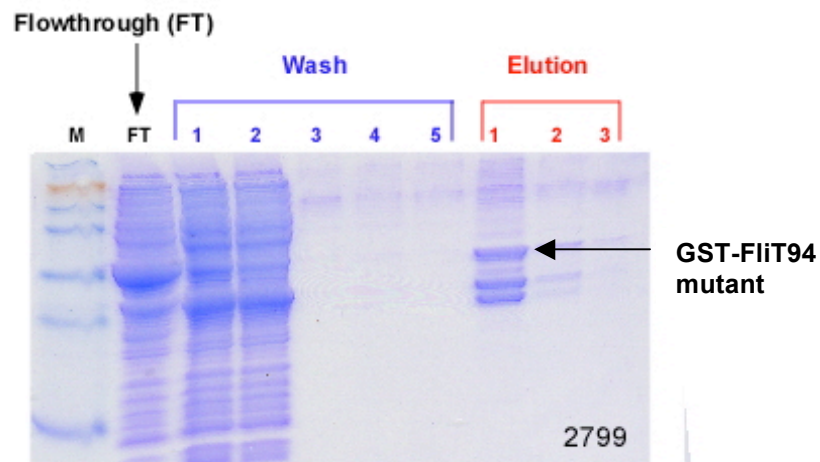
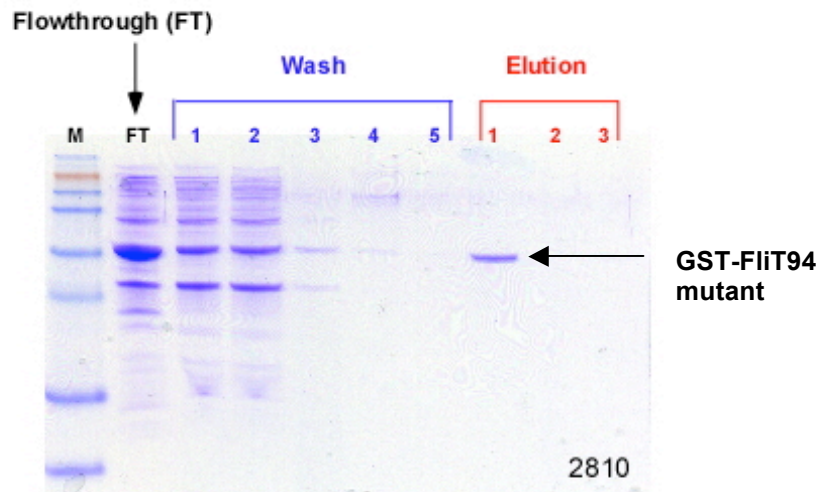
Methods Illustrated for preparing digested proteins (FliT and FliD)



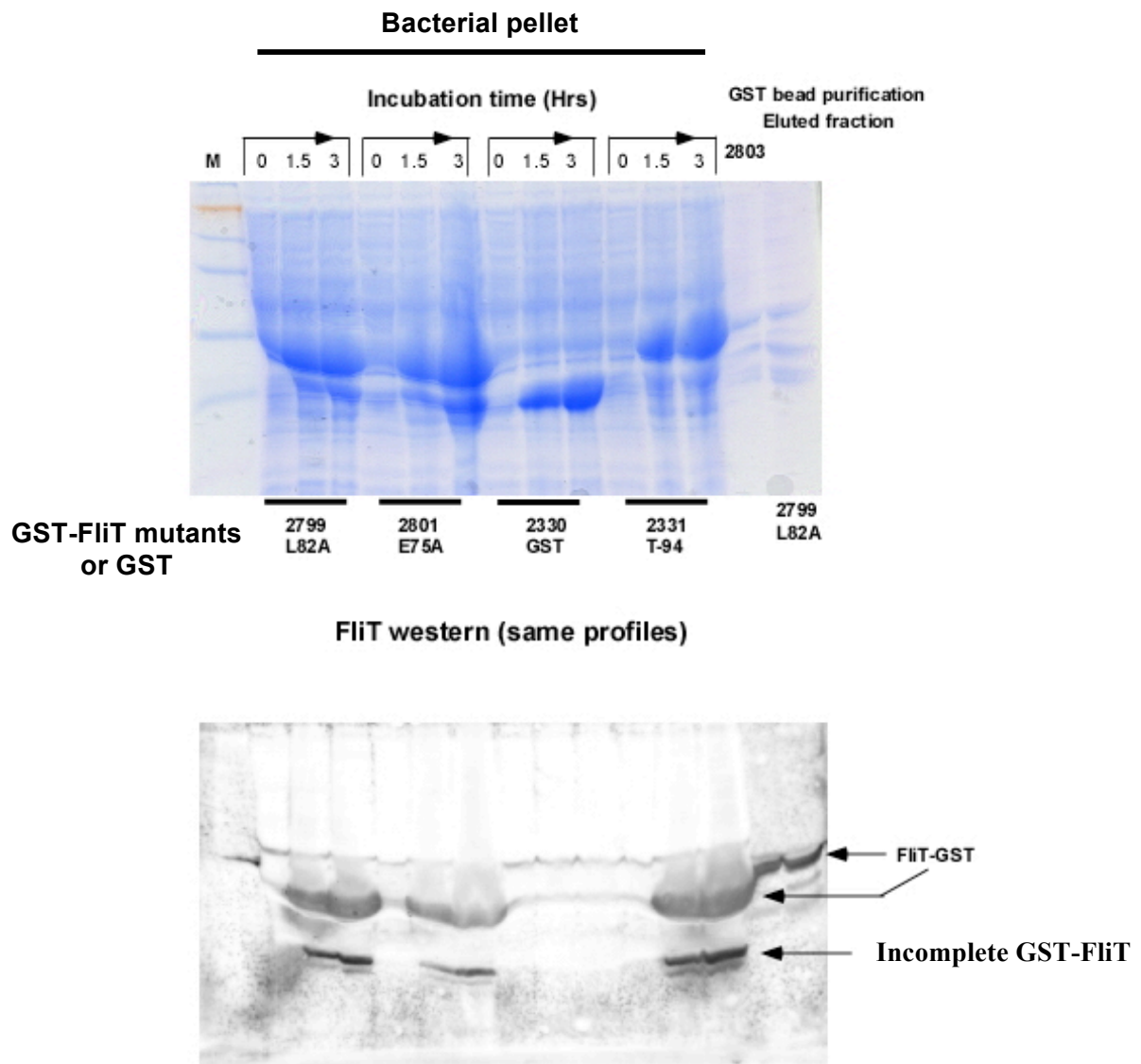
Thrombin digestion of protein: specific cleavage of the sequence
LeuValProArg↓GlySer in recombinant fusion proteins

Appendix F: GST proteins purification

1. GST proteins purified by GST- affinity beads for GST-Flt94 mutants



2. Expression profiles of GST FliT mutants and immune blot (FliT)



Appendix G: Prepare bacterial cells' sample

ODU give us a clue of the amount of bacteria in a sample in relation with the absorbance at 600 of a bacterial culture

Start growing culture by preparing the culture absorbance (λ_{600}) = 0.05

Measuring absorbance (λ_{600}) of overnight culture by diluting the culture (1:10 dilution), the obtained absorbance (λ_{600}) is multiplied by ten to represent the actual absorbance (λ_{600}) (or **A**) of the overnight culture

To prepare 1 litre of bacterial culture with absorbance (λ_{600}) = 0.05, the specific amount of the overnight culture (or **B**) is needed to add to 1 litre of LB media.

$$B (\mu l) = \frac{1000000 * A}{0.05}$$

OD unit (ODU) calculated from the absorbance $\lambda = 600$ of the bacterial culture

Start growing culture Absorbance λ_{600} of culture = 0.05

Stop growing culture Absorbance λ_{600} of collected culture = 0.7-0.8 (or **X**)

The calculation equation representing ODU/ μl of a sample

$$\text{ODU}/\mu l \text{ of a sample} = \frac{\text{Volume of collected culture } (\mu l) * X}{\text{Volume of SDS loading buffer added } (\mu l)}$$

To acquire 1000 ODU of sample, add volume of SDS loading buffer (**Y**) to the bacterial pellet from volume of collected culture (μl)

$$Y (\mu l) = \frac{\text{Volume of collected culture } (\mu l) * X}{1000}$$

Appendix H: PCR information for amplifying *fliT*, *fliD* and *flhDC* gene

	1)	95.0	2 mins	
Denaturation cycle	2)	95.0	30 Secs	18 loops
Annealing cycle	3)	52.0	30 Secs	18 loops
Extension cycle	4)	75.0	2 mins	18 loops
	5)	75.0	5 mins	
	6)	4.0	Pause	

PCR information for Quick Change experiments

	1)	93.0	1 min	
Denaturation cycle	2)	95.0	1 min	18 loops
Annealing cycle	3)	50.0	1 min	18 loops
Extension cycle	4)	72.0	5 mins	18 loops
	5)	72.0	8 mins	
	6)	4.0	Pause	